

MODULATION OF THE HYPERPOLARIZATION
ACTIVATED CATIONIC CURRENT (I_h) AND
SUBTHRESHOLD RESONANCE IN NEOCORTICAL NEURONS

CENTRE FOR NEWFOUNDLAND STUDIES

**TOTAL OF 10 PAGES ONLY
MAY BE XEROXED**

(Without Author's Permission)

CORY VICTOR GILES



Modulation of the Hyperpolarization Activated Cationic Current (I_h) and Subthreshold Resonance in Neocortical Neurons

by

© Cory Victor Giles

A thesis submitted to the School of Graduate Studies

in partial fulfilment of the requirements

for the degree of

Doctor of Philosophy

Faculty of Medicine (Neuroscience)
Memorial University of Newfoundland

October 2005

St. John's

Newfoundland



Library and
Archives Canada

Bibliothèque et
Archives Canada

Published Heritage
Branch

Direction du
Patrimoine de l'édition

395 Wellington Street
Ottawa ON K1A 0N4
Canada

395, rue Wellington
Ottawa ON K1A 0N4
Canada

Your file *Votre référence*
ISBN: 978-0-494-19620-5
Our file *Notre référence*
ISBN: 978-0-494-19620-5

NOTICE:

The author has granted a non-exclusive license allowing Library and Archives Canada to reproduce, publish, archive, preserve, conserve, communicate to the public by telecommunication or on the Internet, loan, distribute and sell theses worldwide, for commercial or non-commercial purposes, in microform, paper, electronic and/or any other formats.

The author retains copyright ownership and moral rights in this thesis. Neither the thesis nor substantial extracts from it may be printed or otherwise reproduced without the author's permission.

AVIS:

L'auteur a accordé une licence non exclusive permettant à la Bibliothèque et Archives Canada de reproduire, publier, archiver, sauvegarder, conserver, transmettre au public par télécommunication ou par l'Internet, prêter, distribuer et vendre des thèses partout dans le monde, à des fins commerciales ou autres, sur support microforme, papier, électronique et/ou autres formats.

L'auteur conserve la propriété du droit d'auteur et des droits moraux qui protègent cette thèse. Ni la thèse ni des extraits substantiels de celle-ci ne doivent être imprimés ou autrement reproduits sans son autorisation.

In compliance with the Canadian Privacy Act some supporting forms may have been removed from this thesis.

Conformément à la loi canadienne sur la protection de la vie privée, quelques formulaires secondaires ont été enlevés de cette thèse.

While these forms may be included in the document page count, their removal does not represent any loss of content from the thesis.

Bien que ces formulaires aient inclus dans la pagination, il n'y aura aucun contenu manquant.


Canada

Abstract

Resonance is a biophysical characteristic of a subset of neurons in which the voltage response of oscillating input peaks at a preferred frequency. Given the widespread distribution of histaminergic neurons and the known physiology of histamine receptors in the CNS, it was hypothesized that histamine modulates the resonance of pyramidal neurons by shifting the activation and kinetics of the hyperpolarization activated cationic current, I_h .

Employing standard whole cell voltage clamp recording, investigation of the modulation of I_h was confounded by a time dependent hyperpolarizing shift of I_h . The addition of cAMP to the recording pipette prevented rundown and resulted in a depolarizing shift in I_h activation consistent with an important role for intracellular cAMP in the maintenance and modulation of I_h .

In the presence of cAMP in the pipette, bath application of histamine, 8-bromo-cAMP, and forskolin, mimicked cAMP-induced changes in I_h . Histamine's action was mimicked by amthamine (H_2 agonist), blocked by tiotidine (H_2 antagonist), and occluded by forskolin, consistent with an H_2 receptor-mediated activation of adenylyl cyclase. H7, a nonspecific protein kinase inhibitor, blocked both the forskolin and histamine-induced effects on I_h consistent with involvement of a phosphorylation event.

Using the Impedance Amplitude Profile (ZAP) methodology to profile the resonant properties of pyramidal neurons, histamine increased both the resonant frequency (f_{res}) and its magnitude (Q) in a concentration-dependent manner that closely resembled histamine's action on I_h . This was confirmed by application of ZD-7288, an

irreversible blocker of I_h , which blocked both the histamine-induced action and resonance.

It is concluded that histamine, acting via H_2 receptor activation of adenylyl cyclase and possibly a protein kinase, shifts the activation of I_h to more depolarized potentials. This action modulates the resonant behaviour of these neurons, which in turn can influence their oscillatory properties and consequently aid in the synchronization of larger neuronal networks.

Table Of Contents

Abstract	ii
Table Of Contents	iv
List of Tables	vii
List of Figures	viii
List of Abbreviations.....	x
Acknowledgements	xvi
1. Introduction.....	1
1.1 Scope of thesis	1
1.2 Histamine in the CNS.....	3
1.2.1 Organization.....	3
1.2.2 H ₁ receptor	8
1.2.3 H ₂ receptor	15
1.2.4 H ₃ receptor	19
1.2.5 Histamine and arousal.....	24
1.2.6 Histamine and homeostasis.....	28
1.2.6.1 Fluid balance	28
1.2.6.2 Feeding	29
1.2.7 Histamine and locomotion	30
1.2.8 Histamine and cognition	31
1.3 Hyperpolarization-activated cationic current (I _h).....	33
1.4 Mechanism of resonance.....	36
1.5 Organization of thesis	45
2. Modulation of the hyperpolarization-activated current (I_h) and prevention of rundown by cyclic AMP in neocortical neurons.....	47
2.1 Introduction.....	47
2.2 Methods and Materials	49

2.3	Results.....	57
2.3.1	Inward rectification by membrane hyperpolarization.....	57
2.3.2	Rundown of I_h	62
2.3.3	K^+ conductance effects on I_h recordings.....	66
2.3.4	I_h is located on apical dendrites.....	72
2.3.5	I_h measurement errors.....	75
2.3.6	cAMP prevents rundown of I_h	81
2.3.7	Modulation of I_h occurs during intracellular cAMP application.....	85
2.3.7.1	cAMP analog.....	90
2.3.7.2	Adenylyl cyclase activator.....	93
2.3.8	Protein Kinase Inhibition.....	96
2.4	Discussion.....	97
2.4.1	cAMP prevents rundown of I_h	97
2.4.2	Activation thresholds can be used to verify I_h I/V results.....	99
2.4.3	Modulation of I_h occurs during intracellular cAMP application.....	101
2.4.4	Protein kinase and I_h activation.....	103
2.4.5	Possible mechanisms of I_h rundown.....	105
3.	Histamine H_2 receptors modulate the hyperpolarization-activated current (I_h) in rat neocortical neurons.....	108
3.1	Introduction.....	108
3.2	Methods and Materials.....	112
3.3	Results.....	113
3.3.1	Histamine modulates I_h	113
3.3.2	Effects of histamine are blocked by the H_2 antagonist, tiotidine.....	120
3.3.3	Effects of histamine are mimicked by the H_2 agonist amthamine.....	132
3.3.4	Adenylyl cyclase activated forskolin mimic histamine-induced actions on I_h	135
3.3.5	Effects of the protein kinase inhibitor H7.....	138
3.4	Discussion.....	143
3.4.1	Histamine does not alter the instantaneous current.....	144
3.4.2	Histamine modulates I_h in neocortical neurons.....	146
3.4.3	Histamine modulation of I_h is mediated by H_2 receptors.....	151
3.4.3	Histamine modulation I_h involves adenylyl cyclase and protein kinase activity.....	153
4.	Histamine modulates subthreshold resonance in rat neocortical neurons.....	156
4.1	Introduction.....	156
4.2	Methods and Materials.....	158
4.3	Results.....	160
4.3.1	Frequency response curves are voltage dependent.....	160
4.3.2	Histamine modulates the frequency response of neocortical neurons.....	166
4.3.3	ZD-7288 prevents histamine modulation of subthreshold resonance.....	170
4.3.4	Tiotidine blocks histamine modulation of subthreshold resonance.....	172

4.4 Discussion.....	177
4.4.1 Subthreshold resonance in neocortical neurons	177
4.4.2 Voltage dependent mechanism of subthreshold resonance.....	184
4.4.3 Histamine modulates subthreshold resonance.....	186
5. Summary and Conclusions.....	188
5.1 Rundown of I_h	188
5.2 Role of protein kinase	189
5.3 Histamine and I_h	190
5.4 Cortical resonance and I_h	190
5.5 Physiological relevance.....	191
5.5.1 Layer V anatomy.....	192
5.5.2 Modulation of cortical I_h	194
5.5.2.1 I_h contribution to membrane potential	195
5.5.2.2 I_h contribution to voltage overshoots and action potential generation.....	196
5.5.2.3 I_h and dendritic integration	198
5.5.2.4 I_h and subthreshold resonance	198
5.5.3 Low frequency activity and behaviour.....	200
5.6 Future research.....	203
Bibliography	205

List of Tables

Table 2.1 $V_{1/2}$ estimation parameters.	80
Table 3.1 Tiotidine concentration-response values for I_h and the resting membrane potential.....	132
Table 3.2 Amthamine concentration response values for I_h and the resting membrane potential.....	135
Table 3.3 Forskolin effects on I_h and the resting membrane potential.	138

List of Figures

Figure 1.1	Summary of H ₁ receptor signalling pathways and membrane responses in the CNS.	11
Figure 1.2	Summary of H ₂ receptor signalling pathways and membrane responses in the CNS.	16
Figure 1.3	Summary of H ₃ receptor signalling pathways and membrane responses in the CNS.	20
Figure 1.4	Impedance frequency response curve (zFRC) showing the contribution of active and passive membrane properties to the formation of resonance.	42
Figure 2.1	Hyperpolarizing voltage step from a holding potential of -57 mV.	52
Figure 2.2	Determining the activation threshold of I _h	54
Figure 2.3	Determining the reversal potential of I _h	55
Figure 2.4	Characterization of I _h in current clamp mode.	58
Figure 2.5	Characterization of I _h in voltage clamp mode.	59
Figure 2.6	The slow component is blocked by CsCl.	61
Figure 2.7	The slow component is eliminated by ZD-7288.	63
Figure 2.8	Rundown of I _h	64
Figure 2.9	Pooled data showing rundown of I _h	67
Figure 2.10	Co-application of TEA and 4-AP block K ⁺ conductances and increases the amplitude of I _h	69
Figure 2.11	Barium chloride (BaCl ₂) decreases K ⁺ conductances and increases the amplitude of I _h	73
Figure 2.12	I _h exists on distal apical dendrites.	76
Figure 2.13	I _h half maximal activation (V _{1/2}) estimations.	79
Figure 2.14	Inclusion of 25 μM cAMP in the internal recording solution precludes rundown of I _h	83
Figure 2.15	cAMP increases the amplitude of I _h and shifts the voltage dependence of I _h	85
Figure 2.16	8-bromo cAMP shifts the voltage dependence of I _h in the presence of cAMP.	88
Figure 2.17	Forskolin shifts the voltage dependence of I _h in the presence of cAMP.	91
Figure 2.18	H7 blocks the forskolin-induced shifts in I _h voltage dependence.	94
Figure 3.1	Histamine increases I _h	114
Figure 3.2	Concentration-response relationships for histamine.	117

Figure 3.3	Histamine increases the fast activation time (τ^2) constant for I_h	119
Figure 3.4	The H_1 antagonist, pyrilamine fails to block the histamine-induced effects on I_h	122
Figure 3.5	The H_1 antagonist, diphenhydramine fails to block the histamine effects on I_h	125
Figure 3.6	The H_3/H_4 antagonist, thioperamide (thio), does not block histamine-induced increase in I_h . 127	
Figure 3.7	The H_2 antagonist, tiotidine blocks the histamine-induced increase in I_h	129
Figure 3.8	Tiotidine antagonizes the action of histamine on I_h in a concentration dependent manner.....	130
Figure 3.9	Tiotidine reduces the histamine induced decrease in the fast activation time (τ^2) constant for I_h	131
Figure 3.10	The H_2 agonist, amthamine, increases I_h	133
Figure 3.11	Concentration-response relationships for amthamine.....	134
Figure 3.12	The H_2 agonist, amthamine, decreases the fast activation time constant (τ^2) for I_h	136
Figure 3.13	Forskolin mimics the histamine-induced changes in I_h	137
Figure 3.14	H7, a non-specific protein kinase inhibitor, blocked the histamine-induced changes in I_h	140
Figure 3.15	Histamine actions on I_h involve adenylyl cyclase and protein kinase activation via H_2 receptors.	141
Figure 4.1	Subthreshold frequency and voltage response of a resonant neuron.	163
Figure 4.2	Histamine modulates subthreshold resonance.	169
Figure 4.3	Histamine increases the f_{res} and Q.....	171
Figure 4.4	Histamine effect on subthreshold resonance is blocked by ZD-7288.....	175
Figure 4.5	ZD-7288 blocks resonance and the histamine induced increases in f_{res} and Q value.....	176
Figure 4.6	Histamine induced effect on subthreshold resonance is blocked by tiotidine.....	180
Figure 4.7	Histamine induced increase in f_{res} and Q value is blocked by tiotidine.	181

List of Abbreviations

AA	arachidonic acid
AC	adenylyl cyclase
A-D/D-A	analog-digital/digital-analog
Amth	amthamine
APV	DL-2-amino-5-phosphonopentanoic acid
arg(Z)	argument of impedance
ASCF	artificial cerebral spinal fluid
ATP	adenosine triphosphate
CaCl₂	calcium chloride
cAMP	adenosine 3',5'-cyclic monophosphate
Cap	capacitance
cGMP	guanosine 3',5'-cyclic monophosphate
CM	capacitance membrane model
CM+S	capacitance membrane model with a simple current
CNBN	cyclic nucleotide binding domain
CNS	central nervous system
cont	control
CREB	cAMP response element-binding
CsCl	cesium chloride
DAG	diacylglycerol
DAP	depolarizing after potential
diphen	diphenhydramine
DOA	diamine oxidase
EC₅₀	median effective concentration
EEG	electroencephalogram

EGTA	ethylene glycol-bis(2-aminoethylether)- <i>N,N,N',N'</i> -tetraacetic acid
E_K	potassium equalibrium potential
ERK/MAP	extracellular signal-regulated kinase/mitogen-activated protein
4-AP	4-aminopyridine
F	Faraday constant
FFT	Fast Fouier Transform
fors	forskolin
f_{res}	resonant frequency
FRS	frequency response surface
GABA	gamma-aminobutyric acid
GABA_A	gamma-aminobutyric acid receptor subtype A
GABA_B	gamma-aminobutyric acid receptor subtype B
GC	guanylyl cyclase
g_h	hyperpolarization activated cationic conductance
$g_{h\text{max}}$	maximum conducatanace
GΩ	gigohms
G-protien	guanine nucleotide bidning protein
H₁	histamine receptor subtype 1
H₂	histamine receptor subtype 2
H₃	histamine receptor subtype 3
H₄	histamine receptor subtype 4
HCN	hyperpolarization activated cyclic nucleotide-gated cationic channels
HCN1	hyperpolarization activated cyclic nucleotide-gated cationic channel isoform 1
HCN2	hyperpolarization activated cyclic nucleotide-gated cationic channel isoform 2
HCN3	hyperpolarization activated cyclic nucleotide-gated cationic channel isoform 3
HCN4	hyperpolarization activated cyclic nucleotide-gated cationic channel isoform 4
HDC	histidine decarboxylase

HEPES	4-(2-hydroxyethyl)-1-piperazineethanesulfonic acid, 4-(2-hydroxyethyl)-1-piperazineethanesulphonic acid
Hde	histidine
hist	histamine
HMT	histamine methyltransferase
H.P.	holding potential
HVACCS	high voltage activated calcium channels
IAA	imidazole acetic acid
I_{AHP}	calcium activated potassium current
I_{Cl}	chloride current
i.c.v	intracerebroventricular
I_f	funny current
I_h	hyperpolarization activated cationic current
I_{K1r}	potassium inward rectifier current
I_{KL}	potassium leak current
I_{Kv3.2}	Kv3 subtype 2 delayed rectifier-type potassium current
IC₅₀	median inhibitory concentration
Ins	instantaneous current
I_M	M-type potassium current
I_{NaP}	persistent sodium current
I_{NaTTXins}	TTX insensitive sodium current
I_{NMDA}	NMDA current
IP₃	inositol triphosphate
I_T	transient low-threshold calcium current
k_m	slope factor
KCl	potassium chloride
KOH	potassium hydroxide
LTP	long term potentiation

MAPK	mitogen-activated protein kinases
MgATP	magnesium adenosine triphosphate
MgCl₂	magnesium chloride
MΩ	megohms
μM	micromolar
mM	millimolar
ms	milliseconds
mV	millivolts
NaGTP	sodium guanine triphosphate
NaCl	sodium chloride
NaHCO₃	sodium bicarbonate
NaH₂PO₄	Sodium dihydrogen phosphate
nM	nanoMolar
NMDA	N-methyl-D-aspartate
NO	nitric oxide
nonREM	non-rapid eye movement
nS	nanoSeimens
ω_h	corner frequency for I _h
ω_{pass}	corner frequency for passive circuit
ω_x	corner frequency for active circuit
pA	picoAmps
pFRC	phase frequency response curve
PIP₂	phosphatidyl-4,5 biphosphate
PKC	protein kinase C
PKA	protein kinase A
PLA₂	phospholipase A ₂

PLC	phospholipase C
Pyril	pyrilamine
Q	quality of resoance
R	gas constant
REM	rapid eye movement
R.M.P.	resting membrane potential
S.E.M.	standard error of the mean
ss	steady state current
T	temperture in Kelvin
τ_h	I_h time constant
τ_m	membrane time constant
τ^2	fast activation time contant
τ_x	active component time constant
TEA	tetraethyammonium chloride
thio	thioperamide
tiot	tiotidine
TM	tuberomammillary nucleus
t-MH	<i>tele</i> -methylhistamine
TTX	tetrodotoxin
V	voltage
V_h	I_h reversial potential
$V_{1/2}$	half maximal activation potential
Z	valence number
Z	impedance
ZAP	impedance amplitude profile
ZD	ZD-7288

zFRC	impedance frequency response curve
$Z(f_{\text{res}})$	impedance at f_{res}
Z_{max}	maximum impedance
Z_{min}	minimum impedance

Acknowledgements

I wish to express my deepest thanks to Dr. Richard Neuman for his support and supervision throughout my program. I also extend my gratitude to Judy Neuman for her tireless work in the preparation of experiments and assistance in writing this thesis. I would also like to express my gratitude to the other members of my Ph.D. supervisory committee, Dr. Carolyn Harley, Dr. Karen Mearow and Dr. Ernie Puil, who monitored my work and provided me with valuable comments. Special thanks, as well, to Dr. Detlef Bieger for his enlightening conversations and scholastic diversions. I am deeply grateful to my fiancée, Gale Warren, for her love, patience and support.

1. Introduction

1.1 Scope of thesis

Although there exists an extensive literature on the electrophysiology of neocortical neurotransmitters the extent of their actions on neocortical oscillatory behaviour remains scant. A goal of this research was to investigate the effects of the neuromodulator, histamine, on subthreshold resonance in rat neocortical pyramidal neurons by means of a novel methodology known as the Impedance Amplitude Profile (ZAP) (Puil, Gimbarzevsky and Miura, 1986; Puil, Gimbarzevsky and Spigelman, 1988)

Many neocortical neurons display subthreshold membrane fluctuations when depolarized to just below spike threshold. These oscillations reflect a close relationship with the neurons' resonant behaviour. Resonance is viewed as a frequency and voltage dependent peak in a neuron's impedance. Within this range of impedance, the neuron exhibits the lowest threshold for excitation (Hutcheon and Yarom, 2000). Central to this phenomenon are the intrinsic active and passive membrane properties that determine the input impedance. All neurons have passive properties made up from the leak conductance and the membrane capacitance. Characterized as a low pass filter, the passive membrane properties function to attenuate higher frequency inputs thereby causing the impedance to decrease and roll off. As well, many neurons contain various active membrane properties, that function as high pass filters that attenuate low frequency inputs (Hutcheon and Yarom, 2000).

Subthreshold to firing, a hyperpolarization activated cationic current, I_h , together with the passive properties, may allow certain neocortical neurons to operate as bandpass

filters. This filter property prevents the neurons, and the networks that embed them, from encoding certain frequencies while promoting others.

The modulation of I_h would have profound implications for the excitability and resonant behaviour of neocortical neurons. It is well established that cyclic nucleotides, in particular adenosine 3',5'-cyclic monophosphate (cAMP), shift I_h activation to more positive potentials (Kaupp and Seifert, 2001; Viscomi, Altomare, Bucchi, Camatini, Baruscotti, Moroni, DiFrancesco, 2001). Although the mechanisms of resonance have been established, to date, there is little evidence showing the influence of neuromodulators on this process. Neocortical networks have long been associated with organized firing patterns and prominent oscillations during sleep and wakefulness. Given the role of histamine in modulating such behavioural states, it is a potential candidate for modulating neocortical resonance. In particular, in the neocortex, the innervation patterns of histamine containing axons (Kohler, Swanson, Haglund and Wu, 1985; Inagaki, Yamatodani, Ando-Yamamoto, Tohyama, Wantanabe, Wada, 1988; Panula, Pivola, Auvinem and Airaksinen, 1989; Manning Wilson, Uhrich, 1996), the pervasiveness of histamine receptors (Palacios, Wamsley and Kuhar, 1981; Bouthenet, Ruat, Sales, Garbarg and Schwartz, 1988; Martinez-Mir, Pollard, Moreau, Arrang, Ruat, Traiffort, Schawartz and Palacios, 1990; Ruat, Traiffort, Bouthenet, Schwartz, Hirschfeld, Buschauer and Schunack, 1990; Pollard, Moreau, Arrang, Schwartz, 1993; Traiffort, Leurs, Arrang, Tardivel-Lacombe, Diaz, Schwartz and Ruat, 1994; Vizuete, Traiffort, Bouthenet, Ruat, Souil, Trardivel-lacombe and Schwartz, 1997; Honrubia, Vilaro, Palacios and Mengod, 2000; Pillot, Heron, Cochois, Tardivel-Lacombe, Ligneau,

Schwartz and Arrang, 2002), and the known actions of histamine receptor activation on cAMP production (Nahorski, Rogers and Smith, 1974; Baudry, Martres, Schwartz, 1975; Hegstrand, Kanof and Greengard, 1976; Palacios, Garbarg, Barbin and Schwartz, 1978; Psychoyos, 1978; Olanas, Oliver and Neff, 1984; Al-Gadi and Hill, 1987), make it a potential modulator of neocortical resonance.

In the present project, based upon preliminary observations, the expected effect of histamine on I_h was occluded by a current rundown, characterized by a time dependent, hyperpolarizing shift in the activation of I_h . This led to investigations of possible factors responsible for the rundown effect. Elimination of the rundown effect allowed for a full investigation into the effect of histamine on subthreshold conductances, in particular I_h , and novel insights into histamine's effect on subthreshold resonance.

To set the context of the following investigations the remaining introductory sections provide a background on histamine anatomy, physiology and major functional correlates in the CNS followed by an overview of the hyperpolarization activated cationic current, I_h , and mechanisms of resonance.

1.2 Histamine in the CNS

1.2.1 Organization

Of the four aminergic systems, serotonin, dopamine, noradrenaline and histamine, research into the actions and role of histamine in the central nervous system (CNS) has received limited attention. It has been over 90 years since Sir Henry Dale first discovered the existence of histamine in animal and plant tissues and over 60 years since the

presence of histamine was described in brain and peripheral nerves in mammals (Schwartz, Arrang, Garbarg, Pollard and Ruat, 1991). Despite this, the acceptance of histamine as a neurotransmitter/neuromodulator has only occurred over the last three decades (Schwartz et al., 1991). Knowledge that has been gathered about the anatomy and effects of the histaminergic system in the CNS suggests that histamine plays a broad regulatory role in brain activity. For example, histamine has been linked to numerous functions and behaviours in the nervous system including: circadian rhythmicity, such as arousal and sleep-wake cycles (Nowak, 1994; Gottesmann, 1999; Passani, Bacciottini, Mannaioni and Blandina, 2000), homeostatic processes, such as fluid balance food intake temperature regulation (Sakata, Yoshimatsu and Kurokawa, 1997; Hass and Panula, 2003), cardiovascular control, cognition and neural plasticity (Bacciottini, Novoa and Cacabelos, 2001; Philipp and Prast, 2001; Gu, 2002) and a variety of brain disorders, such as anxiety and stress (Hill, 1990; Onodera, Yamatodani, Watanabe and Wada, 1994).

A characteristic of the histaminergic system that supports its role as broad modulator of brain activity is the mechanism of its metabolism and release. Histamine is formed from the amino acid L-histidine, which is transported in neurons by a nonspecific, energy-dependent L-amino-acid transport mechanism (Schwartz et al., 1991). Biosynthesis occurs in one step by the enzyme L-histidine decarboxylase. Similar to other aminergic transmitters, newly synthesized neuronal histamine is thought to be stored within vesicles through the actions of the vesicular monoamine-transporter VMAT-2 (Hoffman, Hansson, Mezey, Palkovits, 1998; Travis, Wang, Michael, Caron

and Wightman, 2000). Unlike other aminergic systems, however, histaminergic neurons do not exhibit a high-affinity uptake system for histamine, consistent with its suggested role as a long term modulator of brain activity (Brown, Stevens and Haas, 2001; Haas and Panula, 2003) This role, however, is not static since the rate at which histamine induces its effects is dependent on the rate at which histamine is formed and degraded, i.e., the turnover rate, which is positively correlated to the level of innervation and the activity level of histaminergic neurons (Hough, Khandelwal, Green, 1984; Oishi, Nishibori, Saeki, 1984). After release, histamine is metabolized by two routes: (1) oxidation by diamine oxidase (DOA) leading to imidazole acetic acid (IAA) and (2) methylation by histamine *N*-methyltransferase (HMT) resulting in the production *tele*-methylhistamine (t-MH) (Brown et al., 2001; Haas and Panula, 2003). In the vertebrate CNS histamine degradation occurs almost exclusively through methylation (Hough et al., 1984; Schwartz et al., 1991; Prell, Morrishow, Duoyon and Lee, 1997). In addition to histamine, histaminergic neurons also contain other neuroactive substances such as GABA (Kohler et al., 1985; Ericson, Kohler and Blomqvist, 1991; Alanen, Szabat, Visser and Panula, 1992), met-enkephalin (Airaksinen et al.,1992), galanin (Kohler, Ericson, Watanabe, Polak, Palay, Palay and Palay, 1986; Staines, Yamamoto, Daddona and Nagy, 1986) and substance P (Airaksinen et al.,1992).

Histamine is localized and released in the CNS from at least two cell types: (1) non-neuronal mast cells and (2) neurons with long widely projecting axons with varicosities filled with histamine containing synaptic vesicles (Brown et al., 2001; Haas and Panula, 2003). The latter is more commonly reported. In either case, the action of

histamine does not action occur through a typical arrangement where pre and post-synaptic sites directly apposed each other. Instead, both cell types release histamine into the local extracellular milieu resulting in a concert of effects on a variety of cell types and cell locations (Takgi, Morishima, Hayashi, Watanabe and Wada, 1986; Schwartz et al., 1991)

Another factor that supports the histaminergic system acting as a regulatory center lies in its anatomy. In vertebrates, the histaminergic system is well conserved phylogenetically where histamine synthesis in the CNS occurs exclusively in the tuberomammillary nucleus (TM) located in the posterior hypothalamus (Brown et al., 2001; Haas and Panula, 2003). Anatomical studies in a variety of species have shown that the projection field of histaminergic neurons innervates virtually every area of the brain and parts of the spinal cord through three main pathways, two ascending (ventral and dorsal) and one descending (Kohler et al., 1985; Inagaki et al., 1988; Panula et al., 1989; Inagaki, Toda, Taniuchi, Panula, Yamatodani, Tohyama, Watanabe and Wada, 1990; Manning et al., 1996). The descending pathway has the lowest density of fibers and provides innervation to the midbrain, brain stem, cerebellum and spinal cord (Kohler et al., 1985; Inagaki et al., 1988; Panula et al., 1989). The ventral ascending pathway has the highest density of fibers and provides innervation to the hypothalamus, diagonal band, septum and olfactory tubercle (Inagaki, Toda, Taniuchi, Panula, Yamatodani, Tohyama, Watanabe and Wada, 1990). The dorsal ascending pathway, having a somewhat lower density of fibers than the ventral pathway, innervates the amygdala,

thalamus, hippocampus, and more moderately, the neocortex (Kohler et al., 1985; Inagaki et al., 1988; Panula et al., 1989; Manning et al., 1996).

Less is known about the afferent inputs to the TM. The largest density of afferent fibers originates from the lateral septum, infralimbic cortex and the preoptic nucleus (Ericson, Blomqvist and Kohler, 1991). The known roles of each of these areas correlates well with the behavioural actions of histamine. For example, the lateral septum has been shown to be involved in some forms of learning and spatial behaviours as well as being linked to the inhibition of anxiety and the acquisition of behaviours reinforced by alleviation of anxiety (Thomas and Evans, 1983; Fraser, Poucet, Partlow and Herrmann, 1991; Yadin, Thomas, Grishkat, Strickland, 1993). Similarly, the infralimbic cortex has been linked to inhibition of inappropriate responding that may lead to increased anxiety as well as the control of visceral/autonomic activity such as the control of body temperature and feeding behaviour (Jinks and McGregor, 1997; Quirk, Russo, Barron and Lebron, 2000; Rhodes and Killcross, 2004; Recabarren, Valdes, Farias, Seron-Ferre and Torrealba, 2005). The preoptic nucleus is known for its role in the regulation of sleep and arousal (McGinty and Szymusiak, 2003). More moderate innervation of the TM arising from the brain stem has fibres originating from adrenergic (C1-C3), noradrenergic (A1-A3) and serotonergic (B5-B9) cell groups. The lowest density of fibres originates from the locus coeruleus, substantia nigra and the ventral tegmental area (Ericson, Blomqvist and Kohler, 1989).

To date, four histaminergic receptor subtypes, H₁, H₂, H₃ and H₄, have been identified with H₄ being detected predominantly in peripheral tissues (Palacios et al.,

1981; Bouthenet et al., 1988; Martinez-Mir et al., 1990; Ruat et al., 1990; Pollard et al., 1993; Traiffort et al., 1994; Vizuite et al., 1997; Honrubia et al., 2000; Nguyen, Shapiro, George, Setola, Lee, Cheng, Rauser, Lee, Lynch, Roth, O'Dowd, 2001, Pillot et al., 2002). The following sections provides a brief overview of the three subtypes predominantly found in the CNS.

1.2.2 *H₁ receptor*

The H₁ receptor has a widespread distribution in the CNS (Palacios et al., 1981; Bouthenet et al., 1988; Martinez-Mir et al., 1990; Traiffort et al., 1994). Use of autoradiography and *in situ* hybridization techniques has shown the highest density of H₁ receptors are found in the thalamus, neocortex, basal forebrain, mesopontine tegmentum, raphe nuclei of the reticular formation and the locus coeruleus, all of which play important roles in arousal behaviour. High to moderate densities of H₁ receptors are found in the limbic system, in particular the hypothalamus, septal nuclei, amygdala, hippocampus, nucleus accumbens, and in other areas such as nuclei of the cranial nerves, area postrema and nucleus tractus solitarius. Lower densities are found in the cerebellum, with the exception of the molecular layer, and in the basal ganglia.

Investigations into the pharmacology and biochemistry of each mammalian histamine receptor show they belong to a super-family of seven trans-membrane spanning, G-protein associated receptors. H₁ receptors are primarily coupled to G_{q/11} and phospholipase C (PLC) leading to the formation of two second messengers: inositol 1,4,5-triphosphate (IP₃) and diacylglycerol (DAG) (Daum, Downes and Young, 1984;

Donaldson and Hill, 1986; Carswell, Galione and Young, 1987; Claro, Garcia and Picatose, 1987; Bristrow, Banford, Bajusz, Vedat and Young, 1993; Soria-Jasso, Bahena-Trujillo and Aris-Montano, 1997). A common action of IP₃ is to bind to IP₃ receptors on the endoplasmic reticulum, resulting in the release of intracellular calcium whereas DAG is known for augmenting protein kinase C activity (PKC) (Kirischuk, Tuschick, Verkhatsky and Kettenmann, 1996, Weiger, Stevens, Wunder and Haas, 1997).

In addition, PLC activation has also been linked to the formation of guanosine 3',5'-cyclic monophosphate (cGMP) via a calcium-mediated production of nitric oxide and a subsequent stimulation of guanylyl cyclase (Richelson, 1978). H₁ receptors in neuronal culture and transfected cells have also been shown to couple to phospholipase A₂ (PLA₂) resulting in an enhancement of arachidonic acid formation (Snider, McKinney, Forray, Richelson, 1984; Leurs, Traiffort, Arrang, Tardivel Lacombe, Ruat and Schwartz, 1994). In either case, little is known about the histamine-induced actions of these messengers in the CNS. However, it has been proposed that both arachidonic acid and nitric oxide may act as retrograde signals resulting in presynaptic modulation (Brown et al., 2001). For example, studies of the hypothalamus showed that nitric oxide inhibited and augmented the release of histamine and glutamate, respectively (Prast, Lamberti, Fischer, Tran and Philippu, 1996). Studies involving corticostriatal preparations showed that inhibition of nitric oxide resulted in an increase in histaminergic field potential depression indicating that nitric oxide may act to occlude or inhibit the ability of histamine to depress synaptic transmission (Doreulee, Yanovsky, Flammeyer, Stevens, Haas and Brown, 2001). Histamine-induced production of arachidonic acid

could result in synaptic modulation leading to changes in adaptive neural plasticity, a known effect of PLA₂ activity in the CNS (Volterra, Trotti, Cassutti, Tromba, Galimberti, Lecchi and Racagni, 1992; Massicotte, 2000). For example, in rat hippocampus, an area of high H₁ receptor densities and long-term increase of hippocampal excitability induced by H₁ and H₂ receptor activation, arachidonic acid has been shown to exert a long-lasting facilitatory action on synaptic transmission and may be a significant factor for the expression of long term potentiation (LTP) (Selbach, Brown and Haas, 1997; Nishizaki, Nomura, Matsuoka and Tsujishita, 1999).

H₁ activation has also been linked to the augmentation of H₂ receptor-mediated increases in cAMP production (Baudry et al., 1975; Hegstrand et al., 1976; Palacios et al., 1978; Psychoyos, 1978, Daum, Hill, Young, 1982; Al-Gadi and Hill, 1987; Donaldson and Hill, 1986; Donaldson, Hill and Brown, 1988; Leurs et al., 1994), presumably through activation of PKC (Schwabe, Ohga and Daly, 1978; Hollingsworth, Sears and Daly, 1985; Garbarg and Schwartz, 1988; Donaldson, Brown and Hill, 1989, Leurs et al., 1994). Conversely, H₁ receptors have been indirectly linked to inhibition of cAMP production through an H₁-induced increase in somatostatin-mediated inhibition of adenylyl cyclase activity (Puebla, Ocana Fuentes and Arilla, 1997).

There is considerable evidence for H₁-mediated actions in CNS preparations (Figure 1.1). In the human neocortex, H₁ receptors have been shown to produce excitation through a calcium-independent reduction of a background potassium leak current (I_{KL}), presumably through direct G-protein coupling, resulting in membrane

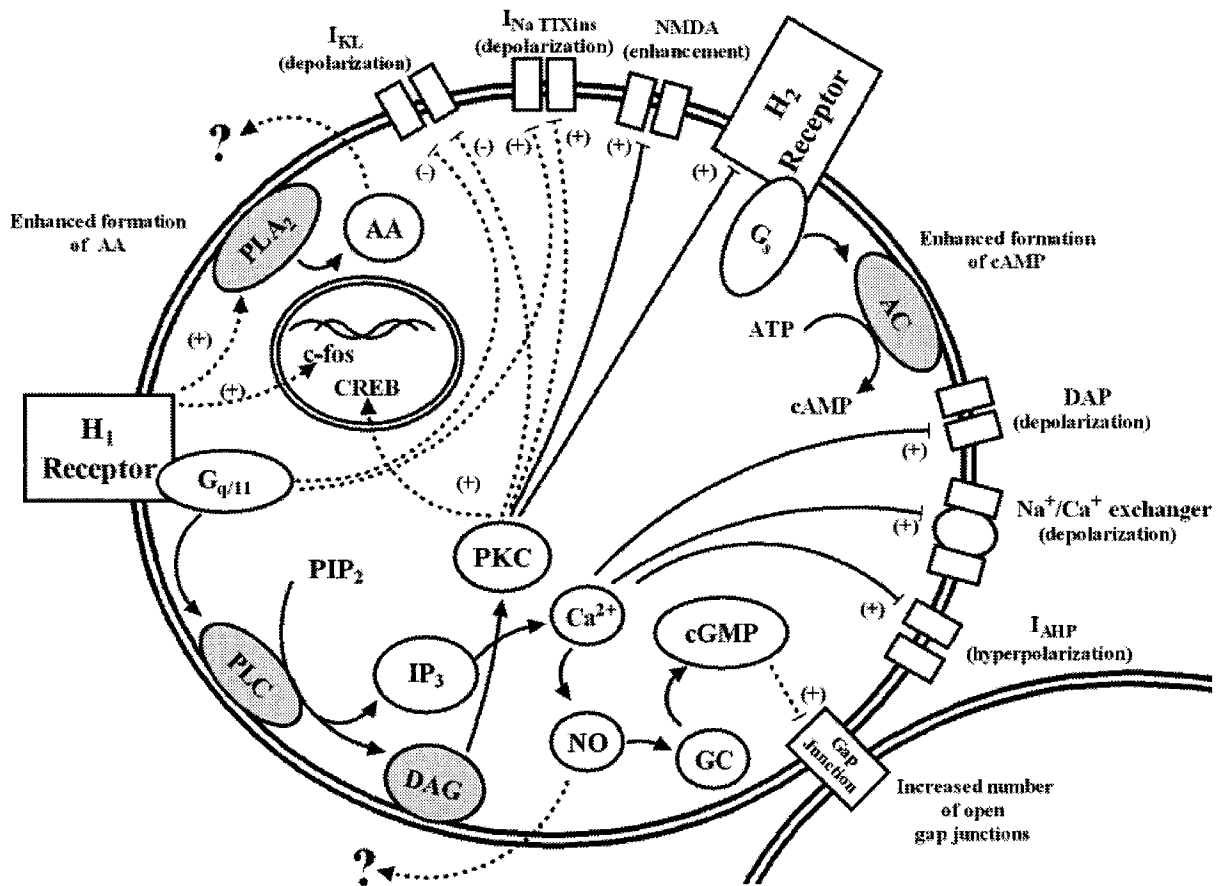


Figure 1.1 Summary of H₁ receptor signalling pathways and membrane responses in the CNS.

Dotted lines signify unclear signal transduction pathways. Plus and negative signs in parenthesis indicate pathway effects, i.e., enhancement or reduction, respectively. Question marks (?) represent undetermined action. H₁ receptors predominantly couple to phospholipase C (PLC) via G_{q/11} G-proteins resulting in the production of two second messengers, inositol-1,4,5-trisphosphate (IP₃) and diacylglycerol (DAG) from phosphatidyl-4,5 biphosphate (PIP₂). IP₃ leads to the release of calcium from intracellular stores. H₁ receptor-induced increases in intracellular calcium can result in production of nitric oxide, a possible retrograde messenger, and the subsequent activation of guanylyl cyclase (GC) leading to the production of cGMP which may increase gap junction conduction. H₁ receptor-induced increases in intracellular calcium have also been shown to increase the calcium activated potassium current (I_{AHP}) resulting in hyperpolarization of the membrane, as well as an increase in a sodium/calcium exchanger and a depolarizing after potential (DAP) via an unknown channel, both resulting in a depolarization of the membrane. DAG enhances PKC activity which leads to the

phosphorylation of various protein targets such as the glutamate NMDA receptor resulting in an enhancement of NMDA-mediated currents. It should also be noted that histamine may also act directly at the NMDA channel. As well, PKC has also been shown to enhance the formation of cAMP by other substances i.e., histamine via the H₂ receptor, coupled to the G_s G-protein. For other effects little is known about the signalling pathways. A commonly observed effect of H₁ receptor activation is the reduction of a potassium leak current (I_{KL}) leading to a depolarization of the membrane. Others include an enhancement of a TTX insensitive sodium current (I_{Na TTXins}) also resulting in a depolarization of the membrane. Other lesser known effects include H₁ receptor-induced c-fos expression, activation of CREB and coupling to phospholipase A₂ (PLA₂) resulting in the production of arachidonic acid (AA), another possible retrograde messenger.

depolarization and facilitation of signal transmission due to a decrease in membrane conductance (Reiner and Kamondi, 1994). Similar H₁ mechanisms have been observed in other tissue preparations. An H₁-mediated block of I_{KL} has been shown in rat hypothalamic supraoptic nucleus, and cat and guinea pig lateral geniculate nucleus (McCormick and Williamson, 1991; Li and Hatton, 1996). A similar effect was also observed in dissociated neostriatal neurons where both H₁ and H₂ receptors mediated a decrease in an unknown K⁺ conductance (most likely I_{KL}) (Munakata and Akaike, 1994).

A synergistic excitatory action was also reported in nucleus basalis cholinergic neurons. However, whether H₁ and H₂ receptors converged on the same physiological mechanism was not determined (Khateb, Fort, Pegna, Jones and Muhlethaler, 1995). Another known action in the neocortex is the facilitation of the N-methyl-D-aspartate (NMDA) receptor-mediated depolarization. (Payne and Neuman, 1997). In the same investigation, the lack of a block of the histamine effect in magnesium free medium also suggests that histamine acts directly via a unique site on the NMDA receptor. Similar histamine receptor independent actions on NMDA receptors were observed on neurons from hippocampal slices, cultures and acutely dissociated preparations (Bekkers, 1993, Vorobjev, Sharonova, Walsh and Hass, 1993; Brown, Fedorov, Haas and Reymann, 1995; Bekkers, Vidovic and Ymers, 1996), as well as in *Xenopus* oocytes expressing recombinant NMDA receptors (Williams, 1994).

In rat cholinergic septal neurons, H₁ receptors have also been shown to produce a calcium independent increase in a TTX-insensitive sodium conductance (Gorelova and Reiner, 1996). In vasopressinergic supraoptic neurons, H₁ receptor-mediated excitation

was shown to occur through the activation of a calcium-dependent Na^+ - Ca^{2+} exchanger and through the calcium dependent enhancement of a depolarizing after potential (DAP) following single firing or burst activity (Smith and Armstrong, 1993, Smith and Armstrong, 1996). Histamine has also been shown to reduce a voltage dependent potassium current, I_M , in bovine adrenal chromaffin cells, presumably through the activation of the H_1 (Wallace, Chen and Marley, 2001). Another action of H_1 receptor activation is an increase in the number of open gap junctions in cultured supraoptic neurons, an effect that was mimicked by application of cGMP analogues (Hatton and Yang, 1996).

Of equal interest, the H_1 receptor has also been linked to increases in the expression of the early-gene c-fos in suprachiasmatic neurons, although the signalling pathway was not investigated (Vizuete, Dimitriadou, Traiffort, Griffon, Heron and Schwartz, 1995). Histamine has also been shown to up-regulate cAMP response element binding (CREB) protein phosphorylation in developing oligodendrocytes, a process which was linked to PKC and mitogen-activated protein kinase (MAPK) activity (Sato-Bigbee, Pal and Chu, 1999). This may suggest that H_1 receptors also play a role in modulating transcriptional control under certain physiological conditions.

Although the data are somewhat limited, H_1 receptors have also been shown to mediate an inhibitory response. For example, in cultured C6 glial cells, H_1 -mediated increases in intracellular calcium via PLC have been shown to increase the conductance of a calcium-dependent potassium channel (I_{AHP}) (Weiger, et al., 1997). This mechanism has been proposed for the H_1 -induced inhibition of firing and hyperpolarization in

hippocampal neurons (Haas, 1981). A similar effect was observed in olfactory bulb interneurons where H_1 receptor activation augments an apamine-sensitive outward current (Jahn, Haas, and Hatt, 1995).

1.2.3 H_2 receptor

In contrast to H_1 receptors, H_2 receptors are present in low densities in the hypothalamus, thalamus and the septum and high densities in the basal ganglia and the cerebellum. On the other hand, similar to H_1 receptor localization, they are found in higher to moderate densities in parts of the limbic system such as the hippocampal formation and the amygdala. They are also present in moderate levels in neocortex, as well as in a number of aminergic cells groups such as the locus coeruleus, substantia nigra and raphe nuclei suggesting a synergistic role (Ruat et al., 1990; Martinez-Mir et al., 1990, Vizuite et al., 1997; Honrubia et al., 2000).

H_2 receptors predominately couple to G_s proteins and adenylyl cyclase resulting in an enhancement of cAMP formation (Nahorski et al., 1974; Baudry et al., 1975; Hegstrand et al., 1976; Palacios et al., 1978; Psychoyos, 1978; Olinas et al., 1984; Al-Gadi and Hill, 1987). As well, it has been suggested that H_2 receptors may also couple to the PLC pathway, independent of adenylyl cyclase. However this has yet to be described in the brain (Wang, Gantz and Del Valle, 1996; Hill, Granellin, Timmerman, Schwartz, Shankley, Young, Schunack, Levi and Haas, 1997; Wang, Hoeltzel, Gantz, Hunter, Del Valle, 1998).

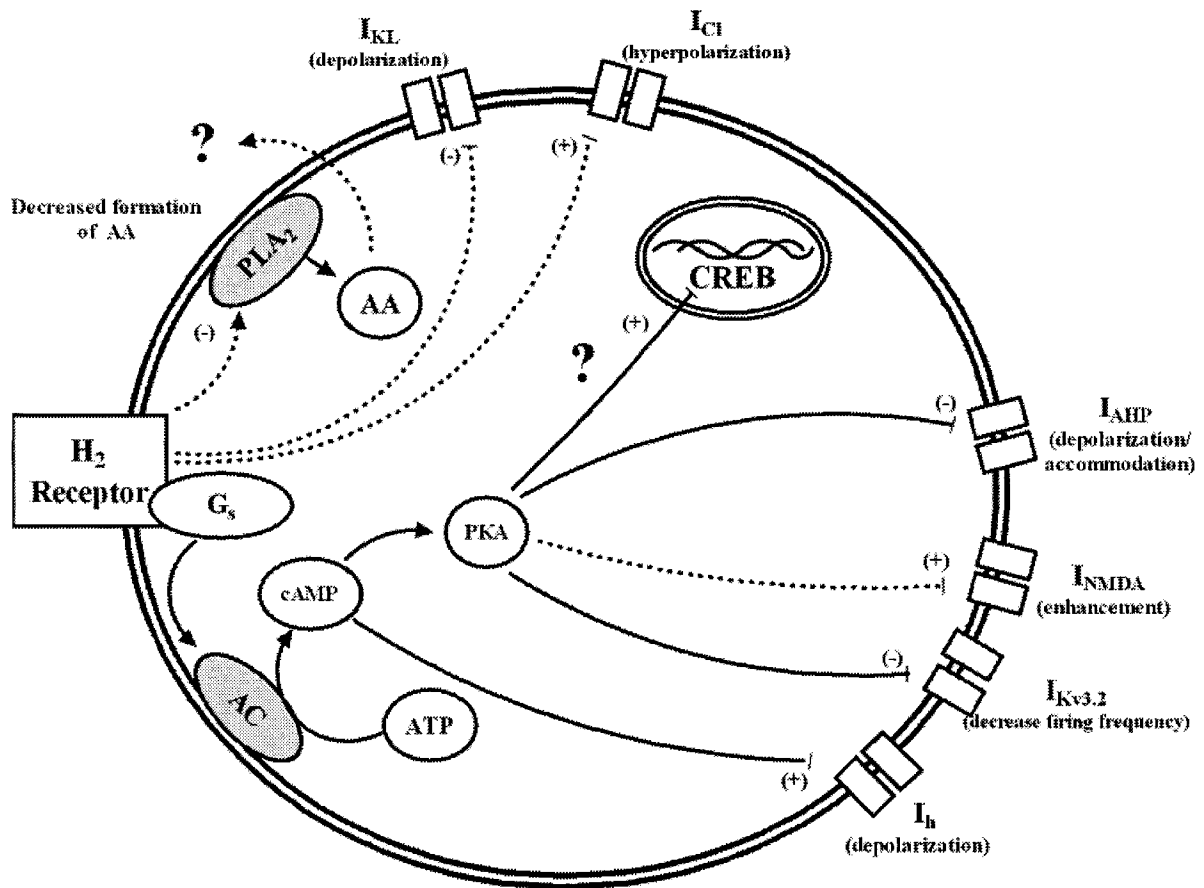


Figure 1.2 Summary of H₂ receptor signalling pathways and membrane responses in the CNS.

Dotted lines signify unclear signal transduction pathways. Plus and negative signs in parenthesis indicate pathway effects, i.e., enhancement or reduction, respectively. Question marks (?) represent undetermined action. H₂ receptors predominantly couple to adenylyl cyclase (AC) via G_s G-protein resulting in the conversion of adenosine triphosphate (ATP) into cyclic adenosine monophosphate (cAMP). Through a direct action, cAMP shifts the voltage dependence of the hyperpolarization activated cationic current (I_h) in a depolarizing direction subsequently resulting in a small depolarization of the membrane and a change in neuronal firing characteristics. Further down stream, cAMP activates protein kinase A (PKA) which acts to reduce the calcium activated potassium current (I_{AHP}) resulting in a depolarization of the membrane and an accommodation of firing. PKA may also activate CREB. Other effects where less is known about the transduction pathways include decreased formation of arachidonic acid (AA), inhibition of potassium leak conductance (I_{KL}) resulting in a depolarization of the membrane, an increase in a chloride conductance (I_{Cl}) resulting in a hyperpolarization of the membrane, and a possible PKA-mediated enhancement of NMDA-mediated currents (I_{NMDA}).

The actions of H₂ receptors produce a mixed degree of excitation and inhibition within the CNS (Figure 1.2). In the rat neocortex, H₂ receptors potentiate excitation by reducing I_{AHP}, resulting in a decrease in spike adaptation (McCormick and Williamson, 1991, McCormick, 1992, McCormick, Wang and Huguenard, 1993). The same action is reported from investigations involving rat hippocampus and dentate gyrus (Haas and Konnerth, 1983; Haas, 1984; Haas and Greene, 1986; Greene and Haas, 1990). Moreover, this mechanism of block occurs in the absence of changes in intracellular calcium levels and most likely involves a cAMP-PKA mediated phosphorylation of the channel (Hass, 1985; Haas and Greene, 1986; Greene and Haas, 1990; Pedarzani and Storm, 1993; Haug and Storm, 2000).

H₁ and H₂ receptor activation may result in opposing physiological responses in some tissue types such as the hippocampus. For example, the H₂ receptor-mediated reduction of I_{AHP} is opposite to that described for H₁ receptors. A similar opposing action may exist in relation to the production and release of arachidonic acid. In Chinese hamster ovary cell lines transfected with guinea pig H₂ receptors, H₂ receptor activation leads to a decrease in the release of arachidonic acid through a cAMP and Ca²⁺ independent pathway (Traiffort, Ruat, Arrang, Leurs, Promelli and Schwartz, 1992).

H₂ receptors have also been linked to a reduction in other potassium conductances. For example, as mentioned previously, H₂ receptor activation leads to a decrease in an unspecified K⁺ conductance in dissociated neostriatal neurons (most likely I_{KL}) resulting in transient increases in excitability (Munakata and Akaike, 1994). H₂ receptor activation also lowers the maximum firing frequency in fast spiking inhibitory

interneurons of the hippocampal formation. This reduction occurs through a PKA dependent block of the Kv3.2 containing potassium channel, a member of the Kv3 superfamily of delayed rectifier-type K^+ channels (Atzori, Lau, Tansey, Chow, Ozaita, Rudy, McBain, 2000).

In the hippocampus and thalamus, H_2 receptor-induced increases in cAMP shift I_h activation kinetics to more positive potentials. This shift results in excitatory action which can switch neuronal activity from burst mode to single spike firing, thus promoting accurate transmission at specific frequencies (McCormick and Williamson, 1991; Pape, 1996; Storm, Winther and Pedarzani, 1996). Conversely, due to the reportedly higher density of I_h channels in hippocampal dendrites, an increase in I_h conductance can negatively influence dendritic spatial integration of synaptic input, thus leading to further modulation of transmission (Magee, 1998).

H_2 receptor activation in the hippocampus can also result in long term increases in excitability via an adenylyl cyclase/PKA-signal transduction cascade. Moreover, this effect is significantly attenuated after application of DL-2-amino-5-phosphonopentanoic acid (APV) indicating an NMDA receptor-dependent component (Selbach et al., 1997).

H_2 receptors have also been shown to mediate inhibition. For example, in ferret GABAergic neurons of the perigeniculate nucleus, H_2 receptor activation resulted in a slow hyperpolarizing response as a result of an increase in membrane Cl^- conductance, an effect only previously seen in invertebrate models (Lee, Broberger, Kim and McCormick, 2004).

Finally, H₂ receptors may also be linked to modulation of transcriptional activity. In the hippocampus, H₂ and H₃ receptor activation has been shown to improve memory consolidation through the phosphorylation of the extracellular signal-related kinase2 (ERK₂) indicating a role in the modulation of neural plasticity (Impey, Obrietan and Storm, 1999; Giovannini, Efoudebe, Passani, Baldi, Bucherelli, Giachi, Corradetti and Blandina, 2003). The mechanism of phosphorylation was not determined, but may have involved the cAMP/PKA pathway. Similarly, given the strong evidence that H₂ receptors predominantly couple to the cAMP/PKA signalling cascade, their activation may result in the upregulation of the transcriptional factor CREB via cAMP-PKA phosphorylation (Sheng, McFadden, Greenberg, 1990; Brown et al., 2001; Hass and Pannula 2003).

1.2.4 H₃ receptor

Compared to the H₁ and H₂ receptors, H₃ receptors are more pervasive in the CNS (Pollard et al., 1993; Pillot et al., 2002). Characteristic of its role as an autoreceptor, H₃ receptors are found in high densities on TM neurons. Outside the TM, H₃ receptors are found in the highest densities in the neocortex, olfactory nucleus, nucleus accumbens, caudate putamen, striatum and the substantia nigra, as well as in many nuclei of the hypothalamus. More moderate densities are found in the hippocampal formation, thalamus and the lower brainstem.

H₃ receptors primarily couple with the G_i/G_o G-protein (Figure 1.3) (Brown and Hass, 1999; Clark and Hill, 1996; Laitinen and Jokinen, 1998; Drutel, Peitsaro, Karlstedt, Wieland, Smit, Timmerman, Panula and Leurs, 2001). Recent cloning investigations have

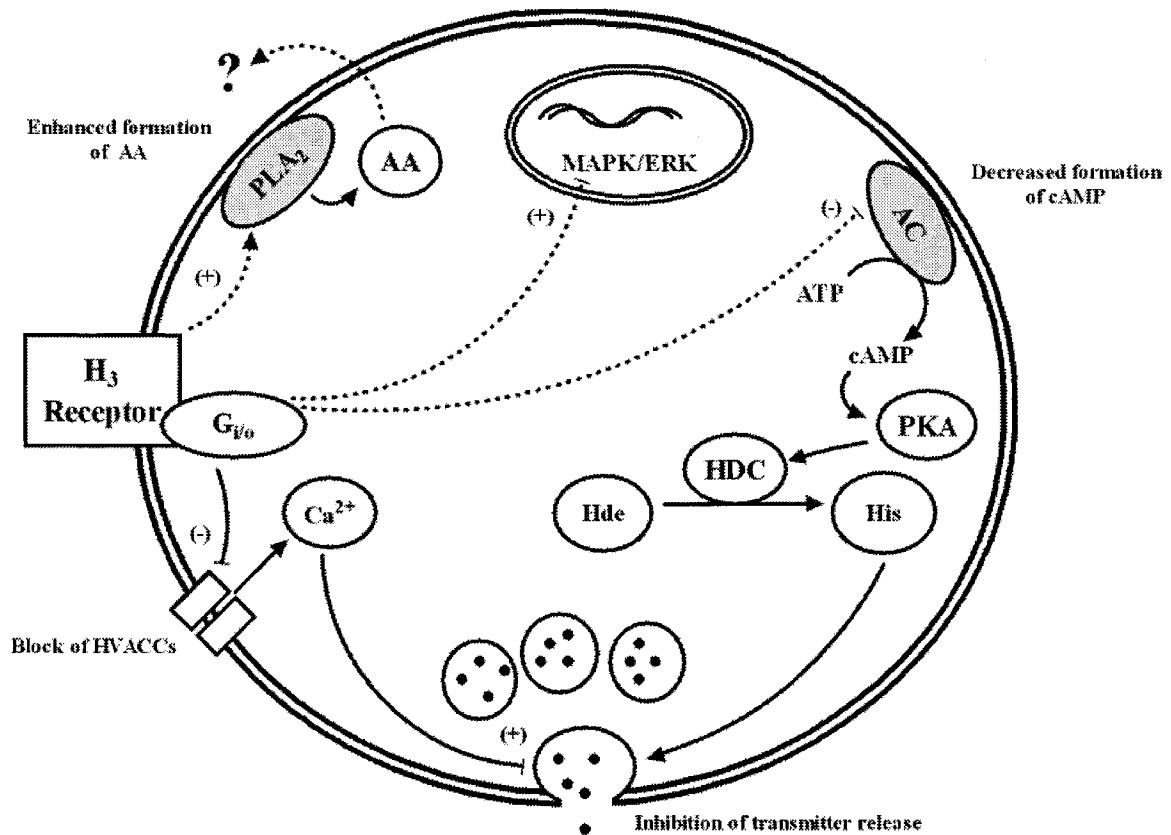


Figure 1.3 Summary of H₃ receptor signalling pathways and membrane responses in the CNS.

Dotted lines signify unclear signal transduction pathways. Plus and negative signs in parenthesis indicate pathway effects, i.e., enhancement or reduction, respectively. Question marks (?) represent undetermined action. H₃ receptors predominantly couple to G_{i/o} G-proteins. The most common action of this coupling is the inhibition of high voltage activated calcium channels (HVACCS), which in presynaptic terminals, results in reduced release of histamine and other neurotransmitters. Other effects, where less is known about the signalling pathways, include increased release of arachidonic acid (AA), inhibition of the adenylyl cyclase (AC)/protein kinase A (PKA) pathway resulting in decreased histamine synthesis and stimulation of the ERK/MAP kinase signalling pathway. (Hde (histidine), HDC (histidine decarboxylase), His (histamine)).

identified H₃-mediated inhibition of forskolin-induced formation of cAMP which suggests the involvement of adenylyl cyclase (Lovenberg, Roland, Wilson, Jiang, Pyati, Huvar, Jackson and Erlander, 1999). Drutel et al. (2001) showed the existence of at least three functional H₃ receptor subtypes, H_{3a}, H_{3b} and H_{3c}, which differentially couple to the G_i protein dependent inhibition of adenylyl cyclase in a number of COS-7 cell lines. Further support of these findings comes from an investigation into the mechanism of H₃ inhibition of histamine synthesis in neocortical neuronal cultures (Gomez-Ramirez, Ortiz and Blanco, 2002). The results of this study showed that histamine synthesis was dependent upon an adenylyl cyclase-protein kinase A pathway, possibly leading to phosphorylation of histidine decarboxylase (Husztli and Magyar, 1984; Joseph, Sullivan, Wang, Kozak, Fenstermacher, Behrendsen and Zahnow, 1990), and that this action was prevented in the presence of imetit, an H₃ receptor agonist.

H₃ receptors have also been linked to ERK/MAP kinase signalling pathway (Drutel et al., 2001; Giovannini et al., 2003). Drutel et al. (2001) showed that the three identified H₃ receptor subtypes differentially couple to the G_i protein dependent phosphorylation and subsequent stimulation of the p44/p42 MAPK. Similarly, as mentioned previously, Giovannini et al. (2003) showed that H₃ receptors' activation resulted in an improvement in memory consolidation that was linked to the phosphorylation of ERK₂. However, unlike the findings of Drutel et al. (2001), the mechanism did not appear to be mediated through a direct H₃ G_i/G_o G-protein mechanism.

Physiologically, H₃ receptors are generally classified as autoreceptors resulting in the inhibition of histamine synthesis (Arrang, Garbarg and Schwartz, 1987; Garbarg, Tuong, Gros and Schwartz, 1989; Oishi, Itoh, Nishibori and Saeki, 1989; Yates, Tedford, Gregory, Pawlowski, Handley, Boyd and Hough, 1999) and release (Arrang, Garbarg and Schwartz, 1983; Arrang, Garbarg, Quach, Dam, Yeramian and Schwartz, 1985; Arrang, Devaux, Chodkiewicz and Schwartz, 1988; Westerink, Cremers, De Vries, Liefers, Tran and De Boer, 2002; Lamberty, Margineanu, Dassel and Klitgaard, 2003), as well as the release of other transmitters including serotonin (Schlicker, Betz and Gothert, 1988; Fink, Schlicker, Neise and Gothert, 1990; Threlfell, Cragg, Kallo, Turi, Coen and Greenfield, 2004), noradrenaline (Schlicker, Fink, Hinterthaler, Gothert, 1989; Fink, Schlicker and Gothert, 1994; Schlicker, Kathmann, Detzner, Exner and Gothert, 1994), dopamine (Schlicker, Fink, Detzner and Gothert, 1993), acetylcholine (Arrang, Drutel, and Schwartz, 1995; Blandina, Giorgetti, Bartolini, Cecchi, Timmerman, Leurs, Pepeu and Giovannini, 1996; Blandina, Giorgetti, Cecchi, Leurs, Timmerman and Giovannini, 1996; Giorgetti, Bacciottini, Bianchi, Giovannini, Cecchi and Blandina, 1997; Prast, Fischer, Tran, Grass, Lamberti and Philippu, 1997; Passani and Blandina, 1998), glutamate (Brown and Reymann, 1996; Brown and Haas, 1999; Doreulee et al., 2001), GABA (Garcia, Floran, Arias Montano, Young and Aceves, 1997; Arias-Montano, Floran, Garcia, Aceves and Young, 2001) and various peptides (Hill et al., 1997).

The most common inhibitory mechanisms of transmitter release in the CNS include inhibition of calcium influx either by (1) blocking presynaptic calcium channels; (2) by enhancing potassium currents or (3) direct G-protein modulation of the cellular

apparatus of transmitter release (Thompson, Capogna and Scanziani, 1993; Wu and Saggau, 1997). Of these, the second is the most commonly reported action for most transmitter systems. Conversely, it is generally accepted that H₃-mediated inhibition of transmitter release occurs via blockade of presynaptic calcium channels; in particular, a direct G_i/G_o G-protein inhibition of high voltage activated calcium channels (HVACCS) (Takeshita, Watanabe, Sakata, Munakata, Ishibashi and Akaike, 1998; Brown and Hass, 1999). For example, in rat dentate gyrus, H₃ inhibition of glutamate release was linked to the reduction of multiple HVACCS including the N and P/Q types (Brown and Haas, 1999). Similarly, in histaminergic neurons of the TM, histamine release was found to be dependent on both P and N type HVACCS (Takeshita et al., 1998). In the neocortex, histamine release was found to depend on the L type HVACC (Washington, Shaw, Li, Fisher and Gwathmey, 2000).

Adding to the complexity of the histaminergic system are the recent findings that a proportion of the H₃ receptor population spontaneously undergoes an allosteric transition, leading to a conformation that can bind G proteins in the absence of an agonist, i.e., constitutive activity. This has been shown in both recombinant receptor (Wieland, Bongers, Yamamoto, Hashimoto, Yamatodani, Menge, Timmerman, Lovenberg and Leurs, 2001; Rouleau, Ligneau, Tardivel-Lacombe, Morisset, Gbahou, Schwartz and Arrang, 2002; Wulff, Hastrup and Rimvall, 2002; Takahashi, Tokita and Kotani, 2003) and in native receptor preparations (Morisset, Rouleau, Ligneau, Gbahou, Tardivel-Lacombe, Stark, Schunack, Ganellin, Schwartz and Arrang, 2000). Similar to the agonist-activated receptors, constitutively active H₃ receptors induce similar effects,

i.e., inhibition of adenylyl cyclase, inhibition of histamine release (Schwartz, Morisset, Rouleau, Ligneau, Gbahou, Tardivel-Lacombe, Stark, Schunack, Ganellin and Arrang, 2003; Takahashi et al., 2003), but have also been shown to elevate arachidonic acid release (Morisset et al., 2000; Rouleau et al., 2002). More over, their existence presents important therapeutic opportunities since antagonists once thought to be pure or neutral have been found to behave as inverse agonists resulting in a reduction of constitutive and basal receptor activity. These results have led to the suggestion that H₃ inverse agonists might be preferred to H₃ neutral antagonists in the treatment of histamine-mediated disorders (Schwartz et al., 2003).

Given the recent discovery that several H₃ isoforms vary in the length of their third intracellular loops, this molecular domain may be responsible for the observed differences in H₃-mediated signalling and presents the possibility that different isoforms have yet to be discovered (Tardivel-Lacombe, Rouleau, Heron, Morisset, Pillot, Cochois, Schwartz and Arrang, 2000; Drutel et al. 2001). On the whole, the evidence suggests that the H₃ receptor is more heterogeneous than first thought and, as a result, is adding a new level of complexity into the function of the histaminergic system in the CNS.

1.2.5 Histamine and arousal

Histamine's role in the CNS is closely related to its property of increasing excitability. In this regard, histamine is commonly associated with the role of mediating arousal. Studies involving several vertebrate species show that histaminergic neurons, when activated, increase wakefulness and arousal. For example, early studies involving

lesions at the level of the posterior hypothalamus induced hypersomnia (Swett and Hobson, 1968; McGinty, 1969). Later studies revealed that brain levels of histamine in rats are highest during the day whereas turnover is highest at night (Orr and Quay, 1975) which parallels the activity of histaminergic firing (Monti, 1993).

Pharmacological studies provide even more convincing evidence for histamine's role in maintaining sleep/wake behaviours. For example, inhibition of the posterior hypothalamus by muscimol, a GABA_A agonist, also leads to a state of somnolence or hypersomnia (Lin, Sakai, Vanni-Mercier and Jouvet, 1989). More direct inhibition, by blocking the histamine synthesising enzyme histidine decarboxylase, results in a depletion of neuronal histamine and a subsequent reduction in the time cats and rats spend awake (Lin, Sakai and Jouvet, 1988; Kiyono, Seo, Shibagaki, Watanab, Maeyama and Wada, 1985). This is also supported by early in-vivo studies in rabbits involving intracerebroventricular (i.c.v.) injections of histamine which favoured wakefulness (Monnier and Hatt, 1969). Similarly, up regulation of neuronal histamine by oral administration of the H₃ antagonist thioperamide also augmented wakefulness in cats while applications of H₃ agonists resulted in a promotion of deep slow wave sleep (Lin, Sakai, Vanni-Mercier, Arrang, Garbarg, Schwartz and Jouvet, 1990; Monti, Orellana, Boussard, Jantos and Olivera, 1991). As well, the waking effects observed in the presence of thioperamide were blocked in the presence of the H₁ antagonist mepryamine consistent with an H₁-mediated increase in wakefulness (Lin et al., 1990). Consistent with this finding, other studies involving the injection (e.g., i.c.v.) of H₁ agonists and antagonists reveal a dose dependent increase and decrease in wakefulness, respectively

(Kalivas, 1982; Monti, Pellejero and Jantos, 1986; Lin et al., 1988; Tasaka, Chung, Sawada and Mio, 1989; Monti, Jantos, Leschke, Elz and Schunack, 1994; Lin et al., 1994; Lin, Hou, Sakai and Jouvet, 1996; Tashiro, Mochizuki, Iwabuchi, Sakurada, Itoh, Watanabe and Yanai, 2002).

Evidence suggesting a role for H₂ receptors in arousal is limited. ICV injections of an H₂ receptor antagonist had little effect on histamine-induced electroencephalogram (EEG) arousal observed in the neocortex and thalamus (Tasaka et al., 1989). Likewise, rats administered with the brain penetrating H₂ antagonist zolantidine showed no significant changes in any of the sleep parameters examined (Monti, Orellana, Boussard, Janto and Olivera, 1990). As well, investigations into the effects of microadministration of the H₂ agonist impromidine into the mesopontine tegmentum showed little change in the cortical EEG and the sleep-wake cycle in freely moving cats (Lin et al, 1996).

Similar to noradrenergic and serotonergic systems, histaminergic neurons are continuously active during wake, reduce discharge during non-rapid eye movement (nonREM) sleep, and cease discharge during REM sleep (Vanni-Mercier, Sakai and Jouvet, 1984). The route by which histamine acts to maintain arousal is complex. At the level of the hypothalamus, the onset of sleep has been traced to neurons in the ventral preoptic area which, when activated, are thought to turn off the histaminergic TM neurons as well as other aminergic neurons via strong monosynaptic GABAergic and galinergic connections (Sherin, Shiromani, McCarley and Saper, 1996; Yang and Hatton, 1997; Sherin, Elmquist, Torrealba and Saper, 1998; Szymusiak, Alam, Steininger and McGinty, 1998). Indirect routes for histamine-induced arousal involve histaminergic

inputs to cholinergic neurons in both the basal forebrain and the mesopontine tegmentum of the brain stem, which subsequently provides direct input to the neocortex and via thalamocortical radiations (Khateb, Serafin and Muhlethaler, 1990; Khateb et al., 1995; Lin et al, 1996; Cecchi, Passani, Bacciottini, Mannaioni and Blandina, 2001). Histamine has also been shown to regulate neocortical arousal by stimulating serotonergic neurons in the dorsal raphe nucleus (Brown, Sergeeva, Eriksson and Haas, 2002). Of these, the cholinergic and serotonergic pathways appear to be essential for producing activation in the neocortex since concurrent blockade of cholinergic and serotonergic inputs to the neocortex abolishes neocortical electrocorticographic activity (Dringenberg and Vanderwolf, 1998). On the other hand, reductions of neocortical histamine through inhibition of histidine decarboxylase had no obvious effect on low voltage fast activity in the neocortex during waking (Servos, Barke, Hough, and Vanderwolf, 1994). Similarly, destruction of the posterior hypothalamus only revealed a severe reduction in normal sleep wake cycles for 3 to 4 days and in evoked cortical low voltage fast activity for 2 to 3 weeks (Denoyer, Sallanon, Buda, Kitahama and Jouvet, 1991).

In contrast, during a cataplexic event (a symptom associated with narcolepsy where muscle tone is lost during a waking state) histamine neurons are active at greater or similar levels to those observed during normal wake states while noradrenergic neurons and serotonergic neurons show complete inactivity or greatly reduced activity. As a result, the role of other aminergic neurons may be more tightly coupled to the maintenance of muscle tone in waking and its loss during REM sleep (John, Wu,

Boehmer and Siegel, 2004), however, an indirect route via cholinergic inputs was not ruled out.

In summary, histamine appears to contribute to arousal indirectly by stimulating other aminergic activating cortical inputs. On the other hand, the direct actions of histamine on the neocortex, i.e., H_1 receptor mediated block of a I_{KL} and facilitation of NMDA receptor mediated currents resulting in excitation, an H_2 mediated block of I_{AHP} resulting in accommodation of firing and H_3 mediated control of neurotransmitter release, most likely play supporting modulatory roles (Wada, Inagaki, Yamatodani and Watanabe, 1991; Dringenberg and Vanderwolf, 1998). For example, in urethane-anaesthetized rats, histamine was shown to primarily facilitate electrocorticogram activation by potentiating the excitatory influence of cholinergic brainstem fibres at the level of the basal forebrain, whereas in the neocortex the action of histamine produced a small suppression of slow delta oscillations (Dringenberg and Kuo, 2003).

1.2.6 Histamine and homeostasis

1.2.6.1 Fluid balance

Fluid balance is strongly associated with histamine stimulation of the supraoptic nucleus resulting in release of vasopressin, which induces antidiuresis (Bhargava, Kulshrestha, Santhakumari and Srivastava, 1973; Tuomisto, Eriksson and Fyhrquist, 1980; Armstrong and Sladek, 1985; Kjaer, Knigge, Rouleau, Garbarg and Warberg, 1994). Similar actions are observed with histamine stimulated renin release following dehydration, which can lead to the eventual production of aldosterone that acts primarily

on the kidney by inducing retention of sodium and water (Matzen, Knigge and Warberg, 1990; Kjaer, Knigge, Jorgensen and Warberg, 1998). This is also supported by studies which show that injection of H₁ and H₂ antagonists into the ventromedial hypothalamus decreased water intake (Magrani, de Castro e Silva, Varjao, Duarte, Ramos, Athanazio, Barbeta, Luz and Fregoneze, 2004).

1.2.6.2 Feeding

Histamine suppression of feeding most likely occurs by H₁ receptor-mediated actions on the ventromedial nucleus of the hypothalamus, an area important in satiety (Sakata, Fukagawa, Ookuma, Fujimoto, Yoshimatsu, Yamatodani and Wada, 1988; Sakata, Ookuma, Fukagawa, Fujimoto, Yoshimatsu, Shiraishi and Wada, 1988). Histamine may also act to suppress feeding behaviour by acting on the mesencephalic trigeminal nucleus, an area that controls mastication (Fujise, Yoshimatsu, Kurokawa, Oohara, Kang, Nakata and Sakata, 1998). Recent studies involving H₁ receptor knock-out mice suggest that histamine suppression of feeding is dependent on leptin, a multifunctional cytokine and hormone, which acts to enhance histamine release and metabolism (Morimoto, Yamamoto, Mobarakeh, Yanai, Watanabe and Yamatodani, 1999; Toftegaard, Knigge, Kjaer and Warberg, 2003). In contrast, histamine has also been shown to influence leptin concentration by inhibiting its expression, thus providing evidence for a bi-directional regulatory loop and a possible pathomechanism for obesity and anorexia (Mercer, Kelley, Haq and Humphries, 1996; Morimoto et al., 1999; Takahashi, Suwa, Ishikawa and Kotani, 2002; Itateyama, Chiba, Sakata and Yoshimatsu,

2003; Sakata, Yoshimatsu, Masaki and Tsuda, 2003; Hegyi, Fulop, Kovacs, Falus and Toth, 2004).

Studies involving energy deficiency in the brain have shown that neural glucoprivation activates histamine neurons in the hypothalamus and results in an augmentation of glycogenolysis in the brain (Oohara, Yoshimatsu, Kurokawa, Oishi, Saeki and Sakata, 1994; Sakata, Kurokawa, Oohara and Yoshimatsu, 1994). As well, histaminergic stimulation of the sympathetic nervous system has been shown to increase lipolysis in the adipose tissue (Takahashi and Shimazu, 1981; Bugajski and Janusz, 1981). Both actions are apparently mediated through the negative feedback loop between histamine neurons and the leptin signaling system (Sakata et al., 2003).

1.2.7 Histamine and locomotion

Histamine has also been shown to induce ambulatory activity. For example, locomotive activity was decreased after inhibition of histamine synthesis and H₃ receptor activation resulting in decreased histamine release (Watanabe and Yanai, 2001, Kubota, Ito, Sakurai, Sakurai, Watanabe and Ohtsu, 2002). Conversely, inhibition of histamine metabolism and application of H₃ receptor antagonists increased locomotive activity (Sakai, Onodera, Maeyama, Yanai and Watanabe, 1992; Sakai, Yamazaki, Onodera, Yanai, Maeyama and Watanabe, 1993). Later studies lend further support, showing that H₁ receptor knock-out mice exhibited impaired locomotor activity and exploratory behaviour, i.e. decreased ambulatory activity in rats (Inoue, Yanai, Kitamura, Taniuchi, Kobayashi, Niimura and Watanabe, 1996; Yanai, Son, Endou, Sakurai and Watanabe,

1998, Yanai, Son, Endou, Sakurai, Nakagawasai, Tadano, Kisara, Inoue and Watanabe, 1998).

1.2.8 Histamine and cognition

Although the enhanced release of other transmitters, such as acetylcholine, play an important role in cognition and learning, histamine may also play an important role (Blandina et al. 1996; Chen, Chen and Kamei, 2001; Bacciottini et al., 2001). Its action, however, is complex and the findings have been contradictory. For example, administration of histidine (Miyazaki, Imaizumi and Onodera, 1995) and H₃ antagonists (Komater, Buckley, Browman, Pan, Hancock, Decker and Fox, 2004) attenuates a scopolamine-induced deficit in task-dependent spatial learning. This effect is likely mediated through H₁ receptor activation (Miyazaki et al., 1996). On the other hand, lesions of the TM region have been shown to facilitate learning, indicating that neuronal histamine may exert a negative influence on learning and memory (Klapdor, Hasenohrl and Huston, 1994; Frisch, Hasenohrl, Krauth and Huston, 1998). Similarly, administration of the H₁ antagonist chlorpheniramine facilitated learning when the compound was administered immediately after training (Frisch, Hasenohrl and Huston, 1997; Hasenohrl, Kuhlen, Frisch, Galosi, Brandao and Huston, 2001). Also, in contrast to other findings, H₃ receptor activation in the basolateral amygdala, an area involved in learning in which certain environmental cues predict threatening events, enhances fear memory (Cangioli, Baldi, Mannaioni, Bucherelli, Blandin and Passani, 2002). Similarly,

increases in cerebral histamine levels through administration of histidine impairs the acquisition of avoidance responses (Rubio, Begega, Santin, Miranda and Arias, 2001).

The role of histamine in cognitive functions may involve synaptic plasticity. Learning is a process by which new information is acquired and memory is the process by which that knowledge is retained. One mechanism by which this is achieved is through long term potentiation (LTP) which enhances or magnifies patterns of synaptic responses elicited by environmental stimuli (Shors and Matzel, 1997). Although there is limited evidence (Brown et al., 1995; Selbach et al., 1997) to suggest a role for histamine in the formation of LTP, its physiology strongly suggests that the potential exists. For example, H₁ receptors are linked to increases in intracellular calcium and activation of PKC and facilitation of NMDA receptor-mediated currents, all of which are important in the initial stages of LTP (Bliss and Collingridge, 1993, Collingridge and Bliss, 1995, Bliss, Collingridge and Morris, 2003). Similarly, H₂ receptor activation of the cAMP/PKA cascade is a potential candidate for generating the transcriptional changes required for the development of LTP in the hippocampus (Frey, Huang and Kandel, 1993, Haas, Sergueeva, Vorobjev and Sharonova, 1995). The heterogeneity of H₃ receptors and their links to regulating transmitter release, i.e., glutamate in the dentate gyrus (Brown and Reymann, 1996), most likely play a broad modulatory role in synaptic plasticity.

1.3 Hyperpolarization-activated cationic current (I_h)

Neurons in the brain and peripheral tissues often exhibit an increased cationic conductance when hyperpolarized to potential negative to the resting membrane potential (Pape, 1996; Robinson and Siegelbaum, 2003). The resulting current, I_h , has a reversal potential at approximately -45 mV and results from the flux of both Na^+ and K^+ ions. The kinetics of activation and deactivation, following hyperpolarization and depolarization, respectively, are a function of voltage and time that can be described by the Hodgkin and Huxley formalism. Once the threshold for activation is reached, steady state activation is preceded by a significant delay during which the inward current develops slowly. Increasing hyperpolarization, up to an approximate maximum of -120 mV, results in an increasing rate of activation and a larger current amplitude. Varying widely among cell types and preparations, the time course of activation ranges from tens to hundreds of milliseconds as described in rod and cone photoreceptors, hippocampal CA1 neurons and entorhinal cortex neurons (Hestrin, 1987; Maricq and Korenbrot, 1990; Magee, 1998, Dickson, Magistretti, Shalinsky, Fransen, Hasselmo and Alonso, 2000), or within the range of seconds, as described in slowly adapting lobster stretch receptors (Edman, Gestrelus and Grampp, 1987). Characteristically, however, the time course ranges from 1 to 2 s at potentials near I_h activation and from 200 to 400 ms at maximal activation potentials (Uchimura, Cherubini and North, 1990; Maruoka, Nakashima, Takano, Ono and Noma, 1994; Harris and Constanti, 1995).

The kinetics of I_h contributes to a number of physiological phenomena including changes in integrative behaviour, action potential generation following membrane

hyperpolarization, resonance and rhythmogenesis, normalization of temporal summation, and regulation of synaptic transmission (McCormick and Pape, 1990a; Foehring and Waters, 1991; McCormick and Huguenard, 1992; Maccaferri, Mangoni, Lazzari and DiFrancesco, 1993; Lamas, 1998; Magee, 1998; Stuart and Spruston, 1998; Doan and Kunze, 1999; Southan, Morris, Stephens and Robertson, 2000; Cuttle, Rusznak, Wong, Owens and Forsythe, 2001; Seutin, Massotte, Renette and Dresse, 2001; Mellor, Nicoll and Schmitz, 2002; Desjardins, Li, Reinker, Muira and Neuman, 2003; Funahashi, Mitoh, Kohjitani and Matsuo, 2003). The recent cloning of a family of four mammalian genes that encode the I_h channel is providing greater insight into the diversity of these channels (Ludwig, Zong, Jeglitsch, Hofmann and Biel, 1998; Santoro, Liu, Yao, Bartsch, Kandel, Siegelbaum and Tibbs, 1998).

Known specifically as the hyperpolarization-activated cyclic nucleotide-gated cationic channels (HCN1-4), the family is 80–90% identical in the core trans-membrane region, but reveals less conservation in the extreme amino and carboxy termini (Kaupp and Seifert, 2001). Each isoform differs in the pattern of expression and activation. In the mammalian brain, HCN3 and HCN4 exhibit weak expression, whereas HCN2 shows strong widespread mRNA expression. HCN1 demonstrates strong, but selective expression (Moosmang, Biel, Hofmann and Ludwig, 1999; Monteggia, Eisch, Tang, Kaczmarek, and Nestler, 2000; Notomi and Shigemoto, 2004). The functional heterogeneity of I_h closely follows the patterns of isoform expression. HCN1, characterized by its more rapidly activating kinetics, is strongly expressed in brain regions that exhibit a rapidly activating I_h , such as layer V neurons of the neocortex and

CA1 neurons of the hippocampus (Santoro, Chen, Luthi, Pavlidis, Shumyatsky, Tibbs and Siegelbaum, 2000). In contrast, HCN4 and HCN2, characterized by their relatively slower activation, are expressed in brain regions that exhibit slowly activating I_h , such as in thalamocortical relay neurons.

A striking feature of the HCN isoforms is the presence of a cyclic nucleotide binding domain (CNBD) in the cytoplasmic carboxy terminus, which alters the voltage dependence when the cyclic nucleotides, cAMP and cGMP bind (Kaupp and Seifert, 2001; Viscomi et al., 2001). It is thought that the presence of the CNBD tonically inhibits I_h channel activation by shifting the gating to more negative potentials. When a cyclic nucleotide binds to the CNBD site, gating of the channel is shifted in the depolarized direction. This action is well described by an allosteric voltage-dependent gating model (DiFrancesco, 1999; Altomere, Bucchi, Camatini, Baruscotti, Viscomi, Moroni, and DiFrancesco, 2001). According to the model, channel opening and shift in kinetics is the combination of two co-existing processes: 1) displacement of voltage sensors on each of the channel subunits and 2) allosteric closed to open transitions involving the binding of cyclic nucleotides whereby I_h has a six fold higher affinity for cAMP in the open state compared to the closed state. The presence of a two step process involving the movement of voltage sensors and a closed to open transition can account for the distinct kinetic features of I_h , such as the delay in current activation and deactivation, and explains the kinetics observed for the 4 HCN isoforms.

Although this provides a strong case for the direct modulation of I_h by cAMP, there is an equally compelling case for an indirect action of cAMP in modulating I_h via a

protein kinase phosphorylation dependent mechanism (Tokimasa and Akasu, 1990; Chang, Cohen, DiFrancesco, Rosen and Tromba, 1991; Yu, Chang, and Cohen, 1993, 1995; Accili, Redaelli and DiFrancesco, 1997; Vargas and Lucero, 2002).

Whether modulation of I_h occurs via a direct or indirect mechanism, it is well established that cyclic nucleotides, in particular cAMP, shift I_h activation to more positive potentials (Pape and Mager, 1992; Pape, 1996; Chen, 1997; Chen, Wang, Siegelbaum, 2001). This depolarizing shift is observed whether the increase results from the application of membrane permeable analogues of cAMP, e.g., 8-bromo-cAMP, or from the stimulated production of cAMP by forskolin (Bobker and Williams, 1989; Tokimasa and Akasu, 1990; Akasu and Shoji, 1994; Larkman and Kelly, 1997; Raes, Wang, Berg, Goethals, Vijver and Bogaert, 1997; Funahashi et al., 2003). Moreover, stimulation of G-proteins positively and negatively coupled to adenylyl cyclase results in a depolarizing or hyperpolarizing shift, respectively, of the activation curve for I_h (Bobker and Williams, 1989; McCormick and Williamson, 1991; Li, Wang, Strahlendorf and Strahlendorf, 1993; Ingram and Williams, 1994; Storm et al., 1996; Svoboda and Lupica, 1998; Gasparini and DiFrancesco, 1999; Vargas and Lucero, 1999; Haas and Selbach; 2000; Bickmeyer, Heine, Manzke and Richter, 2002; Liu, Bunney, Appel, Brodie, 2003).

1.4 Mechanism of resonance

Neuronal oscillations in the brain are pervasive and are strongly correlated with essential functions of the nervous system, such as timing motor performance, sleep, awareness, attention, perception, and learning, all of which aid in synchronizing an

organism's behaviour with its environment (Buzsaki, 1989; Gray, Konig, Engel and Singer, 1989; Steriade, Gloor, Llinas, Lopes da Silva and Mesulam, 1990; Silva, Amitai and Connors, 1991; Murthy and Fetz, 1992; Pinault and Deschenes, 1992; Turbes, 1992; Lampl and Yarom, 1993; Wang, 1993; Steriade, 1996; Steriade, Amzica and Contreras, 1996; Connors and Amitai, 1997; Lampl and Yarom, 1997, Izhikevich, 2002). It has long been speculated that synchronization and rhythmic behaviour of brain activity is a Gestalt phenomenon originating from synaptic interactions in large neuronal pools and/or oscillatory subunits, however, the organization and detailed mechanism for this has yet to be shown.

Although studies into this area have been limited, there has been extensive research into the biophysical characteristics of single neurons and the mechanisms underlying resonance that determine the frequency at which neurons will oscillate and generate action potentials. Resonance is an intrinsic property of neurons, permitting them, and consequently the networks in which they are embedded, to operate as band pass filters preventing the network from encoding certain inputs while promoting those that occur at the neurons' resonant frequencies (Hutcheon and Yarom, 2000). Resonance has been shown in a number of preparations including: trigeminal root ganglion (Gimbarzevsky, Miura and Puil, 1984; Puil et al., 1988); hippocampus (Gimbarzevsky et al., 1984; Leung and Yu, 1998; Pike, Goddard, Suckiling, Gnater, Kasthuri and Paulsen, 2000; Hu, Vervaeke and Storm, 2002); inferior olive nucleus (Lampl and Yarom, 1997); entorhinal cortex neurons (Fransen, Alonso, Dickson, Magistretti and Hasselmo, 2004; Schreiber, Erchova, Heinemann and Hertz, 2004); trigeminal mesencephalic neurons

(Wu, Hsiao and Chandler, 2001); cerebellum (D'Angelo, Nieuwenhuis, Maffei, Armano, Rossi, Taglietti, Fontana and Naldi, 2001); thalamus (Hutcheon, Miura, Yarom and Puil, 1994; Puil, Meiri and Yarom, 1994; Strohmann, Schwartz and Puil, 1994) and neocortex (Gutfreund, Yarom and Segev, 1995; Hutcheon, Miura and Puil, 1996ab; Neuman, Giles, Kong and Puil, 1996; Ulrich, 2002).

Resonance is best investigated through the use of frequency-domain analysis involving Fourier techniques. The resultant output of this analysis is a measure of membrane impedance, a frequency-domain extension of membrane resistance. In neurons with biophysical properties that allow oscillations, a voltage dependent peak in the frequency-impedance plot is observed, also known as the resonant frequency (f_{res}). This resonant peak discriminates between inputs based on frequency content since inputs near f_{res} produce the largest voltage responses and therefore have a higher probability of producing action potentials.

Since the resurgence of frequency domain techniques over the last 20 years, a number of intrinsic biophysical mechanisms necessary for the creation of resonance and oscillations in neurons have been identified (Hutcheon and Yarom, 2000). In short, neuronal resonance results from the interplay between a neuron's passive and active properties. The passive properties are represented in a capacitance membrane (CM) model, also known as the passive model, which is equivalent to a parallel circuit made up of a simple resistor, i.e., leak conductance; and a capacitor, i.e., membrane capacitance (Hutcheon, 1996). This basic circuit, a feature of all neurons, acts like a low pass filter where current inputs at low frequencies, which match the resonant band of frequencies in

a neuron, produce the largest impedance values, and hence larger voltage responses. Higher frequency inputs result in attenuated values due to the roll off of the impedance by the membrane capacitance. The point above which the passive membrane properties begins to attenuate higher inputs is determined by

$$\omega_{pass} = 1/2\pi\tau_m \quad (1)$$

where ω_{pass} is the corner frequency for the passive properties and τ_m is the membrane time constant.

The active properties represent the introduction of a change in the flow of current through the membrane. Also known as the capacitive membrane model with a simple current (CM + S) (Hutcheon, 1996), in terms of the frequency impedance relationship, in order for resonance to be produced the active component behaves in an opposite manner to a capacitor ,i.e., the impedance increases as frequency increases. As a result, the active component behaves as a high pass filter. The point below which the active component attenuates lower frequency inputs is determined by

$$\omega_x = 1/2\pi\tau_x \quad (2)$$

where ω_x is the corner frequency for the active component and τ_x is the time constant of the active component.

Although the CM model is a basic component of all neurons the active components, which produce low frequency attenuation, belong to a class of resonant producing voltage gated currents that are characterized by two specific criteria (Hutcheon, 1996; Hutcheon and Yarom, 2000):

(1) The currents are rectifying in nature in that they actively oppose changes in the membrane voltage. All rectifying currents are characterized by a reversal potential lying in a voltage range where the current is nearly completely deactivated .

(2) The current's time constant is slower than the membrane time constant. As a result, when a neuron is injected with square waves, these currents produce a time dependent voltage signature characterized by sags and rebounds, upon activation and deactivation, respectively, with respect to the near instantaneous passive charging of the membrane, i.e., capacitance. These currents behave similarly when exposed to oscillating inputs made up of multiple frequencies. Due to the slow activation and/or deactivation kinetics, the currents effectively resist changes in the membrane voltage in the low frequency range of the oscillating input. As a result, these currents attenuate the membrane impedance at low frequencies giving the membrane the attribute of a high pass filter.

The combination of these active and passive properties bring together two frequency specific mechanisms: one that attenuates voltage responses to high frequency inputs and another that attenuates responses at inputs arriving at low frequencies (Hutcheon, 1996; Hutcheon and Yarom, 2000). As long as the time constant of the resonant current is slower than the membrane time constant the combination can result in a notch, or band pass filter configuration, which produces a resonant band of frequencies with the largest impedance values occurring at f_{res} (Figure 1.4).

Other active elements, have an opposite arrangement characterized by their fast activation and a reversal potential lying in the voltage range where the current is nearly

completely activated (Hutcheon, 1996). Although they do not have the basic requirement for producing resonance, they can interact with resonant producing currents to amplify or enhance resonance, as well as to sustain membrane oscillations as shown in the thalamus (Hutcheon et al., 1994) and the neocortex, (Hutcheon et al., 1996a). Commonly reported examples include the persistent sodium current, I_{NaP} (Puil et al., 1994; Strohmann et al., 1994; Gutfreund et al., 1995; Hutcheon et al., 1996ab; Hutcheon and Yarom, 2000; D'Angelo et al., 2001; Wu et al., 2001; Hu et al., 2002) and the transient low threshold Ca^{2+} current, I_T (Gutnick and Yarom, 1989; Hutcheon et al., 1994; Strohmann et al., 1994; Lampl and Yarom, 1997, Hutcheon and Yarom, 2000). I_T is a special example since it can produce both resonance and resonance amplification, due to its relatively slow inactivation and fast activation gating properties, respectively (Hutcheon and Yarom, 2000).

Under biological conditions, the CM + S model is more complex. With the exclusion of the membrane capacitance, the passive and active components are made up of multiple ionic currents existing in parallel. The active components can differ dramatically in their voltage dependence resulting in resonant behaviour and amplification occurring over different membrane voltages. For example, resonance in the suprathreshold range (above -65 mV), has been shown to be produced by a K^+ current with the characteristics of the M-current, I_M , in trigeminal root ganglion neurons, trigeminal mesencephalic neurons, hippocampus pyramidal neurons, cerebellar granule cells and pyramidal neurons of the neocortex (Puil et al., 1988; Gutfreund et al., 1995; D'Angelo et al., 2001; Wu et al., 2001; Hu et al., 2002).

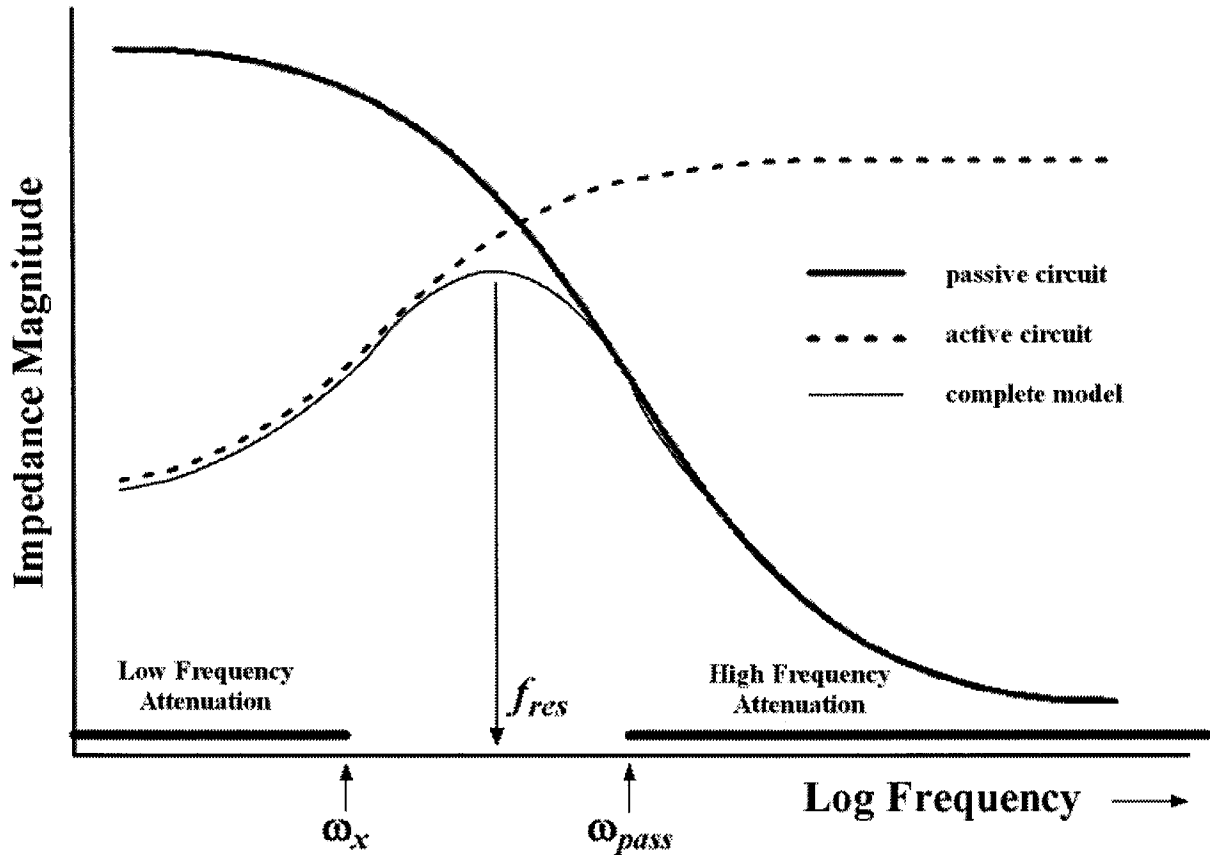


Figure 1.4 Impedance frequency response curve (zFRC) showing the contribution of active and passive membrane properties to the formation of resonance.

At low input frequencies the active circuit (dashed line) dominates the impedance and opposes voltage changes at frequencies below ω_x . At frequencies above ω_x the effect of the active circuit is reduced due to its slow response kinetics giving it the characteristic of a high pass filter. Conversely, the passive circuit (bold solid line), represented by the capacitance and leak component, dominates the impedances beyond frequencies above ω_{pass} . The complete model (thin solid line), formed by the combination of the active and passive circuits, results in a region of unattenuated impedance at intermediate frequencies, i.e., between ω_x and ω_{pass} with the largest impedance values occurring at the resonant frequency (f_{res}). This region gives the model the characteristic of a notch or band pass filter configuration. As a result, input frequencies within this range will produce larger voltage responses and are more likely to influence the firing properties of the neuron.

In the subthreshold voltage range (i.e., below -65 mV) resonance is produced by both I_T and I_h . I_T , with its dual classification, can produce resonance as well as play a regenerative role in the production of oscillations in the thalamus and the inferior olive (Steriade, McCormick and Sejnowski, 1993; Strohmann et al., 1994; Puil et al. 1994; Hutcheon et al., 1994; Lampl and Yarom, 1997). I_h is the most commonly reported subthreshold resonant current which produces resonance in the entorhinal cortex, hippocampus, thalamus and neocortex (Puil et al., 1994; Strohmann et al., 1994; Hutcheon et al., 1996ab; Hu et al., 2002; Ulrich, 2002; Fransen et al., 2004).

Although there has been a great deal of research into the neurological function of neurotransmitters, the full extent of their presynaptic and postsynaptic actions within the cortex are unknown (McCormick, 1992). The study of neurotransmitter effects on frequency response in the neocortex can lead to a greater elucidation of transmitter actions, while providing greater insight into the mechanisms of neocortical resonant behaviour.

Based upon known actions of histamine in the cortex, i.e., H_1 mediated decrease in I_{KL} and H_2 mediated increases in cAMP, modulation of resonance is likely. It is expected that both the frequency of resonance (f_{res}) and the quality of resonance (Q) will be altered. Q is the sharpness of the resonant hump determined by dividing the magnitude of the impedance at f_{res} by the magnitude of the impedance at the lowest frequency sample (see section 4.2 for more detail).

Based on results from Hutcheon et al. (1996a,b) subthreshold resonance in cortical neurons is due to the kinetics of I_h . A possible H_2 modulation of I_h would have

profound implications for the excitability and resonant behaviour of cortical neurons. To increase the activation of I_h the membrane potential has to be moved into a range where it is more active or the kinetics of I_h has to be shifted to a potential where it was previously less active, i.e., via H_2 receptor mediated increases in cAMP. The activation kinetics of I_h are such that as the membrane potential is hyperpolarized its conductance increases while its time constant shortens. A similar effect should be observed if the membrane potential is held constant and histamine shifts the activation of I_h in the depolarizing direction. In addition to a depolarization of the membrane near rest this would also decrease membrane impedance while shifting ω_h to higher frequencies, due to an increase rate of activation, resulting in an increase in the f_{res} and the Q value in a voltage and frequency dependent manner.

Similarly, H_1 receptor modulation of the potassium leak conductance in the neocortex (i.e., reduction) would act to modulate the passive electrical properties of a neuronal membrane. In a simple CM model, the predicted H_1 effect should produce a voltage independent, nonresonant frequency response resulting in a membrane depolarization, an increase in membrane impedance and a shift of ω_{pass} to lower frequencies due to an increase in the membrane time constant. In resonant neurons, where there is interaction of the passive processes and resonant active processes, i.e., I_h , the resultant effect of decreasing a leak conductance is an amplification of resonance and a narrowing of the the band pass frequencies, i.e. a decrease in the f_{res} and a increase in Q (Hutcheon et al.,1996b).

The effect of H₃ activation will depend on the balance of basal H₁ versus H₂ activity and their relative contribution to the membrane potential as well as other H₃ mediated effects on other neurotransmitters. However, due to the predominate presynaptic location of H₃ receptors in neocortical neurons there may be inherent problems in using whole cell techniques to characterize whether or not H₃ receptors function postsynaptically.

1.5 Organization of thesis

Using a novel approach of combining standard whole cell techniques and frequency domain analysis it will be the primary focus of this thesis to investigate the modulation of the hyperpolarization-activated cationic current, I_h, by histamine and its potential role in controlling subthreshold resonance in neocortical neurons.

To investigate the possible modulation of I_h and subthreshold resonance in neocortical neurons Chapter 2 will first focus on measurement errors associated with recording I_h using a whole cell configuration. This includes investigations into whole cell electrode dialysis and displacement of basal levels of cAMP in the cytosol resulting in current rundown of I_h, influence of the space clamp and assessment of analysis techniques. Chapter 3 examines the influence of histamine on ionic conductances in a subthreshold range for neocortical neurons with a specific focus on the modulation of I_h. Based on the known properties of I_h in the production of subthreshold resonance in neocortical neurons, Chapter 4 investigates subthreshold resonance and its modulation by

I_h by employing frequency domain analysis. Chapter 5 provides a summary of the findings and a discussion of their potential physiological relevance.

2. Modulation of the hyperpolarization-activated current (I_h) and prevention of rundown by cyclic AMP in neocortical neurons

2.1 Introduction

To investigate the role of cyclic nucleotides and second messengers in the modulation of I_h , investigators commonly use the whole cell patch clamp method. The whole cell configuration, however, requires rupturing the cell membrane in order to gain a low resistance access to the cell interior. Unavoidable problems with this technique include the disruption of cellular architecture and the displacement of cytosol. For example, Zhou and Lipsius (1993) showed in atrial cells that isoprenaline application during whole cell recording resulted in inconsistent changes in I_f activation and amplitude. In contrast, during nystatin perforated-patch recordings, a less invasive technique resulting in a more physiologically intact cell, isoprenaline application consistently produces a depolarizing shift in I_f activation. Similarly, Difrancesco, Ferroni, Mazzanti and Tromba (1986) observed a loss of I_f in rabbit sino atrial nodes and a corresponding shift of I_f activation to more negative potentials in nearly all cells recorded during whole cell recording. Similar rundown has been observed for other currents as well. For example, Oleson, DeFelice and Donahoe (1993) showed striking differences between perforated patch and whole cell patch methods in the activation, inactivation, and deactivation kinetics and the conductance-voltage relationship of K^+ currents in activated human T cells.

Such rundown might be explained by an *in vitro* related decrease in basal metabolic activity (Duchen, 1990). This, however, is unlikely, due to the less frequent

reporting of current loss using the perforated patch technique under similar experimental conditions (Oleson et al., 1993; Zhou and Lipsius, 1993). Instead, the whole cell technique most likely results in cell dialysis with the intracellular solution leading to a loss of cytoplasmic constituents and second messenger activity and consequently, the loss of ion channel function.

To some extent, an appropriate composition of the pipette solution can minimize the dialysis, maintaining cell function. For example, investigations by Simons and Schneider (1998) of I_M in isolated sympathetic ganglion neurons and by Hughes and Takahira (1998) of the inward rectifying K^+ (I_{Kir}) current in bovine retinal pigment epithelial cells, concluded that rundown of the respective currents was the result of decreased phosphorylation and dephosphorylation regulation that could be prevented or reduced by the addition of a hydrolysable form of adenosine tri-phosphate (ATP) and Mg^{2+} (critical cofactor) to the intracellular solution. Intracellular ATP has also been shown to prevent rundown of NMDA receptor-mediated currents in rat spinal dorsal horn neurons (Wang, Pak and Salter, 1993).

I_h is present in layer V neocortical neurons (Nicoll, Larkman and Blakmore, 1993; Hutcheon et al., 1996a; Schwindt and Crill 1997, Stuart and Spurston, 1998; Moosmang et al., 1999; Monteggia et al., 2000; Notomi and Shigemoto, 2004). While examining how agonists that stimulate cAMP modify the electrophysiological properties of neocortical neurons in response to changing the activation of I_h , a time dependent, hyperpolarizing shift in the activation of I_h and a decrease in current was observed that confounded results. These changes were reminiscent of current rundown observed during whole cell

recording of other membrane currents. It was hypothesized that the whole cell electrode dialyzed the cell thereby lowering the cellular concentration of a factor or factors resulting in the rundown of I_h . Given the presence of the CNBD on the HCN isoforms, the present investigation set out to examine the possibility that rundown may reflect the loss of a cyclic nucleotide.

2.2 Methods and Materials

All experiments were approved by the Institutional Animal Care Committee (IACC), Memorial University of Newfoundland. Postnatal day 8 to 12 Long Evans rats were deeply anesthetized with urethane (1.5 g kg^{-1} , i.p.), the brain removed and 300 - 400 μm thick coronal slices were cut on a Vibratome (Oxford) at 4°C in an artificial cerebral spinal fluid (ACSF) modified by replacing NaCl with an iso-osmotic concentration of sucrose (252 mM) (Aghajanian & Rasmussen, 1989). Slices were cut thin enough to discern cortical layering. After experimenting with various age cohorts, the age cohort of 8 to 12 days old was chosen due to a greater success in achieving whole cell rupture when compared to other cohorts. The slices were transferred to an interface chamber and allowed to gradually return to room temperature ($20 - 24^\circ\text{C}$) over a 60 min recovery period. During this time, the modified ACSF was gradually replaced with the regular ACSF at a rate of 0.5 ml/minute. The composition of the ACSF was (in mM): 126 NaCl, 4 KCl, 2 CaCl_2 , 1.3 MgCl_2 , 1.2 NaH_2PO_4 , 25 Na HCO_3 and 11 D-glucose. Equilibrated with 95% O_2 / 5 % CO_2 , the ACSF had a pH of 7.3. Just prior to a recording session, a slice was hemisected and one section was placed in a submerged type of recording

chamber (0.5 ml volume) and perfused with ACSF at 2 ml min^{-1} at room temperature ($20 - 24 \text{ }^{\circ}\text{C}$). Making use of a dissecting microscope with a graticule eyepiece, electrodes were initially guided to the surface of layer V neocortex, $500 - 700 \text{ }\mu\text{m}$ from the cortical edge of the slice (Kasper, Larkman, Lubke, and Blackmore, 1994a,b).

Whole cell electrodes were fabricated from thin wall borosilicate glass capillary tubing (1 mm O.D.) using a Narashige PP-830 puller and filled with a standard whole cell recording solution containing (mM): 145 potassium gluconate, 5 Na HEPES, 5 NaCl, 3 CsCl, 3 MgATP, 0.3 NaGTP, 11 EGTA, 1 CaCl_2 and titrated with KOH to pH 7.25. Varying concentrations of adenosine 3,5-cyclic monophosphate (cAMP, sodium salt, Sigma) were added to the pipette-solution as noted in the text. The free internal Ca^{2+} concentration equaled 11.7 nM based on calculations using the MaxCelator Software (version 2.5). Initial electrode resistance was 6-8 $\text{M}\Omega$.

Conventional whole cell recordings were made using an Axoclamp 2A amplifier. Low fluid levels in the bath were used to reduce capacitance. Upon entry of the electrode into the bath solution, the amplifier was adjusted to compensate for the liquid junction potential between the electrode solution and the ACSF. Seals to cells were greater than 1 $\text{G}\Omega$ before break through. To compensate for the amplifier offset, a liquid junction potential of -12 mV was calculated using a Junction Potential Calculator (pClamp 8.0) and subtracted from all measured membrane potentials (e.g. recordings at -60 mV were actually -72 mV) (see Zhang and Krnjevic, 1993). Since neocortical pyramidal neurons have extensive dendritic branching, ideal voltage clamp conditions were not possible, i.e., the distribution of the imposed voltage was not iso-potential. To improve the space

clamp, 3 mM CsCl was added to the whole cell recording solution to reduce the shunting effect of K^+ currents (Puil and Werman, 1981). Unless otherwise stated, data for analysis were collected in voltage clamp mode following a 5 min equilibration period after achieving the whole cell configuration. The equilibration period was recorded in current clamp mode, during which the resting membrane potential was monitored and recorded.

To generate voltage clamp protocols as well as to acquire and analyze the voltage and current signals a 40 kHz Labmaster A/D-D/A board was used under control by pClamp 6.0. Both pClamp 6.0 and 8.0 were used for I-V analysis (Axon Instruments, Foster City, Calif.). Traces were recorded and saved to a computer hard drive. Under current clamp, cells were accepted for data analysis only if they had resting membrane potentials ≤ -67 mV, initial spikes overshooting by >10 mV with depolarizing current injection (responses similar to those described for juvenile rat neocortex (McCormick and Prince, 1987; Kasper et al., 1994a,b)) and a voltage sag with hyperpolarizing current injection consistent with the presence of I_h .

To investigate I_h , experiments were conducted in continuous single-electrode mode. Errors due to electrode resistance in this mode were less than 2 mV. Unless otherwise stated, a series of 5 s duration voltage steps were applied in -10 mV increments between -57 mV and -137 mV to neurons held at -57 mV. A 3-5 s time period was allowed between each step to allow for the deactivation of I_h and return to the resting membrane potential. I_h has slow activation kinetics allowing it, and its time constant, to be isolated by fitting the total current with a sum of two exponential terms (Figure 2.1), from the instantaneous and capacitive currents (Scroggs, Todorovic, Anderson, and Fox,

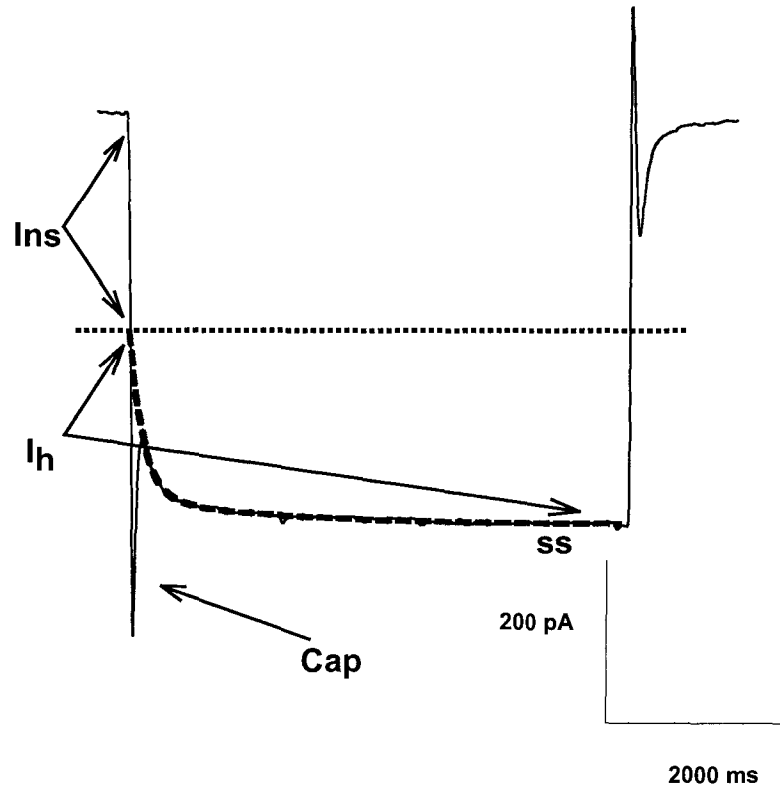


Figure 2.1 Hyperpolarizing voltage step from a holding potential of -57 mV.

The total current is composed of three components, a capacitive current (Cap), an instantaneous current (ins) and a slow current (I_h) (as indicated by arrows). Isolation of I_h and the instantaneous is achieved by fitting the slow current component with a sum of exponential terms (dashed line) between the points where the slow component meets the instantaneous current and reaches steady state (ss).

1994). Where appropriate, a single exponential term was used. Time constants plots were fitted with a best-fit exponential curve.

In order to overcome variations associated with background noise as well as errors associated with the fitting and subtracting of I_h from current traces, the activation point for I_h was initially taken at the voltage where I_h was > 5 pA (Hutcheon et al., 1996a). Due to large variations in the I_h I-V relationships across neocortical neurons, a fixed point of activation resulted in estimation errors, particularly when the recorded I_h was small. To compensate, the current at the point of activation was determined as 3.3% of I_h recorded at the step potential of -137 mV (I_{max}) for each neuron. This was arrived at by dividing 5 pA by 50% of the largest I_{max} recorded (Figure 2.2).

The conductance for I_h was derived from the Hodgkin-Huxley-like formulation:

$$g_h = I_h / (V - V_h) \quad (3)$$

where g_h is the conductance, I_h is the isolated current measured at each voltage (V) and V_h is the reversal potential for I_h . Due to the activation of a number of currents in the voltage range over which the reversal potential for I_h was expected the classical, more accurate method for estimating V_h was not applied. Instead, because I_h is strongly activated at potentials near -100 mV and shows no evidence of inactivation, V_h was extrapolated from the intersection of the instantaneous (chord) current/voltage relationships recorded using 2 s voltage step protocols at holding potentials of -107 mV and -57 mV, i.e. in the presence and absence of I_h (Mayer and Westbrook, 1983) (Figure 2.3).

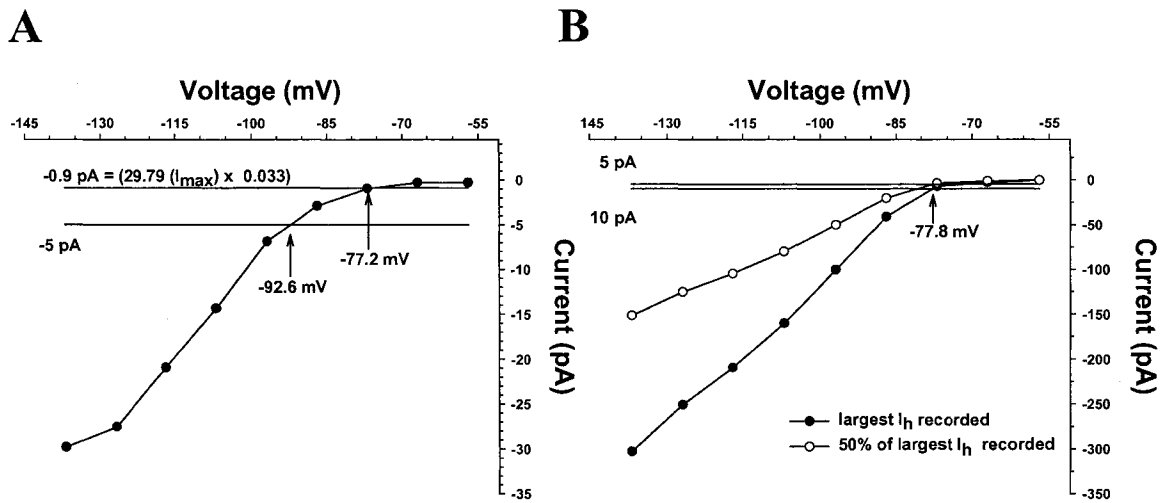


Figure 2.2 Determining the activation threshold of I_h .

I-V curves for I_h in pyramidal cells held at -57 mV and stepped to -137 mV. A: The activation point of I_h was initially defined as the first membrane potential where the current was > 5 pA. Due to large variations in the maximum current (I_{\max}) recorded at -137 mV this standard resulted in overestimations of I_h activation in cells where I_{\max} was small (arrows). To overcome this error, the current at activation was estimated as a proportion (3.3%) of I_{\max} recorded in each cell. In the example shown, the former 5 pA standard resulted in an estimation of -92.6 mV. By taking 3.3% of I_{\max} (0.9 pA) the new activation potential is -77.2 mV. B: I-V curve for the largest I_h recorded is shown. The proportional standard was achieved by dividing the 5 pA standard by half the largest I_{\max} recorded (151.5 pA).

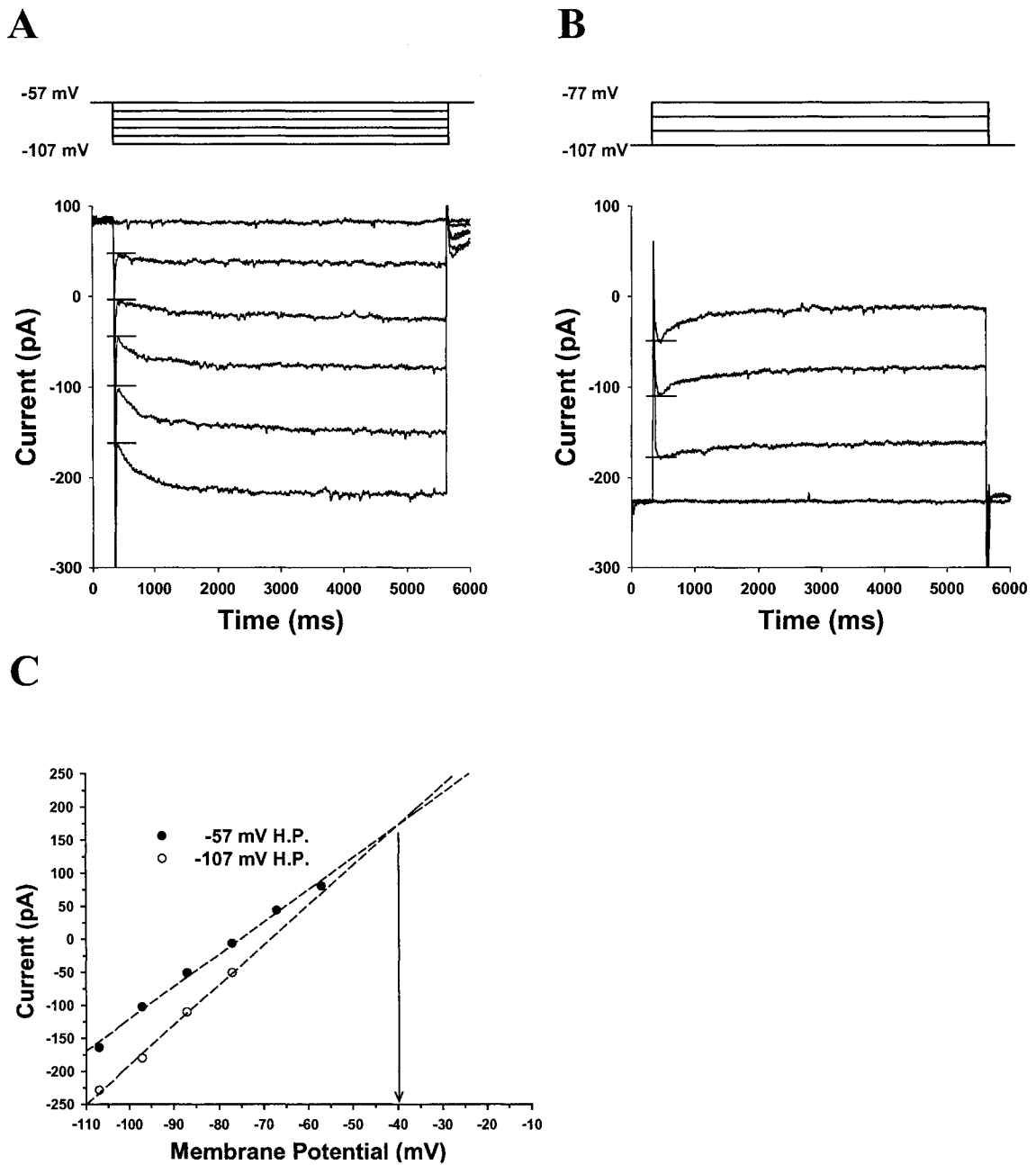


Figure 2.3 Determining the reversal potential of I_h .

A, B: Pyramidal neurons were held at voltages between -57 mV and -107 mV for 2 second intervals and the instantaneous current was extracted for each step (lines). C: Current-voltage (chord) relationships were constructed and V_h was estimated from the intersection of the extrapolated current voltage relation derived at each holding potential (H.P.).

Conductance/voltage relationships were normalized and fitted with a Boltzmann function:

$$g_h/g_{hmax} = 1/1+\exp((V-V_{1/2})/k_m) \quad (4)$$

where g_h is the conductance of I_h at each potential, g_{hmax} is the conductance of I_h at -137 mV, V is the membrane potential, $V_{1/2}$ is the membrane potential of half-maximal activation of I_h , and k_m is the slope factor.

Other compounds used in the study included 8-bromoadenosine-3',5'-cyclophosphate (8br-cAMP sodium salt, Sigma), forskolin (Sigma), H7 dihydrochloride (RBI), 4-ethylphenylamino-1,2-dimethyl-6-methylamino-pyrimidinium chloride (ZD-7288, Tocris), cesium chloride (CsCl, RBI), barium chloride ($BaCl_2$, RBI), tetraethylammonium chloride (TEA, Sigma) and 4-aminopyridine (4-AP, Sigma).

Cortical slices were perfused with tetrodotoxin (TTX, Sigma; $0.250 \mu M$), except during the initial phase where the action potential amplitude was determined. Unless otherwise mentioned, all chemicals and drugs were dissolved in normal ACSF and applied in known concentrations via a three-way tap system for 3 minute durations, after which recordings were started.

Samples sizes represent number of neurons recorded. Drug-induced changes in I_h were evaluated by examination of a wide range of I-V and I_h -V curves measured in control solutions, and in the presence of drug, in the same neuron. For the purpose of averaging responses, all data were converted to log normal value. To measure changes in the amplitude of I_h , I_{max} was converted to a percentage of control ($[\text{Treatment/Control}] \times 100$) before conversion to log normal values (Gaddum, 1945). Average data are

presented as the antilog of the geometric mean \pm S.E.M. Statistical significance of data was assessed with one-way analysis of variance (ANOVA). For multiple pairwise comparisons, the ANOVA was followed by the Bonferroni post hoc test (Instat, Graph Pad Software).

2.3 Results

2.3.1 Inward rectification by membrane hyperpolarization

The results represent data obtained from 62 neurons. The neurons were likely pyramidal neurons based on the recording location in the slice (proximal to layer V), the firing pattern and consistent responses evoked by depolarizing current steps all of which were similar to those described for juvenile rat neocortex, i.e., neurons were identified as regular spiking and intrinsic bursting (McCormick and Prince, 1987; Kasper et al., 1994a,b). Using hyperpolarizing current steps, all neurons showed a prominent inward rectification at voltages negative to the resting potential. This was characterized by a rapid hyperpolarization followed by a depolarizing voltage sag that was both voltage- and time-dependent (Figure 2.4). At current offset, there was a depolarizing overshoot due to the deactivation of I_h that evoked action potentials and low threshold Ca^{2+} spikes.

In voltage clamp mode, stepping the membrane potential -5 to -10 mV below the holding potential (-57 mV) revealed an instantaneous current. Larger voltage steps yielded a non-inactivating slow inward current, which when isolated (see methods), revealed that its rate of activation and amplitude increased with more negative command steps (Figure 2.5). The addition of CsCl (3 mM; $n = 8$) to the ACSF reversibly reduced

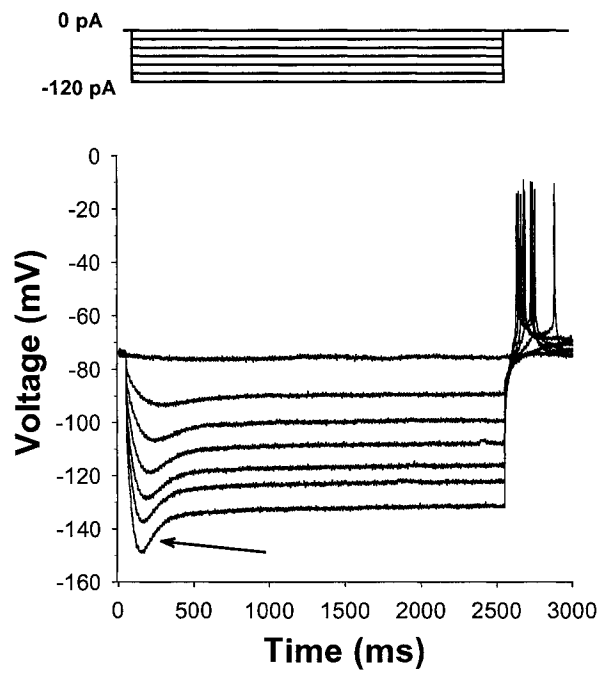


Figure 2.4 Characterization of I_h in current clamp mode.

A: Square hyperpolarizing current pulses evokes voltage responses with a prominent time dependent depolarizing sag (arrow). At the current offset, there was a depolarizing overshoot as a result of I_h deactivation that evoked action potentials and low threshold Ca^{+2} spikes.

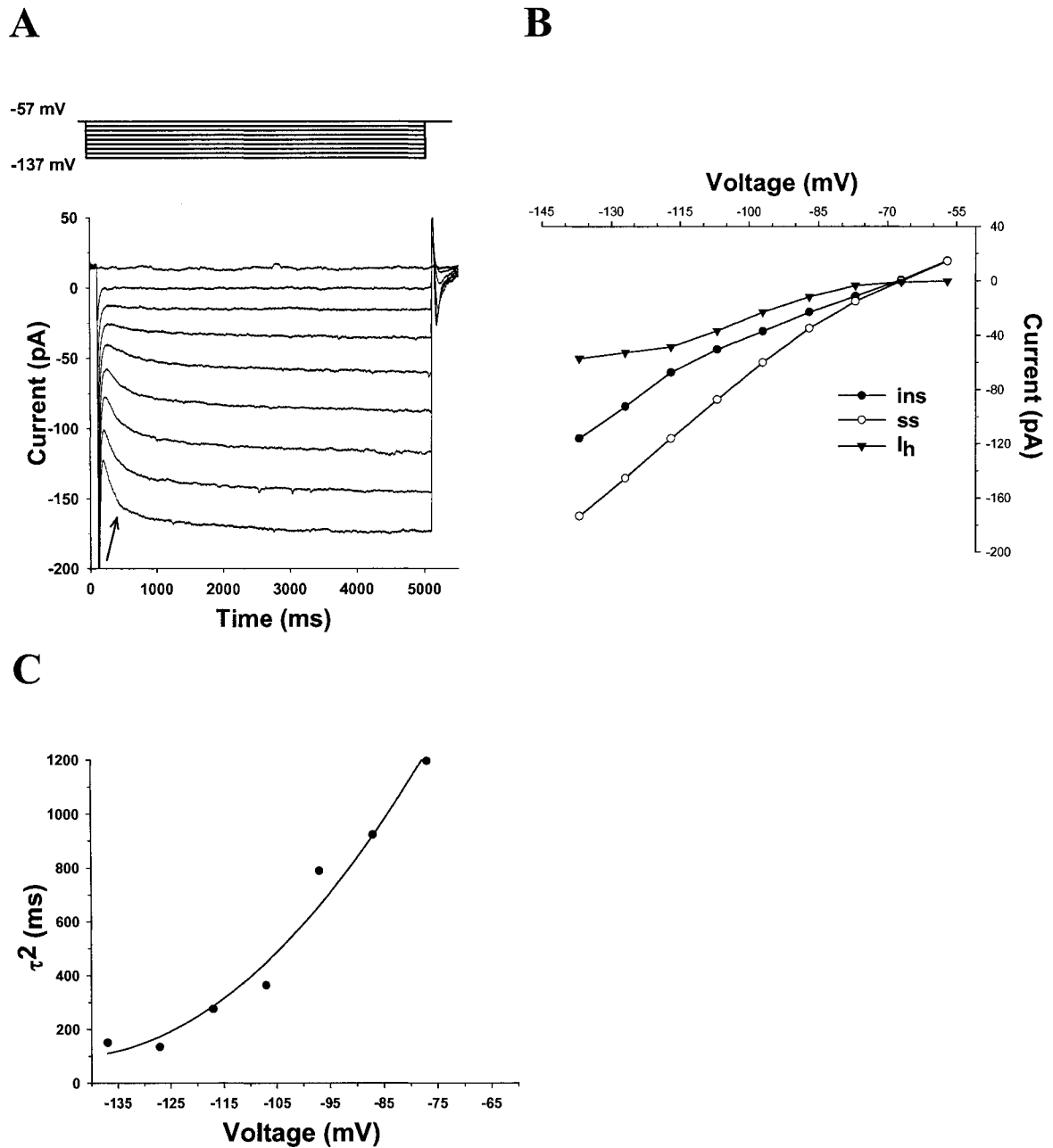


Figure 2.5 Characterization of I_h in voltage clamp mode.

A: Hyperpolarizing voltage steps evoke a slow inward current that exhibits a gradual increase in amplitude with increasing hyperpolarization (arrow). B: I-V curves showing isolated instantaneous (ins) and steady state (ss) current components and the subtracted slow inward current (I_h). C: Plot of the fast activation time constant (τ^2) as a function of

voltage. The fast activation time constant of the slow inward current decreases with increase hyperpolarization (data fitted with a best-fit exponential curve).

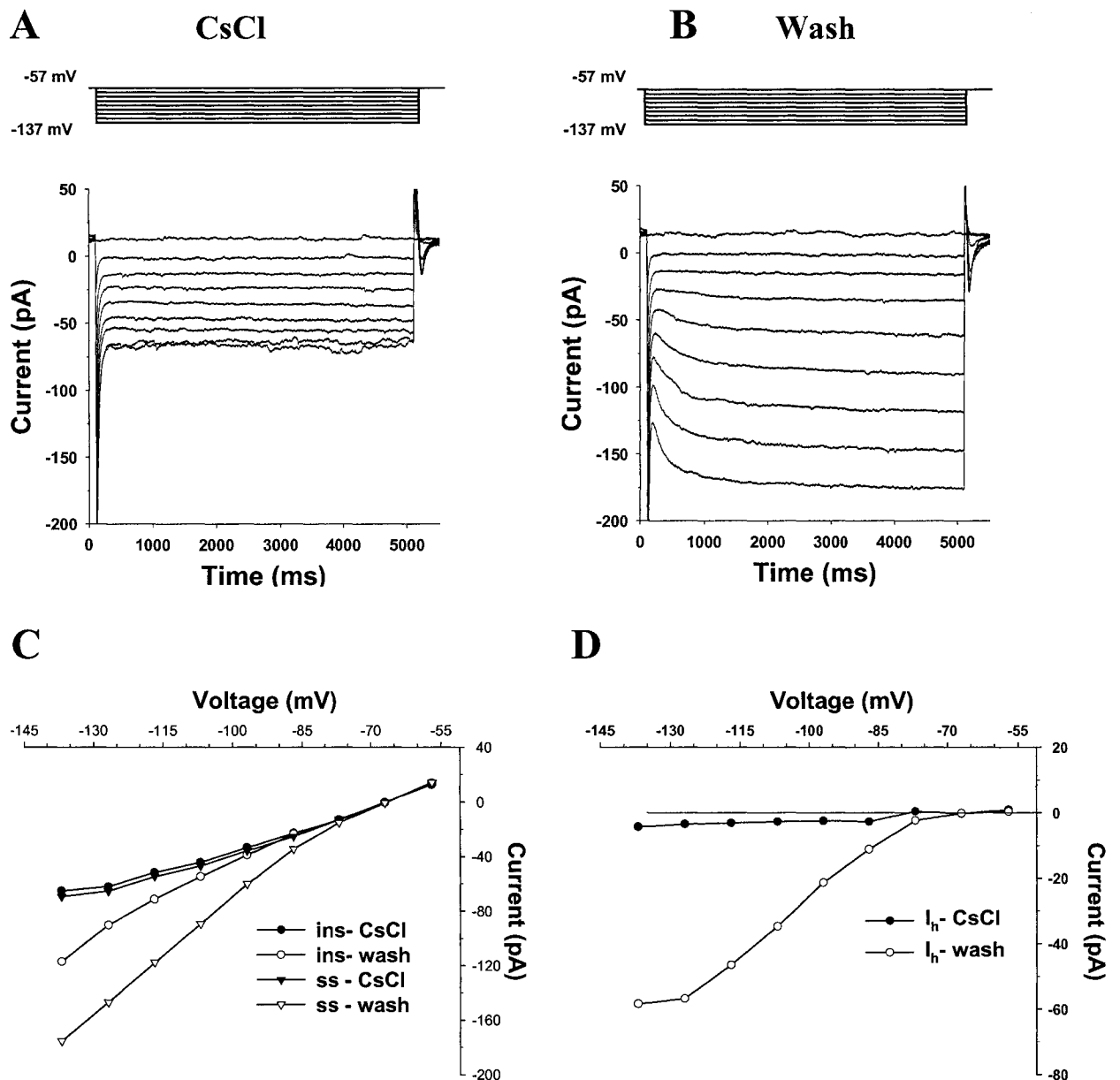


Figure 2.6 The slow component is blocked by CsCl.

Same cell as in Figure 2.5. A, B: Current responses in voltage clamp mode show the reduction and restoration of the slow inward current component after the application and 15 minute wash out of 3 mM CsCl. C: I-V curves for the instantaneous (ins) and steady state (ss) current components after application and washout of CsCl. CsCl reduced the steady state and instantaneous current at potentials negative to -72 mV. D: Subtracted slow current (I_h) component after application and washout of CsCl.

the current and blocked the instantaneous current at potentials negative to -72 mV (Figure 2.6).

Bath application of ZD-7288 (100 μ M, 15 min; $n = 4$), an irreversible inhibitor of I_h (BoSmith, Briggs and Sturgess, 1993; Maccaferri and McBain, 1996; Luthi, Bal, and McCormick, 1998), eliminated the current with no change in the instantaneous current (Figure 2.7). In addition, the mean extrapolated reversal potential, V_h , was -42.5 ± 1.6 mV ($n = 36$) (see methods). Taken together, the voltage- and time-dependence, sensitivity to blockers of this current and the reversal potential are all in keeping with the characteristics of I_h (Pape, 1996). Hereafter, this current is referred to as I_h .

2.3.2 *Rundown of I_h*

I_h recorded with the standard intracellular recording solution exhibited current rundown. Figure 2.8A,B shows current traces from voltage step protocols recorded at 5 and 25 minutes after membrane rupture. Upon initial visual inspection there is an obvious decrease in the steady state of the non-inactivating slow inward current after 25 minutes of recording. Isolating I_h revealed a negative shift in the activation potential (-77.6 mV vs. -85.9 mV) and a reduction in I_{max} (65.2 % of control) (Figure 2.8D). The run down of I_h could not be explained by a deterioration of the whole cell configuration or shunting effect due to a change in membrane conductance as there was no apparent change in the resting membrane potential (-77 mV vs. -76 mV) or the instantaneous current (Figure 2.8C) over the recording period. This also suggests that I_h does not contribute to rest under these conditions.

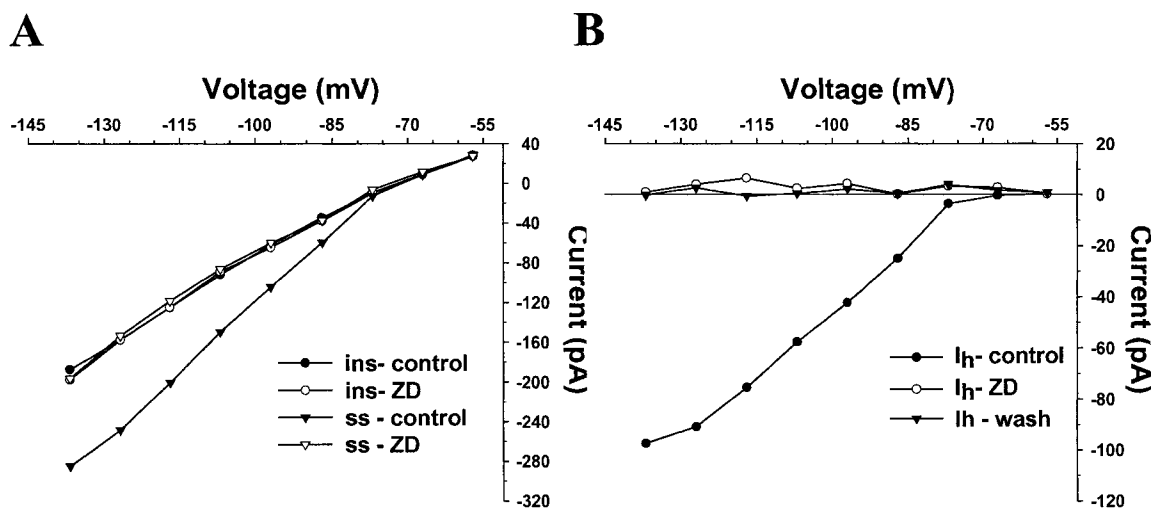


Figure 2.7 The slow component is eliminated by ZD-7288.

A: The I-V curves for the instantaneous (ins) and steady state (ss) current components before and after a 15 minute application of 100 μ M ZD-7288. After application of ZD-7288 the steady state current component was eliminated with no change in the instantaneous component. B: The slow component (I_h) was eliminated after application of ZD-7288 and was irreversible after 15 minutes of wash out.

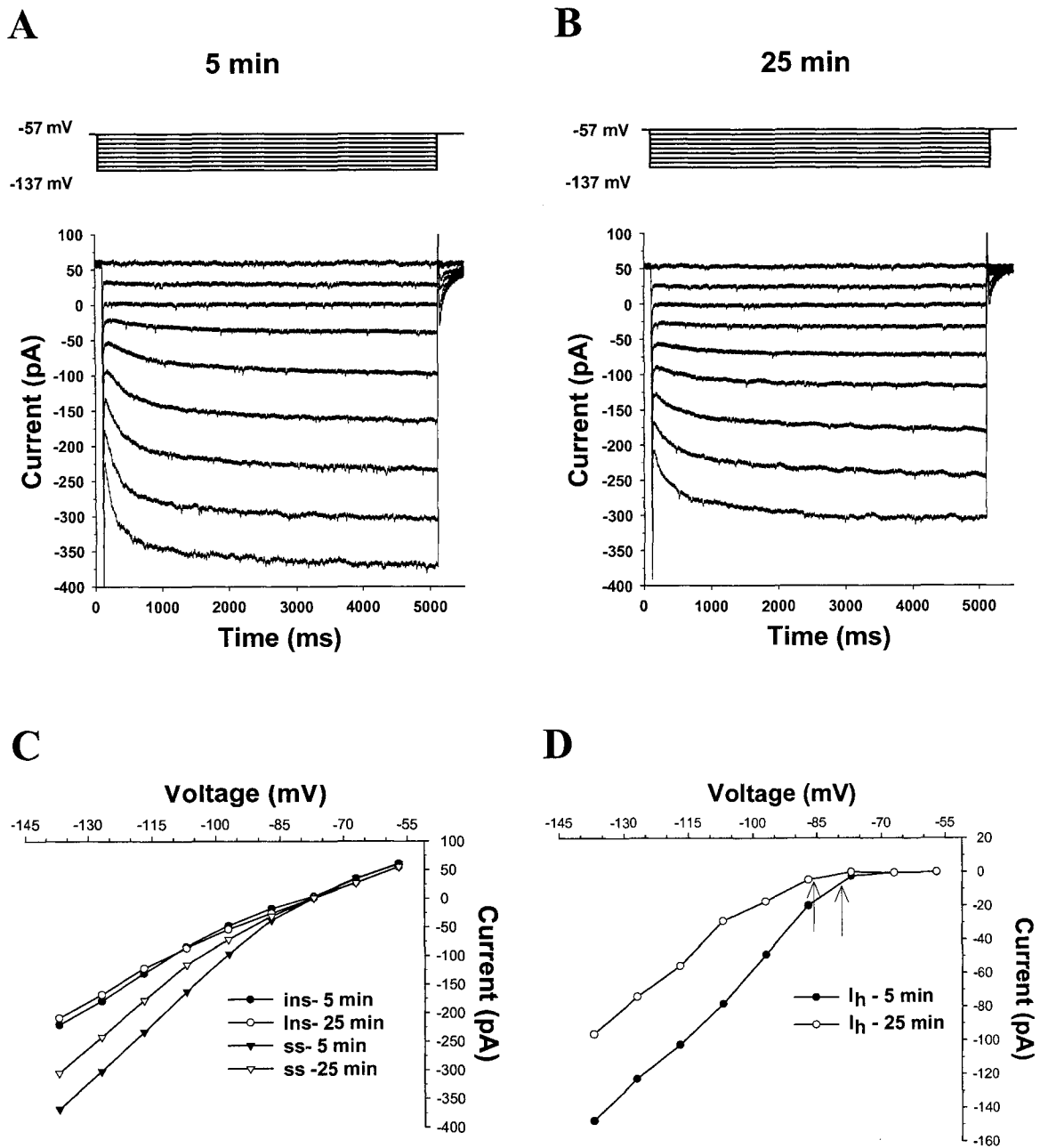


Figure 2.8 Rundown of I_h .

A, B: Current responses to hyperpolarizing voltage steps 5 and 25 minutes after gaining whole-cell access using the standard recording solution. C: I-V curves for the instantaneous (ins) and steady state (ss) current components 5 and 25 min after gaining whole-cell access show a reduction in the steady state after 25 minutes of recording with no observed change in the instantaneous component. D: I-V curves for I_h 5 min and 25

min after achieving whole cell access. Subtracted I_h shows a reduction in amplitude as well as a shift in activation in the hyperpolarizing direction after 25 min of recording (-77.6 mV vs. -85.9 mV, arrows).

Pooling data for I_h and the instantaneous current (mean \pm S.E.M., $n = 5$) verified these initial observations (Figure 2.9). After 25 minutes of recording there was a hyperpolarizing shift in the I_h activation threshold (-76.8 ± 0.8 mV vs. -89.0 ± 3.7 mV; $P < 0.05$) and a reduction in I_{\max} ($69.6 \pm 3.4\%$ of control; $P < 0.001$) (Figure 2.9A). The change in the activation threshold was also accompanied by a decreased rate of activation, indicative of a slowing of the voltage-dependent fast activation time constant over the entire voltage range examined (Figure 2.9B). Recordings at times longer than 25 minutes from membrane rupture revealed even further rundown characterized by a further hyperpolarizing shift of the I_h activation kinetics (data not shown). Similar to initial observations, there was no change in instantaneous current (Figure 2.9C) or the resting membrane potential (-78.0 ± 3.6 mV vs. -76.4 ± 2.5 mV, Bonferroni, $P > 0.05$).

2.3.3 K^+ conductance effects on I_h recordings

Theoretically, a decrease or increase in the membrane length constant could, in effect, result in an increase or decrease in the attenuation of the voltage clamp. If the greater proportion of I_h channels are at a higher density in the most distal pyramidal apical dendrites (Stuart and Spurston, 1998; Williams and Stuart, 2000; Berger, Larkum and Luscher, 2001; Lorincz, Notomi, Tamas, Shigemoto and Nusser, 2002), a change in membrane conductance could change the population of I_h channels that contribute to the current recorded. Changes in I_h , due to this error, may be interpreted as a physiological modulation of I_h as a result of experimental protocols when, in actuality, it may be an indirect effect due to changes in neuronal electrotonic properties. Although the observed

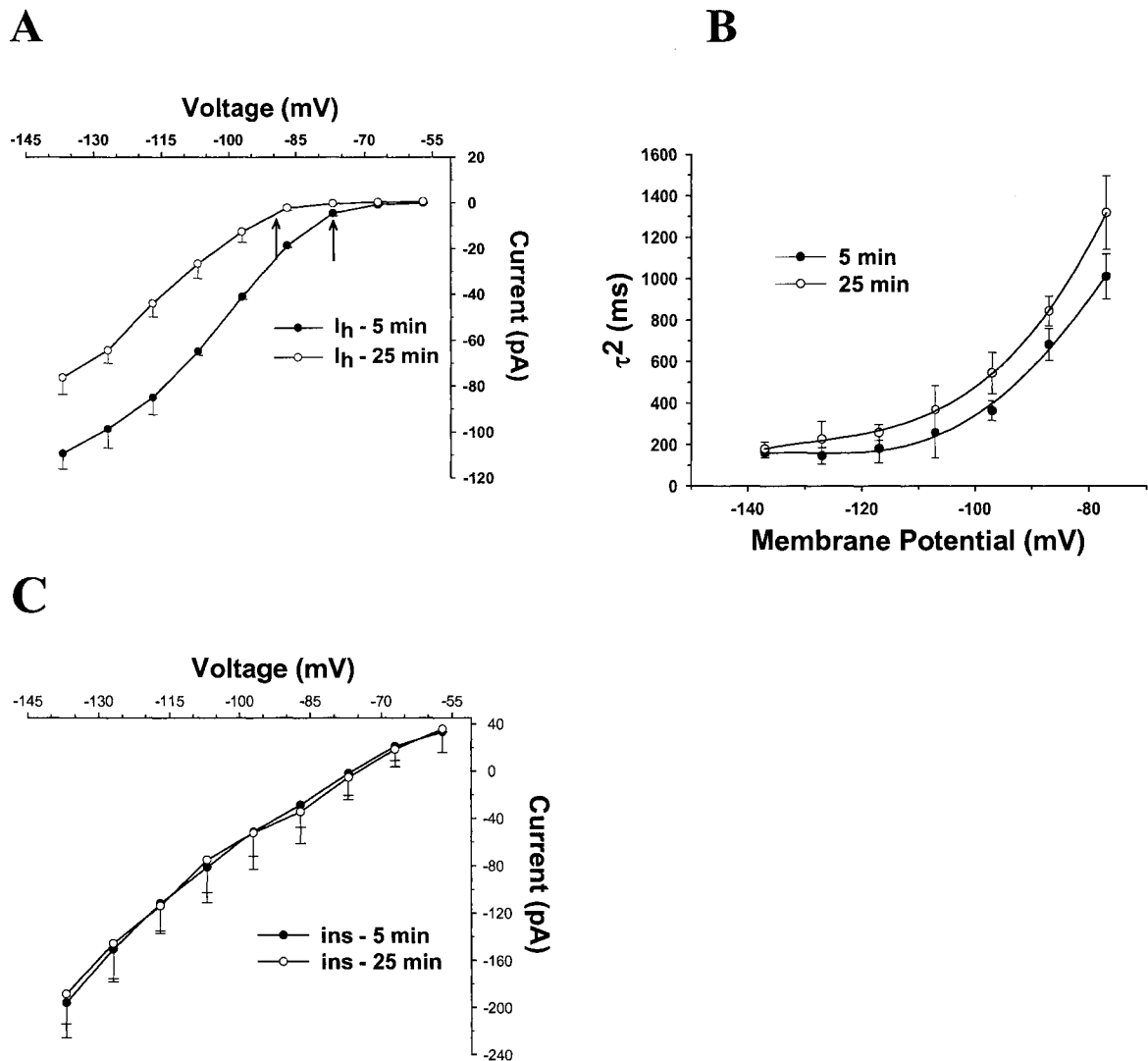


Figure 2.9 Pooled data showing rundown of I_h .

Pooled data (mean \pm S.E.M., $n = 5$). A: I-V curves for I_h shows the significant shift in the activation of I_h (arrows) 25 minutes after gaining whole-cell access. B: Plot of fast activation time constant as a function of voltage. Consistent with a negative shift in activation there is a slowing of the fast activation time constant (τ^2) at more depolarized potentials. The mean difference at -75 mV (25 min - 5 min) was ~ 309 ms. C: I-V curves for the instantaneous current (ins) show no change between the 5 minute and 25 minute responses.

run down of I_h does not appear to be related to a shunting effect due to changes in other membrane conductances, as there was no apparent change in the instantaneous current across the voltage range tested, the possibility that changes in the membrane conductance can result in changes in recorded I_h , i.e., space clamp errors, was investigated. For example, the K^+ inward rectifier (I_{Kir}) is active in the same voltage range of I_h and shares a similar pattern of channel density in neocortical dendrites (Takigawa and Alzheimer, 1999).

To decrease membrane conductance, thereby increasing the length constant of the neuron and increasing the distance of voltage clamp control from the site of puncture, experiments were conducted using two test solutions containing potassium current blockers: (1) a solution containing 10 mM TEA and 1 mM 4-aminopyridine (4-AP), and (2) a solution containing 1 mM $BaCl_2$, a blocker of the K^+ inward rectifier (I_{Kir}). To examine the effects of a decrease in membrane conductance on the rundown of I_h , neurons were recorded at 5 minutes and 25 minutes after rupture, i.e., to ascertain that rundown had occurred, followed by a bath application of the potassium current blockers.

Similar to previous control observations, I_h exhibited a rundown over the 25 minute recording period characterized by a shift in activation in the hyperpolarizing direction (-76.5 ± 0.5 mV vs. -85.9 ± 1.4 mV, Bonferroni, $P < 0.01$), and a decrease in I_{max} (70.0 ± 7.6 % of 5 min, Bonferroni, $P < 0.05$) (Figure 2.10A) with no change in the resting membrane potential (75.7 ± 1.2 mV vs. 75.3 ± 0.8 mV, Bonferroni, $P > 0.05$) or observed change in the instantaneous current (Figure 2.10B).

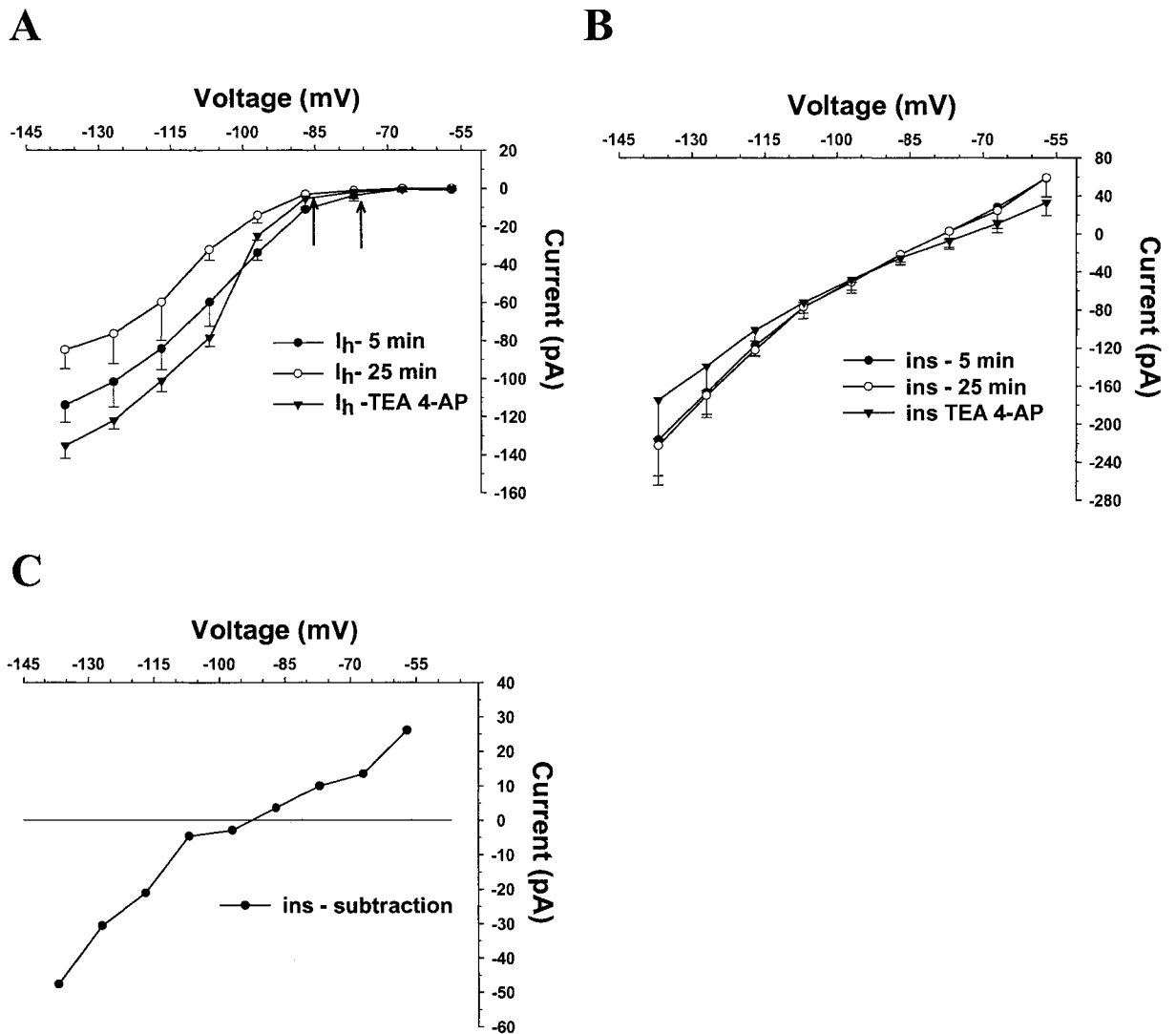


Figure 2.10 Co-application of TEA and 4-AP block K^+ conductances and increases the amplitude of I_h .

Pooled I-V curves (mean \pm S.E.M., $n = 5$) 5 minutes and 25 minutes after gaining whole cell access followed by bath co-application of 10 mM TEA and 1 mM 4-AP. A: I-V curves for I_h . Similar to previous observations rundown of I_h occurs over 25 minutes of recording as indicated by a hyperpolarizing shift in activation (arrows) and a decrease in current amplitude. Co-application of TEA and 4-AP appeared to prevent further rundown in the activation of I_h and increased I_{max} to levels comparable to the 5 min response. B: Pooled I-V curves for the instantaneous current (ins) show no change between the 5 minute and 25 minute response whereas co-application of TEA and 4-AP reduced the instantaneous current along the entire voltage range tested. C: Subtraction of

the 25 min and TEA/4-AP instantaneous I-V curves shows the change in current. The point of 0 current flux was ~ -92 mV. Given the known pharmacological effects of TEA and 4-AP, this was interpreted as the reversal potential for K^+ .

Co-application of TEA and 4-AP, however, resulted in a decrease in instantaneous component along the entire voltage range tested and a depolarization in the resting membrane potential (-75.3 ± 0.8 mV at 25 minutes vs. 69.0 ± 1.6 mV, Bonferroni, $P < 0.05$). Subtraction of pooled I-V for the instantaneous current (25 min – cocktail) revealed an extrapolated reversal potential of -92.3 mV, indicative of a reduction in K^+ conductance (Figure 2.10C). This was confirmed by estimating the reversal potential for K^+ using the Nernst equation:

$$E_K = RT/ZF * (\ln([K^+]_o/[K^+]_i)) \quad (5)$$

Where E_K is the value of the membrane potential at which K^+ is in equilibrium, R is the gas constant (8.3 J / K mol), Z is the valence of K^+ (1^+), T is the temperature in Kelvin (298.2), F is the Faraday constant (96,487 C/mol), and $[K^+]_o$ and $[K^+]_i$ is the concentration of K^+ outside and inside the cell (4 mM and 145 mM, respectively, based on known K^+ concentrations in the ACSF and the intracellular solution). The estimated E_K was -93.3 mV.

Given that externally applied TEA or 4-AP have no known effects on I_h (Budde, White and Kay, 1994; Roth and Hausser, 2001), the decrease in the K^+ conductance appeared to alter the I-V relationship of I_h . There appeared to be a reduction in the rate of rundown as there was no change in the activation of I_h compared to records taken at 25 min (-85.9 ± 1.4 vs. -84.6 ± 0.8 mV, Bonferroni, $P > 0.05$). As well, I_{max} , was increased above the 25 min response (70.1 ± 7.6 % vs. 120.3 ± 3.9 %, Bonferroni, $P < 0.01$) and

appeared to be reversed to levels comparable to the 5 min recordings (Bonferroni, $P > 0.05$). Running the experiments using BaCl_2 ($n = 4$) produced similar results (Figure 2.11).

Results from both experiments are consistent with an increase in K^+ conductance, independent of I_h , which appears to shunt the effectiveness of the voltage clamp. As a result, depending on recording site and the level of membrane conductance, I_h responses may be masked, reduced and/or irregular compared to neuronal preparations where the distribution of voltage under voltage clamp approaches iso-potential conditions.

2.3.4 I_h is located on apical dendrites

To investigate the possibility that I_h channels are more densely populated on the most distal dendrites rather than the soma or proximal dendrites, approximately 500 microns of the outer cortical tissue was manually removed using a scalpel with the assistance of a dissecting microscope equipped with a graticule eyepiece. The intention was to remove most of the apical dendritic branching of the layer V pyramidal neurons leaving only the soma and a part of the proximal portion of the apical dendritic trunk intact. After completion of the dissection procedure, the tissue was placed back in the interface storage chamber for 1- 2 hours to allow for recovery and sealing of the dissected dendritic trunks. To record from neurons with the shortest segments of dendritic trunks, the recording electrode was placed near the site of dissection before insertion into the cortical slice.

To avoid rundown effect recordings were taken 5 mins after puncture. Neurons

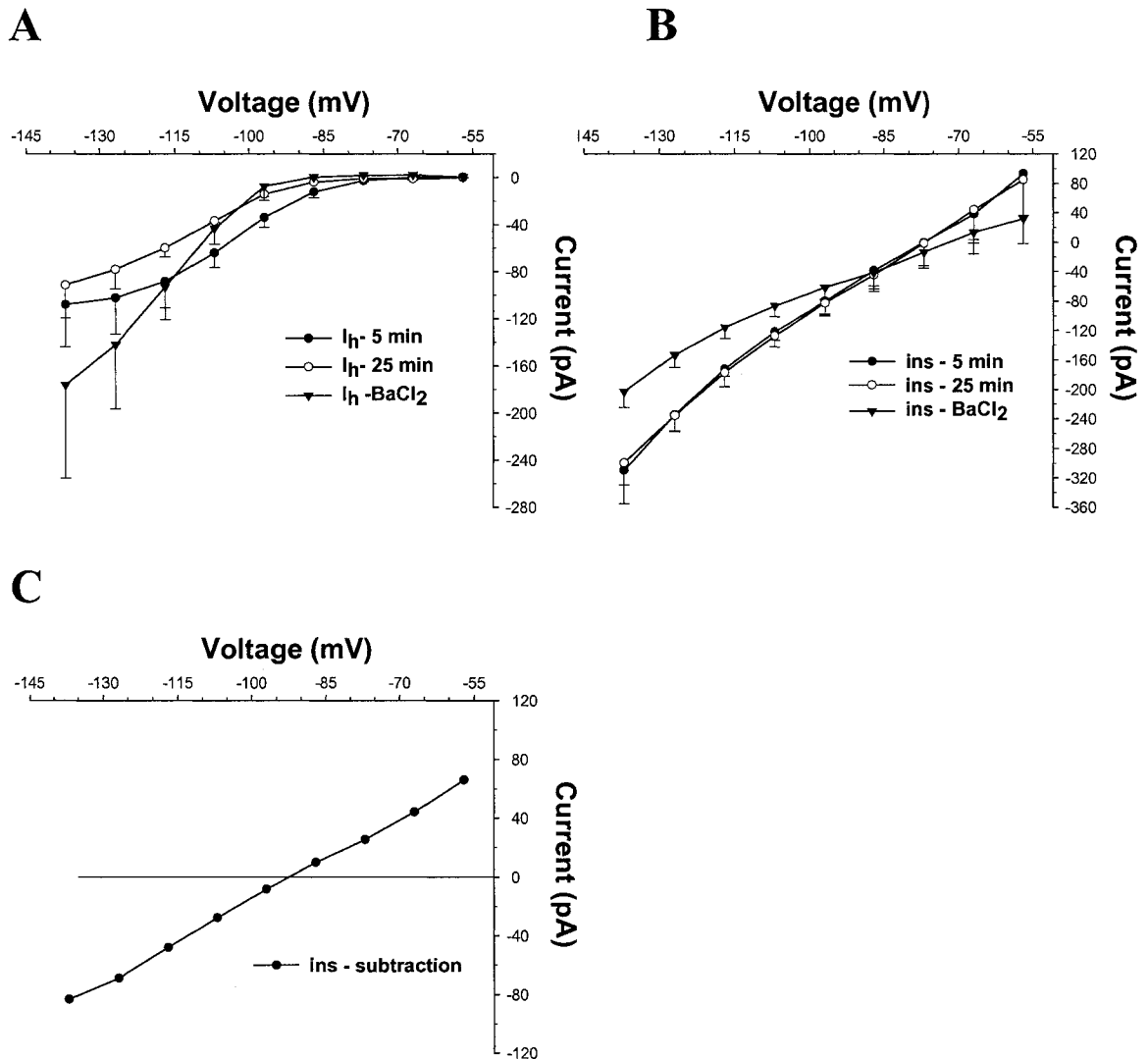


Figure 2.11 Barium chloride (BaCl₂) decreases K⁺ conductances and increases the amplitude of I_h .

Pooled data (mean \pm S.E.M., $n = 4$) 5 minutes and 25 minutes after gaining whole cell access followed by a bath application of 1 mM BaCl₂. A: I-V curves for I_h . Similar to previous observations, I_h exhibited rundown over the 25 minute recording period characterized by a negative shift in the activation threshold (-77.3 ± 2.1 mV vs. -89.0 ± 1.3 mV, Bonferroni, $P < 0.05$), and an observed decrease in I_{max} (85.0 ± 2.5 % of 5 minute response, Bonferroni, $P > 0.05$) Application of BaCl₂ appeared to prevent further rundown as the activation threshold of I_h was not significantly different compared to the 25 min recording (-89.0 ± 1.3 mV vs. -85.7 ± 3.3 mV, Bonferroni, $P > 0.05$). I_{max} ,

however, was significantly increased above the 25 min and 5 min responses (154.3 ± 15.7 % of 25 minute response, Bonferroni, $P < 0.01$). B: I-V curves for the instantaneous current (ins). There was no observed difference between the 5 minutes and 25 minutes responses and no significant change in the resting membrane potential (76.3 ± 1.3 mV vs. 75.8 ± 0.6 mV, Bonferroni, $P > 0.05$). Application of BaCl_2 resulted in decrease in instantaneous current along the entire voltage range tested and a significant depolarization in the resting membrane potential (-75.8 ± 0.6 mV at 25 minutes vs. 70.8 ± 0.7 mV, Bonferroni, $P < 0.01$). C: Mean difference between the instantaneous current at 25 min and after application of BaCl_2 . The extracted reversal potential, taken at the intersection where the current flux equals 0 pA, was -92.4 mV.

with dendritic removal showed a stable resting membrane potential that was not significantly different from neurons with intact dendrites (76.1 ± 0.9 (n = 4) vs. mV -74.8 ± 3.4 mV (n = 8), Bonferroni, $P > 0.05$). Consistent with this observation there was only a slight decrease in the instantaneous current (Figure 2.12B,C). On the other hand, although the isolation of I_h revealed no difference in the activation threshold (-77.8 ± 2.1 mV vs. -76.2 ± 1.3 mV, Bonferroni, $P > 0.05$) when compared to neurons with intact dendrites (Figure 2.12A), there was an approximate 60% reduction in I_{max} (36.9 ± 14.1 pA vs. 97.1 ± 13.1 pA, Bonferroni, $P < 0.01$). The results are consistent with the notion that the dissection of the dendrites reduces the number of channels responsible for I_h and the instantaneous current. As well, in 3 of the 4 neurons which had their dendrites removed, I_h reached an expected maximum current asymptote at voltages near -137 mV, compared to only 1 of the 8 neurons with intact dendrites, consistent with increased potential uniformity.

2.3.5 I_h measurement errors

Approximately 90% of I_h recordings did not appear to reach an asymptote at the most hyperpolarized test potentials, i.e., -137 mV. Since the accurate recording of I_h I-V relationships appeared to be influenced by the space clamp the possibility that clamping irregularities in measuring the voltage dependence of I_h was examined. To test this assumption, two methods of estimating the half maximal activation of I_h ($V_{1/2}$) were utilized: (1) the commonly used method of fitting normalized conductance values

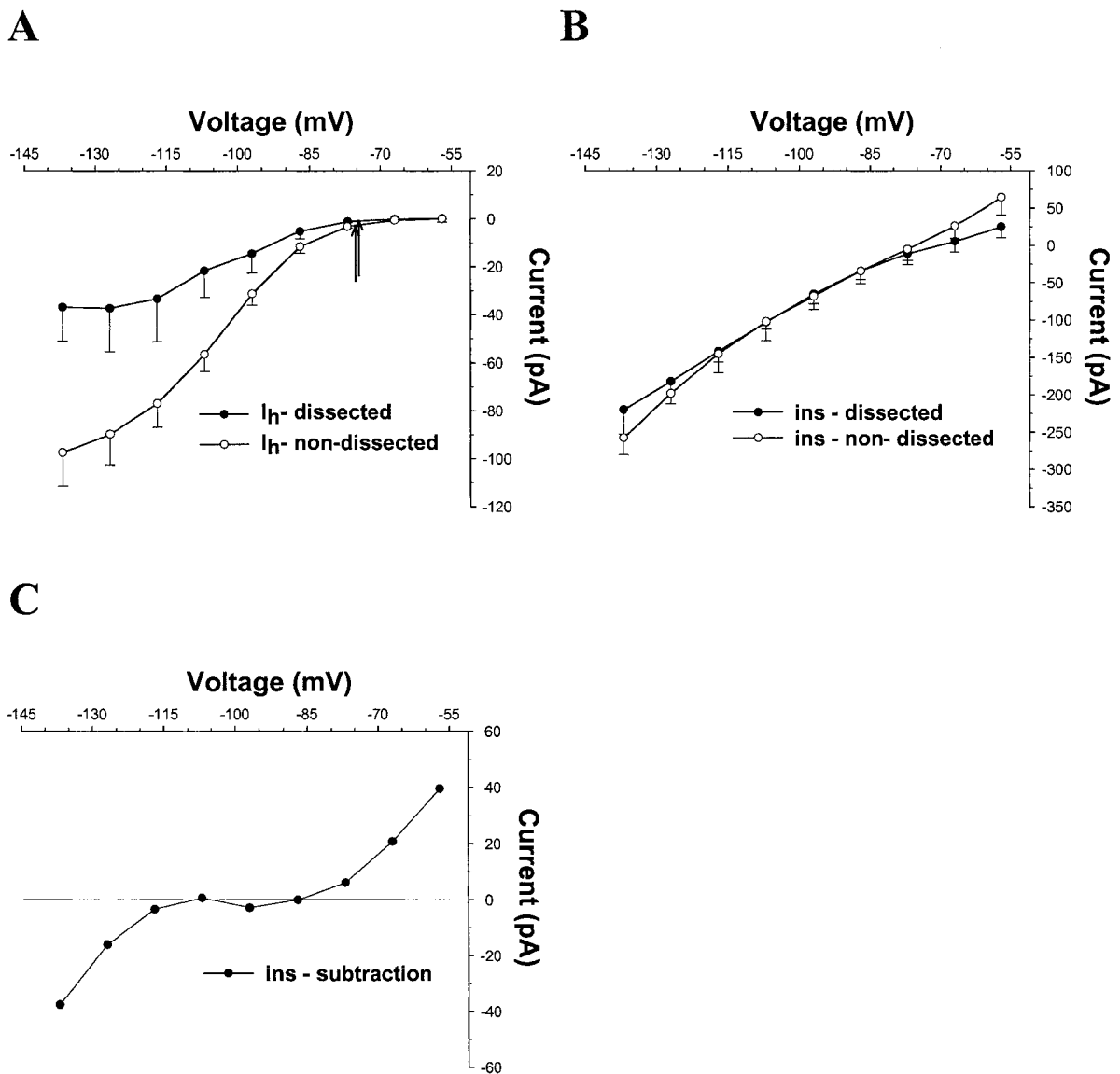


Figure 2.12 I_h exists on distal apical dendrites.

Pooled data (mean \pm S.E.M.) from cells with removal of apical dendrites ($n = 4$) and neurons with intact apical dendrites ($n = 8$) taken 5 minutes after achieving whole cell access. A: I-V curves for I_h from neurons with and without apical dendrites intact (arrows); however, I_{max} was significantly decreased in neurons without dendrites consistent with a decrease in the number of I_h channels. Also, in contrast to neurons with intact dendrites, neurons without dendrites showed I_h reaching an asymptote at the maximum negative test potentials, indicative of more iso-potential voltage clamp conditions (1/8 vs. 4/5, respectively). B: I-V curves for the instantaneous current from

neurons with and without apical dendrites. Neurons without dendrites show a small decrease in the amount of current at the most positive and most negative test potentials, indicative of a reduction in the number of channels responsible for the instantaneous current. C: Mean difference between the instantaneous current in neurons with and without dendrites intact. Due to comparisons made from different cells the reversal potential could not be estimated from a single subtraction of pooled results. The average reversal potential based on individual subtractions equalled -93.7 mV.

reflecting the shape of the I-V relationship for I_h and (2) a theoretical calculation based on a Hodgkin Huxley formalism as a function of the activation potential for I_h which is less dependent on the I-V relationship (equation 6) (Figure 2.13).

Six neurons with varying I_h amplitude and activation potentials were divided into 2 groups of 3 cells. In the first group, (cells 1 to 3) the I-V curves for I_h reflected a more linear I-V relation at more hyperpolarized voltage steps, indicative of I_h responses under the influence of space clamp errors (Figure 2.13A). In the second group (cells 4 to 6) the I-V curves for I_h appeared to reach a maximum current asymptote, an apparent ideal voltage response for I_h (Figure 2.13B).

In method (1), the conductance - voltage (g_h/V) curves were calculated for both groups (see methods, equation 3) and the conductance was normalized (g_h/g_{max}), where g_{max} was taken to be the value of g_h at -137 mV. Normalized conductance plots were fitted with a Boltzman equation (equation 4) allowing for the estimation of $V_{1/2}$ and the slope factor (k_m) for each cell.

In method (2), experimentally observed activation potentials were substituted into the Hodgkin-Huxley model solved for $V_{1/2}$:

$$V_{1/2} = V - k_m \ln((g_h(V - V_h)/I_h - 1)) \quad (6)$$

Where V is the activation threshold potential observed for each cell, k_m is the slope factor derived from the Boltzman equation fits in method 1, g_h is g_{hmax} derived from equation 2, V_h is the estimated reversal potential for I_h (-42.6 mV), and I_h is the activation

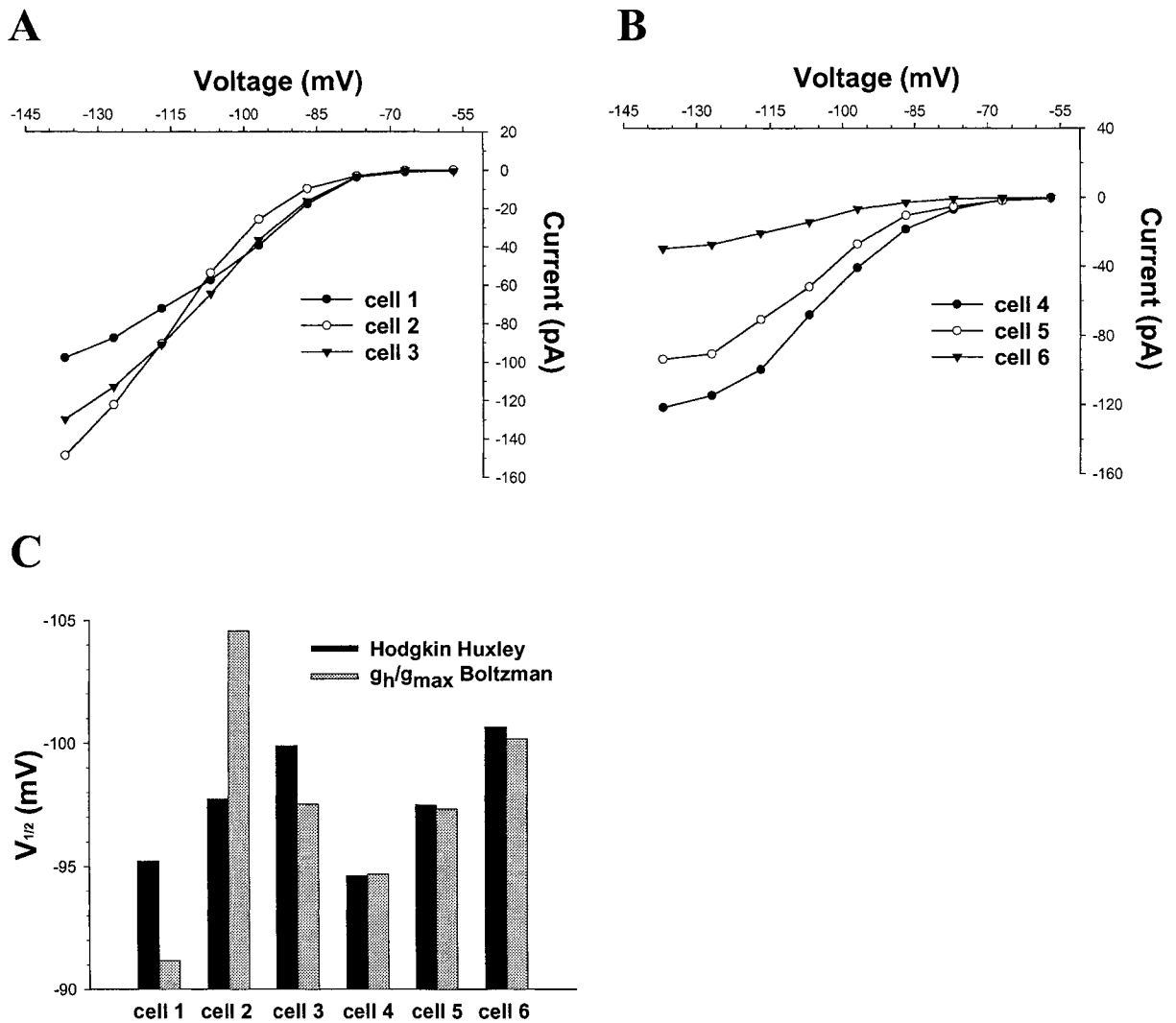


Figure 2.13 I_h half maximal activation ($V_{1/2}$) estimations.

A, B: I-V curves of I_h with varying I_{max} for neurons not reaching (cells 1- 3) and reaching (cells 4 - 6) a maximum current asymptote. C: A comparison of derived $V_{1/2}$ values using theoretical Hodgkin Huxley computations (equation 6) and g_h/g_{hmax} Boltzman fits (equation 4). In neurons where I_h does not reach a maximum asymptote the theoretical and g_h/g_{hmax} derived $V_{1/2}$ values did not match. In contrast, for cells where I_h appeared to reach a maximum current asymptote, both the theoretical and extracted values were near identical. This indicates that the traditional g_h/g_{hmax} method to estimate $V_{1/2}$ values may result in inaccurate estimations of I_h voltage kinetic variations when space clamp conditions are not ideal. On the other hand all neurons show similar activation potentials (~ -73 to -78 mV) indicating that I_h activation is a more accurate estimate of shifts in I_h kinetics in these preparations.

current, i.e. 3.3% of I_{\max} . Estimation parameters used in the Hodgkin Huxley computations for each cell are shown in Table 2.1.

Table 2.1 $V_{1/2}$ estimation parameters.

Cell	Maximum Asymptote	Activation Current (pA)	Activation Potential (mV)	$g_{h\max}$ (nS)	k_m
1	No	3.2	-76.7	1.0	7.7
2	No	4.9	-77.8	1.6	8.2
3	No	4.3	-77.8	1.4	9.1
4	Yes	1	-78.4	0.3	9.0
5	Yes	4.0	-73.0	1.4	9.5
6	Yes	3.1	-75.7	1.1	8.9

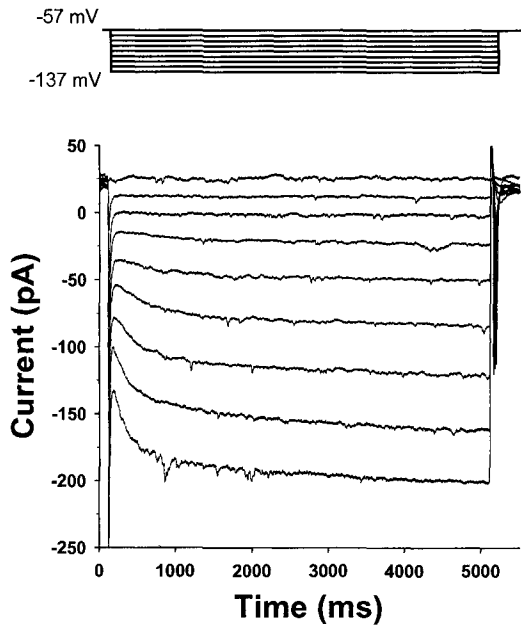
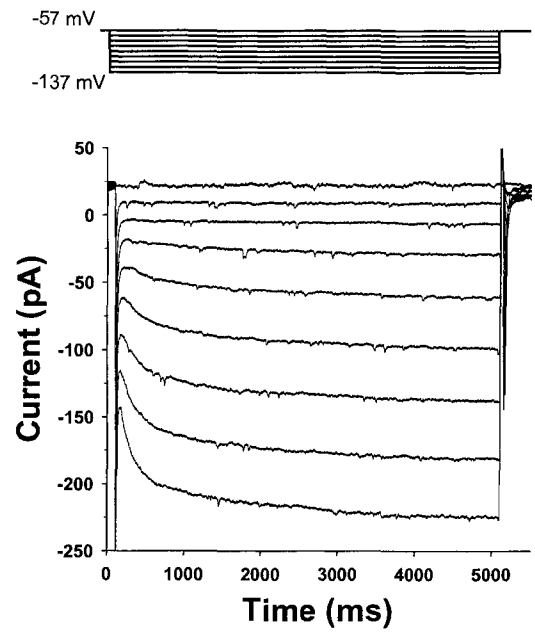
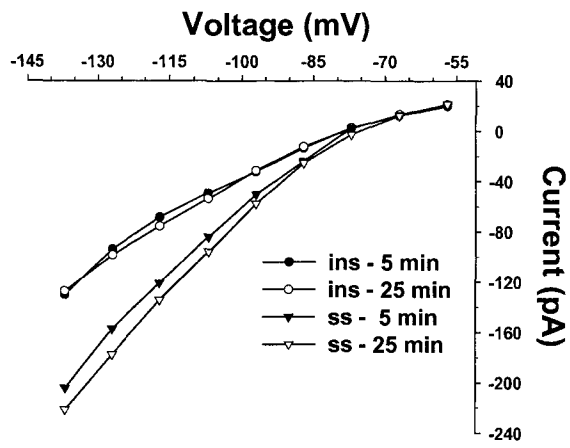
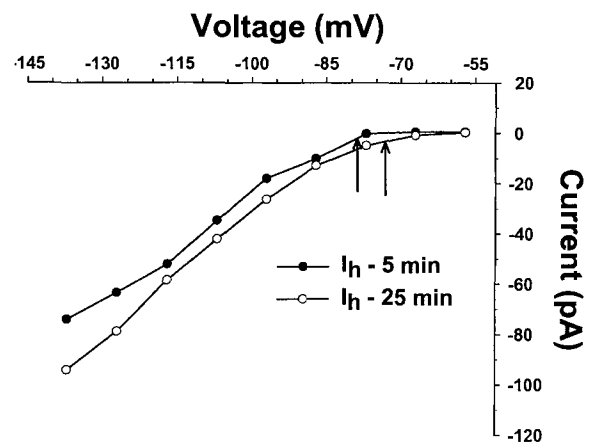
Theoretically, if the I_h response from each cell accurately represented I_h activation, both methods of estimating $V_{1/2}$ should approximately match. Comparisons of both methods for deriving $V_{1/2}$ show that a greater disparity exists in the first group where I_h did not reach a maximum current asymptote (Figure 2.13C). Subtraction of $V_{1/2}$ values derived from both methods reveal differences ranging from -4 mV to 7 mV, 40% to 70 % of the commonly observed maximal shifts in I_h voltage dependence (± 10 mV). In contrast, the second group, where I_h appeared to reach a maximum current asymptote, revealed differences ranging from -0.5 mV to 0.6 mV. Even with CsCl present in the pipette recording solution, the results show that in preparations with less than ideal voltage clamp conditions, standard methods of estimating I_h parameters, i.e., $V_{1/2}$, may yield poor fits. In such cases, the better method for estimating I_h parameters should rely

less on the shape of I -V relationship. Comparison of the activation potential from both groups (Table 2.1) shows little difference, 73 - 78 mV, in values. As a result of the high variability in I_h maximum responses observed through this study, the activation potential was employed as an estimate of shifts in I_h kinetics.

2.3.6 *cAMP prevents rundown of I_h*

Given that no change in the instantaneous current occurs during rundown of I_h , the observed rundown appears to occur independent of other changes in the membrane conductance, i.e., is not the result of masking or changes in space clamp conditions. In light of the TEA and 4-AP results, however, the possibility that changes in conductances outside the range of the space clamp may be influencing the I_h I -V relationships could not be ruled out since changes in membrane conductance could be occurring outside the recording range of the space clamp. In any case, whether the rundown is due to a direct action via I_h channels or a masking affect, or some combination of both, the possibility that whole cell recording conditions may lead to the loss of intracellular elements required for normal voltage dependent activation of I_h was examined.

Since cyclic nucleotides modulate I_h , cell dialysis by the whole cell electrode might reduce the concentration of free cyclic nucleotides resulting in current rundown. This possibility was assessed by including 25 μ M cAMP in the pipette solution to stabilize the nucleotide concentration of the cytoplasm. Figure 2.14 shows an example where application of cAMP prevents the rundown phenomena, and enhances parameters

A**B****C****D**

E

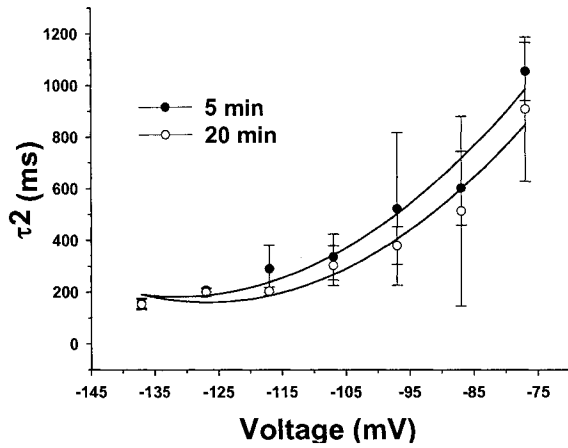


Figure 2.14 Inclusion of 25 μM cAMP in the internal recording solution precludes rundown of I_h .

A, B: Current responses to hyperpolarizing voltage steps 5 and 25 minutes after gaining whole-cell access using the internal recording solution containing 25 μM cAMP. After 25 minutes of recording there was an increase in recorded current. C: I-V curves for the instantaneous (ins) and steady state (ss) current components. After 25 minutes of recording there is an increase in the steady state current with no change in the instantaneous current. D: I-V curve for I_h shows a positive shift in activation (~ 6 mV, arrows) after 25 minutes of recording and an increase in amplitude. E: Plot of mean fast activation time constant as a function of voltage (mean \pm S.E.M., $n = 4$). Inclusion of 25 μM cAMP increases the rate of activation for I_h at potentials near activation. The mean difference at -75 mV (25 min - 5 min) was ~ 146 ms.

associated with I_h activation. Recordings taken after 25 minutes of whole cell access revealed a depolarizing shift in the activation threshold for I_h (-78.7 mV vs. -72.7 mV), an increase in I_{max} (127% of control), as well as an increased rate of activation, i.e., a decrease in the activation time constant. In addition, the resting membrane potential was depolarized by approximately 3 mV with no observed change in the instantaneous current consistent with a contribution of I_h to rest.

Figure 2.15 illustrates the concentration-response relationship for different pipette concentrations of cAMP (5, 10, 25, 50, 100 μ M) and the activation threshold, resting membrane potential, and % change in I_{max} . To pool data a sample of recordings from 4 to 7 neurons were collected for each concentration. Each recording was based on a single pipette concentration of cAMP. Recordings were taken 25 minutes after achieving whole cell access to ascertain that rundown did not occur and to allow for the transfer of cAMP to the cell interior. Control recordings, i.e., 0 added cAMP, were taken 5 minutes after whole cell puncture and assumed to represent normal basal conditions.

Over the concentration range examined there was a significant depolarizing shift in the activation threshold of I_h ($P = 0.0048$), increase in I_{max} ($P = 0.0001$) and depolarization of the resting membrane potential ($P = 0.0006$). The concentration-dependent shift in I_h activation was fitted by a Hill equation with a half maximal shift at $6.7 \pm 0.6 \mu$ M and a Hill coefficient of 1.6 ± 0.3 . Similarly, the half maximal shift and Hill coefficient for the resting membrane potential was $8.9 \pm 1.6 \mu$ M and 1.5 ± 0.4 , respectively. Comparisons of control conditions ($n = 7$) and 100 μ M cAMP ($n = 4$)

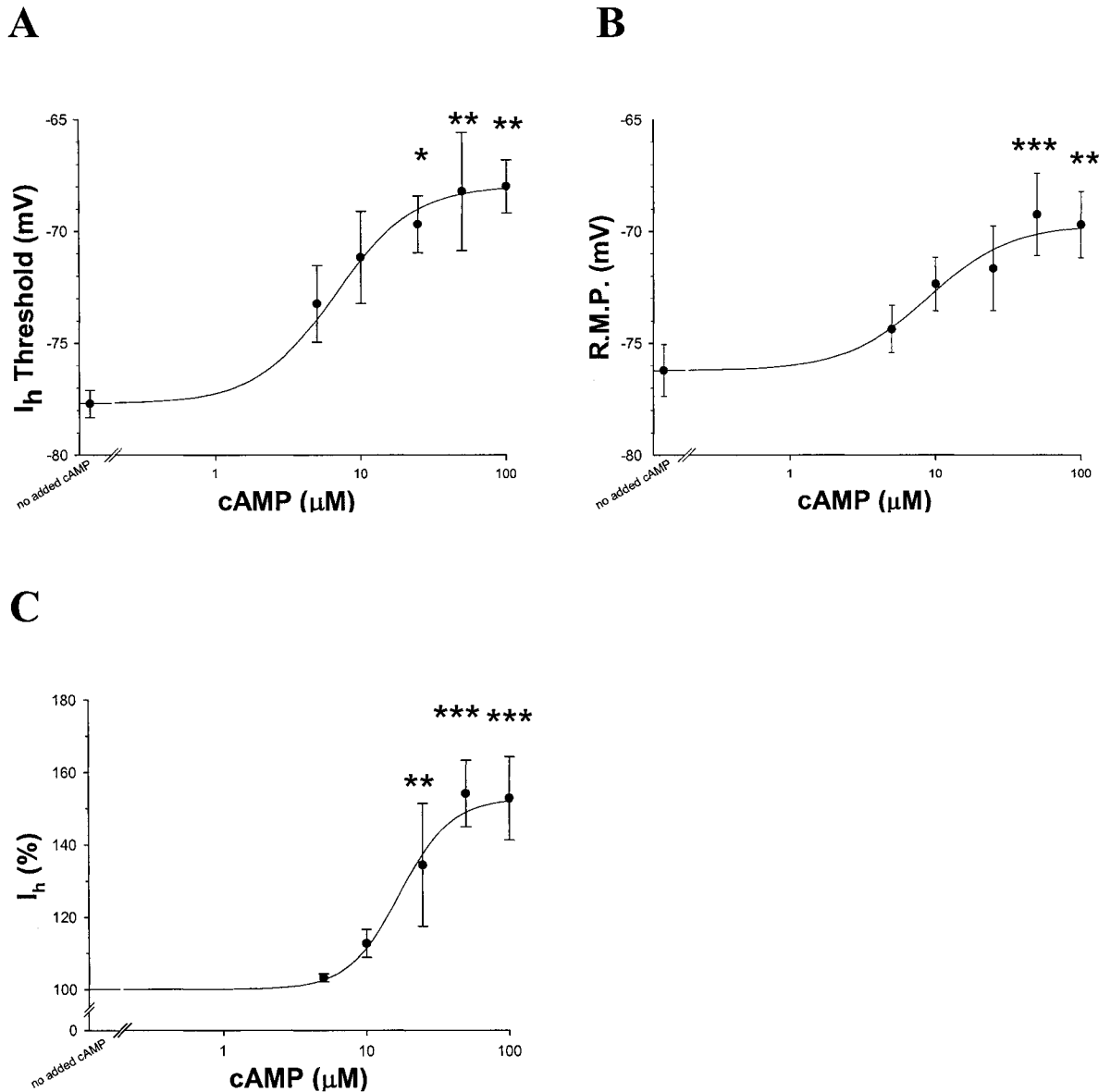


Figure 2.15 cAMP increases the amplitude of I_h and shifts the voltage dependence of I_h .

Pooled data (mean \pm S.E.M.). A, B, C: Added cAMP in the pipette was effective in inducing changes in I_h over a concentration range of 5 to 100 μM (100 μM , $n = 4$; 50 μM , $n = 7$; 25 μM , $n = 4$; 10 μM , $n = 7$; 5 μM , $n = 7$; control, $n = 7$). A: The I_h threshold is shifted in a depolarizing direction in a concentration dependent manner with a maximum shift of ~ 10 mV. B: The resting membrane potential (R.M.P.) is depolarized with increasing cAMP pipette concentrations with a maximum depolarization of ~ 6 mV indicating a contribution of I_h to the R.M.P. C: Change in I_h amplitude is plotted as the

mean change in I_h at -137 mV (I_{max}) as determined by $((I_{max} \text{ treatment} / I_{max} \text{ control}) \times 100)$ The amplitude of I_h (% of 5 minute recording) increased in a concentration-dependent manner by intracellular loading of cAMP. Maximum effect equalled $\sim 153\%$ of control. * $P < 0.05$, ** $P < 0.01$, *** $P < 0.001$ vs. control.

revealed an approximate 10 mV rightward shift in the activation threshold of I_h (77.7 ± 0.6 mV vs. 68.0 ± 1.2 mV, Bonferroni, $P < 0.01$). Over the same concentration range, the resting membrane potential was shifted from -76.2 ± 1.2 mV to -69.9 ± 1.5 mV, i.e. ~ 6 mV (Bonferroni, $P < 0.001$). As well, I_{\max} was significantly increased to 152.9 ± 11.5 % of control, (Bonferroni, $P < 0.001$). Unlike the cAMP-induced changes in activation and the resting membrane potential, however, both the half maximal shift (17.2 ± 1.5 μ M) and the Hill coefficient (2.4 ± 0.4) were almost twice as large. The latter may reflect not only cAMP-induced changes in g_h , but also changes in another current affecting the space clamp in a voltage-dependent manner.

2.3.7 Modulation of I_h occurs during intracellular cAMP application

To examine the possibility that a fixed basal level of intracellular cAMP is important to reveal the physiological modulation of I_h , the effects of compounds known to mimic parts of the cAMP cascade, with, and without, 1 μ M cAMP in the recording pipette were determined. This low concentration of cAMP was used to maintain a constant basal concentration of cAMP while at the same time not saturating cAMP levels before application of each compound, i.e., 1 μ M is near the base of the cAMP concentration curve for modulating I_h . These studies included raising the intracellular cAMP concentration by 3 min application of the membrane permeant cAMP analogue 8-bromo cAMP or forskolin, to stimulate intrinsic adenylyl cyclase. To ensure sufficient time for rundown to occur, and to ascertain the stability of I_h activation during internal

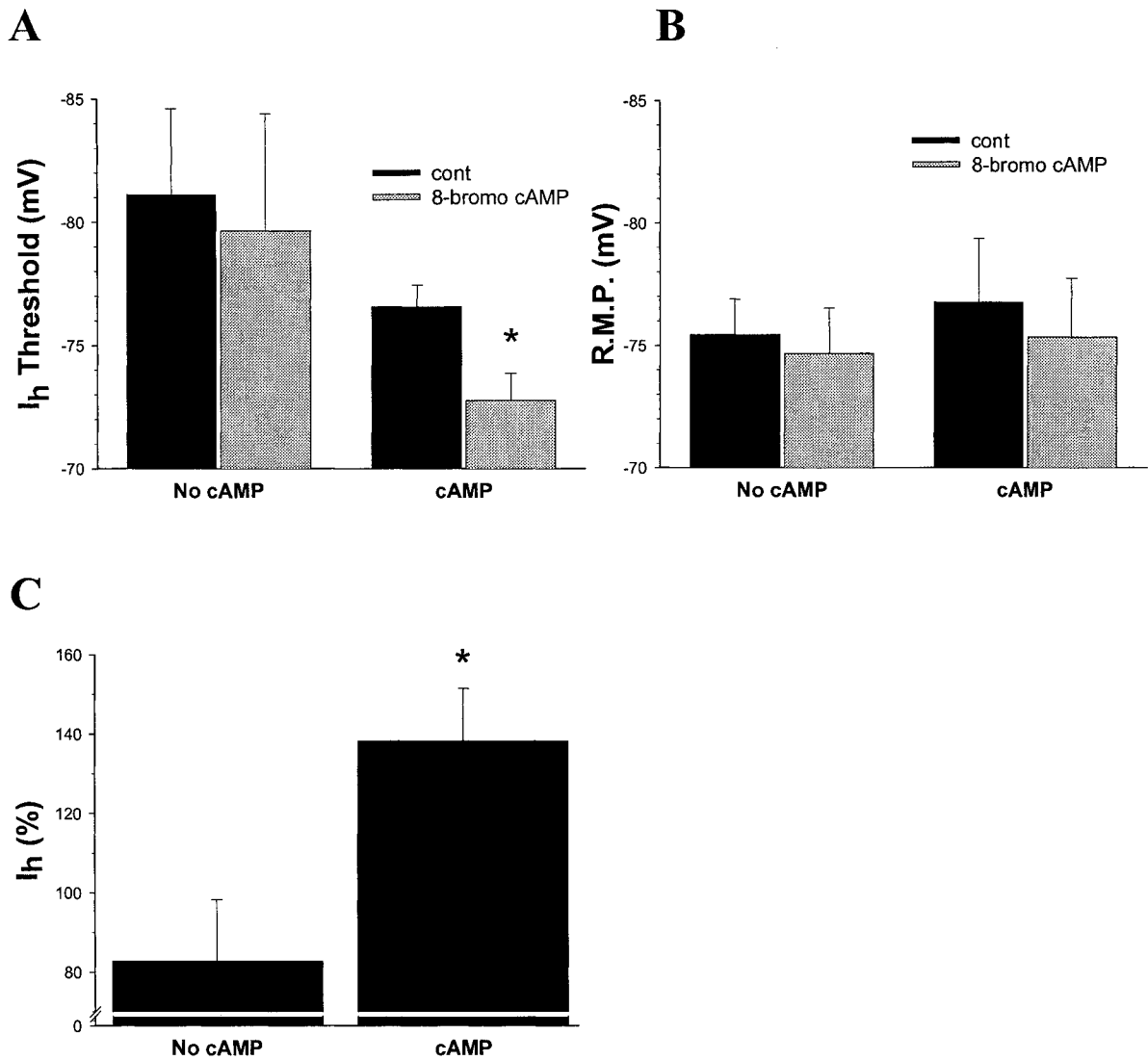


Figure 2.16 8-bromo cAMP shifts the voltage dependence of I_h in the presence of cAMP.

Pooled data (mean \pm S.E.M.). A: Histogram showing the effects of bath application of 8-bromo cAMP (1 mM) in the absence and presence of 1 μ M cAMP in the pipette solution on the activation threshold of I_h . With no cAMP present, bath application of 8-bromo cAMP did not significantly alter I_h activation when compared to control. With cAMP present in the pipette solution, bath application of 8-bromo cAMP results in a significant depolarizing shift of I_h activation. B: Histogram showing resting membrane potential with and without 1 μ M cAMP included in the pipette recording solution. Bath application of 8-bromo cAMP results in no apparent change in the resting membrane potential with and

without cAMP present in the pipette solution. C: Histogram showing the effects of 8-bromo cAMP on the amplitude of I_h (I_{max} as % of control) with and without 1 μ M cAMP present in the pipette recording solution. With no cAMP present in the pipette solution, bath application of 8-bromo cAMP did not significantly alter the amplitude of I_h . With cAMP present in the pipette solution, bath application of 8-bromo cAMP results in a significant increase in the amplitude of I_h . * $P < 0.05$ vs. control, $n = 3$.

application of 1 μ M cAMP, two controls were recorded at 5 min and 15 - 20 min, respectively.

2.3.7.1 cAMP analog

In the absence of added 1 μ M cAMP in the recording pipette solution, bath application of 8-bromo-cAMP (1 mM, 3 min, n = 3) did not alter the activation threshold of I_h (-81.1 ± 3.5 mV vs. -79.6 ± 4.8 , Bonferroni, $P > 0.05$), I_{\max} (82.8 ± 15.5 % of control, Bonferroni, $P > 0.05$) or the resting membrane potential (-75.4 ± 1.5 mV vs. -74.7 ± 1.9 mV, Bonferroni, $P > 0.05$) when compared to control (Figure 2.16). Although I_h exhibited rundown, application of 8-bromo cAMP prevented further rundown of I_h over the time period that test recordings were performed. Consistent with the prevention of rundown, control recordings made using recording pipettes containing 1 μ M cAMP resulted in the stable activation of I_h (~ -77 mV), compared to control recordings made in the absence of cAMP. Moreover, the presence of a fixed pipette concentration of cAMP unmasked the effects of bath application of 8-bromo-cAMP (1 mM, n = 3) resulting in a significant shift (~ 4 mV) in the activation threshold of I_h in the depolarizing direction (-76.6 ± 0.9 mV vs. -72.8 ± 1.1 mV, Bonferroni, $P < 0.05$) and an increase in I_{\max} (134.1 ± 15.6 % of control, Bonferroni, $P < 0.05$). Consistent with the small shift in the activation of I_h , there was no change in the resting membrane potential (-76.8 ± 2.7 mV vs. -74.4 ± 2.5 mV, Bonferroni, $P > 0.05$).

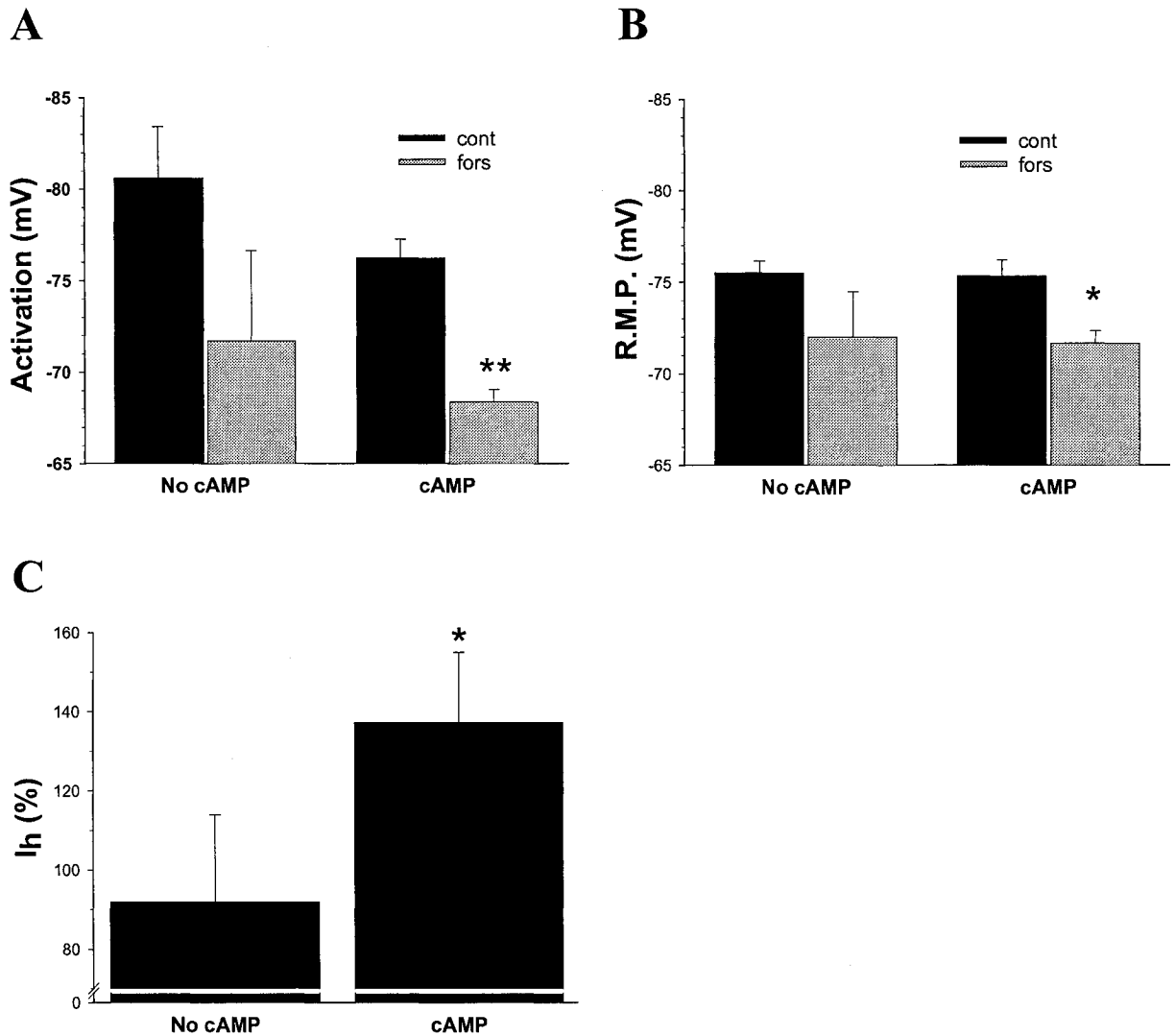


Figure 2.17 Forskolin shifts the voltage dependence of I_h in the presence of cAMP.

Pooled data (mean \pm S.E.M.). A: Histogram showing the effects of bath application of forskolin (fors, 50 μ M) on I_h activation in the absence and presence of 1 μ M cAMP in the recording pipette with no cAMP present, bath application of forskolin did not significantly alter I_h activation when compared to control (cont). With cAMP present in the pipette solution, bath application of forskolin results in a significant depolarizing shift in I_h activation. B: Histogram showing the effects of forskolin on the resting membrane potential with and without 1 μ M cAMP present in the pipette recording solution. With no cAMP present in the pipette solution, bath application of forskolin did not significantly alter the resting membrane potential when compared to control. With cAMP present in

the pipette solution, bath application of forskolin results in a significant depolarization of the resting membrane potential. C: Histogram showing the effects of forskolin on the amplitude of I_h (I_{max} as % of control) with and without 1 μ M cAMP present in the pipette recording solution. With no cAMP present in the pipette solution, bath application of forskolin did not significantly alter the amplitude of I_h . With cAMP present in the pipette solution, bath application of forskolin results in a significant increase in the amplitude of I_h . * $P < 0.05$, ** $P < 0.01$ vs. control, $n = 4$.

2.3.7.2 *Adenylyl cyclase activator*

Application of forskolin (50 μ M, $n = 4$) in the absence of cAMP failed to significantly alter I_h (Figure 2.17). There was, however, an observed mixing of stimulation and rundown during recording. Records taken just after completing the 3 minute forskolin application showed evidence of stimulation as evidenced by a depolarizing shift of the activation threshold of I_h in the depolarizing direction when compared to control (-80.6 ± 2.8 mV vs. -71.7 ± 4.9 mV, Bonferroni, $P > 0.05$) (Figure 2.17A). Subsequent voltage steps, however, revealed a reduction in the I_{max} (91.9 ± 22.0 % of control, Bonferroni, $P > 0.05$) (Figure 2.17B) and an apparent hyperpolarizing voltage shift in the I-V relationship (data not shown), indicating a rapid washout of the forskolin effect and rundown of I_h before completion of the voltage clamp protocol. In addition, there was no change in the resting membrane potential (-75.5 ± 0.6 mV vs. -72.0 ± 2.5 mV, Bonferroni, $P > 0.05$) (Figure 2.17C).

Similar to the results with the cAMP analog, the effects of forskolin were clearly revealed in the presence of added cAMP. With 1 μ M cAMP present in the recording pipette, bath application of forskolin (50 μ M, $n = 4$), resulted in a significant shift (~ 8 mV) in the activation threshold of I_h in a depolarizing direction (-76.2 ± 1.0 mV vs. -68.4 ± 0.7 mV, Bonferroni, $P < 0.01$) and a significant increase in I_{max} (137.2 ± 17.8 % of control, Bonferroni, $P < 0.05$). In keeping with previous observations, changes in I_h was accompanied by significant depolarization of the resting membrane potential (~ 4 mV) (-75.3 ± 0.9 mV vs. -71.7 ± 0.7 mV, Bonferroni, $P < 0.05$).

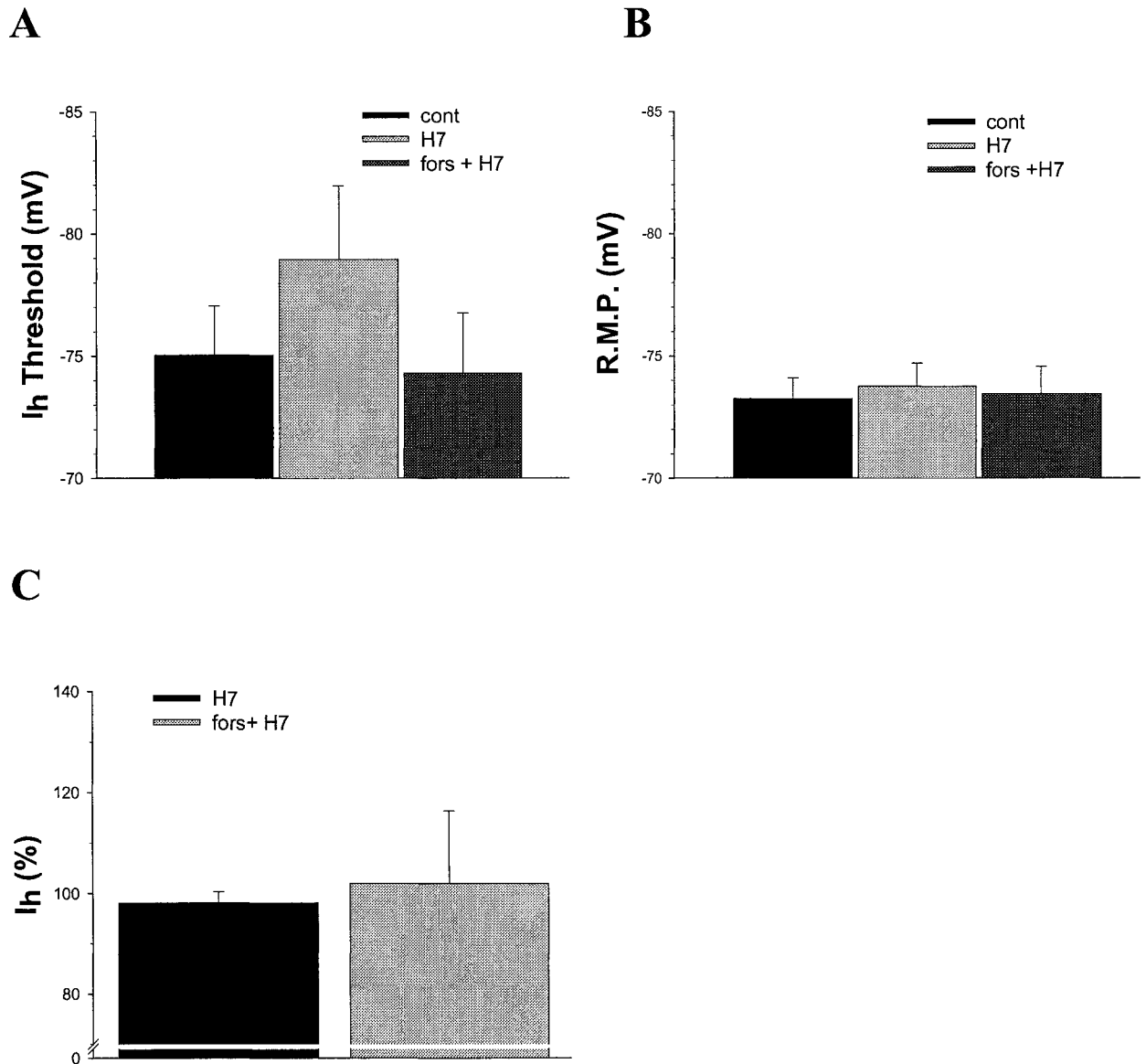


Figure 2.18 H7 blocks the forskolin-induced shifts in I_h voltage dependence.

Pooled data (mean \pm S.E.M., $n = 4$). A: Histogram showing the effects of bath application of H7 (100 mM) followed by co-application of H7 and forskolin (fors, 50 μ M) on I_h activation (1 μ M cAMP present in the pipette recording solution). H7 had no significant effect on the activation of I_h when compared to control (cont) and blocks the forskolin-induced depolarizing shift in I_h activation. B: Histogram showing the effects of bath application of H7 followed by co-application of H7 and forskolin on the resting

membrane potential. H7 had no significant effect on the resting membrane potential when compared to control and blocked the forskolin-induced depolarization. C: Histogram showing the effects of bath application of H7 followed by co-application of H7 and forskolin on the amplitude of I_h (I_{max} as % of control). H7 had no significant effect on the amplitude of I_h when compared to control and blocked the forskolin-induced increase.

2.3.8 Protein Kinase Inhibition

To investigate the possible involvement of phosphorylation through protein kinase stimulation in the modulation of the voltage- and time-dependent characteristics of I_h , forskolin (50 μM) was co-applied with H7 (100 μM), a nonspecific protein kinase inhibitor. H7 was continuously bath applied for the remainder of testing once control current samples were collected. To ascertain the stability of I_h activation during internal application of 1 μM cAMP, two controls were recorded at 5 and 15-20 minutes before H7 application. Voltage clamp protocol was taken 10 minutes after applying H7 to allow sufficient time for inhibition to occur.

Figure 2.18 shows pooled results for I_h measured in 4 neurons. H7 had no effect on the activation threshold I_h (-75.0 ± 2.0 mV vs. -78.9 ± 3.0 mV, Bonferroni, $P > 0.05$) or I_{max} (98.1 ± 2.2 % of control, Bonferroni, $P > 0.05$), nor did it alter the resting membrane potential (-72.3 ± 0.9 mV vs. -74.8 ± 0.9 mV, Bonferroni, $P > 0.05$). As well, H7 had no effect on the instantaneous component. In the presence of H7, forskolin was ineffective in altering I_h activation (74.8 ± 0.9 mV vs. -74.3 ± 2.5 mV, Bonferroni, $P > 0.05$), I_{max} (102.01 ± 14.4 % of control, Bonferroni, $P > 0.05$) or the resting membrane potential (-74.8 ± 0.9 mV vs. -73.8 ± 1.1 mV, Bonferroni, $P > 0.05$). The effects of H7 application implicate an involvement of a phosphorylation step that modulates the voltage- and time-dependent characteristics of I_h .

2.4 Discussion

2.4.1 cAMP prevents rundown of I_h

The slowly activated current activated by hyperpolarization in rat neocortical neurons displayed a biophysical and pharmacological profile characteristic of the profile for I_h found in other neuronal preparations. This includes a voltage-dependent current activation, voltage-dependent kinetics, sensitivity to external Cs^+ and irreversible blockade by ZD-7288 and a reversal potential of approximately -40 to -45 mV (Mayer and Westbrook, 1983; Uchimura et al., 1990; Harris and Constanti 1995; Khakh and Henderson, 1998; Funahashi et al., 2003).

Given the evidence that supports the direct regulation of I_h by cAMP (Tsien, Giles, and Greengard, 1972; Tokimasa and Akasu, 1990; Pedarzani and Storm, 1995) GTP and Mg ATP were added to the recording pipette solution, thus eliminating them as possible factors that underwent dialysis. This did not, however, rule out the possibility of a washout of intracellular cAMP or a factor or factors leading to a disruption of the G_s -adenylyl cyclase cascade governing the production of cAMP. Alreja and Aghajanian (1995) reported the loss of spontaneous firing in locus coeruleus neurons during whole cell recording was due to decreased production or wash out of endogenous cAMP, preventable by the addition of cAMP to the pipette solution. Similarly, Ferrier, Zhu, Redondo and Howlett (1998) showed the addition of 8-bromo-cAMP to the whole recording solution compensated for a disruption of the cAMP–PKA cascade preventing the loss of a voltage sensitive release mechanism for cardiac contractions in guinea pig ventricular myocytes. Similarly, rundown of calcium dependent potassium and chloride

currents measured in isolated cells from rat lacrimal glands was prevented by the internal application of inositoltrisphosphate (IP₃) suggesting that the washout substance was an unknown co-factor of phospholipase C or the GTP binding protein governing the production of IP₃ (Marty and Zimmerberg, 1989).

Without testing for another missing constituent, the addition of cAMP to the pipette solution was a quick test of this hypothesis. The absence of cAMP in the pipette solution resulted in an approximate 10 mV shift in the activation threshold of I_h in the hyperpolarizing direction after 15-20 minutes of recording. Conversely, the addition of 25 μM cAMP to the pipette solution occluded any rundown of I_h, produced a positive shift of I_h activation, increased the amplitude of I_h, and depolarized the resting membrane potential. These results support the notion that whole cell recording conditions leading to “rundown” of I_h in neurons proximal to layer V rat neocortex are dependent upon basal levels of intracellular cAMP.

The concentration-response relationship for cAMP was examined by varying the concentration of cAMP in the pipette over a range from 5 to 100 μM. Raising the cAMP concentration resulted in a 10 mV shift in I_h activation, consistent with the 7 to 10 mV depolarizing shifts observed with other neuronal preparations (Alreja and Aghajanian, 1995; Ingram and Williams, 1996; Raes et al., 1997; Frere and Luthi, 2004). As well, intracellular loading of cAMP revealed a concentration-dependent 6 mV depolarization of the resting membrane potential. Since there was no apparent change in the instantaneous current, the change in the resting potential is consistent with a contribution of I_h to resting equilibrium. This finding is also in keeping with previous findings that the

membrane potential hyperpolarizes following application of known blockers of I_h (Maccaferri et al., 1993; Pape, 1994, Raes et al., 1997; Doan and Kunze, 1999). The EC_{50} for cAMP ranged from 6.7 μM for the activation of I_h to 8.8 μM for the depolarization of the resting membrane potential. The EC_{50} for cAMP-induced changes in I_h amplitude was considerably higher (17.2 μM) suggesting more than one mechanism may be at play, e.g., reducing a masking conductance. However, one cannot rule out the possibility that this finding may be due to distortions in I-V relationship for I_h as a result of a poor space clamp. Each of the findings for cAMP concentration were substantially higher than the 0.2 μM to 0.55 μM range reported for dorsal root ganglion neurons, sino atrial nodes and the broadly distributed HCN2 isoform (DiFrancesco, 1994; Raes et al., 1997; Ludwg et al., 1998). Whether this reflects a real difference or degradation of cAMP in the patch pipette by intracellular phosphodiesterases (Alreja and Aghajanian, 1995) remains to be established.

2.4.2 Activation thresholds can be used to verify I_h I/V results

Initially, it was speculated that longer recording times might result in changes in the electrotonic conductive properties of the neuron due to a deterioration of the whole cell electrode seal or an increase in the neuron's active and/or passive instantaneous current components. In either case, one would expect a decrease in the membrane length constant due to a decrease in membrane resistance. This, in effect, would decrease the distance from the site of whole cell puncture that could be effectively voltage clamped in each neuron. For example, Schwindt and Crill (1997) showed that a block of calcium

activated potassium currents by tetraethylammonium chloride (TEA) in neocortical pyramidal neurons resulted in an increase in dendritically transmitted current as a result of a reduced shunting effect. This is also supported by observations made by Stuart and Spruston (1998) when recording from neocortical pyramidal apical dendrites. Utilizing simultaneous whole cell patch recordings from the soma and apical dendrites, they showed that a non-uniform distribution of Cs-sensitive and Cs-insensitive resting conductances generated "leaky" apical dendrites, which differentially influenced the integration of spatially segregated synaptic inputs. When these conductances were blocked, there was a significant decrease in the steady-state voltage attenuation and an increase in EPSP integration in a manner that depended on the location of the recording electrodes.

Similarly, studies have shown that activation of other currents that directly alter the membrane conductance, such as the potassium inward rectifier, I_{Kir} , can mask the appearance of I_h (Watts, Williams and Henderson, 1996; Cathala and Paupardin-Tritsch, 1999). Indeed, our findings from experiments involving the block of K^+ conductances suggest that an apparent modulation of I_h can be attributed to changes in the membrane conductance. While the addition of CsCl to the pipette solution partially overcomes this masking by blocking many K^+ channels, it does not provide a full block of all channels as evident from the additional block of K^+ channels resulting from the bath application of $BaCl_2$, TEA, and 4-AP. As well, the addition of CsCl to the pipette solution will not overcome the problem associated with the extensive dendritic branching characteristic of layer V neocortex pyramidal neuron morphology and the distribution of I_h channels. Due

to the size of the cells and the length and arborization of dendritic processes, the farther from the site of whole cell access, the less likely that the voltage across the membrane will be under the control of the voltage clamp. As a result, the membrane potential will deviate from the command potential as a function of the distance from the whole cell pipette.

These types of errors in the space clamp are well documented in large neurons, such as layer V pyramidal neurons and Purkinje neurons, and result in distortion of recorded I-V relationships, making it difficult to characterize neuronal currents (Spruston, Jaffe, Williams and Johnson, 1993; Roth and Hausser, 2001; Schaefer, Helmstaedter, Sakman and Korngreen, 2003; Castelfranco and Hartline, 2004). As well, due to the apparent non-uniform distribution of I_h , where the density of I_h channels increases along the somato-dendritic axis, I_h -induced attenuation increases with distance from the soma. This, in combination with the non-uniformity of imposed voltage, makes measurement of I_h less accurate at larger potentials. Utilizing I_h activation threshold can reduce space-clamp errors, since the current shunt is smaller near activation resulting in less attenuation of I_h . In addition, activation threshold data can be used to input theoretical I/V values and verify observed data in those cells where recordings appear to reach more isopotential conditions (Magee, 1998; Stuart and Spruston, 1998; Desjardins et al., 2003).

2.4.3 Modulation of I_h occurs during intracellular cAMP application

The present study provides two other lines of evidence which support a role for intracellular cAMP in regulating and maintaining I_h in neocortical pyramidal neurons.

First, the application of the membrane permeable cAMP analogue, 8-bromo-cAMP, mimicked the effect of intracellular loading with cAMP from the pipette. This effect was only observed during the co-presence of cAMP in the recording pipette. The effect is not surprising since, in the absence of a background concentration, it is difficult to demonstrate an imposed change in sub-membrane levels of intracellular cAMP. Secondly, the adenylyl cyclase activator, forskolin, produced a similar action to the cAMP analogue. Interestingly, in the absence of intracellular loading of cAMP, 3 min application of both forskolin and 8 bromo cAMP, although forskolin more so, delayed rundown of I_h , consistent with the stimulation of adenylyl cyclase and a resultant transient increase in sub-membrane levels of cAMP. The effect, however, rapidly washed out, presumably due to washout of the compounds from the bath and dialysis of the cell interior by the recording pipette.

In the presence of intracellular loading of cAMP, the application of 8-bromo-cAMP and forskolin produced an increase in the amplitude of I_h and reduced the time course of activation, consistent with effects reported for other preparations, including prepositus hypoglossi, sympathetic, nodose ganglion, primary afferent, primary auditory, CA1 hippocampus and area postrema neurons (Bobker and Williams, 1989; Tokimasa and Akasu, 1990; Ingram and Williams, 1994, Ingram and Williams, 1996; Chen, 1997; Bickmeyer et al., 2002; Funahashi et al., 2003).

Unlike forskolin, 8-bromo-cAMP did not produce as large a positive shift in I_h activation. While this inconsistency is difficult to explain, such variability is not uncommon. Opposite to the results produced by 8-bromo-cAMP, application of forskolin

in sino-atrial nodes produced a depolarizing shift in the activation curve of I_h , but did not increase the current amplitude (DiFrancesco et al., 1986). This may be the result of better voltage clamping in these cells where the neuron was iso-potential and, correspondingly, there was a uniform activation of I_h channels. In the present study, the increase in current amplitude observed after application of both forskolin and 8-bromo-cAMP may have resulted from activation of previously inactive channels, thus leading to an increased contribution of I_h . In addition, the lack of consistency may be the result of the heteromultimeric assembly of the HCN isoforms and other protein sub-units. While the molecular basis and the basic channel activation mechanism for I_h is likely the same in all tissue types, the efficacy and action of cAMP, its analogues, as well as activators of adenylyl cyclase may differ, accounting for the observed variations in channel kinetics. In the present study, this may explain the lack of a comparable activation shift of I_h by 8-bromo-cAMP. As a result, a full concentration dependency for each compound should be examined in future experiments. For example, studies employing cardiac tissue show the HCN1 isoform, the predominate channel expressed in the neocortex, to be far less responsive to the action of cAMP than HCN2 and HCN4 isoforms. In addition, variations in the gating mechanism of the S4 trans-membrane domain for each isoform may also help explain differences in the kinetics of I_h (Accili, Proenza, Baruscotti and DiFrancesco, 2002).

2.4.4 Protein kinase and I_h activation

Protein phosphorylation has long been identified as a major mechanism involved

with the regulation of ion channel function, as has been described for Ca^+ , K^+ and Na^+ channels (Reuter, Stevens, Tsien and Yellen, 1982; Trautwein and Hescheler, 1990; Cantrell, Smith, Goldin, Scheuer and Catterall, 1997; Hoffman and Johnson, 1998; Winklhofer, Matthias, Seifert, Stocker, Sewing, Herget, Steinhauser and Saaler-Reinhardt, 2003)

I_h is also regulated by protein phosphorylation. For example, the application of the protein kinase inhibitors, H7 and H8, shift the activation of I_h to more negative potentials in canine Purkinje fibres (Chang et al., 1991). Other experiments involving canine Purkinje fibers, isolated canine ventricular myocytes and rabbit sino-atrial node myocytes have shown the application of the phosphatase inhibitor calyculin A results in a positive shift in the activation of I_h , suggesting the involvement of phosphorylation (Yu et al., 1993, 1995; Accili, Redaelli and DiFrancesco, 1997). While these particular studies did not identify the specific kinase responsible, parallel experiments have suggested PKA involvement. Thus, in dissociated bullfrog sympathetic neurons, application of H8 decreases the peak amplitude of I_h , whereas the protein kinase C activator, phorbol 12-myristate 13-acetate, is without effect (Tokimasa and Akasu, 1990). In rat olfactory neurons, application of the specific PKA inhibitor, H89, induced a hyperpolarizing shift in $V_{1/2}$ and a decrease in current amplitude of I_h . Moreover, the activation of PKA with cBIMPS and the internal perfusion of the catalytic subunit of PKA right-shifted the activation of I_h , whereas the specific PKA peptide inhibitor blocked both effects (Vargas and Lucero, 2002).

In the present examination, the effects of H7 application implicate phosphorylation in the functional regulation of I_h in neocortical neurons. In the absence of forskolin, however, H7 did not significantly influence I_h suggesting there is little basal PKA activity and the requirement for increased levels of cAMP through the activation of the adenylyl cyclase.

Although the specific kinase involved was not examined, given the role of cAMP as a second messenger modulator of I_h , PKA is a likely candidate. In light of this, however, a possible role of other kinases, such as protein kinase C (PKC) or the tyrosine kinases, cannot be ruled out (Cathala and Paupardin-Tritsch, 1997; Wu and Cohen, 1997). This is further supported by the work of Vargas and Lucero (2002), who noted that application of the specific PKA inhibitor, H89, produced only a partial effect compared to K252a, a nonspecific protein kinase inhibitor, indicating that other unidentified kinases are involved, at least in their preparation.

2.4.5 Possible mechanisms of I_h rundown

Current rundown through numerous ion channels takes place when the membrane is excised or the cell is internally dialyzed. In either case, such treatment reveals the regulation of channel function by intracellular factors and that rundown can result from the loss of intracellular constituents or dephosphorylation (Forscher and Oxford, 1985; DiFrancesco et al, 1986; Horn and Korn, 1992; Oleson et al., 1993; Wang et al., 1993; Zhou and Lipsius, 1993; Hoshi, 1995; Hughes and Takahira, 1998; Simons and Schneider, 1998; Tang and Hoshi, 1999). In the present study, rundown of I_h was

accompanied by a decrease in current amplitude and a decreased rate of activation, suggesting a loss of I_h channels in the open state as well as a change in gating kinetics. Rundown was prevented by intracellular loading of cAMP but was not mimicked by application of protein kinase inhibitors. This suggests the observed changes in I_h may be the product of more than one process.

Whereas the presence of the CNBD in the HCN channel confirms a direct rather than a phosphorylation-dependent activation of I_h , it does not discount the possibility of secondary regulation of I_h function via phosphorylation of I_h directly or phosphorylation of a protein modifying the kinetics of I_h . For example, the description of I_h cyclic nucleotide and voltage dependent kinetics by the allosteric voltage-dependent gating model (Section 1.3) provides a plausible mechanism for phosphorylation that may act to increase the probability of the open state, thus allowing for the preferential binding of cAMP, or changes in the sensitivity of I_h to voltage (DiFrancesco, 1999; Altomere, Bucchi, Camatini, Baruscotti, Viscomi, Moroni, and DiFrancesco, 2001).

Another possible mechanism may involve an indirect masking of I_h due to an increase in a secondary conductance. Based on the results from section 2.3.3, an increase in potassium currents over time could result in an increasing decay of the effectiveness of the voltage clamp and a shunt of recorded I_h . As well, given the low affinity of the HCN1 isoform for cAMP in the neocortex, the observed increase in I_h activation with added cAMP and block by protein kinase inhibition might be in part the result of their actions on a masking conductance. For example, the reduction of I_{Kir} in neuronal and myocyte culture preparation, a current which shares a similar activation range as I_h , has been shown

to depend on increased levels of cAMP and PKA activation (Koumi, Wasserstrom and Ten Eick, 1995a,b; Wischmeyer and Karschin, 1996; Takigawa and Alzheimer, 1999). Similarly, in studies involving principal neurons of the rat substantia nigra pars compacta, Cathala and Paupardin-Tritsch (1999) suggested that an observed inhibition of I_h by noradrenaline and dopamine was secondary to a shunting effect induced by the activation of the I_{Kir} .

3. Histamine H₂ receptors modulate the hyperpolarization-activated current (I_h) in rat neocortical neurons

3.1 Introduction

In Chapter 2 it was shown that (1) a fixed level of intracellular cAMP is required for the maintenance of the hyperpolarization activated current, I_h, in rat neocortical neurons and (2) cAMP can shift the voltage kinetics of I_h in a concentration dependent manner. Given these findings, it reasonable to presuppose that I_h in neocortical neurons is subject to modulation by a number of endogenous compounds known to activate and inhibit the adenylyl cyclase cascade. However, this has yet to be shown. A potential candidate for modulating I_h in the neocortex is histamine.

Unlike other brain areas where histaminergic axons are randomly oriented and irregularly spaced, innervation of the neocortex forms a distinct plexus of evenly distributed fibers innervating layers II-VI. The exception is layer I where there is a slight increase in fiber density and parallel orientation to the pial surface. Despite the lower density of innervation, autoradiography and *in situ* hybridization studies show high densities of each receptor subtype in the neocortex with only minor pattern differences across species (Hass and Panula, 2003).

H₁ receptor binding in the neocortex of the rat and guinea pig is observed in all neocortical layers with a higher density observed in layer VI (Palacios et al., 1981; Bouthenet et al., 1988). In the guinea pig, these results were confirmed by means of H₁ mRNA localization (Traiffort et al., 1994). Similarly, H₁ receptor binding is observed in

all neocortex areas and layers of humans and monkeys. In addition to layer VI, however, higher densities of H₁ receptors are also observed in layer V (Martinez-Mir et al., 1990).

In the rat neocortex, H₃ receptor binding is observed in all neocortical areas and layers with a higher density rostrally and in layers IV-VI (Pollard et al., 1993). Similar patterns were observed for H₃ mRNA expression (Pillot et al., 2002).

In guinea pig, monkey and human neocortex, H₂ receptor binding sites are dense in layers I-III, moderate in layers V-VI and low in layer IV. (Ruat et al., 1990; Martinez-Mir et al., 1990; Vizuete et al., 1997; Honrubia et al., 2000). In monkey and human, *in situ* hybridization studies confirm the receptor binding results (Honrubia et al., 2000). There are, however, some conflicting results from *in situ* hybridization studies of guinea pig. Here, H₂ receptor mRNA was more dense in layers III and V with low to moderate densities in layers I, II, IV and layer VI, respectively (Vizuete et al., 1997). This may however, be explained by differences in the somatic location of protein synthesis and the location of receptor expression, which is most likely occurring in the dendrites that overlay multiple neocortical layers.

Although histamine plays diverse roles in the CNS, there is limited evidence for histamine action in the neocortex. Neocortical H₁ receptors are predominantly linked to excitatory responses through two mechanisms: first, a calcium-independent reduction of a background potassium leak (I_{K1}) shown in human neocortex, resulting in membrane depolarization and facilitation of signal transmission due to a decrease in membrane conductance (Reiner and Kamondi, 1994), and secondly, a facilitation of the N-methyl-

D-aspartate (NMDA) receptor-mediated depolarization shown in rats (Payne and Neuman, 1997).

Neocortical H₃ receptors have been studied more extensively and have been shown to be involved in a number of physiological effects. This includes inhibition of histamine synthesis and metabolism (Arrang et al, 1987; Garbarg, Tuong, Gros and Schwartz, 1989; Oishi, Itoh, Nishibori and Saeki, 1989; Yates, Tedford, Gregory, Pawlowski, Handley, Boyd and Hough, 1999) and histamine release (Arrang et al., 1985; Westerink et al., 2002; Lamberty, Margineanu, Dassel and Klitgaard, 2003). The H₃-induced decrease in neocortical histamine activity has also been shown to be inversely correlated with the incidence of spindles and with spectral power of low frequency (1-5 Hz) EEG activity in freely behaving rats. However, the exact mechanism of this relationship was not investigated (Valjakka, Vartiainen, Kosunen, Hippelainen, Pesola, Olkkonen, Airaksinen, Tuomisto, 1996). In addition to regulation of histamine synthesis and release, neocortical H₃ receptors have been shown to regulate the release of a number of other neocortical transmitters including acetylcholine (Blandina et al., 1996; Blandina et al., 1996; Passani and Blandina, 1998), noradrenaline (Fink et al., 1994; Schlicker et al., 1994; Schlicker et al., 1989) and serotonin (Schlicker et al., 1988; Fin et al., 1990).

A well-documented action of neocortical histamine is the H₂ receptor activation of adenylyl cyclase and resultant increase in intracellular cAMP (Baudry et al., 1975; Hegstrand et al., 1976; Psychoyos, 1978; Al-Gadi and Hill, 1987). To date, however, neocortical H₂ receptors have only been shown to potentiate excitation through a reduction of I_{AHP} resulting in a decrease in action potential spike adaptation (McCormick

and Williamson, 1991, McCormick, 1992; McCormick, Pape and Williamson, 1991; McCormick, Wang and Huguenard, 1993)

Although the neocortex has a higher density of the hyperpolarization-activated cyclic nucleotide-gated cationic 1 (HCN1) channels (Moosmang et al., 1999; Monteggia et al., 2000, Notomi and Shigemoto, 2004), which have a lower affinity for cAMP (Kaupp and Seifert, 2001; Viscomi et al., 2001), histamine modulation of neocortical I_h is plausible. First, HCN2 channel isoforms, which have a higher affinity for cAMP (Kaupp and Seifert, 2001; Viscomi et al., 2001), have been found to be colocalized with HCN1 on the most distal dendrites of pyramidal neurons (Notomi and Shigemoto, 2004). Second, the apparent coexistence of I_h and H_2 receptors on neocortical dendrites suggests H_2 activation, via activation of adenylyl cyclase, could modulate I_h . A similar mechanism is observed in thalamic relay neurons, that have a high density of HCN2, and hippocampal pyramidal neurons that have a high density of both HCN1 and HCN2, where H_2 receptor activation of adenylyl cyclase results in an enhancement of I_h by shifting its activation kinetics to more positive potentials (McCormick and Williamson 1991; Storm et al., 1996; Moosmang et al., 1999; Monteggia et al., 2000, Notomi and Shigemoto, 2004). This excitatory action may act to switch neuronal activity from burst to single spike firing which is associated with shifts from slow-wave sleep to waking and attentiveness (Pape and McCormick, 1989; McCormick and Williamson, 1991, McCormick, Pape and Williamson, 1991). Hutcheon et al (1996a,b) has also suggested a similar role for the modulation of I_h and resonance leading to the promotion of accurate neural transmissions of specific frequencies. Similarly, due to the higher density of I_h in

neocortical dendrites (Stuart and Spurston, 1998; Williams and Stuart, 2000; Berger et al., 2001; Lorincz et al., 2002), an increase in I_h conductance can negatively influence dendritic spatial integration of synaptic input (van Brederode and Spain, 1995; Schwindt and Crill, 1997; Stuart and Spurston, 1998; Williams and Stuart, 2000; Berger et al., 2001; Berger, Senn and Luscher, 2003).

Based upon the results in chapter 2, which show that stable levels of cAMP can modulate I_h in the neocortex, it was hypothesized that histamine should shift the voltage kinetics of I_h in a concentration-dependent manner via H_2 receptor activation of adenylyl cyclase.

3.2 Methods and Materials

(For detailed methods see Section 2.2.) To prevent current rundown of I_h and to maintain a constant basal concentration of cAMP, while at the same time not saturating cAMP levels, 1 μ M cAMP was added to the pipette-solution in all the present experiments. To ascertain that rundown had not occurred controls were taken at 5 and 25 mins after whole cell rupture. Compounds in this study included forskolin (Sigma), H7 dihydrochloride (RBI), histamine (Sigma), amthamine dihydrobromide (Tocris), diphenhydramine hydrochloride (RBI), pyrilamine maleate (RBI), thioperamide maleate (RBI) and tiotidine (Tocris).

3.3 Results

3.3.1 Histamine modulates I_h

Using the procedure outlined in Chapter 2 for isolating the instantaneous and I_h current components, the effect of histamine on 23 neurons proximal to layer V neocortex was characterized using whole cell voltage clamp recordings. Figure 3.1 illustrates control currents recorded in response to a series of -10 mV voltage steps (5s) from a holding potential of -57 mV to -137 mV and the current voltage (I-V) relationships for the isolated components plotted as a function of voltage. Using the same voltage protocol, bath application of 50 μ M histamine increased the overall current compared to control (Figure 3.1B). Figure 3.1C shows the I-V relationships of the instantaneous and steady state currents for control conditions and in the presence of histamine. The instantaneous and steady state current components were isolated as described in Chapter 2 methods. Note that histamine produced an increase in the steady state current with little or no change in the instantaneous current when compared to control. Figure 3.1D shows the isolated I_h (subtracting the instantaneous from the steady state currents) for control conditions and after the application of histamine. Histamine results in a more depolarized activation of I_h (-78.3 mV vs. -68.6 mV) as well as a substantive increase in I_{max} (153.7% of control).

The effectiveness of histamine was examined by determining the concentration-response relationship for I_h activation and amplitude using five concentrations of histamine (1, 5, 10, 20, 50 μ M). Histamine significantly shifted the activation of I_h in a

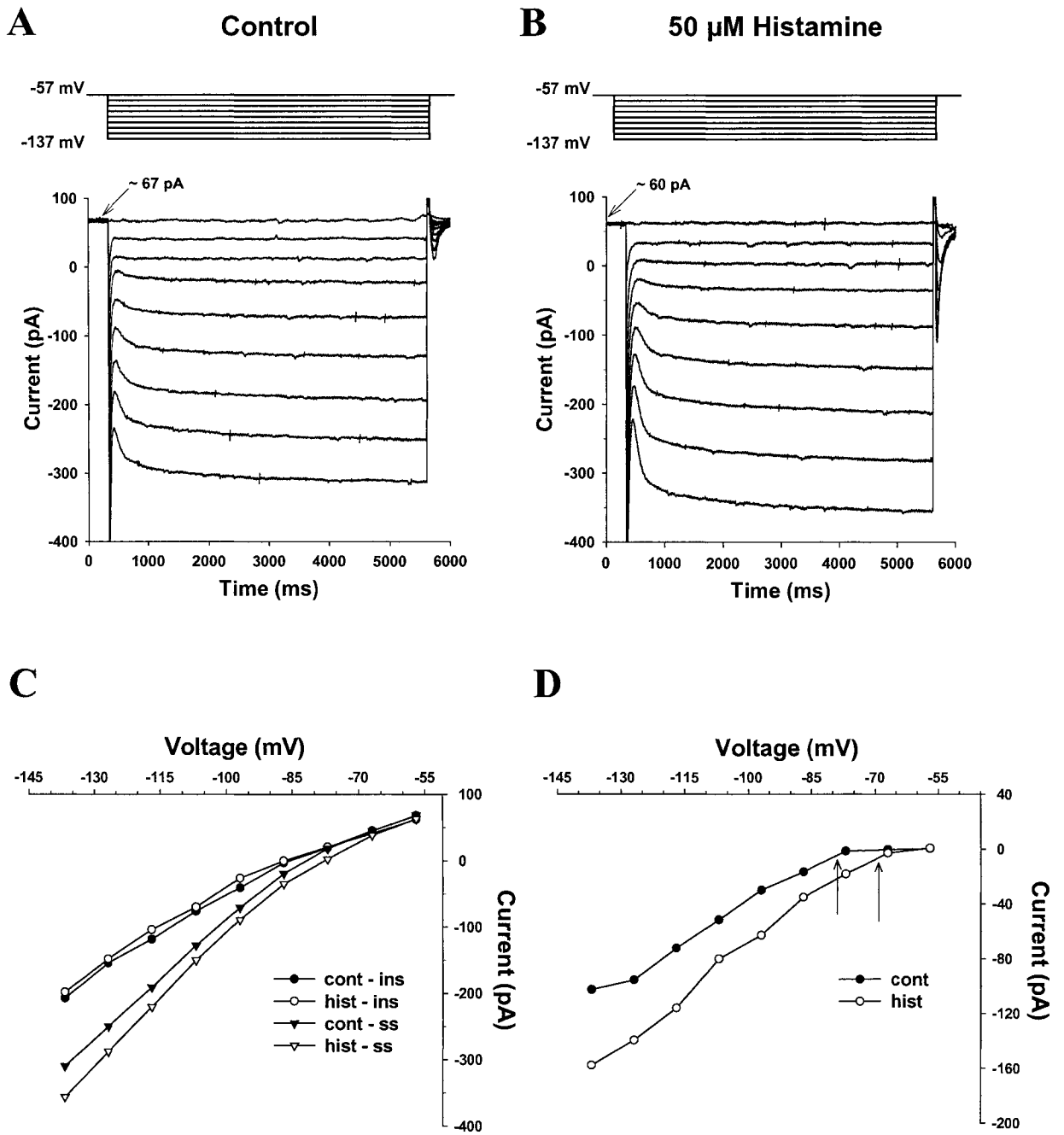


Figure 3.1 Histamine increases I_h .

A: The hyperpolarizing voltage steps (top) elicited the activation of a time-dependent current response that reflects I_h . (see Chapter 2) B: (same neuron as in A) Application of 50 μ M histamine (hist) increased the amplitude of the steady state current (ss) in a

voltage dependent manner. Application of histamine also resulted in a depolarization of the resting membrane potential by approximately 3 mV as evidenced by decrease in the current (~ 7 pA) required to maintain the neuron at a holding potential of -57 mV (arrows). C: I-V curves showing the isolated instantaneous (ins) and steady state currents as a function of the step voltage, in control conditions (cont) and in the presence of histamine. Both instantaneous and steady state currents are derived from exponential fits to the slowly activating inward current allowing for the isolation of I_h from the instant and capacitive component curves (see Chapter 2). Histamine increased the steady state current at all voltage steps negative to -67 mV, but had little effect on the instantaneous current. D: I-V curves for I_h derived from the subtraction of the instantaneous and steady state components for control and histamine. Application of histamine resulted in an increase in current amplitude and an earlier activation (arrows) when compared to control.

depolarizing direction ($P = 0.0009$) and increased I_{\max} in a concentration-dependent manner ($P = 0.0001$) (Figure 3.2A,C). Comparisons of control ($n = 7$) and $50 \mu\text{M}$ histamine ($n = 6$) shows an approximate 9 mV shift in I_h activation (-77.6 ± 1.3 mV vs. -69.1 ± 1.2 mV, Bonferroni, $P < 0.01$) and 165.4 ± 7.5 % (Bonferroni, $P < 0.001$) increase in I_{\max} . The concentration-dependent shift in I_h activation was fitted by a Hill equation with a half-maximal shift at $4.1 \pm 0.3 \mu\text{M}$ and a Hill coefficient of 1.9 ± 0.1 . Fitting the concentration-dependent increase in the amplitude of I_h revealed a higher half-maximal increase at $7.5 \pm 0.3 \mu\text{M}$ and a Hill coefficient of 2.6 ± 0.3 indicating a different efficacy of histamine on the conductance of I_h .

Consistent with the contribution of I_h to rest, histamine also significantly depolarized the resting membrane potential in a concentration-dependent manner ($P < 0.018$) with a maximum depolarization of 4 mV (Bonferroni, $P < 0.05$) (Figure 3.2B). Similar to the concentration-dependent shift in I_h activation, the concentration dependent effect of histamine on the resting membrane potential reached a half-maximal depolarization at $5.6 \pm 0.7 \mu\text{M}$ and a Hill coefficient of 1.7 ± 0.3 .

Figure 3.3 shows fast activation time constants plotted as a function of voltage in control conditions and after application of $50 \mu\text{M}$ histamine. Time constants were determined from the exponential fits of I_h and fitted with a best-fit exponential curve. Consistent with a shift in the activation kinetics of I_h , the activation time of I_h is decreased in the presence of histamine when compared to control (a difference of ~ 456 ms at -77 mV).

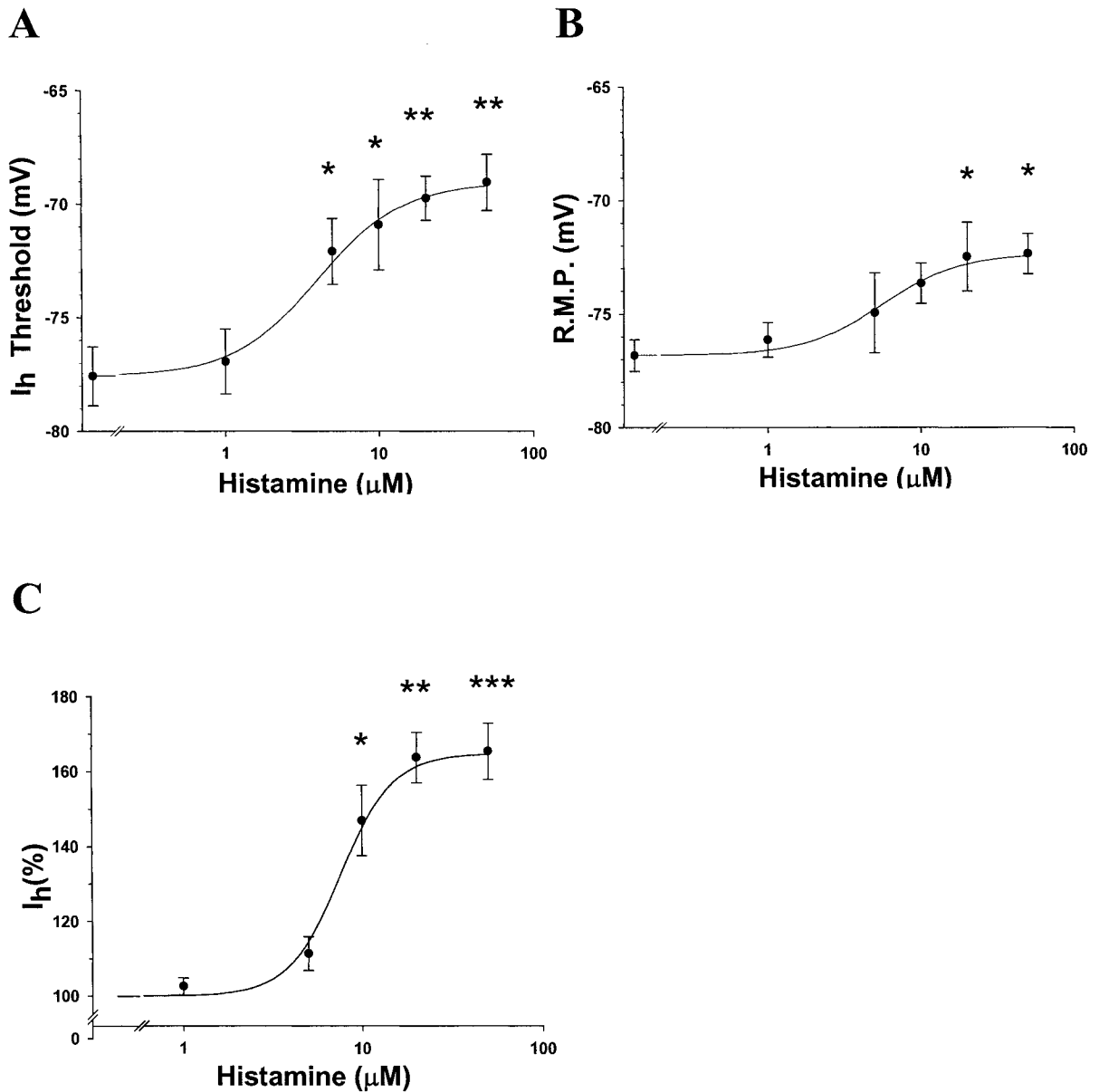


Figure 3.2 Concentration-response relationships for histamine.

Pooled data (mean \pm S.E.M). A, B, C: Histamine was effective in inducing changes in I_h over a concentration range of 1 to 50 μM (control, $n = 7$; 1 μM , $n = 6$; 5 μM , $n = 3$; 10 μM , $n = 3$, 20 μM , $n = 5$; 50 μM , $n = 6$). A: The I_h threshold is shifted in a depolarizing direction in a concentration-dependent manner with a maximal shift of ~ 8 mV. B: The resting membrane potential (R.M.P.) is depolarized with increasing histamine concentrations with a maximal depolarization of ~ 4 mV indicating a contribution of I_h to

the R.M.P.. C: Change in I_h amplitude is plotted as the mean change in I_h at -125 mV (I_{max}) as determined by $((I_{max} \text{ treatment} / I_{max} \text{ control}) \times 100)$. Increasing histamine concentration results in a concentration-dependent increase in I_{max} . Maximum effect for $50 \mu\text{M}$ histamine equalled $\sim 165\%$ of control. $*P < 0.05$, $** P < 0.01$, $*** P < 0.001$ vs. control.

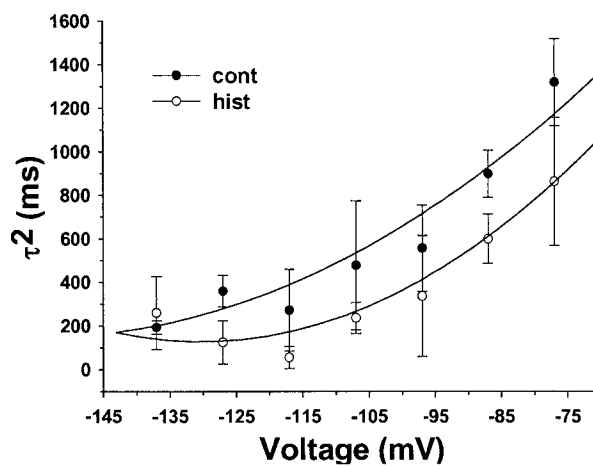


Figure 3.3 Histamine increases the fast activation time (τ^2) constant for I_h .

Pooled fast activation time constants ($\tau^2 \pm$ S.E.M., $n = 6$). Plot of time constant as a function of voltage. Bath application of 50 μ M histamine (hist) results in a faster activation of I_h at more depolarized potentials. The mean difference at -77 mV (cont - hist) was ~ 456 ms.

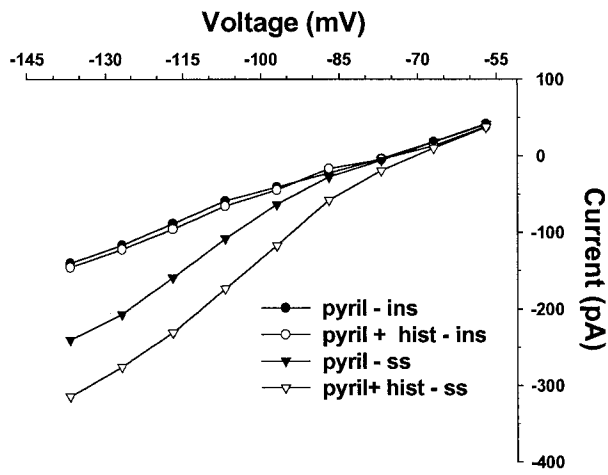
From these data it was concluded that histamine shifts the voltage- and time-dependent kinetics of I_h to more depolarized potentials, as well as increasing I_h . Since histamine did not alter the instantaneous current over the voltage range examined it seems plausible that the effects on I_h are not the result of unmasking following the reduction of another current.

3.3.2 *Effects of histamine are blocked by the H₂ antagonist, tiotidine*

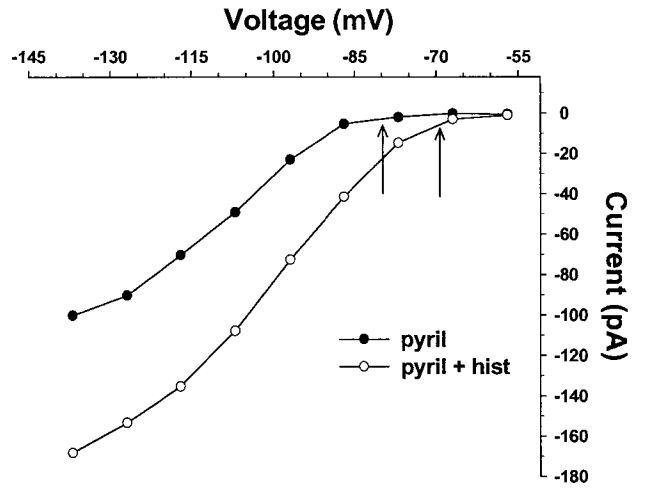
To determine the receptor subtype mediating the histamine response, experiments were repeated in the presence of a number of histamine antagonists. These included the H₁ antagonists, pyrilamine and diphenhydramine, the H₂ antagonist, tiotidine, and the H₃/H₄ antagonist, thioperamide. Histamine effects did not readily wash out so antagonists were bath applied continuously after control recordings and tested after 10 minutes followed by application of 50 μ M histamine.

Figure 3.4 shows that the H₁ antagonist, pyrilamine, fails to block the histamine-induced effects on I_h . I-V curves of steady state and instantaneous components shows that histamine in the presence of pyrilamine results in an increase in the steady state current with little change in the instantaneous current when compared to pyrilamine alone (Figure 3.4A). Subtraction of I_h revealed the previously observed patterns of histamine effects including a shift in I_h activation (-80.0 mV vs. -69.1 mV) and an increase in I_{max} (-100.1 pA vs. 168. pA) (Figure 3.4B). Pooled data (n = 4) show that histamine in the presence of pyrilamine, compared to pyrilamine alone, produces a significant shift in the activation threshold of I_h from -76.1 ± 1.8 mV to -69.9 ± 0.9 mV (~ 6 mV) (Bonferroni, *P*

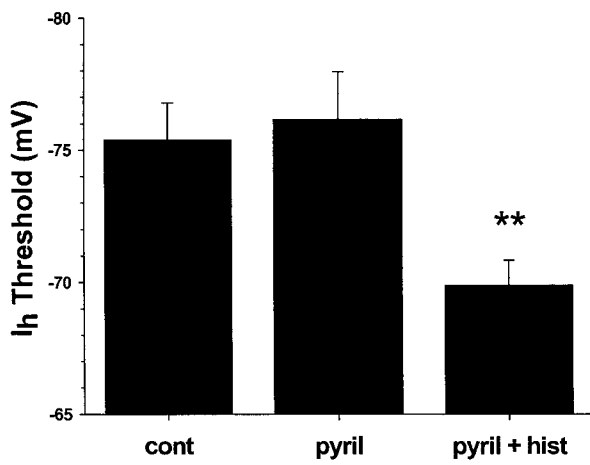
A



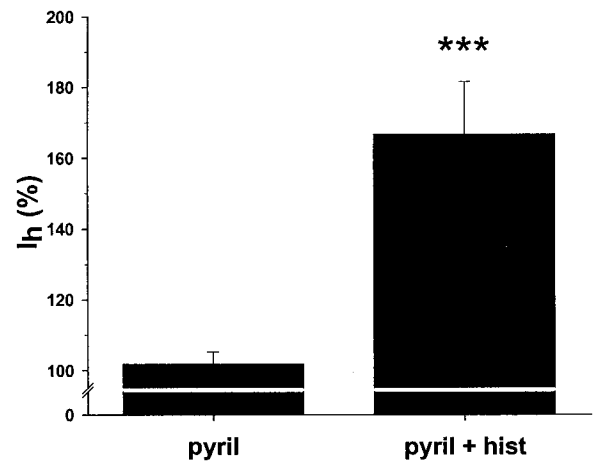
B



C



D



E

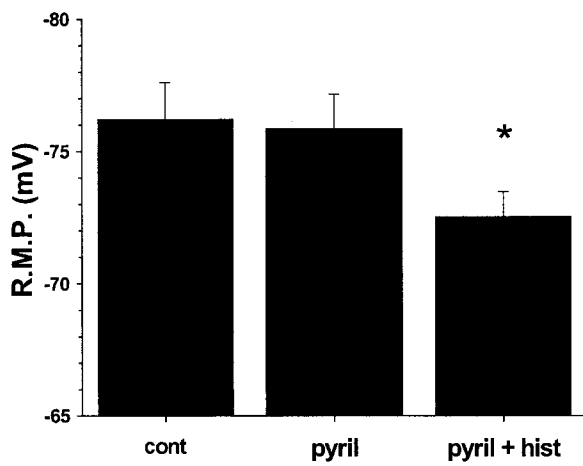


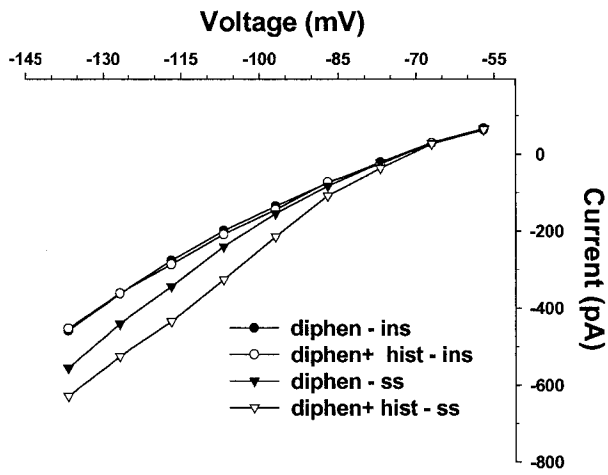
Figure 3.4 The H₁ antagonist, pyrilamine fails to block the histamine-induced effects on I_h.

A: I-V curve of the isolated instantaneous (ins) and steady state (ss) currents as a function of voltage, in 1 μ M pyrilamine (pyril), and 50 μ M histamine in the presence of pyrilamine (pyril + hist). Application of histamine in the presence of pyrilamine increased the steady state current with no effect on the instantaneous current. B: I-V curves for I_h (same neuron as in A). Histamine increased the current amplitude and produced earlier activation (arrows) despite the presence of pyrilamine. C, D, E: Pooled data (mean \pm S.E.M.). C, D: Histamine resulted in a significant depolarized shift in the activation threshold of I_h and a significant increase in the amplitude of I_h (I_{max} as % of control) despite the presence of pyrilamine. D: Histamine induced a significant depolarization of the resting membrane potential (R.M.P.) despite the presence of pyrilamine. * $P < 0.05$, ** $P < 0.01$, *** $P < 0.001$ vs. pyril, n = 4.

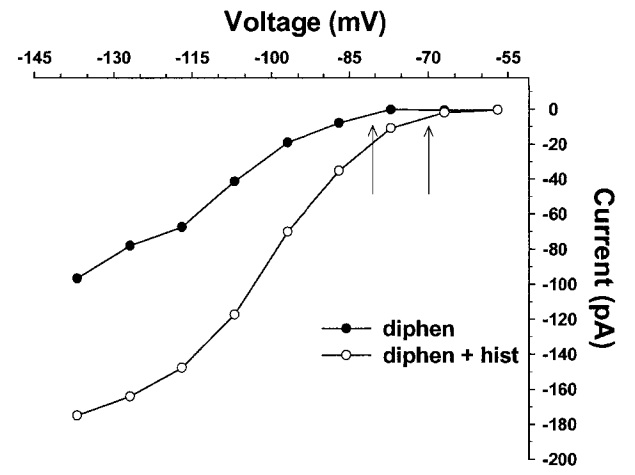
< 0.01) and a significant increase in I_{\max} from $101.9 \pm 3.4\%$ to $166.7 \pm 14.9\%$ of control (Bonferroni, $P < 0.001$) (Figure 3.4C,E). Similarly, histamine significantly depolarized the resting membrane potential from -75.9 ± 1.3 to -72.5 ± 0.9 mV (~ 3 mV) (Bonferroni, $P < 0.05$). There was no difference between control conditions and pyrilamine in I_h activation, I_h amplitude, or the resting membrane potential (Bonferroni, $P > 0.05$). There was also no difference between the effects of histamine when applied alone and when applied in the presence of pyrilamine (Bonferroni, $P > 0.05$) (Figure 3.15A,B,C). Similar experiments involving diphenhydramine produced comparable results (Figure 3.5).

Figure 3.6 shows that the H_3/H_4 antagonist, thioperamide, also failed to block the histamine-induced changes in I_h and the resting membrane potential. In the presence of thioperamide, histamine produced an increase in the steady state current with no change in the instantaneous current (Figure 3.6A). Isolation of I_h revealed a positive shift in the activation threshold of I_h (-81.4 mV vs. -76.1 mV) and an increase in I_{\max} (148.7% of control) (Figure 3.6B). Pooled data ($n = 4$) show that histamine in the presence of thioperamide, compared to thioperamide alone, produces a significant shift in the activation threshold of I_h from -76.7 ± 1.6 mV to -70.5 ± 0.9 mV (~ 6 mV) (Bonferroni, $P < 0.01$) and a significant increase in I_{\max} from $100.6 \pm 4.6\%$ to $169.9 \pm 7.2\%$ of control (Bonferroni, $P < 0.001$) (Figure 3.6C,E). Consistent with previous observations, histamine also significantly depolarized the resting membrane potential from -75.5 ± 0.6 to -72.1 ± 1.1 mV (~ 3 mV) (Bonferroni, $P < 0.05$). There was no difference between control conditions and thioperamide for I_h activation and amplitude or the resting membrane potential ($P > 0.05$). In keeping with the absence of a thioperamide block,

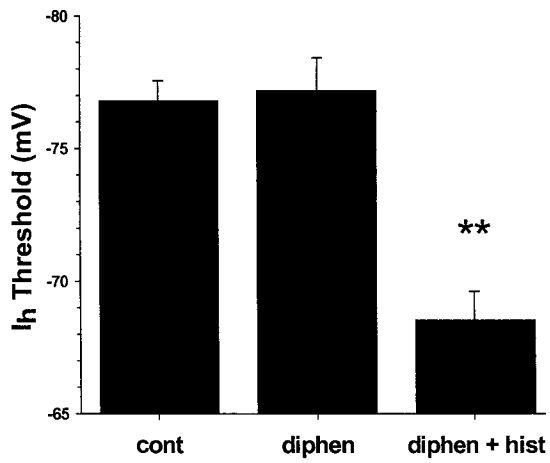
A



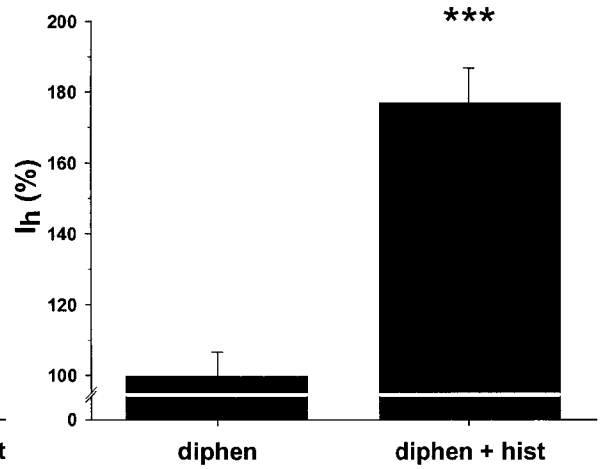
B



C



D



E

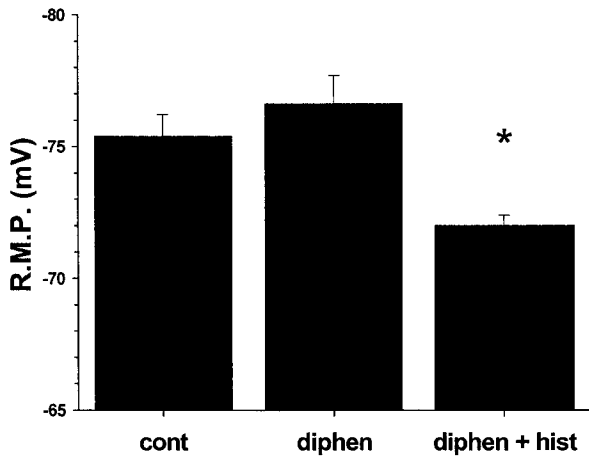


Figure 3.5 The H₁ antagonist, diphenhydramine fails to block the histamine effects on I_h.

A: I-V curve of the isolated instantaneous (ins) and steady state (ss) currents as a function of voltage, in 1 μ M diphenhydramine (diphen) and 50 μ M histamine in the presence of diphenhydramine (diphen + hist). Application of histamine in the presence of diphenhydramine increased the steady state current with no effect on the instantaneous current. B: I-V curves for I_h (same neuron as in A). Histamine increased the current amplitude (96.7 pA vs. 175.0 pA) and produced earlier activation (-80.4 mV vs. -71.0 mV, arrows) despite the presence of diphenhydramine. C, D, E: Pooled data (mean \pm S.E.M.). C, D: Histamine resulted in a significant depolarized shift in the activation threshold of I_h (-77.2 ± 1.2 mV vs. -68.5 ± 1.1 mV, $P < 0.01$) and a significant increase in the amplitude of I_h (99.7 ± 6.8 % vs. 176.8 ± 9.9 % of control, $P < 0.001$) despite the presence of diphenhydramine. D: Histamine induced a significant depolarization of the resting membrane potential (R.M.P.) despite the presence of diphenhydramine (-76.6 ± 1.1 mV vs. -72.0 ± 0.4 mV, $P < 0.05$). * $P < 0.05$, ** $P < 0.01$, *** $P < 0.001$ vs. diphen, n = 4.

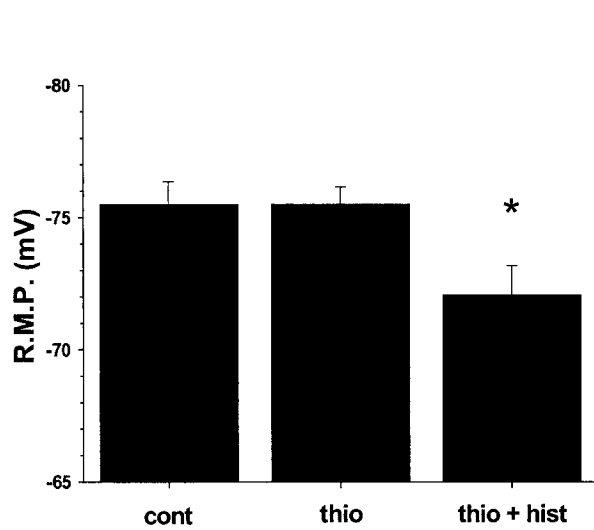
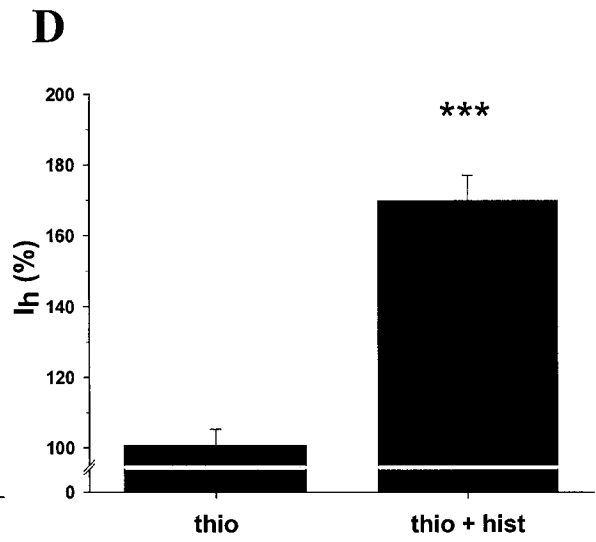
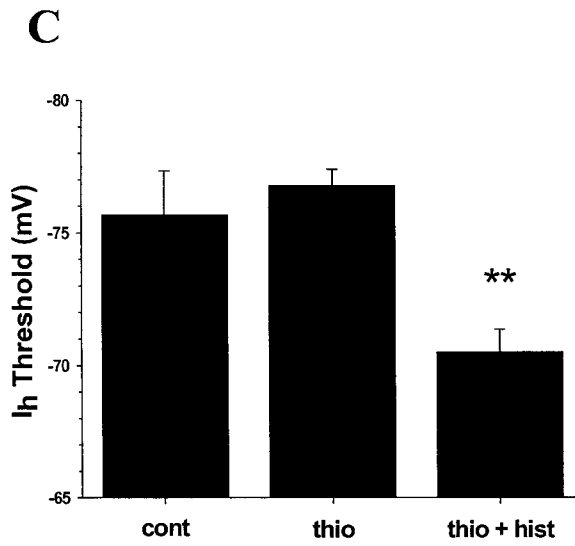
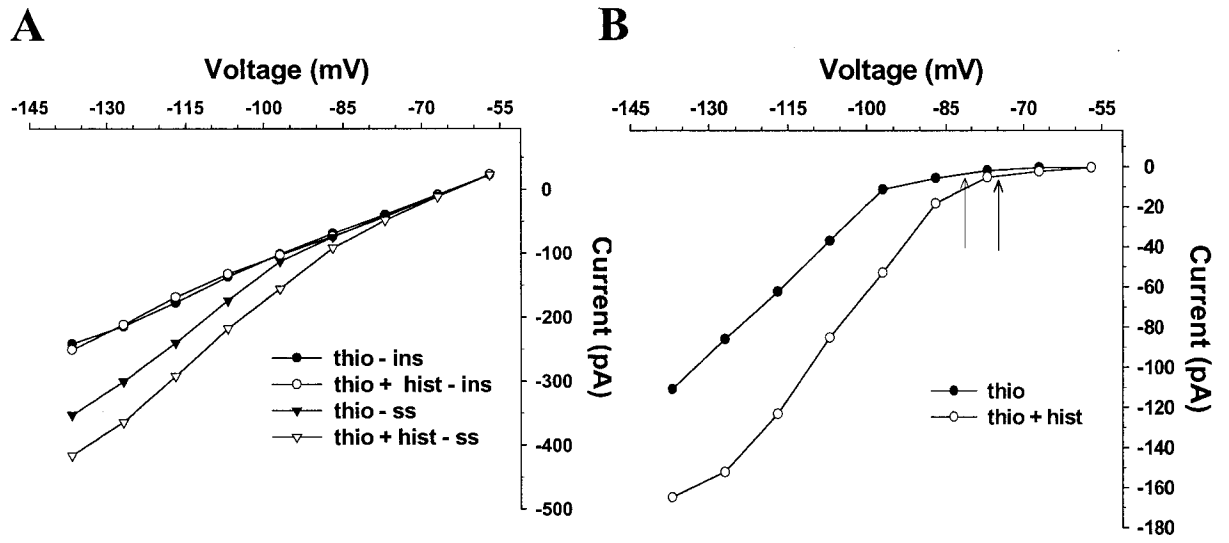


Figure 3.6 The H₃/H₄ antagonist, thioperamide (thio), does not block histamine-induced increase in I_h.

A: I-V curve showing the isolated instantaneous (ins) and steady state (ss) currents as a function of voltage, in 1 μ M thioperamide (thio) and 50 μ M histamine in the presence of thioperamide (thio + hist). Application of histamine in the presence of thioperamide increased the steady state current at all voltage steps negative to -67 mV with no effect on the instantaneous current. B: Isolated I-V curve for I_h (same neuron as in A). Histamine increased the current amplitude and produced earlier activation (arrows) despite the presence of thioperamide. C,D,E: Pooled data (mean \pm S.E.M.) C, D: Histamine resulted in a significant depolarized shift in the activation threshold of I_h and a significant increase in the amplitude of I_h (I_{max} as % of control) despite the presence of thioperamide. D: Histamine induced a significant depolarization of the resting membrane potential (R.M.P.) despite the presence of thioperamide. * $P < 0.05$, ** $P < 0.01$, *** $P < 0.001$ vs. thio, n = 5.

there was no difference between the effects of histamine applied alone and applied in the presence of thioperamide (Bonferroni, $P > 0.05$) (Figure 3.15A,B,C).

Unlike the H_1 and H_3/H_4 antagonists, the H_2 antagonist, tiotidine, blocked the histamine-induced effects. Figure 3.7 shows that tiotidine (500 nM) blocked the histamine-induced increase in the steady state current and prevented the depolarizing shifts in the activation threshold of I_h (-77.8 mV vs. -77.2 mV) as well as the increase in I_{max} (102.0% of control). Figure 3.8 shows the concentration-response relationships for 4 different concentrations of tiotidine (5, 10, 100, 500 nM) on the histamine-induced effects on I_h activation, I_h amplitude and the resting membrane potential. Tiotidine significantly blocked the histamine-induced shift in I_h activation ($P = 0.0063$), increase in amplitude ($P = 0.0001$) and depolarization of the membrane potential ($P = 0.0173$) in a concentration-dependent manner (see Table 3.1 for IC_{50} and Hill coefficient values). Comparisons of histamine control conditions ($n = 6$) and histamine in the presence of 500 nM tiotidine ($n = 4$) show a near complete block of the histamine-induced shift in the activation threshold of I_h (-69.1 ± 1.2 vs. -75.7 ± 1.2 mV, Bonferroni, $P < 0.05$) and increase in I_{max} (165.4 ± 7.5 % vs. 105.2 ± 9.3 %, Bonferroni, $P < 0.001$) (Figure 3.8A,C). As well, consistent with a tiotidine block of histamine shift in the activation threshold of I_h , there was also no apparent change in I_h activation time (Figure 3.9). A similar blocking effect was observed for the histamine-induced depolarization of the resting membrane potential (-72.4 ± 0.9 mV vs. -75.7 ± 0.8 mV, Bonferroni, $P < 0.05$) (Figure 3.8C).

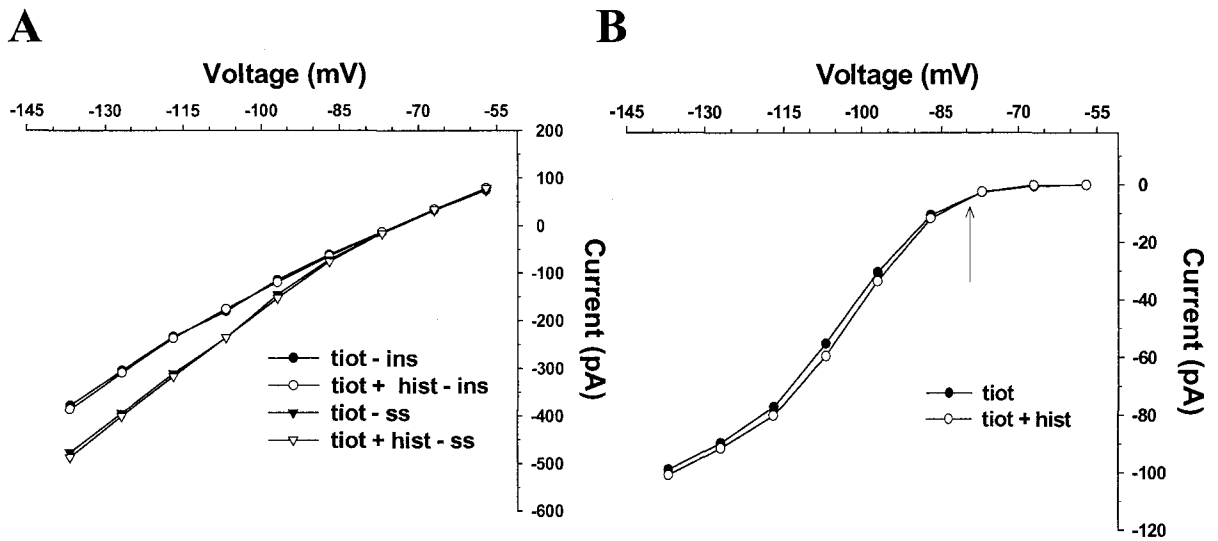


Figure 3.7 The H_2 antagonist, tiotidine blocks the histamine-induced increase in I_h .

A: I-V curves showing the isolated instantaneous (ins) and steady state (ss) currents as a function of voltage, in 500 nM tiotidine (tiot) and 50 μ M histamine in the presence of tiotidine (tiot + hist). Tiotidine blocked the histamine-induced increase in the steady state current at all voltage steps with no effect on the instantaneous current. B: Isolated I-V curves for I_h . Tiotidine prevents the histamine-induced increase in current amplitude and early activation (arrow).

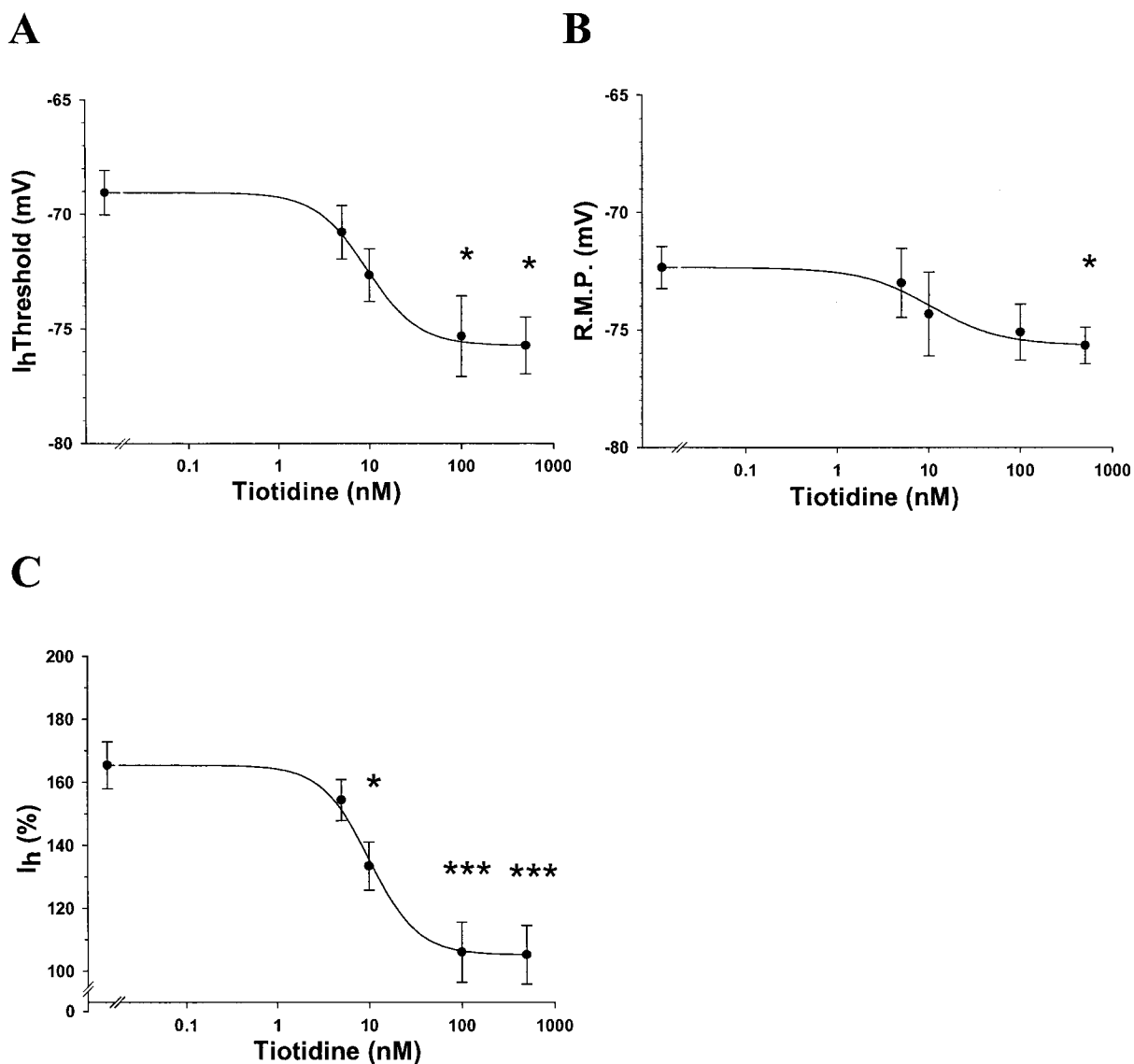


Figure 3.8 Tiotidine antagonizes the action of histamine on I_h in a concentration dependent manner.

Pooled data (mean \pm S.E.M.). Tiotidine antagonized histamine-induced changes in I_h over a concentration range of 5 to 500 nM (control, $n = 4$; 5 nM, $n = 3$; 10 nM, $n = 3$; 100 nM, $n = 2$, 500 nM, $n = 4$). Each neuron was exposed to one concentration of tiotidine followed by a single application of 50 μ M histamine. A: Plot of mean threshold for I_h shows a concentration-dependent block of the histamine-induced depolarized shift in early I_h activation. B: Block of histamine-induced depolarization of the resting membrane potential (R.M.P.). D: Tiotidine blocks the histamine-induced increase in I_h amplitude (I_{max} as a % of control). $P > 0.05$, $*P < 0.05$, $***P < 0.001$ vs. control.

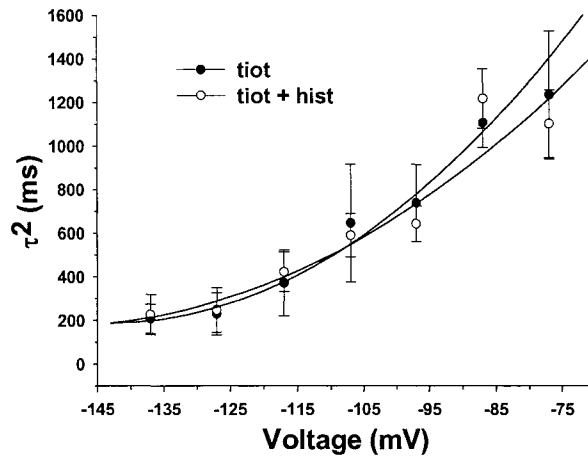


Figure 3.9 Tiotidine reduces the histamine induced decrease in the fast activation time (τ^2) constant for I_h .

Pooled data (mean \pm S.E.M., $n = 4$). Plot of the fast activation time constant for I_h as a function of voltage in 500 nM tiotidine (t_{iot}) and 50 μ M histamine in the presence of tiotidine (t_{iot + hist}). Tiotidine reduces the histamine induced decrease in activation time for I_h . The mean difference at -77 mV (t_{iot} - (t_{iot + hist})) was ~134 ms (compare to Figure 3.3).

The results from the antagonist experiments indicate that the histamine effects on I_h and the resting membrane potential are mediated through the H_2 receptor subtype.

Table 3.1 Tiotidine concentration-response values for I_h and the resting membrane potential.

Effect	IC ₅₀ (nM)	Hill coefficient
I_h activation threshold	10.1 ± 1.2	1.3 ± 0.2
I_h amplitude	10.1 ± 0.6	1.7 ± 0.1
resting membrane potential	10.6 ± 3.2	1.1 ± 0.5

3.3.3 Effects of histamine are mimicked by the H_2 agonist amthamine

To further confirm that histamine was acting via H_2 receptors, experiments were conducted using the H_2 specific agonist amthamine. Figure 3.10 shows the effects of amthamine (25 μ M) for a sample neuron. Bath application of amthamine resulted in an increase in the steady state current with no effect on the instantaneous current as well as a depolarizing shift in the activation threshold of I_h (-79.6 mV vs. -71.5 mV) and an increase in I_{max} (157.2 % of control). These effects were similar to the observed histamine effects shown in Figure 3.1.

Concentration response relationships were constructed using 4 concentrations of amthamine (0.5, 1, 10, 25 μ M) (Figure 3.11). Amthamine significantly shifted the activation threshold of I_h ($P = 0.0011$), increased I_h amplitude ($P = 0.0002$) and

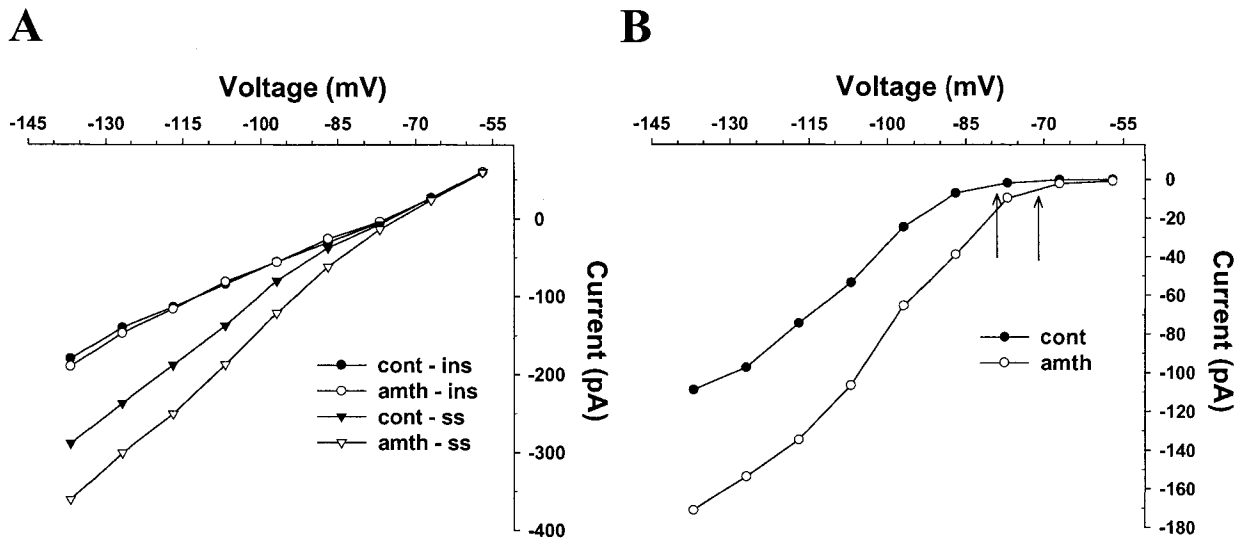


Figure 3.10 The H_2 agonist, amthamine, increases I_h .

A: I-V showing the isolated instantaneous (ins) and steady state (ss) currents as a function of voltage, in control conditions (cont, solid circles and triangles) and in the presence of 25 μ M amthamine (amth). Application of amthamine increased the steady state current at all voltages negative to -67 mV with no effect on the instantaneous current. B: Isolated I-V curves for I_h (same neurons as in A). Application of amthamine resulted in an increase in current amplitude and earlier activation (arrows) similar to the effect of histamine shown in Figure 3.1 D.

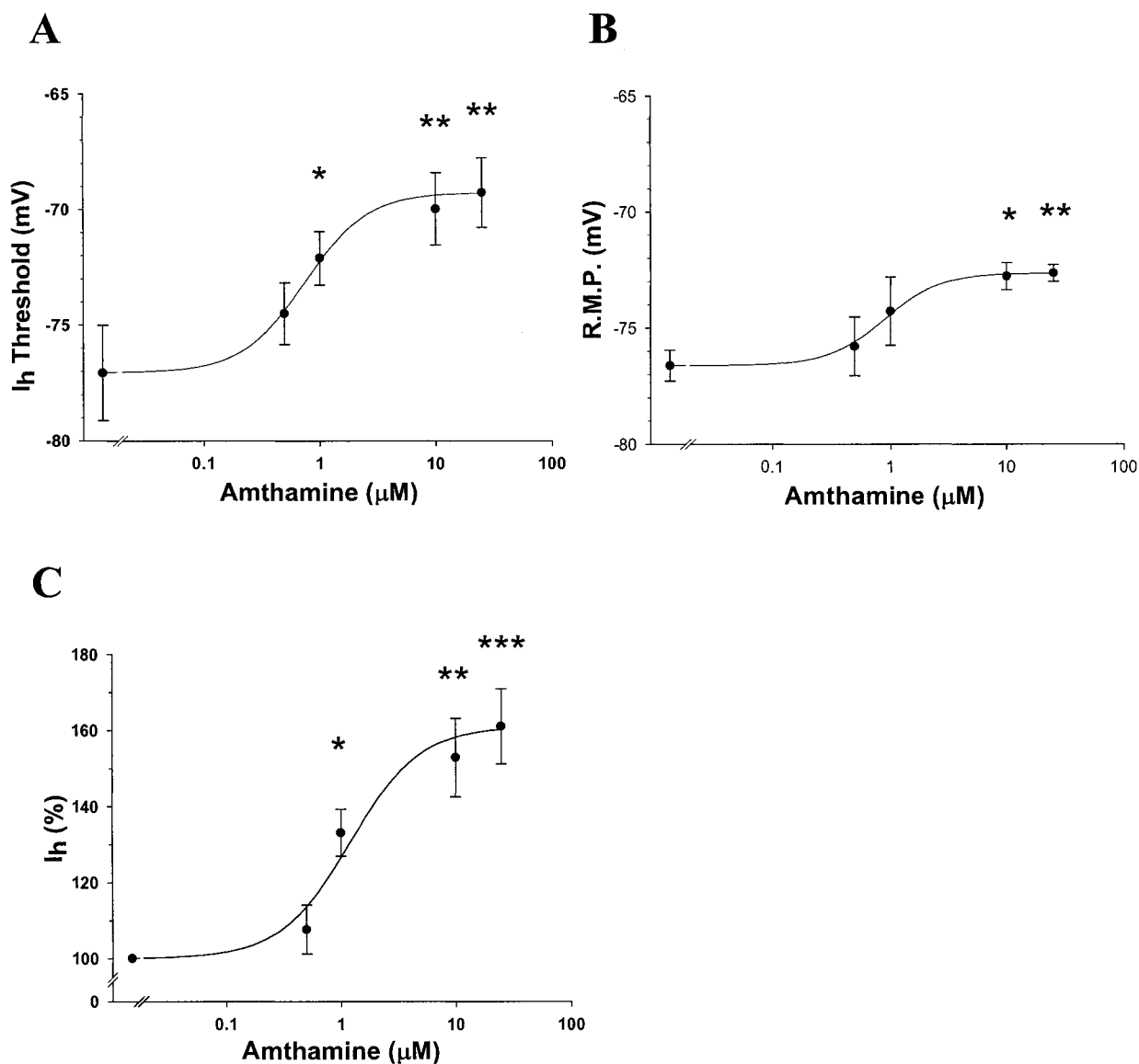


Figure 3.11 Concentration-response relationships for amthamine.

Pooled data (mean \pm S.E.M.). A, B, C: Amthamine was effective in inducing changes in I_h over a concentration range of 0.5 to 25 μ M (control, $n = 3$; 0.5 μ M, $n = 3$; 1 μ M, $n = 4$; 10 μ M, $n = 4$, 25 μ M, $n = 3$). A: The activation threshold of I_h was significantly shifted in a depolarizing direction with a maximum shift of ~ 8 mV. B: In keeping with I_h contribution to rest, the R.M.P. was depolarized with increasing amthamine concentrations with a maximum depolarization of ~ 4 mV. C: Increasing amthamine concentrations also results in a concentration dependent increase in the amplitude of I_h (I_{max} as % of control). The maximum effect equalled 161% of control. * $P < 0.05$, ** $P < 0.01$, *** $P < 0.001$ vs. control.

depolarized the resting membrane potential ($P = 0.0192$) in a concentration-dependent manner (see Table 3.2 for EC_{50} and Hill coefficient values). Comparison of control conditions ($n = 3$) and 25 μM amthamine ($n = 3$) revealed a significant depolarizing shift (~ 8 mV) in the activation threshold of I_h (-77.1 ± 2.1 vs. -69.3 ± 1.5 , Bonferonni, $P < 0.001$). The maximum concentration-dependent increase in I_{max} was 161.1 ± 9.9 % of control (Bonferonni, $P < 0.001$). The maximum depolarization in the resting membrane potential was 4 mV (-76.6 ± 0.7 vs. -72.6 ± 0.4 , Bonferonni, $P < 0.05$). Similar to histamine, amthamine also decreased the activation threshold time of I_h (a difference of ~ 472 ms at -77 mV) (Figure 3.12).

Table 3.2 Amthamine concentration response values for I_h and the resting membrane potential.

Effect	EC_{50} (nM)	Hill coefficient
I_h activation threshold	0.7 ± 0.1	1.6 ± 0.4
I_h amplitude	1.2 ± 0.3	1.4 ± 0.2
resting membrane potential	0.9 ± 0.0	2.0 ± 0.1

3.3.4 Adenylyl cyclase activator forskolin mimics histamine-induced actions on I_h

Given the evidence that H_2 receptors couple to adenylyl cyclase resulting in an increased formation of intracellular cAMP, the combined effects of histamine and forskolin, an activator of adenylyl cyclase was investigated. Figure 3.13 shows the

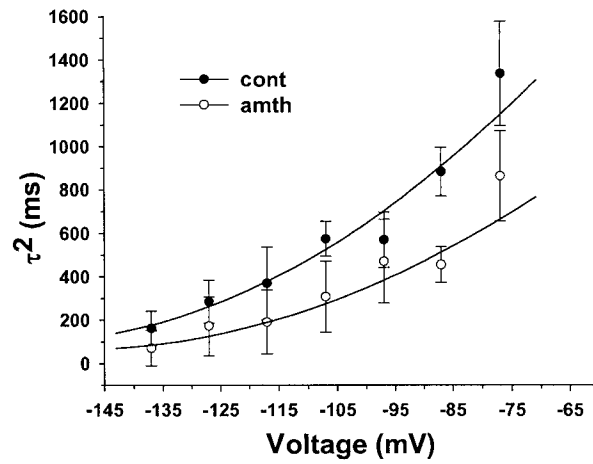


Figure 3.12 The H₂ agonist, amthamine, decreases the fast activation time constant (τ^2) for I_h.

Pooled data (mean \pm S.E.M., n = 3). Plot of the fast activation time constant for I_h as a function of voltage. Similar to the effects of histamine found in Figure 3.3, the application of amthamine (amth) results in a faster activation of I_h at more depolarized potentials. The mean difference at -77 mV (cont – amth) was \sim 472 ms.

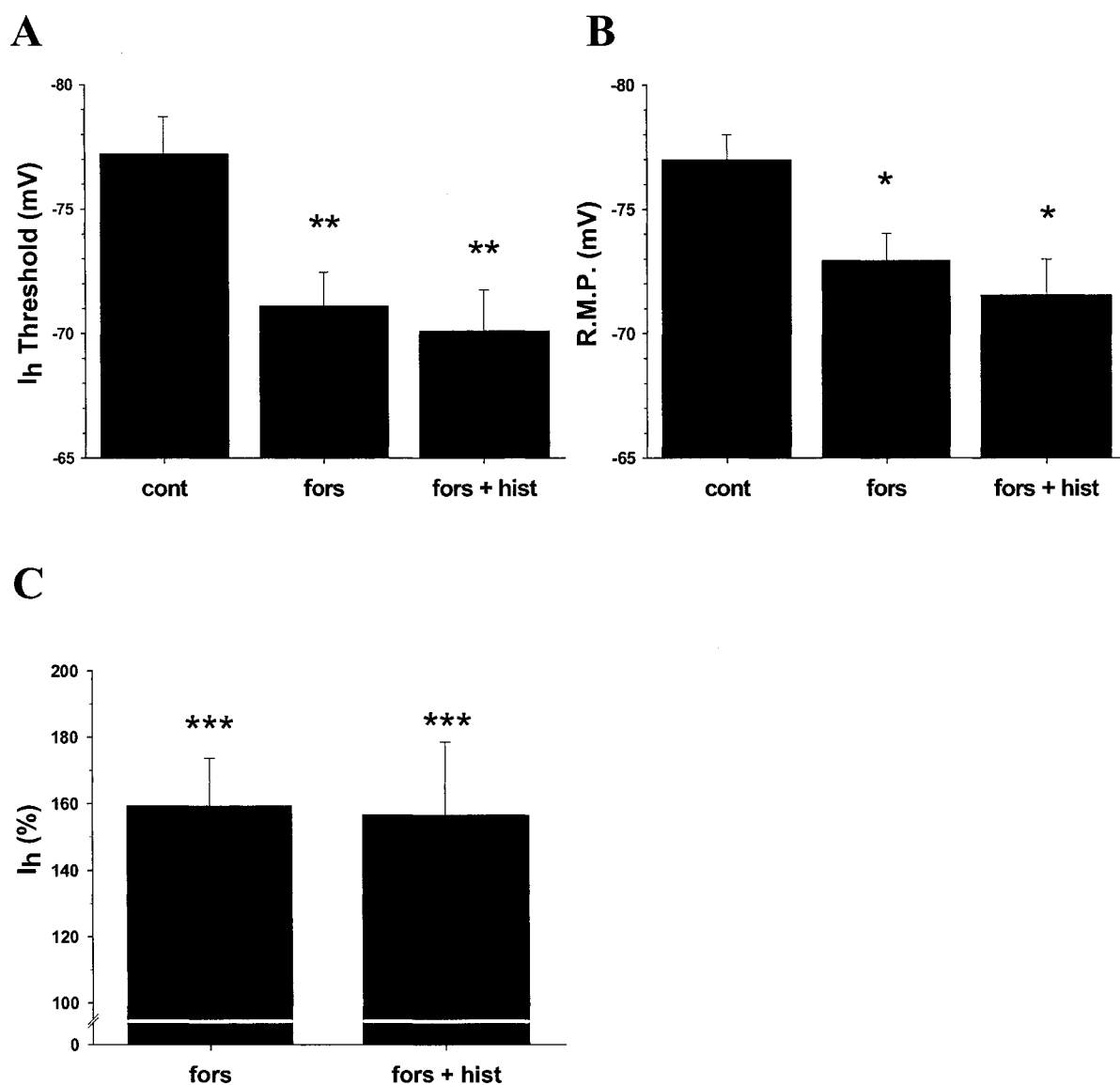


Figure 3.13 Forskolin mimics the histamine-induced changes in I_h .

Figures show the effects of 100 μ M forskolin (fors) and 50 μ M histamine (hist) in the presence of forskolin. A, B, C: Compared to control (cont), forskolin induces a significant depolarizing shift in the activation threshold of I_h , depolarization of the resting membrane potential (R.M.P.) and increase in the amplitude of I_h (I_{max} as a percent of control). In each of the above, the addition of histamine showed no significant additive effect to the forskolin-induced changes in I_h ($P > 0.05$). * $P < 0.05$, ** $P < 0.01$, *** $P < 0.001$ vs. control, $n = 3$.

effects of forskolin (100 μM) alone and in the presence of histamine (50 μM). Compared to control, both forskolin and the co-application of forskolin and histamine significantly shifted the activation threshold of I_h in a depolarizing direction (Bonferonni, $P < 0.01$), increased the current amplitude of I_h ($P < 0.001$), and depolarized the resting membrane potential (Bonferonni, $P < 0.05$) (see Table 3.3 for values). In each of the parameters examined, forskolin and the co-application of forskolin and histamine were not different ($P > 0.05$). Moreover, comparison of histamine with co-application of forskolin and histamine shows they were not additive (Bonferonni, $P > 0.05$). From this it was concluded that a similar mechanism of adenylyl cyclase activation is responsible for the observed histamine effects (Figure 3.15A,B,C).

Table 3.3 Forskolin effects on I_h and the resting membrane potential.

Effect	Control	forskolin	forskolin + histamine
I_h activation threshold (mV)	-77.2 ± 1.5	-71.1 ± 1.4	-70.1 ± 1.6
I_h amplitude (I_{max} % of control)	100	159.3 ± 14.4	156.6 ± 21.9
resting membrane potential (mV)	-77.0 ± 1.0	-73.0 ± 1.1	-72.5 ± 1.4

3.3.5 Protein kinase inhibitor H7Blocks histamine effects on I_h

Among the recent developments in the study of I_h has been the cloning of a family of hyperpolarization-activated cyclic nucleotide-gated cationic channels (HCN1-4) and

the discovery of a cyclic nucleotide binding domain in the cytoplasmic carboxy terminus, which mediates a direct response to cyclic nucleotides, most notably cAMP (Kaupp and Seifert, 2001; Viscomi et al., 2001). Although it is generally accepted that cAMP mediates an action on I_h through direct binding to the channel there is conflicting evidence on the involvement of secondary effectors such as phosphorylation by a protein kinase (Tokimasa and Akasu, 1990; Chang et al, 1991; Yu et al, 1993, 1995; Accili et al, 1997; Vargas and Lucero, 2002; Zong, Eckert, Yuan, Wahl-Schott, Abicht, Fang, Li, Mistrik, Gerstner, Much, Baumann, Michalakis, Zeng, Chen and, Biel, 2005). To investigate the possibility that histamine modulation of I_h involves protein kinase activation, a set of experiments were conducted with H7, a non-selective protein kinase inhibitor. Similar to the antagonist experiment protocol, H7 (100 μ M) was continuously bath applied after control recordings followed by application of 50 μ M histamine.

Figure 3.14 shows the effects of H7 alone and the effects of histamine with H7 present ($n = 4$). Comparisons of H7 and histamine with H7 present show a near complete block of the histamine-induced shift in the activation threshold of I_h (-78.1 ± 0.5 vs. -77.0 ± 1.1 mV, Bonferroni, $P > 0.05$) and increase in I_{max} (90.4 ± 7.7 %, vs. 97.0 ± 8.4 %, Bonferroni, $P > 0.05$)(Figure 3.14A,C). A similar blocking effect was observed for the histamine-induced depolarization of the resting membrane potential (-76.7 ± 1.4 mV vs. -76.2 ± 1.0 mV, Bonferroni, $P > 0.05$) (Figure 3.14B). For each parameter, the control condition and H7 were not significantly different ($P > 0.05$).

These results were verified by comparison of histamine alone to histamine in the presence of H7 (Figure 3.15 A,B,C). The activation threshold of I_h after co-application of

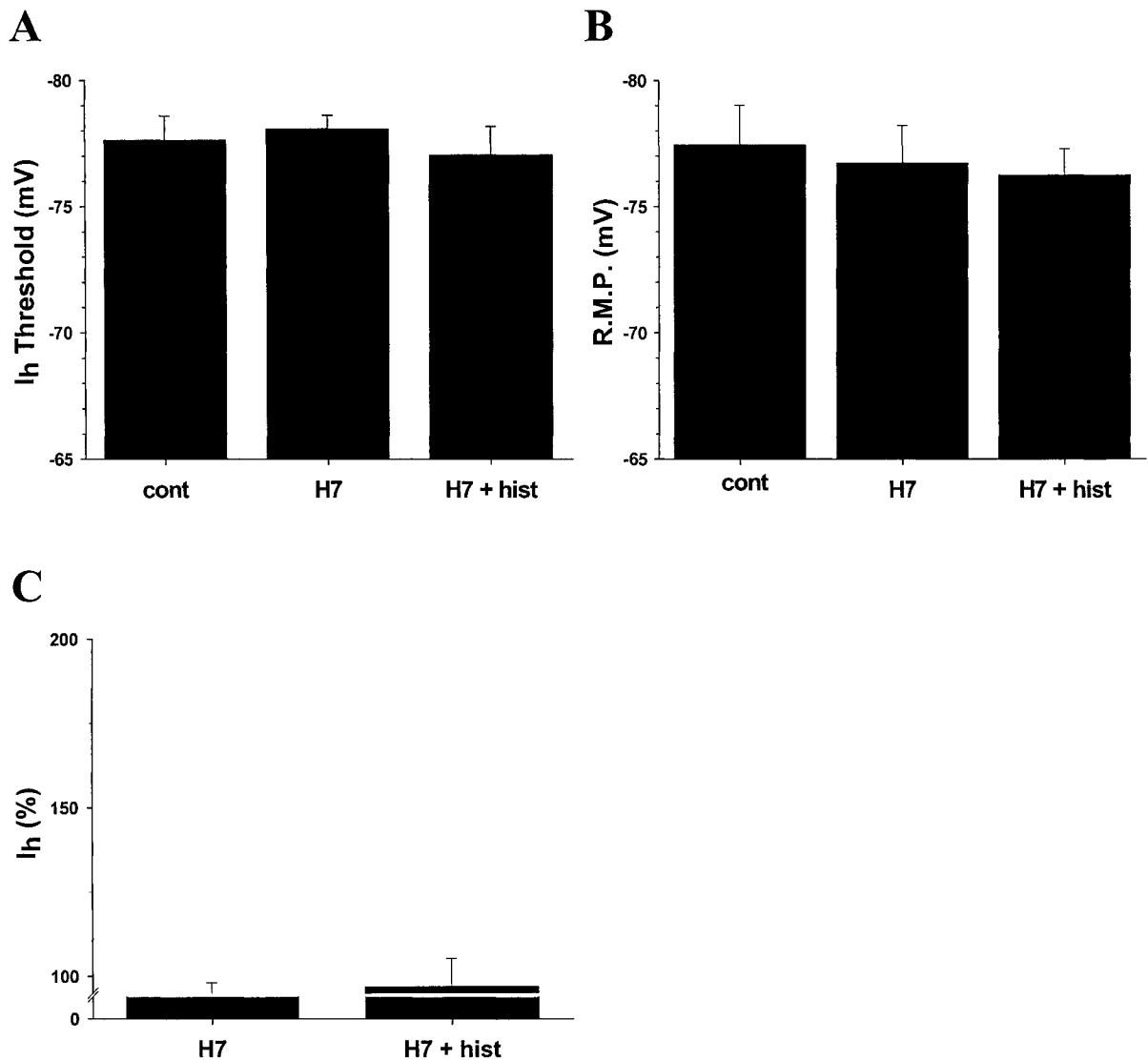


Figure 3.14 H7, a non-specific protein kinase inhibitor, blocked the histamine-induced changes in I_h .

Figures show the effects of 10 μ M H7 and 50 μ M histamine with H7 present. A: H7 prevents the histamine-induced depolarized shift in the activation threshold of I_h . B: H7 blocks the histamine-induced depolarization of the resting membrane potential (R.M.P.). C: H7 blocks the histamine-induced increase in the amplitude of I_h (I_{max} as a percent of control). In each of the above, there was no significant difference between H7 and control (cont) with H7 present. $P > 0.05$, $n=4$.

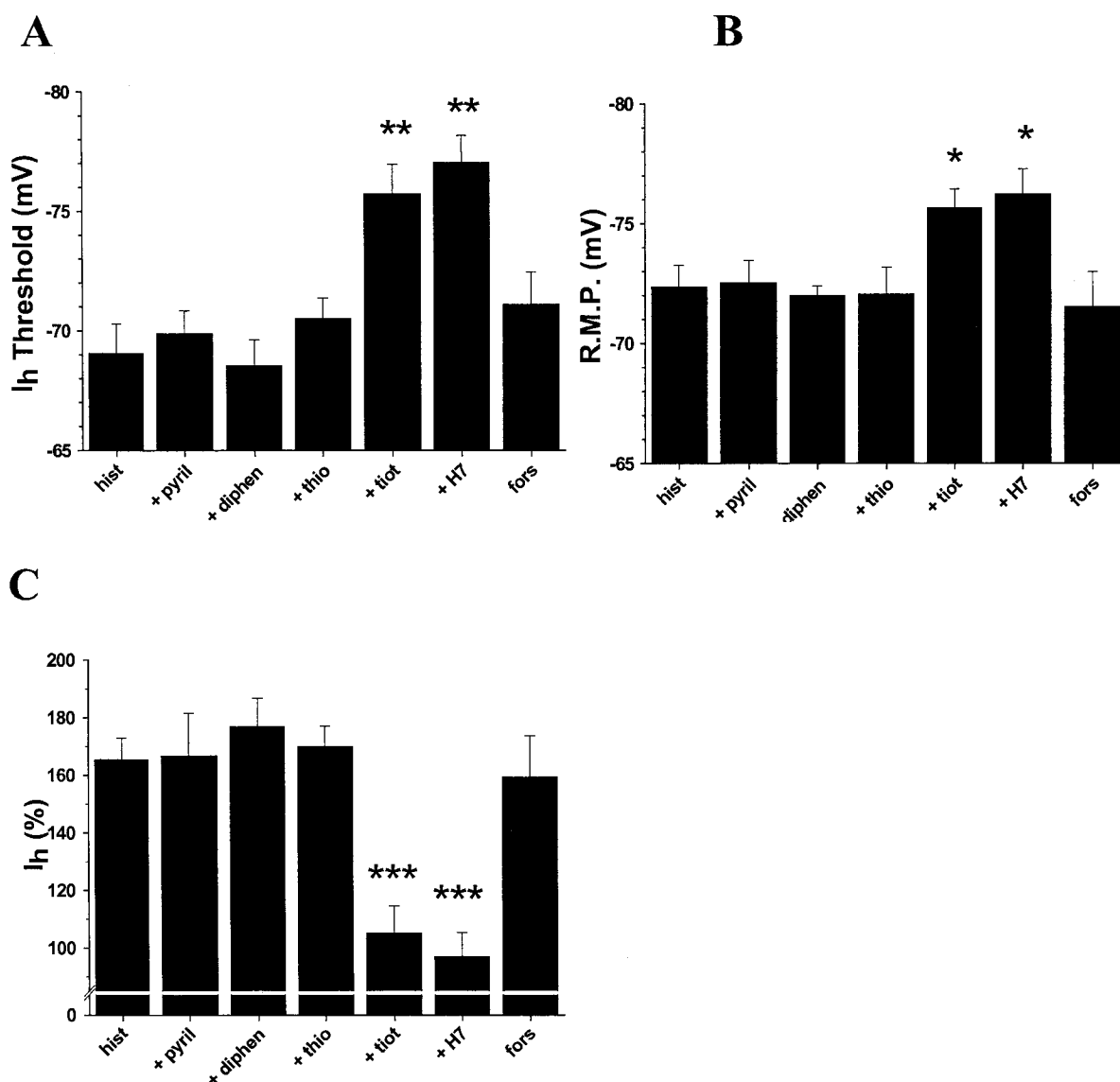


Figure 3.15 Histamine actions on I_h involve adenylyl cyclase and protein kinase activation via H₂ receptors.

Figures show the effects of 50 μ M histamine alone (hist, n = 6) and in the presence of 1 μ M pyrilamine (+ pyril, n = 4), 1 μ M diphenhydramine (+ diphen, n = 4), 1 μ M thioperamide (+ thio, n = 4), 500 nM tiotidine (+ tiot, n = 4), 10 μ M H7 (+ H7, n = 4) and 50 μ M forskolin (+ fors, n = 3). A,B,C: The histamine-induced depolarizing shift in the activation threshold of I_h, depolarization of the resting membrane potential (R.M.P.), and increase in the amplitude of I_h was significantly blocked by the H₂ antagonist, tiotidine, but not by H₁ antagonists, pyrilamine and diphenhydramine, or by the H₃/H₄ antagonist,

thioperamide, consistent with an action via the H₂ receptor subtype. In addition, the histamine-induced actions were mimicked by forskolin and blocked by H7, consistent with activation of adenylyl cyclase and some unknown protein kinase. * $P < 0.05$, ** $P < 0.01$, *** $P < 0.001$ vs. histamine.

histamine and H7 was significantly lower compared to application of histamine alone (Bonferonni, $P < 0.01$). A similar effect was observed for the amplitude I_h (Bonferonni, $P < 0.001$) and the resting membrane potential (Bonferonni, $P < 0.05$).

3.4 Discussion

The results shown demonstrate that histamine produces two effects on I_h located on layer V neocortical neurons: (1) a shift in the activation kinetics to more positive potentials; and (2) an increase in current amplitude. Both effects were concentration dependent (1-50 μM). The same effects were replicated in a concentration-dependent manner by the H_2 agonist amthamine (0.5 - 25 μM). In addition, the histamine effects were blocked in a concentration-dependent manner by the H_2 antagonist tiotidine (5 - 500 nM) with no observed block by the H_1 antagonists diphenhydramine and pyrillamine, or by the H_3/H_4 antagonist thioperamide. These data are consistent with histamine acting via the H_2 receptor subtype. The actions of histamine were also mimicked by the adenylyl cyclase activator, forskolin. Moreover, the co-application of histamine and forskolin produced no additive effect when compared to histamine alone. This suggests that the observed effects were mediated by activating adenylyl cyclase, resulting in an increase in production of the second messenger cAMP. As well, similar to the results in Chapter 2, the histamine-induced shift in I_h voltage kinetics and increase in current amplitude were blocked by the non-specific protein kinase inhibitor H7 suggesting the involvement of an unknown secondary effector.

3.4.1 Histamine does not alter the instantaneous current

Similar to the cAMP results shown in the previous chapter, histamine did not have an effect on the instantaneous current. This rules out the possibility that the observed effects, namely the increase in I_h current amplitude, were secondary to a change in the effectiveness of the space clamp. Although the localization of the recording pipette on layer V neocortical neurons was unknown, recording most likely took place on the soma or close to the soma on the dendrite. If histamine were to block the instantaneous current, (e.g., K^+) this effect would lead to a reduction in leakage of the axial current through the somatic and dendritic membranes. Consequently, histamine application would improve space clamp conditions permitting the recording of I_h located more distally from the recording site of the pipette as a result of improved flow of axial current. The contribution of more I_h channels would increase I_{max} . When the membrane conductance is increased, the opposite effect is observed. For example, in rat substantia nigra pars compacta neurons, dopamine and noradrenaline increase the inward rectifying potassium current (I_{Kir}) and decrease I_h . In the presence of barium and internal cesium, both of which reduce I_{Kir} , the dopamine and noradrenaline effect on I_h is occluded. In this system, the dopamine and noradrenaline actions on I_h are due to the shunting effect of increasing I_{Kir} conductance (Cathala and Paudpardin-Tritsch, 1999). Similar results were shown in rat substantia nigra zona compacta neurons with the GABA_B agonist baclofen, i.e., the I_h current is reduced in the presence of a baclofen-induced increase in I_{Kir} (Watts, Williams and Henderson, 1996). The modulation of I_{Kir} by histamine would be a potential candidate action since, like I_h , I_{Kir} channels are disproportionately expressed in the

dendrites of neocortical pyramidal neurons compared to the soma (Takigawa and Alzheimer, 1999).

Rather surprisingly, there was no change in the instantaneous current observed with histamine in the present results. However, the reason may lie in the voltage range tested (-57 to -137 mV) and experimental protocol used. Based on the voltage range tested, potential potassium currents included the voltage independent I_{KL} , the hyperpolarization activated I_{Kir} , I_M and possibly, the calcium-activated I_{AHP} . Of these, only I_{KL} and I_{AHP} in the neocortex are modulated by histamine via the H_1 and H_2 receptors, respectively (Reiner and Kamondi, 1994; McCormick, 1992). It is unknown why histamine does not show modulation of either in the present study as both H_1 and H_2 receptors show a consistent pattern of distribution in all layers of the neocortex across a variety of mammalian models (see section 3.1). A possible factor may involve the age of the animals used and the degree of adjacency of each channel to histamine receptors. There is little evidence, however, suggesting age-related changes in histamine-induced modulation of the above currents.

In the case of I_{AHP} , its activation is generally associated with transient intracellular calcium increases resulting from action potential activity (Strafstorm, Schwindt, Flatman and Crill, 1984; Lorenzon and Foehring, 1992; Yang, Seamans and Gorlova, 1996). Since the experiments were conducted in TTX and step potentials did not extend beyond a holding potential of -57 mV, the activation of I_{AHP} may not have occurred. H_1 receptor activation could potentially activate I_{AHP} without depolarizing the neurons as a result of PLC-IP3 mediated increases in intracellular calcium as shown in glial cells (Weiger et al.,

1997). However, this effect has yet to be reported in brain slice preparations. Finally, the inclusion of cesium chloride in the intracellular recording solutions may occlude the expected histamine-induced effect as internal cesium blocks I_{AHP} (Puil and Werman, 1981).

Other currents, such as the persistent sodium current (I_{NaP}) in the neocortex, activated at potentials as low as -68 mV, would be blocked by application of TTX (Hutcheon et al., 1996a). The low threshold calcium current (I_T) with its complex activation/inactivation kinetics would only activate upon repolarization from negative voltage steps and therefore would not contribute to the initial instantaneous component. Moreover, neither I_T nor I_{NaP} have been shown to be modulated by histamine in any preparation.

The known H_1 enhancement of glutamate NMDA receptor-mediated currents may allow it to contribute to potentials closer to rest (Payne and Neuman, 1997). Under the present experimental conditions, however, it is unlikely that the NMDA current would contribute substantially to the instantaneous component in the voltage range tested as the voltage-dependent magnesium block is typically not removed at potentials less than -20 mV. As well, the presence of TTX in the present experiments would greatly reduce the background release of glutamate and subsequently, NMDA channel activation.

3.4.2 Histamine modulates I_h in neocortical neurons

The present study demonstrates that histamine concentrations of $1 - 50$ μ M consistently shift the voltage dependent activation of I_h in the depolarizing direction with

a maximal mean shift of approximately 9 mV from a mean control activation of -77 mV. The same dose range also produces an apparent increase in I_h conductance as illustrated by a maximal mean increase in current amplitude of approximately 160 % above control. The shift in I_h activation was also characterized by a dose-dependent depolarization of the resting membrane potential with a maximum mean depolarization of 4 mV. The observed EC_{50} values for each curve, ranging from 4 - 8 μ M, were somewhat higher than the 1 - 3 μ M reported for H_1 -mediated IP hydrolysis found in other tissue types (Leurs et al., 1994; Khateb et al., 1995). In keeping with an H_2 -mediated effect, the EC_{50} values for each curve more closely match the 7 - 9 μ M values observed for histamine-stimulated activation of adenylyl cyclase and formation of cAMP in guinea pig neocortex and hippocampus (Buadry et al, 1975; Hegstrand et al, 1976; Olianas et al., 1984). Moreover, the EC_{50} of 5 μ M reported for the histamine-induced activation of adenylyl cyclase in hippocampal tissue closely matches that observed in the present study (Olianas et al., 1984). It should be noted that the histamine-induced increase in firing observed in the hippocampus as a result of activation of adenylyl cyclase may not solely reflect an enhancement of I_h since the effect of increasing cAMP has also been shown to block I_{AHP} in the same tissue type (Hass and Konnerth, 1983; Haas, 1984; Haas and Greene, 1986). Overall, given that histamine was bath applied in an iso-concentration manner and that a high affinity uptake system for histamine has yet to be reported, the concentrations used most likely reflect relevant physiological levels (Brown et al., 2001).

With the exception of the increase in current amplitude, the response of I_h to histamine presents similarities to those observed for histamine (McCormick and

Williamson, 1991), as well as, noradrenaline and serotonin in thalamic relay neurons (Pape and McCormick, 1989, McCormick and Pape, 1990b; Lee and McCormick, 1996). The similarities include an increase in the I_h steady state current, a positive shift in the I_h activation curve, and an enhancement of the I_h activation rate. The ionophoretic application of 300 – 500 μM concentration of histamine used in the thalamic relay studies (Pape and McCormick, 1989), which was suggested to be comparable to 30 – 50 μM bath application, also closely matches the concentration response observed in the present study. The shift in the activation threshold in the present results (8.5 mV) was slightly more positive compared to the histamine-induced shift observed in the thalamic relay neurons (7.5 mV). Notwithstanding differences in tissues preparations, one explanation for this difference in shift may be the use of internal CsCl in the present study. This would permit the recording of I_h located more distally from the recording site of the pipette and, as a result, would translate into a greater shift in I_h activation, i.e., improved current recording.

Another likely explanation is the ionotophoretic technique used in the thalamic study which generally provides for small volume, highly localized, high concentration applications of drugs. The bath application technique used in the present study would result in a more iso-concentration bath condition, which may lead to a greater observed effect. As well, histamine dose-response relationships were not examined in the thalamic relay studies. Given the greater expression of the HCN2 channel subtype found in thalamic neurons (Moosmang et al., 1999; Monteggia et al., 2000; Notomi and Shigemoto, 2004) which has a greater sensitivity to intracellular cAMP producing

maximal shifts in activation of +20 mV (Kaupp and Seifert, 2001; Viscomi et al., 2001), a complete dose dependency profile under the same conditions as the present study may result in greater histamine-induced shifts in I_h activation in that tissue. In neocortical tissue, in particular layer V pyramidal neurons, the greater expression of the HCN1 subtype with its lower sensitivity to cAMP and smaller resultant shifts of +4 mV suggests that the histamine-induced changes in I_h activation in the present study reflect greater than maximal shifts. Alternatively, since both HCN1 and HCN2 channel subtypes are colocalized on the distal dendrites of neocortical pyramidal neurons, the observed histamine-induced shift in I_h may represent intermediate kinetics properties, i.e., between +4 and +20 mV shift, respectively (Chen, Wang and Siegelbaum, 2001; Notomi and Shigemoto, 2004).

A major difference in the present results and those reported by McCormick and Williamson (1991) was our observed histamine-induced increase in the peak current of I_h (I_{max}) with increasing hyperpolarization. Again, this may result from a difference in methods. In thalamic relay neurons, current responses elicited using negative voltage step protocols, similar to those used in the present study, show a similar histamine-induced increase in the I_h steady state current at potentials negative to -60 to -65 mV. To circumvent the observed increase in I_h , however, which was interpreted as a possible limitation of the single electrode voltage clamp technique, the I_h I-V curves were constructed using tail current analysis. This technique, which allows for the measurement of I_h inactivation near the resting membrane potential, and consequently near the reversal potential for I_h , results in a reduction in current amplitude (McCormick

and Williamson, 1991). Other studies of I_h using the same tail current technique revealed similar results for noradrenaline and serotonin (Pape and McCormick, 1989, McCormick and Pape, 1990b, Lee and McCormick, 1996). As well, the use of micro-electrodes in the thalamic studies could translate into larger current errors due to the high resistance of the electrodes, which may confound the results.

In other neuromodulation studies employing the same technique to construct I_h I-V relationships used in the present experiments (i.e., subtracting the instantaneous current from the steady state current elicited during the voltage step) both increases and decreases in I_h amplitude have been reported. For example, in rat hippocampal pyramidal neurons, a serotonin-induced increase in cAMP resulted in both an increase in the amplitude of I_h as well as a positive shift in activation (Gasparini and DiFrancesco, 1999). Similarly, both 8-bromo-cAMP and forskolin have the same effect in area postrema neurons (Funahashi, Mitoh, Kohjitani and Matsuo, 2003) Conversely, in rat hippocampal interneurons and pig nodose ganglion neurons, opioids linked to inactivation of adenylyl cyclase, induced a decrease in the amplitude and rate activation of I_h (indicative of a negative shift in I_h voltage kinetics) (Svoboda and Lucpica, 1998). Similar decreases in I_h were reported for dopamine and baclofen in ventral tegmental neurons of the rat mid brain using the same current extraction method.

Notwithstanding the differences in methods, the present study suggests that histamine augments the amplitude of I_h in addition to shifting I_h activation to more depolarized potentials with a resultant depolarization of the resting membrane potential. These effects imply that histamine is activating H channels that are not activated by

hyperpolarization alone or that histamine increases H channel conductance. The latter is somewhat supported by the differences in the histamine EC_{50} and slope factor for I_h activation and amplitude, implicating a concentration-dependent divergence of histamine action. It should be noted, however, that the concentration dependency for I_h amplitude and shift might reflect the apparent limitations of the space clamp (see Chapter 2). For example, the histamine-induced effect on I_h may be secondary to a blocking effect on other channels (e.g., K^+) located on the distal dendrites that contribute little to the recorded instantaneous current. Whether this possible effect is due to direct actions of histamine postsynaptically or whether it is due to effects elicited through histamine induced/inhibited presynaptic release of histamine or other neurotransmitters is unknown. In any case an unrecorded reduction in membrane conductance would act to reduce the leak of I_h in the distal direction resulting in an overall increase in I_h flow in the proximal direction. As well, an improvement in the space clamp would further accentuate this effect due to the higher density of I_h channels located on neocortical distal dendrites (Stuart and Spruston, 1998; Berger et al., 2001, Notomi and Shigemoto, 2004).

3.4.3 Histamine modulation of I_h is mediated by H_2 receptors

In the absence of a histamine-induced change of other currents, the apparent increase in conductance and depolarization of the resting membrane potential results from an enhancement of I_h . Moreover, based on the experiments involving known histamine agonists and antagonists, histamine actions appear to be mediated by H_2 receptors.

Bath application of H₁ antagonists, diphenhydramine and pyrilamine, and the H₃/H₄ antagonist, thioperamide, failed to block the histamine-induced effects on I_h. Also worthy of mention is the lack of a significant effect on I_h or the instantaneous current when comparing antagonist actions to control in the absence of histamine. In particular, the lack of response for thioperamide suggests that there is little or no endogenous transmitter release, i.e., histamine. This presumably reflects the block of synaptic transmission in the presence of TTX. Consistent with an H₂-mediated effect, the enhancement of I_h by histamine was blocked by the H₂ antagonist tiotidine in a concentration-dependent manner and mimicked by the H₂ agonist amthamine in a concentration-dependent manner with no change in the instantaneous current. In thalamic relay neurons the block of the histamine-induced effect on I_h by tiotidine and the lack of a block in the presence of diphenhydramine were also attributed to an H₂-mediated effect in that tissue, consistent with the present findings.

Also in support of these findings, *in situ* hybridization and receptor binding studies of the H₂ receptor subtype in guinea pig neocortical tissue show a high density of H₂ receptor gene transcripts in layer V neocortex with a high expression of H₂ receptors on the pyramidal dendrites (Vizuete et al., 1997). The localization of the H₂ receptor and H₂ effects also fits with the disproportionately higher density of I_h on the apical dendrites of layer V pyramidal neurons (Stuart and Spruston, 1998; Berger et al., 2001; Notomi and Shigemoto, 2004). The present results with histamine, in combination with the localization of I_h and H₂ receptors in layer V pyramidal neurons, suggests that the

location of H₂ receptors on neocortical neurons allows the control of I_h on the apical dendrite.

3.4.3 Histamine modulation I_h involves adenylyl cyclase and protein kinase activity

Similar to the cAMP results in Chapter 2, the adenylyl cyclase activator forskolin mimicked the effect of histamine thus providing further support for the role of intracellular cAMP in regulating and maintaining I_h in neocortical pyramidal neurons. Furthermore, co-application of forskolin and histamine was not additive compared to applications of histamine alone, consistent with the actions of histamine being mediated by the activation of adenylyl cyclase. These observations are consistent with present findings that histamine is acting via H₂ receptors, which have long been associated with adenylyl cyclase activation and with increases in intracellular cAMP in the neocortex and other tissue preparations (Nahorski et al., 1974, Baudry et al., 1975; Hegstrand et al., 1976, Psychoyos, 1978; Olianias et al., 1984, Ezeamuzie and Philips, 2000; Zawilska, Woldan-Tambor, Nowak, 2002).

Also in keeping with the cAMP results in Chapter 2, application of H7, a nonspecific protein kinase inhibitor, blocked the histamine-induced effects again suggesting the involvement of a protein kinase in the modulation of I_h in neocortical neurons. Moreover, the fact that applications of H7 in the absence of histamine did not significantly alter I_h suggests that the protein kinase activity is dependent upon intracellular levels of cAMP and is occurring downstream of the histamine-induced activation of adenylyl cyclase. To date, most evidence supporting modulation of I_h

through phosphorylation and dephosphorylation mechanisms, an outcome of kinase activity, has been shown in cardiac tissue (Yu, Chang and Cohen, 1993, 1995; Accili Redaelli, Difrancesco, 1997). For example, in Purkinje fibers and isolated ventricular myocytes, treatment with calyculin A, a protein phosphatase inhibitor, resulted in a positive shift in the activation curve of I_h (Yu et al., 1993, 1995). Conversely, treatment of Purkinje fibers with protein kinase inhibitors H7 and H8 resulted in a negative shift in the activation curve of I_h (Chang, Cohen, Difrancesco, Rosen and Tromba, 1991). Moreover, the effects of H8 were not observed in the absence of activation of the cAMP cascade, similar to the present findings. Protein kinase inhibitors decrease the peak amplitude of I_h in dissociated bullfrog sympathetic neurons (Tokimasa and Akasu, 1990). Vargas and Lucero (2002) reported similar negative shifts, as well as a significant decrease in I_h conductance, in rat olfactory receptor neurons after treatment with K252a, another non-specific protein kinase inhibitor. In further support of the present findings, they observed I_h activation time constants resembling those of HCN1 channels, the HCN channel subtype most expressed in layer V neocortex (Moosmang et al., 1999; Monteggia et al., 2000, Notomi and Shigemoto, 2004).

Although there is substantial evidence to suggest protein kinase involvement in the modulation of I_h , identification of the exact kinase involved has been ambiguous at best. For example, in rat olfactory receptor neurons, the observed negative shift was shown to be due only in part to the inhibition of protein kinase A (PKA), since the specific PKA inhibitor H-89 replicated only in part the K252a effect (Vargas and Lucero, 2002). This suggests that, in addition to PKA, other protein kinases may be been involved

in the modulation of I_h . This is likely, as other kinases, such as PKC and tyrosine kinase, have also been implicated in the modulation of I_h in rat substantia nigra pars compact and sinoatrial node myocytes, respectively (Cathala and Paupardin-Tritsch, 1997, Wu and Cohen, 1997, Zong et al., 2005). Similarly, given that studies of the structural components of single H_2 receptors have been shown to activate both adenylyl cyclase and PLC pathways, the involvement of more than one kinase in the modulation of I_h in the present study is plausible (Wang et al., 1998).

4. Histamine modulates subthreshold resonance in rat neocortical neurons

4.1 Introduction

Although the generation of synchronized oscillations in the neocortex is dependent on a network of both excitatory and inhibitory inputs (Silva, et al., 199; Flint and Connors, 1996; Lukatch and MacIver, 1997; Castro-Almancos, 2000; Castro-Almancos and Rigas, 2002; Timofeev, Bazhenov, Sejnowski and Steriade, 2002), groups of neurons can be driven rhythmically by intrinsic pacemaker properties. Layer V neocortical pyramidal neurons in the neocortex have long been known to show intrinsic 5 to 12 Hz rhythmic patterns of burst firing and appear to play a pacemaker role in promoting certain synchronized oscillations (Silva, Amital and Connors, 1991; Amitai, 1994; Flint and Connors, 1996; Lukatch and MacIver, 1997). Given this inherent property, it likely that layer V neurons are an important site for modulation which can result in the switching of neocortical activity between different rhythmic states.

An intrinsic mechanism, which can influence these rhythmic patterns, is resonance (see section 1.4). Resonance may enable neurons to selectively assimilate bombardments of synaptic input and communicate action potentials over a preferred band of frequencies to postsynaptic targets (Hutcheon and Yarom, 2001; Izhikevich, Desai, Walcott, Hoppensteadt, 2003; Richardson, Brunel and Hakim, 2003). Since certain frequencies are resonant for some neurons whereas others do not exhibit resonant responses, resonance may have a selectivity role in communications between neurons. This selectivity can be modulated by changing the frequency content of synaptic input

and by modulating the intrinsic factors that determine resonance. Together, this presents the CNS with a dynamic rewiring mechanism that occurs on short time scales without any long-term plastic changes in the synaptic circuitry. For example, changes in the frequency content of input may reduce the activity of previously active neurons if the input no longer contains their preferred band of frequencies. Conversely, a change in input may increase the activity of other neurons because the frequency content matches their resonant bands (Hutcheon et al., 1996a,b; Izhikevich et al., 2003; Richardson et al., 2003). A change in input strength can have a similar effect (Richardson et al., 2003). As well, theoretically, direct modulation of resonant mechanisms can change the preferred band of frequencies (Hutcheon and Yarom, 2001).

In layer V pyramidal neurons of the neocortex, I_h in combination with the passive properties produces subthreshold resonance (Hutcheon et al., 1996a,b; Ulrich, 2002). Since a specific active process such as I_h can regulate the frequency response of neurons, it follows that modulation of the process will influence resonant behaviour. For example, Hutcheon et al. (1996b) showed in modeling studies of neocortical resonance that changes in the parameters of I_h , which could represent changes induced by intrinsic modulatory factors, altered neocortical resonance. Modulation of I_h would therefore have important implications for the control of cortical activity such as in the maintenance and generation of burst firing (Foehring and Waters, 1991).

The study of neurotransmitter effects on the frequency response of neurons is a new field of neuromodulator investigation, which can lead to a greater elucidation of transmitter actions and insight into the control of resonant behaviour. In Chapter 3,

histamine was shown to shift the activation kinetics of I_h to more depolarized potentials, and increased I_{max} . Given the evidence that I_h is responsible for the formation of subthreshold resonance in neocortical neurons it was hypothesized that the histamine-induced effects on I_h in the neocortex would also result in the modulation of subthreshold resonance.

4.2 Methods and Materials

(For detailed methods see Section 2.2)

The impedance (Z) amplitude profile (ZAP) method was used to investigate the subthreshold frequency domain of neocortical neurons (Puil et al., 1986; Puil et al., 1988). In current clamp mode, neurons were held at potentials between -57 to -97 mV, in 10 mV increments. At each potential, a computer generated ZAP waveform was injected into the neuron and the resulting voltage output was digitally recorded and stored on a computer hard drive. Data collection and analysis were completed using ZAP Acquisition (version 3.5) and ZAP Analysis (version 4.01) software developed by Dr. Ernie Puil's laboratory (Figure 4.1A).

The ZAP waveform is a swept-sine-wave alternating current with a constant amplitude and finite duration that changes frequency linearly from 0.2 to 60.0 Hz. The ZAP input was derived by the formula

$$I(t) = a\sin(bt^3) + dc, \quad (7)$$

where I is the input current, t is time, a is the amplitude, b is the band-width of input and dc is the holding current.

To ensure the relationship between the current input and voltage response was approximately linear, which is required for accurate frequency domain analysis, the current amplitude was adjusted at each holding potential such that the maximum voltage response was less than 20 mV peak to peak.

The impedance, a complex number made up of real and imaginary parts, was calculated based upon the ratio of the fast Fourier-transforms (FFT) of the voltage response and current input using the formula

$$Z = Z_{\text{real}} + Z_{\text{imaginary}} = \text{FFT}(V)/\text{FFT}(I). \quad (8)$$

Final impedance calculations were based on the average of three ZAP sweeps and were presented in two frequency response forms: impedance frequency response curves (zFRC) and phase shift frequency response curves (pFRC) (Fig 4.1B,C). The strength of resonance (Q) and the resonant frequency (f_{res}) were calculated from the zFRC (Fig 4.1D).

$$Q = Z_{\text{max}}/Z_{\text{min}} \quad (9)$$

where Z_{max} is the impedance recorded at the peak of the zFRC and Z_{min} is the impedance recorded at the lowest frequency sampled (Koch, 1984). The f_{res} was determined as the frequency at Z_{max} as shown in equation 10.

$$Z(f_{\text{res}}) = Z_{\text{max}} \quad (10)$$

To prevent current rundown of I_h and to ensure a stable basal level of cAMP without saturating intracellular cAMP levels, 1 μM cAMP was added to the pipette-solution in all the present experiments. To ascertain that rundown had not occurred controls were taken at 5 and 15-20 mins after whole cell rupture. Compounds in this study included histamine

(Sigma), tiotidine (Tocris) and 4-ethylphenylamino-1,2-dimethyl-6-methylamino-pyrimidinium chloride (ZD-7288, Tocris).

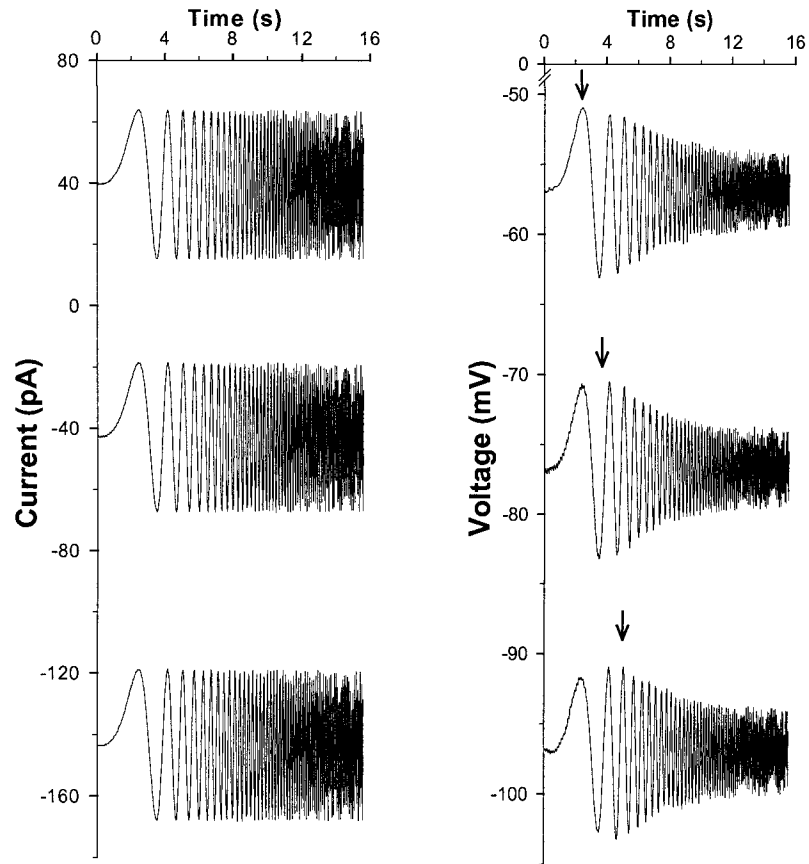
Drug and voltage induced changes in impedance profiles were evaluated by comparison of the impedance in control solutions, and in the presence of drug, in the same neuron. For the purpose of averaging responses, all data were converted to log normal value. Average data are presented as the antilog of the geometric mean \pm S.E.M. Statistical significance of data was assessed with two-way analysis of variance (2 way ANOVA) (Excel, Microsoft Office 2000).

4.3 Results

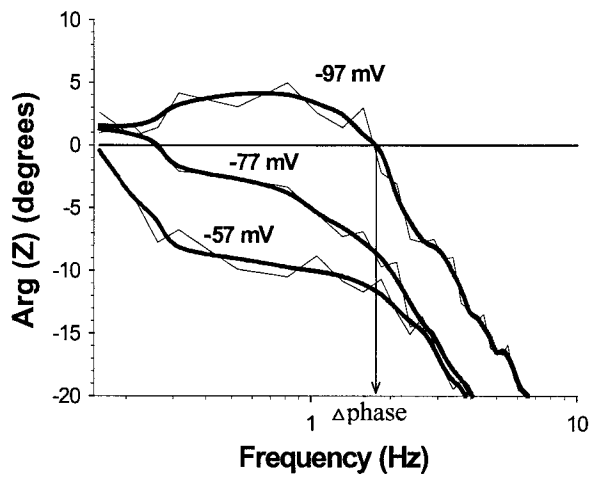
4.3.1 Frequency response curves are voltage dependent

The results represent data obtained from 16 neurons. Figure 4.1A shows layer V neocortical neuron subthreshold (-57 mV to -97 mV) voltage responses to constant ZAP waveform inputs. Typically, the amplitude of voltage oscillations was largest during the earlier part of the ZAP sweep (0 to 6s, which represents lower frequency inputs), followed by a steady decline for the remainder of the input (7 - 16s, which represented a current input at higher frequencies). With increased hyperpolarization, however, there are distinct differences in the amplitude and timing of the voltage response. In the example shown, the voltage trace at -57 mV represents a feature of nonresonance where the zFRC is wedge shaped due to the largest voltage response occurring at the lowest frequency

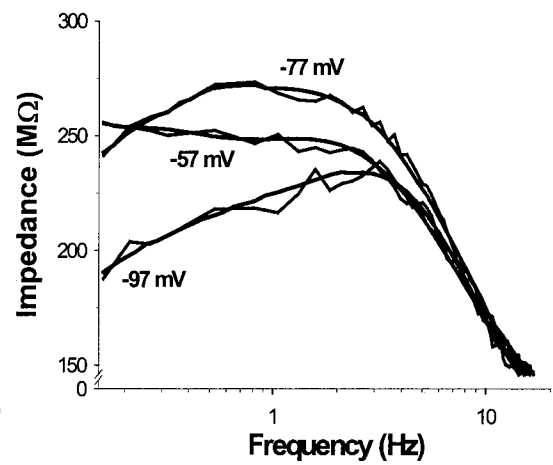
A



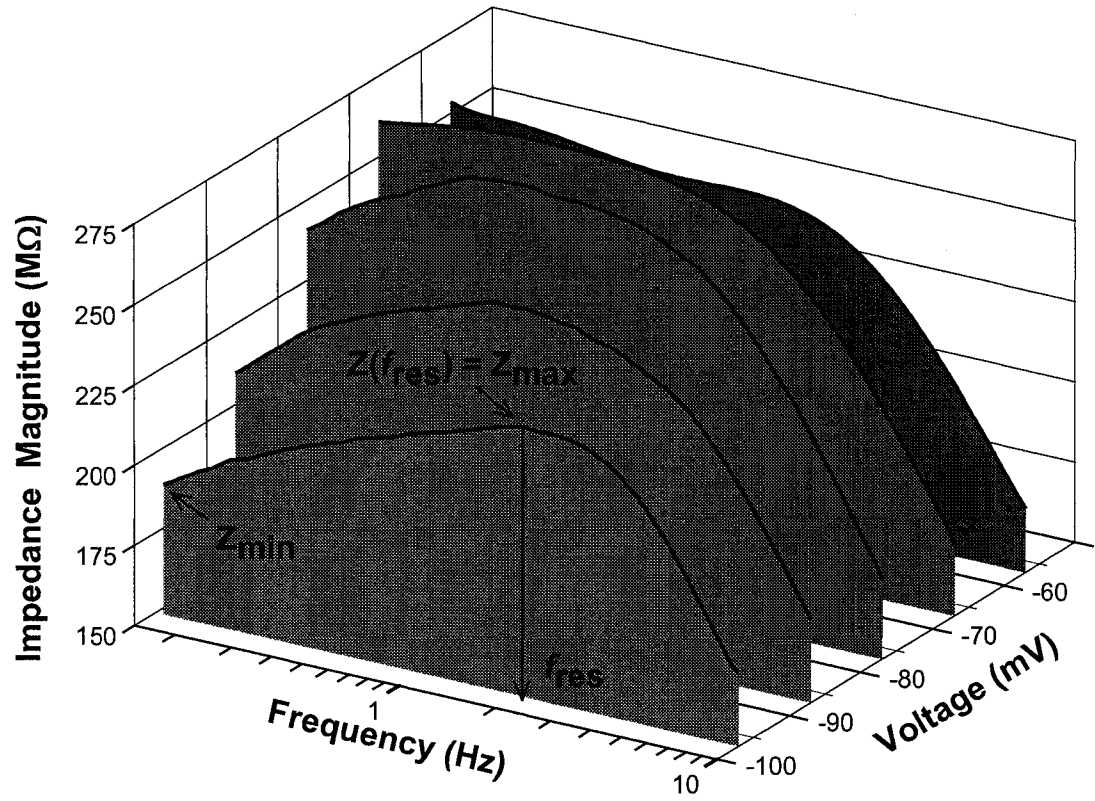
B



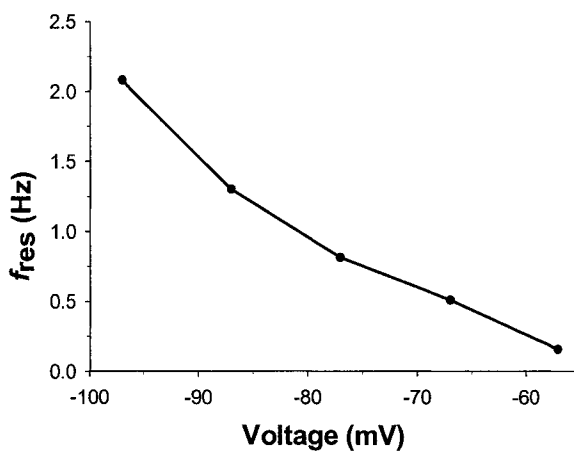
C



D



E



F

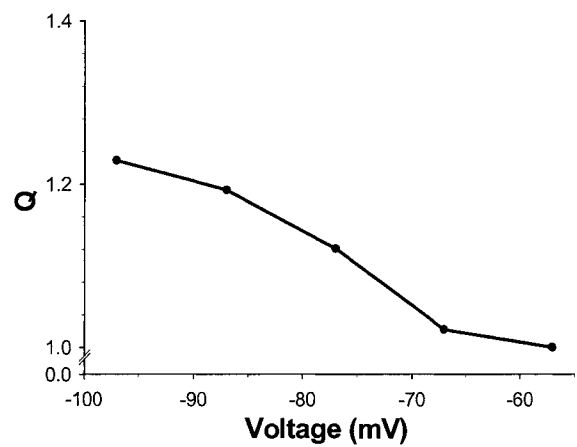


Figure 4.1 Subthreshold frequency and voltage response of a resonant neuron.

A: Examples (at -57 , -77 and -97 mV) of ZAP current inputs (left) and voltage responses (right) in a resonant neuron under current clamp mode. Voltage trace reflects an average response from three ZAP sweeps. Current input was adjusted to achieve a voltage response of less than ± 10 mV at each holding potential. Increasing hyperpolarization from -57 mV shows a change in the voltage amplitude with increasing frequency (arrows). B, C, D: To investigate the frequency preference of neurons, their phase frequency response curve (pFRC) and impedance frequency response curve (zFRC) were determined. B: pFRC shows a voltage and frequency dependent rightward shift in the phase with increasing hyperpolarization. At -97 mV the voltage leads the current up to ~ 1.8 Hz followed by the current leading the voltage for higher frequencies. Smooth line reflects a 5 point average of the data. C: In keeping with B, the zFRC shows a voltage and frequency dependent rightward shift in the maximum impedance as well as an overall decrease in the impedance with increasing hyperpolarization. Smooth lines were fitted by eye to the data. D: Three dimensional plot of impedance as a function of frequency and voltage using fitted lines. At potentials negative to -67 mV the neuron reveals resonance. Maximum impedances were observed just negative to the resting membrane potential (-64 mV) between -67 and -77 mV. IFRC for -97 shows that the maximum impedance (Z_{\max}) corresponds to the resonant frequency (f_{res}). The minimum impedance (Z_{\min}) is taken as the impedance at the lowest frequency recorded (0.2 Hz). Note the decrease in Z_{\min} and Z_{\max} and the rightward shift in f_{res} at potentials negative to -77 mV. E: Plot for f_{res} as a function of voltage. The value of f_{res} increases with increasing hyperpolarization from a minimum of 0.2 Hz at -57 mV to 2.1 Hz at -97 mV. F: Plot of the quality of resonance (Q) as a function of voltage. Q represents the ratio of Z_{\max} and Z_{\min} (Z_{\max}/Z_{\min}). Similar to f_{res} , Q increases with increasing hyperpolarization ranging from a value of 1 at -57 , representing a non-resonant condition, to 1.2 at -97 mV.

input. Although the voltage response at -57 mV shown in Figure 4.1A represents a feature of nonresonance, most cells in this study showed a slight spindle shape response (12 of 16) where there was an attenuation of the voltage amplitude at the lowest frequencies followed by larger voltage amplitudes at intermediate frequencies. In contrast, the voltage traces negative to -67 mV reveal characteristics of strong resonance characterized by a more prominent spindle shape. Moreover, the peak of these spindles, which closely represents f_{res} , occurred later with increased hyperpolarization, consistent with a shift of f_{res} to higher frequencies.

The pFRCs for the same neuron shows the voltage dependence of the phase shift (Figure 4.1B). The phase shift is the argument of impedance ($\arg(z)$) between the input and output at each frequency. In short, the $\arg(z)$ can be determined from the complex plane of impedance by taking the angle between the horizontal or real impedance and the complex impedance vector. $\arg(z)$ values in the positive quadrant represent the voltage leading the current whereas values in the negative quadrant represent the current leading the voltage. A phase shift occurs when there is a change from the positive to the negative plane or vice-versa. The frequency at which $\arg(z) = 0$ is the point at which both the voltage and current are in phase, representing the approximate mid value of the surrounding resonant band of frequencies, i.e., f_{res} .

In the example shown, a phase shift is not evident at -57 mV since $\arg(z)$ occurs in the negative quadrant for all frequencies. At potentials negative to -67 mV, there is a change in the pFRC where the phase angle crosses the horizontal axis (0°) at intermediate frequencies, indicating that the voltage is leading the current up to that point. Similar to

the time shift in the voltage amplitude in 4.1A, the phase shift increases with increasing hyperpolarization (0.2 Hz at -77 mV and 1.8 Hz at -97 mV).

The zFRCs shown in Figures 4.1C and D reveal the typical voltage dependent nature of impedance seen throughout this study. In the low frequency range, up to a maximum of 10 Hz, the impedance magnitudes were highly voltage dependent. This includes an increase followed by a decrease in the impedance at potentials negative to -57 mV with peak values typically occurring at -67 mV and -77 mV. A specific feature in this range is the formation of subthreshold resonance. This is characterized by an attenuation of the impedance at lower frequencies relative to intermediate frequencies with increased hyperpolarization. This gives the zFRC a humped shape. At frequencies greater than 10 Hz, the impedance values show little voltage dependence consistent with the high frequency attenuation of the passive membrane properties, i.e., ω_{pass} .

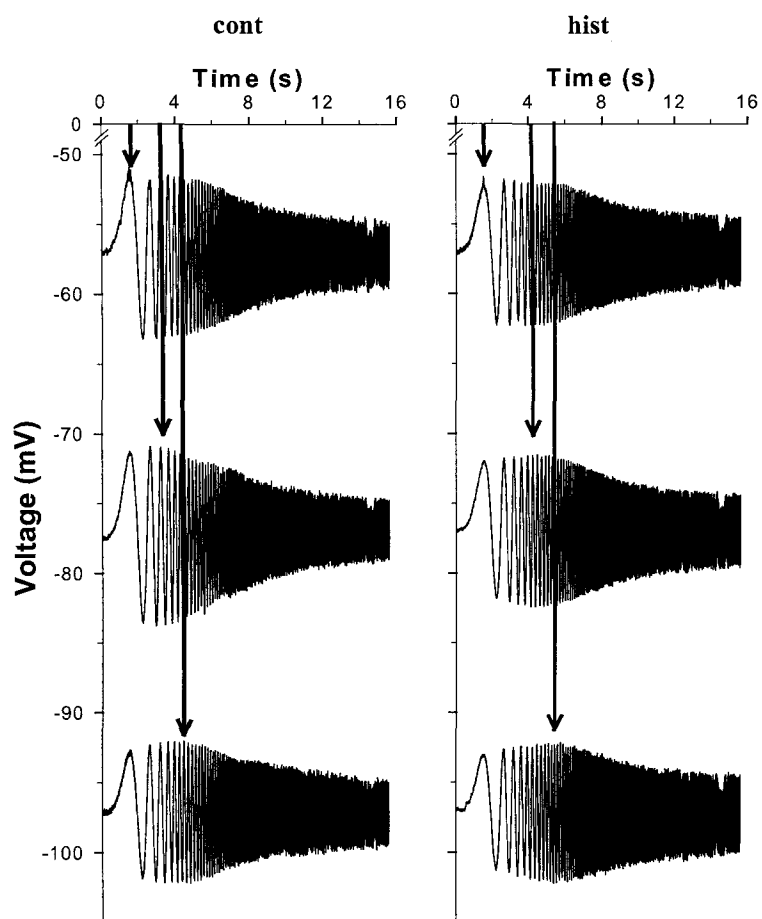
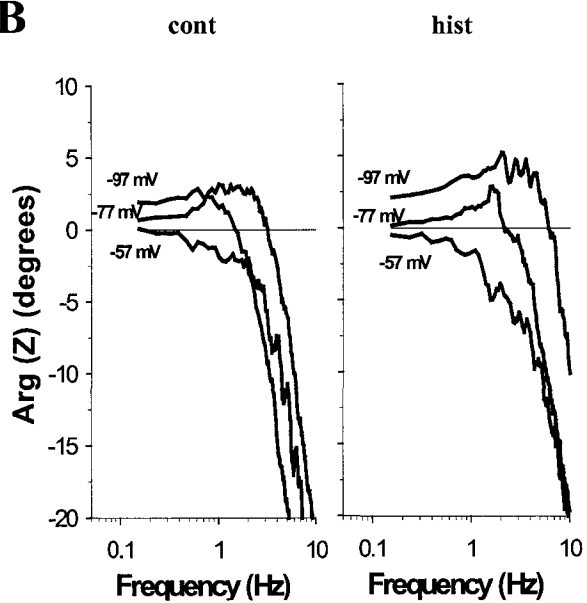
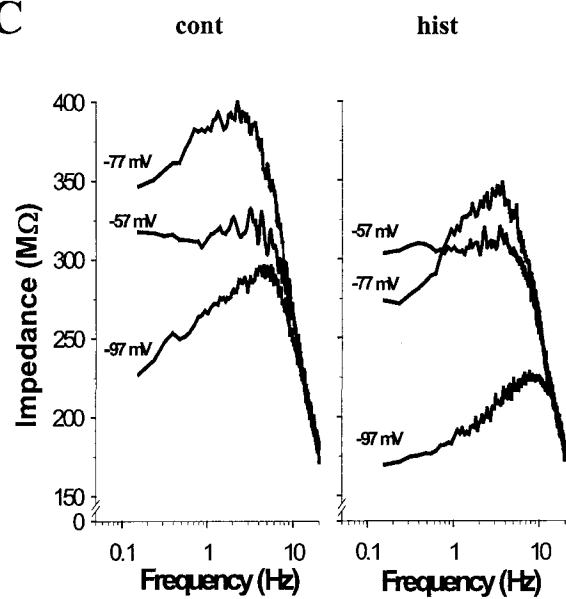
Figure 4.1 D shows a 3-dimensional frequency response surface (FRS) made up of zFRCs determined at 10 mV interval holding potentials. The membrane is clearly resonant at potentials negative to -67 mV. The features of resonance, as described by f_{res} and the Q value, were also voltage dependent (Fig 4.1E, F). The f_{res} value increases almost linearly from 0.2 Hz at -57 mV to 2.1 Hz at -97 mV, consistent with the enhanced attenuation of the impedance at lower frequencies with increased hyperpolarization. Moreover, while f_{res} increases steadily with increased hyperpolarization, the Q value remains stable near 1 up to -67 mV after which it increases to an approximate asymptotic value of 1.2.

4.3.2 Histamine modulates the frequency response of neocortical neurons

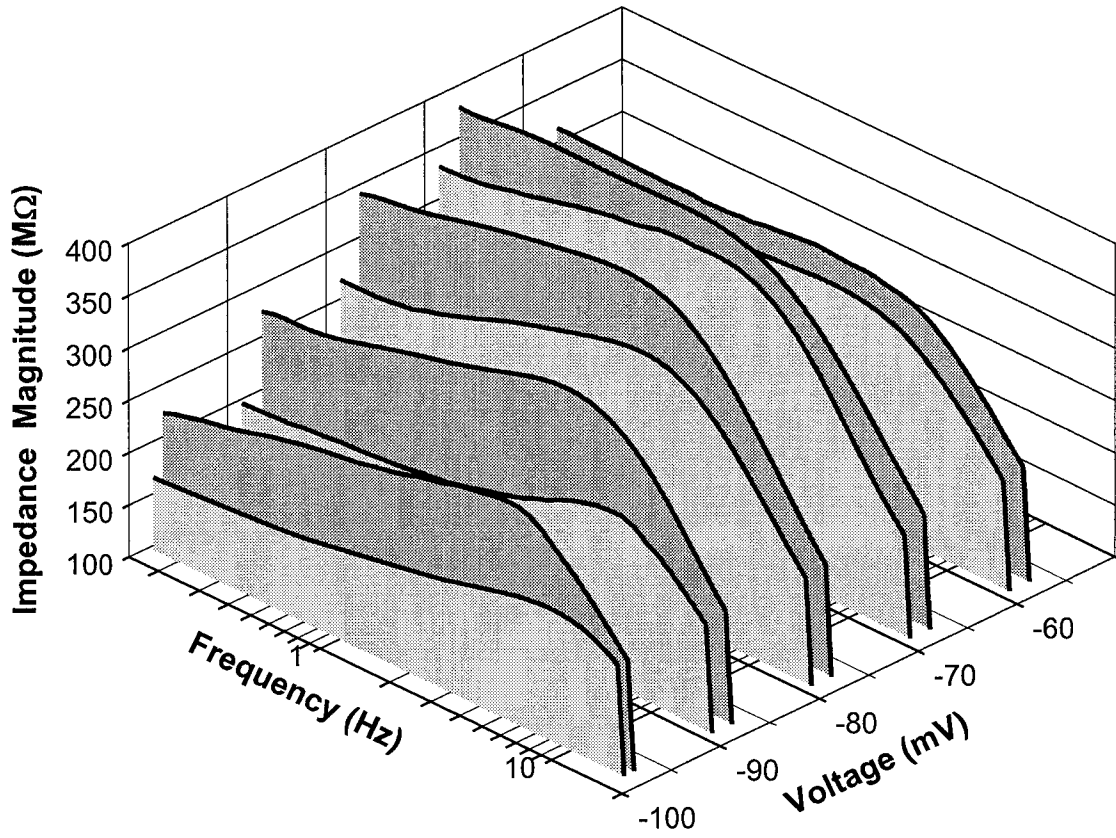
To investigate modulation of the frequency response of neocortical neurons, 50 μM histamine was applied after control ZAP recordings. The control in Figure 4.2A shows the typical voltage dependent formation of the spindle shape voltage response with increased hyperpolarization. Application of histamine had little effect on the voltage response at the holding potential of -57 mV. In contrast, the voltage response at more negative potentials showed a shift in the peak amplitude to higher frequency inputs (Figure 4.2A). Consistent with the observed change in the voltage response, histamine had no effect on the phase shift at -57 mV (0.2 vs. 0.3 Hz). However, the phase shift occurred at higher frequencies when the neuron was hyperpolarized (1.4 Hz vs. 2.2 Hz at -77 mV and 2.4 Hz vs. 6.3 Hz at -97 mV, Figure 4.2B).

Similarly, although the zFRCs show a slight resonance hump at -57 mV, histamine had no effect. On the other hand, the more prominent feature of resonance, consistently observed at potentials negative to -67 mV, showed strong histamine modulation which included a rightward shift in the frequency of Z_{max} and an overall decrease in the impedance up to a 10 Hz input frequency (Figure 4.2 C and D).

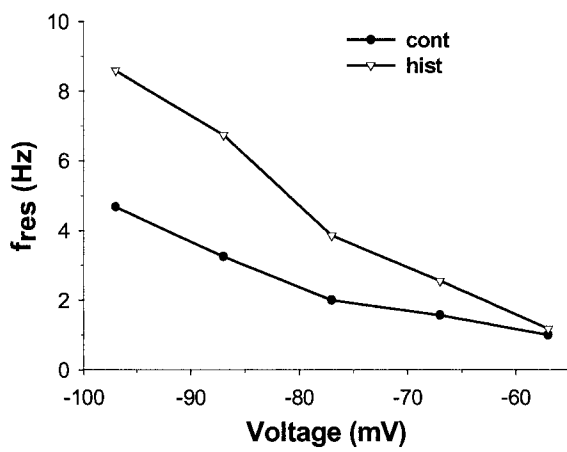
Consistent with this finding, histamine increased f_{res} at -67 mV through to -97 mV with little effect at -57 mV (Figure 4.2E). In addition, pooled data (Figure 4.3A) revealed that the increase in f_{res} was voltage dependent between -57 mV to -97 mV as well as significantly larger after application of 50 μM histamine (2 way ANOVA, $P < 0.01$, $n = 7$).

A**B****C**

D



E



F

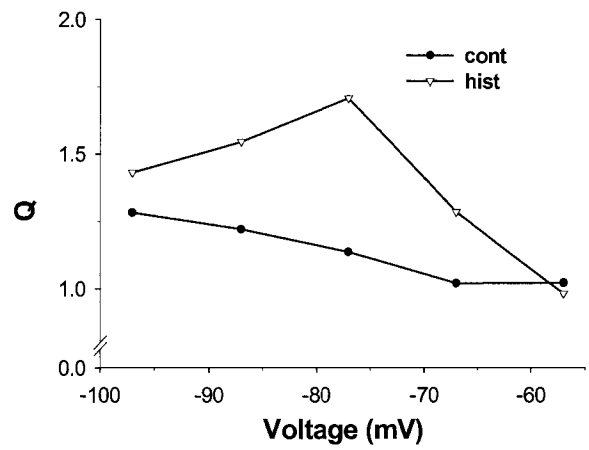


Figure 4.2 Histamine modulates subthreshold resonance.

Sample neuron represents the largest f_{res} recorded. A: Sample subthreshold voltage responses (at -57 , -77 and -97 mV) to ZAP current inputs for control (cont, left) and 50 μM histamine (hist, right). Histamine shifts the peak voltage amplitude to the right with hyperpolarization at -77 mV (3.2 s vs. 4.7s) and -97 mV (4.5 s vs. 5.6 s), but not -57 mV (1.5 s vs. 1.5 s) (arrows). Note that histamine has little or no effect at -57 mV. B: pFRC shows a voltage and frequency dependent rightward shift in phase in the presence of histamine. In control, at -97 mV, the voltage leads the current up to ~ 2.4 Hz compared to 6.3 Hz in the presence of histamine. C: Similarly, the zFRC shows a histamine induced voltage and frequency dependent rightward shift in the maximum impedance (Z_{max}) as well as an increase in the low frequency attenuation of impedance at more negative potentials. D: Three dimensional plot of impedance as a function of frequency and voltage using fitted lines in control (dark grey) and in the presence of histamine (light gray). Histamine decreases Z_{min} and Z_{max} and shifts f_{res} to the right at potentials negative to -67 mV compared to control E: Plot for f_{res} as a function of voltage. The f_{res} is increased in the presence of 50 μM histamine at -67 mV and lower. In control, f_{res} was 1.0 Hz at -57 mV and 4.7 Hz at -97 mV compared to 1.1 Hz and 8.6 Hz, respectively, in the presence of histamine. F: Plot of Q as a function of voltage. Similar to f_{res} , histamine increased Q for all voltages tested. Q peaked at -77 mV followed by a decline at more hyperpolarized potentials.

Histamine had no effect on the Q value at -57 mV (1.1 vs. 1.0) whereas at -67 mV and lower, the histamine-induced decrease in the impedance was characterized by a larger decrease in Z_{\min} compared to Z_{\max} , resulting in an increase in the Q value (Figure 4.2F). Moreover, when compared to the control condition, Q peaked at -77 mV (1.1 vs. 1.7) and declined with further hyperpolarization. Pooled data (Figure 4.3B) revealed a similar trend where the increase in the Q value was voltage dependent between -57 mV to -97 mV and was significantly larger after application of $50 \mu\text{M}$ histamine (2 way ANOVA, $P < 0.05$, $n = 7$) with the largest increase occurring near -77 mV (1.1 ± 0.1 vs. 1.4 ± 0.1).

4.3.3 ZD-7288 prevents histamine modulation of subthreshold resonance

In keeping with I_h production of subthreshold resonance it was speculated that blocking I_h would eliminate resonance and its modulation by histamine. To investigate this hypothesis, $100 \mu\text{M}$ ZD-7288 was bath applied for 5 minutes and neurons were stepped to -127 mV under current clamp mode to verify the elimination of the depolarizing voltage sag characteristic of I_h activation. Following block of I_h , the ZAP method was used before and after application of $50 \mu\text{M}$ histamine.

In all cells tested, ZD-7288 had no effect on the slight resonant properties at -57 mV, consistent with the lack of I_h activation in this range. With increased hyperpolarization (-67 to -97 mV), however, the characteristic spindle shaped voltage response observed in the control was absent in all neurons during ZD-7288 application. The voltage response, instead, was characterized by a wedge shape with the peak

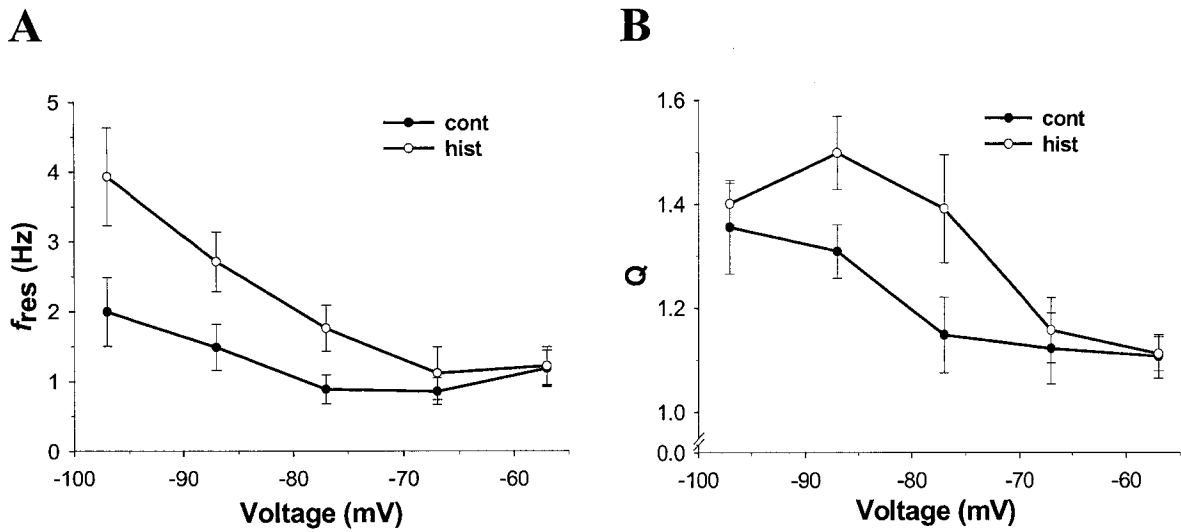


Figure 4.3 Histamine increases the f_{res} and Q.

Pooled data (mean \pm S.E.M., $n = 7$). A: Plot of f_{res} as a function of voltage. Compared to the control condition (cont), the voltage dependent increase in f_{res} is significantly increased in the presence of 50 μM histamine (hist) (2 way ANOVA, $P < 0.01$). B: Plot of Q value as a function of voltage. Histamine significantly increased the voltage dependent increase in Q value when compared to the control condition (2 way ANOVA, $P < 0.05$). Again there is no change at -57 mV with the greatest effect observed in the range of -77 mV to -87 mV. Similar to Figure 4.2 E, histamine produced less effect on Q at more hyperpolarized potentials.

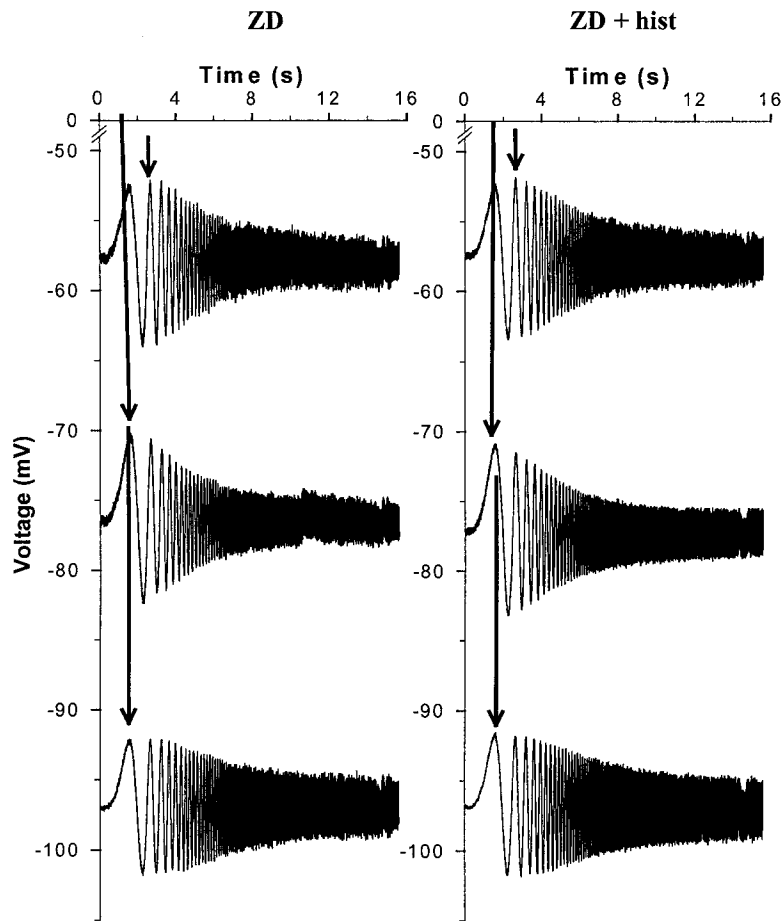
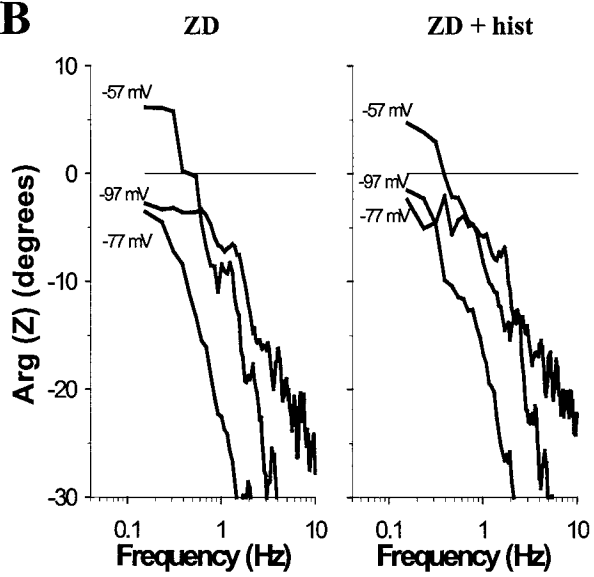
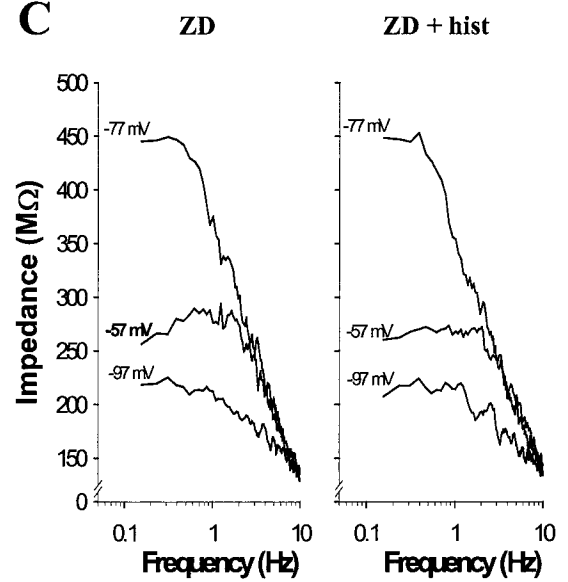
amplitude occurring at the lowest frequencies, a characteristic of nonresonant neurons (Figure 4.4A). Moreover, no phase shift was evident within the same voltage range (Figure 4.4B). In a similar vein, there was no voltage dependent low frequency attenuation of the impedance in the zFRCs and FRS (Figures 4.4C and D). For example, in the trace shown, the f_{res} ranged from 0.2 Hz at -67 mV to 0.3 Hz at -97 mV and the Q values approximated 1.0 (Figure 4.4E,F). Moreover, application of histamine had no effect. This was further verified by pooling the data (Figure 4.5A,B) revealing that the voltage dependence of f_{res} and the Q value, as well as the effect of histamine, were not statistically significant (2 way ANOVA, $P > 0.05$, $n = 5$).

Notwithstanding the absence of resonance in the hyperpolarized range, the general shape of the FRS was maintained. This included an overall increase in impedance peaking at approximately -67 mV to -77 mV, followed by a decline at more negative holding potentials.

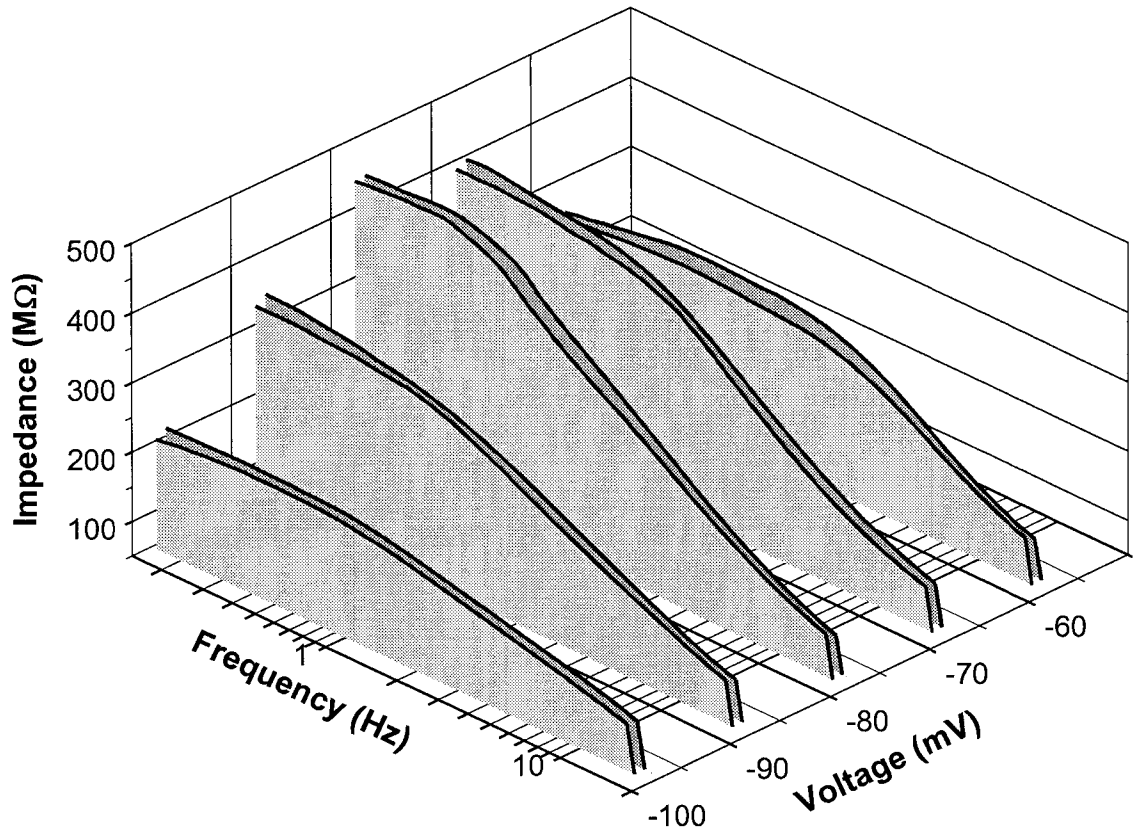
4.3.4 Tiotidine blocks histamine modulation of subthreshold resonance

The above results show that histamine acts to modulate subthreshold resonance through actions on I_h . Given that histamine modulates I_h via the H_2 receptor subtype (see chapter 3), blocking this receptor should prevent histamine action on subthreshold resonance. To investigate this hypothesis, 500 nM tiotidine was continuously bath applied after achieving whole cell rupture. The ZAP recordings were then made before and after application of 50 μM histamine.

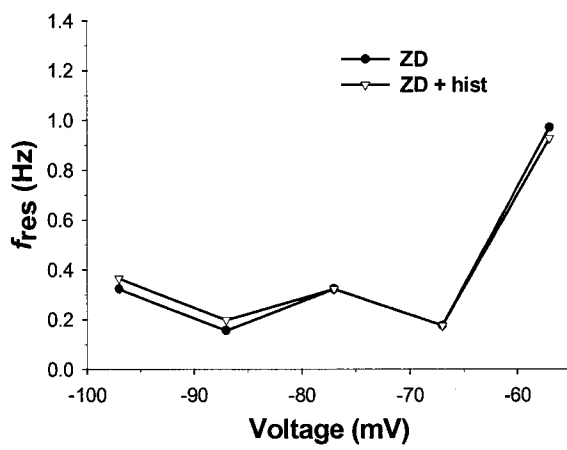
Figure 4.6A shows that tiotidine had little effect on the formation of the spindle

A**B****C**

D



E



F

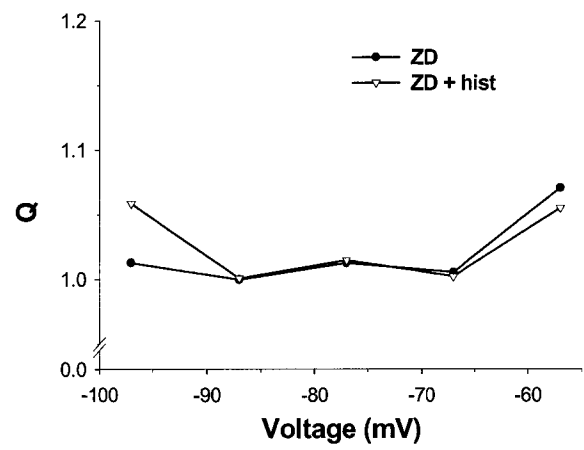


Figure 4.4 Histamine effect on subthreshold resonance is blocked by ZD-7288.

A: Sample subthreshold voltage responses (at -57, -77 and -97 mV) to ZAP current inputs for 100 μ M ZD-7288 (ZD, left) and ZD plus 50 μ M histamine (ZD + hist, right). ZD blocks the shift in peak voltage amplitude previously observed with increasing hyperpolarization (left, arrows). In the presence of ZD, histamine has no effect on the voltage amplitude (arrows). Note the small resonant effect observed at -57 mV is unaffected by ZD and histamine. B: pFRC shows that ZD eliminates the phase shift previously observed with increasing hyperpolarization. There is no effect on the shape of the pFRC by histamine with ZD present. C: The zFRC also shows that ZD eliminates resonance by blocking the low frequency attenuation at more negative potentials. Histamine has no effect on the zFRC with ZD present. D: Three dimensional plot of impedance as a function frequency and voltage using fitted lines in ZD (dark grey) and in the presence of histamine (light gray). ZD eliminates resonance at potentials negative to -67 mV resulting in Z_{\min} equaling Z_{\max} . The elimination of resonance blocks the histamine-induced effects on the zFRC. E: Plot of f_{res} as a function of voltage. The f_{res} closely equals the lowest sampled frequency (0.2 Hz) at -67 mV and lower. Histamine has no effect on f_{res} in the presence of ZD. F: Plot of Q as a function of voltage. Similar to f_{res} , the histamine-induced effect is blocked in the presence of ZD. Note that ZD results in a Q value close to 1 for potentials of -67 and lower, consistent with the elimination of resonance.

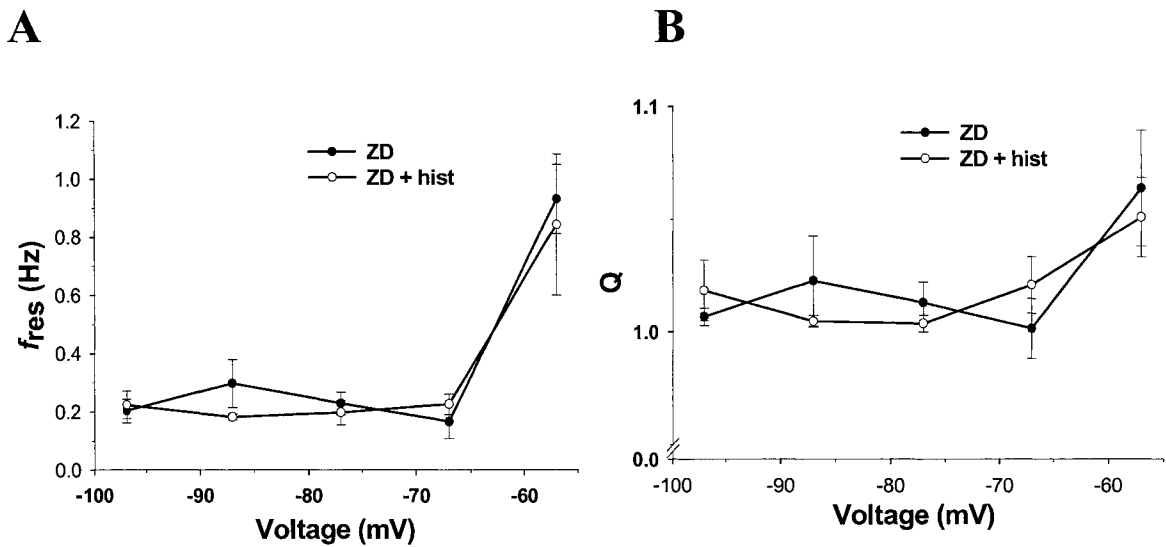


Figure 4.5 ZD-7288 blocks resonance and the histamine induced increases in f_{res} and Q value.

Pooled data (mean \pm S.E.M., $n = 5$). A: Plot of f_{res} as a function of voltage showing the mean. At potentials of -67 mV and lower, f_{res} equals the lowest frequency sampled. $100 \mu\text{M}$ ZD-7288 (ZD) eliminated the hyperpolarized voltage dependent increase of f_{res} and the increase induced by $50 \mu\text{M}$ histamine (ZD + hist) (2 way ANOVA, $P > 0.05$). F: Plot of Q (mean \pm S.E.M.) as a function of voltage. ZD eliminated the hyperpolarized voltage dependent increase in Q and the histamine induced increase in Q at potentials of -67 mV and lower (2-way ANOVA, $P > 0.05$). Note that ZD has no effect on the f_{res} or Q at the holding potential of -57 mV.

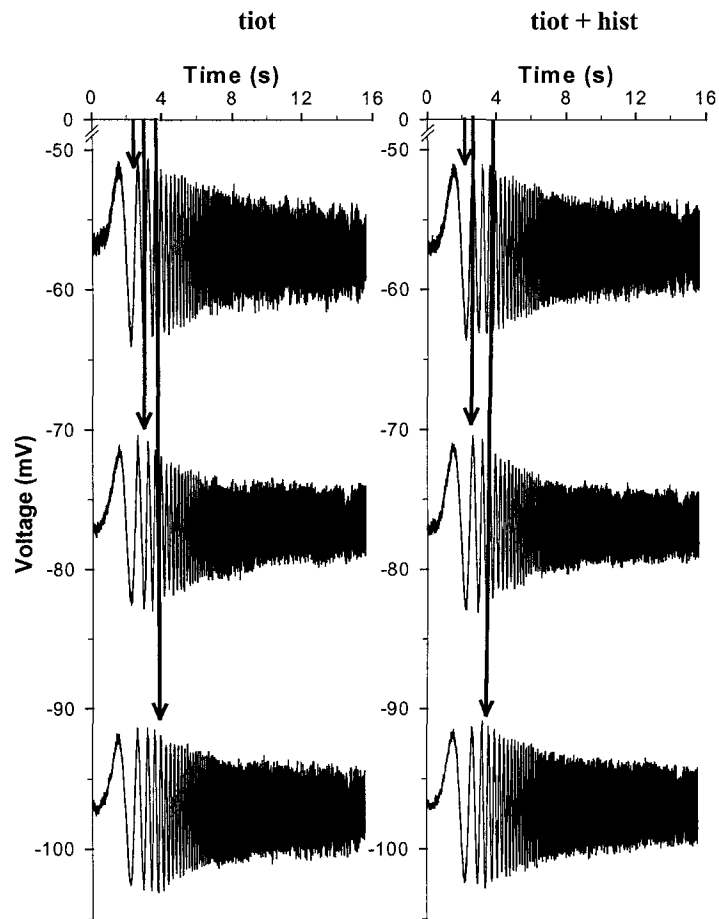
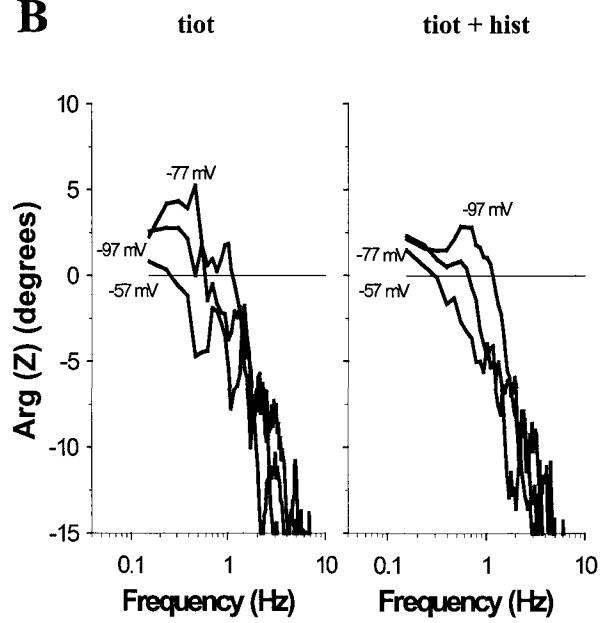
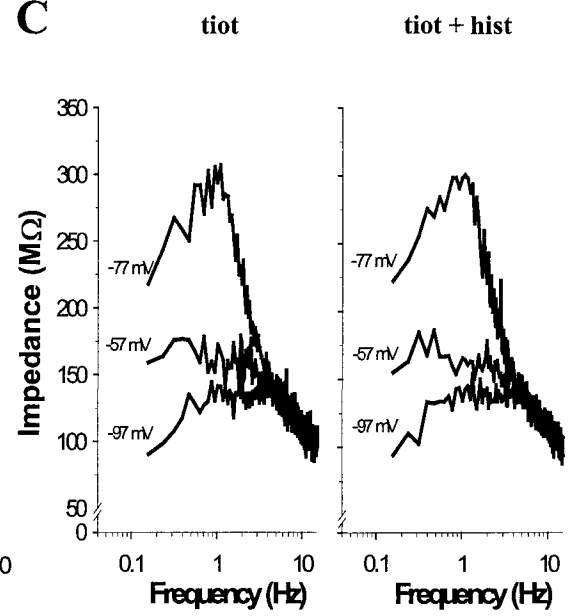
shape voltage response with increased hyperpolarization. However, tiotidine blocked the histamine-induced shift in the peak amplitude to higher frequency inputs. Similarly, the histamine-induced increase in the phase shift to higher frequencies also was absent with increased hyperpolarization (Figure 4.2B).

In keeping with these findings, the control zFRCs show the prominent resonant features consistently observed at potentials negative to -67 mV. However, histamine had little or no effect on impedance (Figure 4.4 C and D). For example, there was little difference between the f_{res} (0.5 Hz vs. 0.5 Hz at -67 mV, 1.8 Hz vs. 1.7 Hz at -97 mV) and the Q value (1.1 vs. 1.1 at -67 mV, 1.5 Hz vs. 1.5 Hz at -97 mV) under control conditions when compared to histamine (Figure 4.5E,F). In addition, pooled data (Figure 4.7) revealed that, although the increase in f_{res} and the Q value was voltage dependent between -57 mV to -97 mV, there was no difference in the increase between control conditions and post-application of histamine (2 way ANOVA, $P < 0.05$, $n = 3$).

4.4 Discussion

4.4.1 Subthreshold resonance in neocortical neurons

Past studies in the neocortex have shown I_h to play a major role in attenuating excitatory postsynaptic potentials, as well as in temporal and spatial summation (Nicoll et al., 1993; Schwindt and Crill, 1997; Stuart and Spruston, 1998; Berger et al, 2001; Berger et al. 2003). In addition to this role, I_h has also been shown to create a band pass filter configuration or resonance in neocortical neurons, which may act to filter somatic and dendritic input (Hutcheon et al., 1996a,b; Ulrich, 2002).

A**B****C**

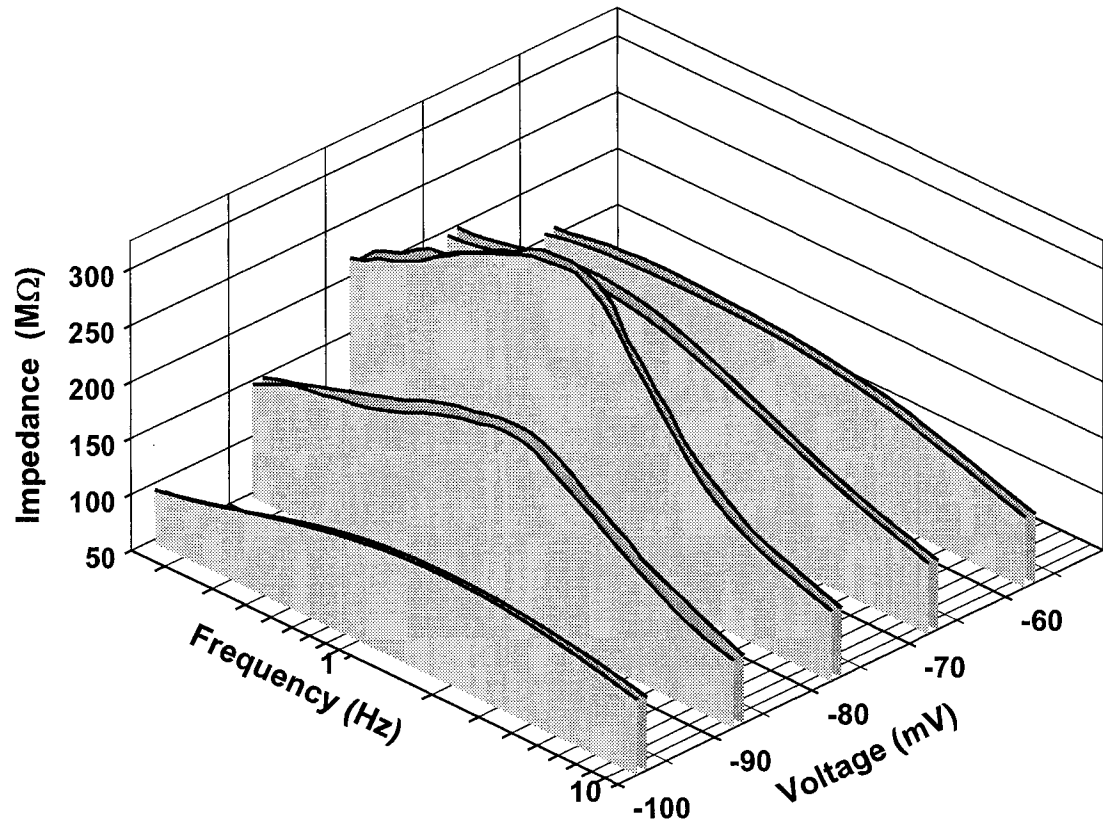
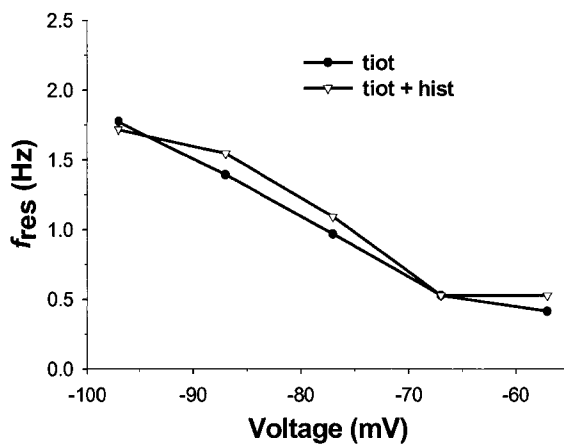
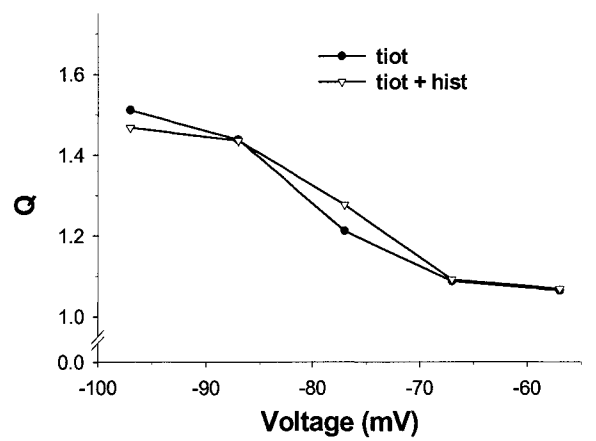
D**E****F**

Figure 4.6 Histamine induced effect on subthreshold resonance is blocked by tiotidine.

A: Sample voltage responses (at -57 , -77 and -97 mV) to ZAP current inputs resonant neuron for 500 nM tiotidine (tiot, left) and tiotidine plus 50 μ M histamine (tiot +hist, right). Tiotidine has no effect on the resonant properties observed at -67 mV and lower, but blocks the histamine-induced shift in voltage amplitude (arrows). B: pFRC shows that tiotidine blocks the histamine induced rightward shift in phase. C, D: The zFRC also shows that tiotidine blocks the histamine induced voltage dependent rightward shift in frequency (Z_{\max}) as well as the increase in the low frequency attenuation of impedance with hyperpolarization. E: Plot for f_{res} as a function of voltage. Histamine has no effect on f_{res} in the presence of tiotidine F: Plot of Q value as a function of voltage. Similar to f_{res} , histamine has no effect on Q in the presence of tiotidine.

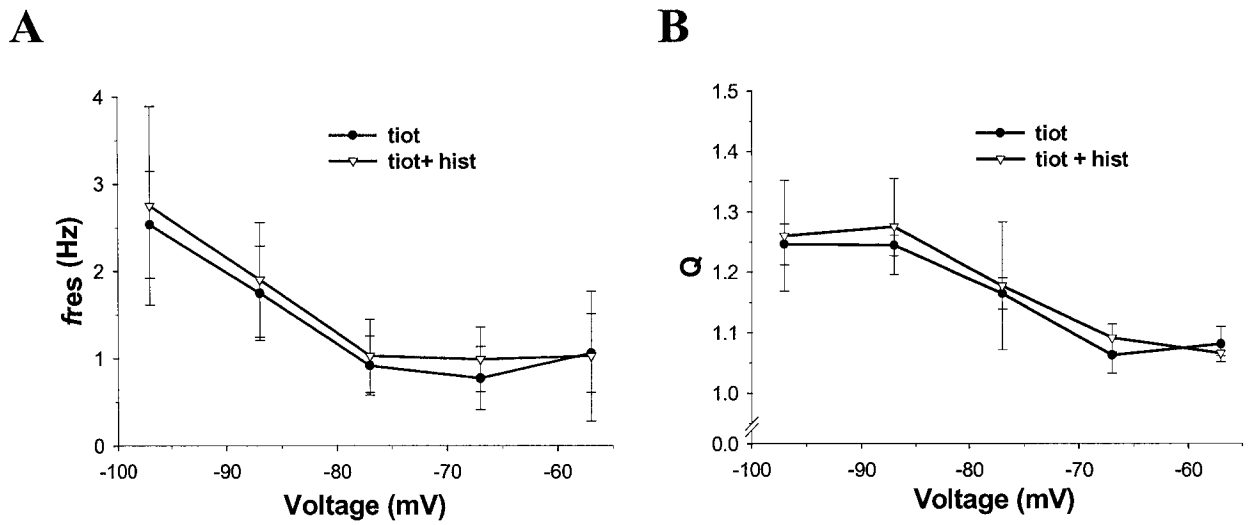


Figure 4.7 Histamine induced increase in f_{res} and Q value is blocked by tiotidine.

Pooled data (mean \pm S.E.M., $n = 3$). A, B.: Plot for f_{res} and Q value as a function of voltage. Tiotidine (500 nM) blocks the histamine (50 μ M) induced increase in f_{res} and Q value (2-way ANOVA, $P > 0.05$).

Consistent with these findings, the present study shows that layer V neocortical pyramidal neurons possess I_h dependent subthreshold resonance in the delta (0.2 - 4 Hz) and theta range (4 – 12 Hz). The features of subthreshold resonance in these neurons were shown to be modulated by histamine, an action most likely occurring through the modulation of I_h , which results in a voltage dependent increase in the sharpness and frequency of resonance. This may be the first time that the neuronal frequency response behaviour of neocortical neurons has been shown to undergo modulation by an intrinsic compound.

Similar to the findings of Hutcheon et al. (1996a,b), the subthreshold resonance observed in this study has many points of similarity with the activation threshold and kinetics of I_h shown in Chapter 2 and 3: (1) the voltage dependence of I_h activation closely resembles that of resonance (i.e., -67 mV and below); (2) the voltage dependent slow time course and rectifying nature of I_h are consistent with the range of observed phase shifts and resonant frequencies; (3) resonance was absent in the presence of ZD-7288, similar to the block of I_h and resonance by Cs^+ and ZD-7288 shown by Hutcheon et al. (1996a) and Ulrich (2002), respectively; (4) the histamine-induced shift in f_{res} and the Q value is consistent with the histamine-induced shift in I_h activation and in increased conductance; (5) the block of the histamine-induced effect on resonance by the H_2 receptor antagonist tiotidine is consistent with the tiotidine block of the histamine induced effect on I_h shown in Chapter 3.

Under control and experimental conditions both f_{res} and the Q value were highly voltage dependent. Similar to the resonance effects reported by Hutcheon et al. (1996a)

and Ulrich (2002) f_{res} increased almost linearly from -67 mV with increased hyperpolarization. The average f_{res} at -97 mV (~ 1.5 Hz) was close to the 1.0 - 3.0 Hz delta range reported by Hutcheon et al. (1996a,b), but lower than the 6.0 Hz and higher theta range reported by Ulrich (2002) at similar holding potentials. The difference from the latter is likely due to the strong temperature dependence of resonance in these neurons compare to resonance shown in the present study ($35 - 36^{\circ}\text{C}$ vs. room temperature). Similar temperature dependent results were observed for subthreshold resonance in the hippocampus where changes in the recording temperature from 33°C to 38°C shifted f_{res} from 4.0 to 9 Hz, respectively (Hu et al., 2002). Again this can be explained by changes in the parameters of I_h , since the time constants can be 6 to 11 times faster at body temperature compared to those at room temperature (Spain, Schwindt and Crill, 1987). Indeed, Hutcheon et al. (1996b) showed in a model of neocortical I_h dependent resonance that substituting I_h kinetics to reflect those at physiological temperatures increased the subthreshold frequencies an order of magnitude higher than those observed at room temperature. The resultant resonant frequencies, occurring in the theta and alpha range (5 - 15 Hz), indicate that I_h is capable of making contributions to rhythmic activity in awake animals (see section 5.2.3).

The Q value showed a similar increasing trend with hyperpolarization reaching a near asymptote value at potentials less than -70 to -80 mV. Again the average maximum value (~ 1.3) was similar to the maximum range of 1.4 – 1.5 observed by Hutcheon et al. (1996a). It should be noted that the above values reflect observations made in the presence of TTX, a known blocker of the class II low frequency amplifier, I_{Nap} . As a

result, the Q value could be substantially higher in the range where I_h and I_{NaP} overlap (i.e. ~ -65 mV), based on results from Hutcheon et al. (1996a). This would also have the effect of decreasing the resonant bandwidth at more depolarized potentials and thus may act to finely tune neuronal input near the firing threshold.

Another interesting observation was the slight resonant feature observed in the depolarized range. Although resonance in this range was not the focus of the present study, it does reinforce the variety of resonant mechanisms found in other neocortical studies such as those involving current I_M (Gutfreund et al., 1995).

4.4.2 *Voltage dependent mechanism of subthreshold resonance*

Assuming physiologically relevant temperatures, the voltage dependence of resonance provides evidence that I_h is only functionally significant in processing inputs of less than 20 Hz. This can be explained in terms of the CM + S or reduced membrane model (RM) which contains only a passive component made up of I_{Leak} and the membrane capacitance, and I_h , a class I current (Hutcheon et al., 1996a; Hutcheon and Yarom, 2000). As discussed in section 1.4, the passive component acts as a low pass filter which attenuates inputs at frequencies above $1/2\pi\tau_m$ and is unaffected by changes in the membrane potential. In the absence of I_h the zFRC is characterized by a Q value of 1, with f_{res} occurring at the lowest input frequency and no change in magnitude of Z_{max} or Z_{min} for all holding potentials.

The introduction of I_h into the model results in a contribution of rectifying inward current which, in effect, counteracts changes in the membrane potential with

hyperpolarization. During a repolarizing event, a characteristic of oscillating inputs, I_h has an opposite effect by slowly deactivating. This allows for a time dependent decreased contribution to depolarization at potentials above the point where I_h initially activates thus explaining why I_h dependent resonance is observed beyond its activation. If the frequency and magnitude of the input is such that enough time is available for the activation and deactivation of I_h , the zFRC will be characterized by an attenuation of the impedance at that frequency. On the other hand, as the input frequency increases, less time is available for activation and deactivation, thus I_h acts to pass higher frequencies. Similar to the passive component, the frequency at which I_h stops responding to oscillating input is determined by its kinetics (i.e. $1/2\pi\tau_h$). Unlike the passive component, however, the kinetics of I_h change with increased hyperpolarization resulting in both an increase in the activation rate and conductance, as shown in Chapter 2 and 3. Assuming the range of the low and high frequency attenuation do not overlap (i.e. $1/2\pi\tau_h < 1/2\pi\tau_m$) a band of non-attenuated frequencies will exist between both filters, the peak of which represents f_{res} . As I_h activates with increased hyperpolarization $1/2\pi\tau_h$ increases, thus shifting and narrowing the band of non-attenuated frequencies (i.e., increasing f_{res}), as well as decreasing the impedances at the low frequencies, thereby increasing Q . Since the magnitude of impedance at f_{res} is greatest and therefore more likely to initiate firing, the position of the I_h activation curve and its level of conductance can determine to what extent I_h contributes to changes in the subthreshold range and spike initiation. In the present study, the observed change in the phase shift, the frequency at which the voltage leads the current, f_{res} and the Q value are consistent with the above explanation.

4.4.3 Histamine modulates subthreshold resonance

The histamine-induced rightward shift in the pFRC and zFRC is consistent with the histamine-induced shift in I_h activation. Indeed, similar to the ~ 10 mV maximum shift in activation induced by 50 μ M histamine, the f_{res} observed at -77 mV under control conditions closely matches f_{res} at -67 mV after application of histamine. A simple shift in the activation kinetics does not, however, explain f_{res} becoming increasingly larger with hyperpolarization after application of histamine. This may be due to an additive effect of the histamine-induced increase in I_h conductance as evidenced by the observed increase in I_{max} shown in Chapter 3. Based on investigations by Hutcheon et al. (1996a), and assuming that all other factors are kept constant, a two fold increase in the conductance of I_h at -70 mV acts to decrease the overall impedance of the membrane circuit while increasing both f_{res} and the Q value by a factor of 1.3.

The same model can explain the decrease in Q at potentials negative to -77 mV. The zFRC for I_h is opposite to that of the passive circuit being characterized by low impedance values at lower frequencies, followed by increasing impedances at intermediate frequencies and asymptotic impedances at higher frequencies. With increased hyperpolarization, the rate of activation for I_h increases, which acts to move the range of low frequency attenuation towards the range of high frequency attenuation. The point of intersection between the two ranges determines the magnitude of Q. When the point of intersection is within the range of asymptotic impedances, Q is at its maximum. As the range shifts further, such that it begins to intersect the range of low frequency

attenuation, Q will become increasingly smaller. Theoretically, if $1/2\pi\tau_h$ becomes larger than $1/2\pi\tau_m$, Q will equal 1 and resonance disappears.

Overall, histamine induces a shift of f_{res} to higher frequencies and decreases the impedance magnitude in a voltage dependent manner. A more distinct action of histamine is the formation of a voltage dependent bell shaped increase in Q with an approximate peak near -87 mV and the greatest increase near -77 mV. Therefore, unlike control conditions, where both the Q and f_{res} increase with hyperpolarization, histamine acts to finely tune a neuron's frequency responses close to I_h activation and the resting membrane potential. Depending on the position of I_h activation relative to the threshold for action potential generation this may have important functional implications in synchronizing neuronal activity in the networks that include histamine sensitive components.

5. Summary and Conclusions

5.1 Rundown of I_h

The results from the investigations presented in the preceding chapters provide new insights into histamine modulation of the hyperpolarization activated cationic current, I_h , and subthreshold resonance in cortical neurons.

Under whole cell recording conditions, preliminary investigations into I_h revealed a time dependent hyperpolarizing shift in I_h activation and decreased current that confounded interpretation. Failure to observe a change in the resting membrane potential or the instantaneous current over the course of the recording period suggested that the rundown of I_h did not result from deterioration in the whole cell configuration or shunting due to an increased membrane conductance. It was therefore concluded that the rundown resulted from cell dialysis by the recording pipette leading to the loss of one or more intracellular factors required for the normal function of I_h channel activity. Further experiments revealed that a basal level of intracellular cAMP was required for the maintenance of I_h . Addition of cAMP to the pipette solution prevented rundown of I_h and produced a concentration-dependent (5 - 100 μ M) depolarizing shift in I_h activation, increased amplitude of I_h , and depolarization of the resting membrane potential. The requirement for cAMP was further supported by the failure to observe the expected modulation of I_h by the cAMP analogue 8-bromo-cAMP and the adenylyl cyclase activator forskolin in the absence of added cAMP to the pipette filling solution.

5.2 Role of protein kinase

Interestingly, the effects of the non-specific protein kinase inhibitor H7 blocked both the forskolin and histamine-induced action on I_h suggesting the possible involvement of phosphorylation in the regulation of I_h . This contrasts with findings that I_h is directly modulated by cAMP. This direct modulation likely occurs in cortical neurons, but does not exclude other possibilities such as a secondary regulation of I_h via direct phosphorylation of I_h , phosphorylation of a protein that modifies the cAMP cascade, or a protein kinase-induced reduction of a shunt conductance that resulted in an improved space clamp. Support for this can be found in Chapter 2 where it was observed that reducing K^+ conductances partially mimics the effects of cAMP in preventing rundown as well as increasing the amplitude of I_h . Simply reducing a shunt however, cannot fully explain the observed results since reducing K^+ conductances had no effect on the activation of I_h . As well, the lack of a cAMP-induced change in the instantaneous current undermines this possibility. Similarly, the lack of an H7 effect on I_h , in the absence of forskolin and histamine, suggests there is little in the way of basal protein kinase activity. As a result, protein kinase activity is not likely involved in the rundown of I_h , consistent with a direct action by cAMP. Overall, it would appear there is a combination of processes at play, although further experiments are required to evaluate the implications of these observations.

5.3 Histamine and I_h

Histamine-induced a concentration-dependent (1 - 50 μ M) depolarizing shift in the activation of I_h , increased the amplitude of I_h , and depolarized the membrane potential. These effects closely mimic those observed with the addition of cAMP to the recording pipette. Furthermore, the effects of histamine were occluded during co-application of forskolin, consistent with histamine actions being induced through the mechanism of adenylyl cyclase activation. Neither H_1 nor H_3 antagonists altered basal activity or histamine-induced actions. On the other hand, histamine's effects were blocked in a concentration-dependent manner by tiotidine (5 – 500 nM), an H_2 receptor antagonist, and mimicked by amthamine (0.5 – 25 μ M), an H_2 receptor agonist. These results are consistent with an H_2 receptor-mediated action.

5.4 Cortical resonance and I_h

Based on data from the ZAP experiments in Chapter 4, neurons proximal to layer V possess I_h dependent subthreshold resonance in the delta to theta range (1 - 8 Hz) at potentials negative to -67 mV. This is supported by the following points of similarity with the activation kinetics of I_h shown in Chapters 2 and 3: (1) the voltage dependence of I_h activation closely resembles that of resonance (i.e., -67 mV and below); (2) the voltage dependent time course of I_h is consistent with the range of observed phase shifts and resonant frequencies; (3) resonance was eliminated in the presence of ZD-7288.

The frequency (f_{res}) and magnitude of resonance (Q) were voltage dependent. Resonant frequencies, at room temperature, under control conditions averaged close to 1

Hz near rest (-70 to -75 mV) and above 2 Hz at -97 mV. Q showed a similar voltage dependent trend with average values ranging between 1.1 and 1.4, respectively. Consistent with the histamine-induced shift in I_h activation and increased conductance, histamine was also shown to modulate the resonant behaviour of neocortical neurons. This was characterized by a shift in f_{res} (~ 1.5 Hz near rest, ~ 4 Hz at -97 mV) and an overall decrease in the impedance up to an input frequency of 10 Hz. Also, in keeping with the histamine-induced shift in I_h activation, the increased current resulted in an increase in Q over the range of -67 to -97 mV with the greatest change observed just below the resting membrane potential (-77 mV).

5.5 Physiological relevance

The histaminergic system plays a role in cortical activation in part by direct widespread hypothalamo-cortical projections, and indirectly, by stimulating the cholinergic system originating from the nucleus basalis magnocellularis and the substantia innominata (Khateb et al., 1990; Khateb et al., 1995; Lin et al., 1996; Cecchi et al., 2001). More is known about the modulation of the indirect routes and rather less about the complementary role of the hypothalamo-cortical histaminergic projections. The work in this thesis provides new insights into direct histaminergic influence on the cellular mechanisms of cortical activity. Although it is beyond the scope of this body of work to ascertain the global effects of modulation on these neurons, the following subsections provide a brief overview of the physiological implications of these findings.

5.5.1 *Layer V anatomy*

This thesis focused on recordings from neurons proximal to cortical layer V. Layer V neurons have intrinsic oscillatory properties which probably gives them an important role in promoting synchronized activity and, hence, they represent a potentially important site for modulation of cortical activity during wakefulness and sleep (Silva, et al., 1991; Amitai, 1994; Flint and Connors, 1996; Lukatch and MacIver, 1997). To better understand how changes in layer V activity may affect brain physiology, a good starting point is to provide an overview of the neural circuitry outlined by their dendritic and axonal morphology.

Layer V is integrated into a system of neocortical and sub-cortical neural circuits that are characterized by a high degree of feed forward and feedback connections (Thomson and Bannister, 2003). The anatomy of this region is primarily characterized by large burst firing pyramidal neurons contained in upper layer Va. These neurons are thought to have an important role in processing excitatory and inhibitory cortical activity since their dendrites form extensive arborizations in upper cortical layers (I-IV), thereby allowing them to directly access the afferent inputs from these superficial regions (Thomson and Bannister, 2003). In addition, since layer V receives little or no input from the thalamus, this dendritic organization allows for direct and indirect contact from thalamocortical inputs originating from specific thalamic nuclei, i.e., the lateral geniculate nucleus (LGN), the inhibitory nucleus reticularis thalami, and non specific thalamic nuclei, i.e., the pulvinar (Thomson and Bannister, 2003). Communication between the neocortex and the thalamus represents one of the most important circuits in

the corticolimbic system. The thalamus is the centre for a massive convergence of both afferent information from the periphery and efferent cortical feedback. In keeping with its morphology, the thalamus plays an important role in the integration and/or selective channelling of information received from the sensory periphery and the neocortex (Choe, 2004). Also contained in upper layer Va, as well as the lower layer Vb, are smaller regular spiking pyramidal neurons, which are characterized by shorter dendritic arborizations that, for the most part, do not extend beyond layer III (Thomson and Bannister, 2003).

Depending on the cortical area, efferent projections from layer V pyramidal neurons target a number of cortical and sub-cortical areas. Cortical projections include a dense axonal arborization within layer V, as well as horizontal projections within layers V and VI giving rise to ascending branches that project into the superficial layers which provides a means for negative feedback through contact with inhibitory neurons (Burkhalter and Bernardo, 1989; Fujita and Fujita, 1996). As well, layer V axons form long horizontal projections that extend beyond local cortical regions to innervate other high order cortical areas, e.g., trans-callosally (Gilbert and Wiesel, 1979).

Layer V is only one of two neocortical layers, the other is layer VI, which provides excitatory innervation to the thalamus (White and Hersh, 1982; Jones 2001). Layer V neurons target only the pulvinar and are a major driving force of excitatory input to the thalamus (Jones 2001; Shipp, 2003). The pulvinar, the largest nucleus in the thalamus, plays a crucial role in attention and motor processing and acts to coordinate

neocortical information processing by facilitating and sustaining the formation of synchronized activity (Guillery and Sherman, 2002; Shipp, 2003).

Other subcortical targets include the superior colliculus and the pons, mainly via the large pyramidal neurons, as well as the striatum, via the smaller regular spiking neurons. The superior colliculus plays an important function in combining and processing multiple sensory inputs to guide adaptive motor response such as ocular motor control and organism orientation within environmental maps (King, 2004). The pons is important in the control of arousal and sleep (Baghdoyan, Spotts and Snyder, 1993; Douglas, Demarco, Baghdoyan and Lydic, 2004) and is an important input relay for corticocerebellar connections involved in motor cognitive processing (Schmahmann and Pandya, 1997). The striatum, made up of the caudate nucleus and the putamen, largely serves as the input nucleus for the basal ganglia and plays a role in the control and selection of motor programs such as locomotion, posture, eye movements, breathing, chewing, swallowing and expression of emotions (Grillner, Hellgren, Menard, Saitoh and Wikstrom, 2005).

5.5.2 *Modulation of cortical I_h*

Findings of this thesis provides evidence that the I_h current found in layer V neurons is modulated by increasing the intracellular level of cAMP or by a histamine-induced activation of the H_2 receptor subtype. Shifting the activation threshold of I_h in the depolarizing direction, as well as increasing its amplitude, has important implications for the excitatory behaviour of these neurons, including changes in integration near the

resting membrane potential, contribution to voltage overshoots and action potential generation, dendritic integration, and membrane resonance. It is worth noting that none of these actions are mutually exclusive but, rather, they act together to modify the behaviour of these neurons and consequently the circuits to which they contribute. This may allow neurons, which are hard wired, to change functionality with changes in behavioural state.

5.5.2.1 I_h contribution to membrane potential

Shifting the activation threshold of I_h , as shown in this thesis, alters the resting membrane potential. This action will result in two major outcomes. First, there will be an increase in the amount of I_h current active at rest and a depolarization of the membrane towards the I_h reversal potential (~ -40 to -45 mV) resulting in an increase in membrane excitability. Although a higher density of I_h channels exists on the dendrites of cortical pyramidal neurons, a shift in I_h activation may depolarize the axon hillock because the inward current in the dendrites in part flows out through the soma thereby bringing the membrane potential closer to threshold for spike generation. Second, this effect is complemented by a decrease in the membrane input resistance, allowing the membrane to counteract hyperpolarizing fluctuations, and thus stabilizing the membrane near rest. Note, however, that since both the amount of I_h and its rate of activation increases at potentials negative to I_h activation, the extent to which I_h can induce these effects will depend on the timing and amplitude of inputs. In any event, a positive shift in the I_h activation curve suggests that that I_h will stabilize the membrane and reduce

hyperpolarizing influences, since the membrane impedance is lower and the faster kinetics of I_h will better limit higher frequency hyperpolarizing drive. In addition, a shift towards threshold will enable I_h to be more readily incorporated into the ongoing synchronized /tonic activity of the neuron.

5.5.2.2 I_h contribution to voltage overshoots and action potential generation

Whether I_h contributes directly to the generation of action potentials was not examined in this study. Depending on the shift in I_h activation, and the level and timing of tonic depolarization during firing, I_h can contribute to depolarization, repolarization, and repetitive spiking. This can be explained by its activation kinetics and the mixed Na^+/K^+ nature of its current. If I_h is active at rest or the membrane has been sufficiently hyperpolarized to activate I_h , the deactivation kinetics allow for an outward current at potentials positive to its reversal potential, contributing to repolarization and reducing spike amplitude, and an inward current at potentials negative to the reversal potential contributing to depolarization. As well, depending on the extent of I_h activation and its enhancement by histamine, the rebound overshoots resulting from the slow deactivation of I_h may move the membrane potential to spike threshold, particularly after repetitive spiking where there may be a deep hyperpolarizing response. Moreover, a positive shift in I_h activation increases the likelihood of an overlap with the activation range of other depolarizing conductances. For example, Hutcheon et al. (1996a) showed that the rebound following hyperpolarization and activation of I_h was reduced after application of TTX, which they argued provided evidence that I_h activated rebound overlaps the

activation range for the persistent sodium current, I_{NaP} . This overlap also has important consequences for the production of subthreshold resonance (discussed below).

Similarly, I_h may also interact with the low threshold transient Ca^{2+} current, I_T , in the generation of Ca^{2+} -mediated bursts which may lead to spike generation closely resembling the I_h - I_T burst firing mechanism observed in studies of thalamic relay and cortical neurons (McCormick and Pape, 1990a; Foehring and Waters, 1991; Bazhenov, Timofeev, Steriade and Sejnowski, 2002). The existence of this mechanism, however, may be limited since I_T tends to be expressed in only a small population of pyramidal neurons (Pare and Lang, 1998). As well, an I_h - I_T mechanism would depend on situations where hyperpolarization of the membrane allowed for the removal of I_T inactivation, whereas a positive shift in I_h activation would decrease the likelihood of this occurring. Thus, McCormick and Williamson (1991) showed that a histamine H_2 -mediated positive shift in I_h resulted in a reduction of I_T -mediated burst firing and an increase in single spike activity in thalamic relay neurons. The same effect may result in the reduction of cortical I_T -mediated burst firing. Although it has yet to be shown, I_T could also produce resonance in cortical neurons as has been shown for the thalamus and the inferior olivary nucleus (Steriade et al., 1993; Strohmann et al., 1994; Puil et al. 1994; Hutcheon et al., 1994; Lampl and Yarom, 1997). If so, the effect of histamine could reduce or eliminate this resonance.

5.5.2.3 I_h and dendritic integration

As stated previously, a positive shift in I_h activation would decrease membrane impedance at more depolarized potentials, resulting in an increased ability of the membrane to rectify hyperpolarization. This effect would also play an important role in shaping both excitatory and inhibitory postsynaptic potentials, i.e., EPSPs and IPSPs respectively, by changing the membrane's electrotonic properties. Studies of I_h in layer V cortex reveal a gradient of dendritic I_h characterized by an increase in current density with increasing distance from the soma (Stuart and Spurston, 1998; Williams and Stuart, 2000; Berger et al., 2001; Lorincz et al., 2002). The increased presence of I_h in the distal dendrites has been shown to decrease both the time and length constants of the membrane upon activation, resulting in a decreased probability of temporal and spatial integration of synaptic input (van Brederode and Spain, 1995; Schwindt and Crill, 1997; Stuart and Spurston, 1998; Williams and Stuart, 2000; Berger et al., 2001; Berger, et al., 2003). Although a histamine-induced increase in I_h would increase this shunt, it would also act to selectively facilitate synaptic input near f_{res} due to its resonant producing properties.

5.5.2.4 I_h and subthreshold resonance

As a low frequency resonant current, I_h is but one mechanism of many by which the brain can promote, integrate and stabilize coherent activity. For example, depending on state of activity such as the duration and amplitude of neural oscillations, the brain appears to have multiple mechanisms at the cellular and network level to handle a broad range of synchronized frequencies. In the neocortex, the characteristics of I_h makes it an

ideal candidate for the modulation of low frequency input in the subthreshold range near rest. As the membrane is depolarized beyond the range of I_h activation the potassium current I_M , may contribute to resonance (Gutfreund et al., 1995; Hu, et al., 2002.). Typical high frequency gamma oscillations, i.e. 30 - 40 Hz, which far outstretch the response capabilities of both I_h and I_M , have been shown to involve a number of currents responsible for spike frequency adaptation, e.g., slowly inactivating K^+ currents and I_{NaP} (Wang, 1993; Fuhrmann, Markram and Tsodyks, 2002). In addition, higher level network interactions involving inhibitory interneurons can elicit both slow (Budd, 2005) and fast (Steriade, Timofeev, Durmuller and Grenier, 1998; Brunel, 2000; Sanchez-Vives and McCormick, 2000; Steriade, 2001) cortical rhythms.

As shown in Chapter 4, the membrane impedance determined by I_h is highly dependent on frequency. As a result, I_h acts to attenuate excitatory synaptic input at frequencies below ω_h (see section 1.4, equation 2), and in relative terms facilitate excitatory input in the region where resonance is observed, i.e., the region where impedance is elevated. The very nature of this range of high impedance provides for a filtering mechanism that converts synaptic input at the resonant frequency into larger voltage responses than inputs of equal amplitude at frequencies above and below this range. The modulation of I_h acts to shift this peak and the characteristic change in the overall impedance to higher frequencies, thereby influencing the frequency response behaviour of cortical neurons. Moreover, based on modeling studies by Hutcheon et al. (1996b), a depolarizing shift in I_h activation would lead to a greater probability of I_h - I_{NaP} overlap resulting in even greater amplification of the high impedance region. This is

further accentuated by the fact that I_h is moving further away from the resonant attenuating effects of the K^+ current, I_{Kir} .

This thesis did not directly examine resonance-action potential coupling, however, other studies on pyramidal neurons have shown that resonance leads to an enhanced likelihood of generating spikes in response to oscillatory input at or near f_{res} (Hutcheon et al., 1996ab, Ulrich 2001). Further support for this action comes from studies that have confirmed that the subthreshold frequency preference of neurons is clearly communicated in preparations in which the level of synaptic noise is comparable to that prevailing *in vivo* (Richardson, Brunel and Hakim, 2003). If this is the case, histamine's effect of modulating I_h activation has important functional implications in synchronizing neuronal activity, the overall effect being the tuning of cortical activity to specific "preferred" frequencies.

5.5.3 *Low frequency activity and behaviour*

Assuming normal physiological conditions, I_h may contribute to the oscillatory activity in the brain at frequencies spanning the alpha, theta and delta ranges, i.e. 1 - 15 Hz (Hutcheon et al., 1996ab). Within this range, modulation of I_h by histamine may act to shift the frequency response of neocortical neurons and consequently the networks to which they contribute in a manner similar to the concentration-dependent results shown in the preceding chapters. For example, increased firing of histaminergic neurons should result in increased levels of histamine in the cortex similar to that observed during waking states. A decrease in the firing of histaminergic neurons should have the opposite

effect as expected during the transition to sleep (Orr and Quay, 1975; Monti, 1993). In fact, this is the case *in vivo* where histamine levels in the frontal neocortex were found to be 3.8 times higher during waking compared to sleep like states, indicating that histamine released in the neocortex is strongly related to the sleep-wake cycles and arousal (Chu, Huang, Qu, Eguchi, Yao and Urade, 2004). Noting that an additional excitatory effect of histamine in the neocortex is the H₁-mediated block of a K⁺ leak conductance, I_{KL}, the actions of histamine on neocortical I_h via the H₂ receptor may offer a modulating contribution to the transition of neocortical activity between slow wave sleep and more tonic desynchronized states observed during waking (Reiner and Kamondi, 1994; Steriade, 1996; Bazhenov et al., 2002; Dringenberg and Kuo, 2003).

Histamine modulation of I_h may also lead to changes in other waking related behavioural states that are commonly associated with rhythmic cerebral activities over the 1- 20 Hz range. For example, the 7 - 12 Hz EEG activity in the brain is associated with cognitive behaviours including attention (Yamagishi, Callan, Goda, Anderson, Yoshida and Kawato, 2003), memory tasks (Caplan, Madsen, Raghavachari and Kahana, 2001; Raghavachari, Kahana, Rizzuto, Caplan, Kirschen, Bourgeois, Madsen and Lisman, 2001; Rizzuto, Madsen, Bromfield, Schulze-Bonhage, Seelig, Aschenbrenner-Scheibe and Kahana, 2003) and synchronization of primary sensory input, associated with changes in behavioural context and expectancy (Von Stein, Chianga and Konjg, 2000). A similar range of rhythmic activity has also been linked to a number of motor behaviours including fluid self-administration tasks (Fontanini and Katz, 2005) and

patterned motor activity during and after exploratory behaviour (Nicoletis, Baccala, Lin and Chapin, 1995; O'Connor, Berg and Kleinnfeld, 2002).

Cortical rhythmic activity in the low frequency range has also been linked to pathological conditions as well. Studies involving examination of physiological tremor, commonly associated with epilepsy and Parkinson's disease, show that a 6 - 14 Hz coherence between cortical and electromyogram (EMG) recordings result from a direct corticomuscular transmission and that the rhythms are determined within cortical networks (Hellwig, Haussler, Schelter, Lauk, Guschlbauer, Timmer and Lucking, 2001; Raethjen, Lindemann, Dimpelmann, Wenzelburger, Stolze, Pfister, Elger, Timmer and Deuschl, 2002). Furthermore, it is likely that modulation of I_h may play a role in the control of rhythmic activity associated with these pathologies. For instance, the generation of slow wave paroxysmal activities (2 - 3 Hz) in the neocortex were shown to depend on the interaction of I_h , a calcium activated potassium current, I_{KCa} (most likely I_{AHP}), and I_{NaP} and that I_h may play a significant role in determining the threshold for slow wave intracortical seizures (Timofeev, Bazhenov, Sejnowski and Steriade, 2002; Timofeev, Grenier and Steriade, 2004). Similarly, in mutant stargazer mice, a model for generalized non-convulsive spike wave epileptic seizures, the current amplitude of I_h in layer V was found to be three times larger than in control neurons and it was suggested that this increase contributes to a hyperexcitable network and a subsequent a lower threshold for the onset of seizure activity (Di Pasquale, Keegan and Noebels, 1997).

5.6 Future research

Future research in this area should focus on histamine modulation of cortical rhythms. First, a histamine-induced change in subthreshold resonance and action potential coupling must be confirmed. Second, the effects of histamine should be examined under a variety of oscillatory activities. Early preliminary observations for this thesis showed that application of NMDA could repeatedly induce large amplitude oscillatory activity in these neurons and therefore could be used as an *in vitro* model. In contrast, other experiments should examine the effects of histamine on *in vivo* rhythmic activity. This could be achieved by recording from identifiable sites within known corticocortico or corticothalamic circuits. Other necessary experiments include investigations into histamine induced actions in the supra threshold voltage range and the possible interactions with subthreshold responses, e.g., a closer examination of I_h and I_{NaP} , I_T , and I_M and how histamine may act to change the interactions of these conductances and the frequency response of cortical neurons.

Future experiments should include the use of infrared differential interference contrast video microscopy in combination with independent manipulators for recording electrodes. In addition to quick identification of neurons, this visual technique allows for the detailed placement of a recording pipette, e.g., dendritic recordings. Multiple pipette placements along the soma and the dendrites may provide for a better control and understanding of space clamp errors, i.e., histamine modulation of secondary conductances that may have confounded the present results. Such studies also may permit

examination of the roles of histamine and resonance on coherence between neocortical neurons.

Bibliography

- Accili, E.A., Proenza, C., Baruscotti, M., and DiFrancesco, D. From funny current to HCN channels: 20 years of excitation. *News Physiol.Sci.* 17:32-37, 2002.
- Accili, E.A., Redaelli, G., and DiFrancesco, D. Differential control of the hyperpolarization-activated current (I_f) by cAMP gating and phosphatase inhibition in rabbit sino-atrial node myocytes. *J.Physiol.* 500:643-651, 1997.
- Airaksinen, M.S., Alanen, S., Szabat, E., Visser, T.J., and Panula, P. Multiple neurotransmitters in the tuberomammillary nucleus: comparison of rat, mouse, and guinea pig. *J.Comp.Neurol.* 323:103-116, 1992.
- Akasu, T. and Shoji, S. cAMP-dependent inward rectifier current in neurons of the rat suprachiasmatic nucleus. *Pflugers Arch.* 429:117-125, 1994.
- Al-Gadi, M. and Hill, S.J. The role of calcium in the cyclic AMP response to histamine in rabbit cerebral cortical slices. *Br.J.Pharmacol.* 91:213-222, 1987.
- Alreja, M. and Aghajanian, G.K. Use of the whole-cell patch-clamp method in studies on the role of cAMP in regulating the spontaneous firing of locus coeruleus neurons. *J.Neurosci.Methods.* 59:67-75, 1995.
- Altomare, C., Bucchi, A., Camatini, E., Baruscotti, M., Viscomi, C., Moroni, A., and DiFrancesco, D. Integrated allosteric model of voltage gating of HCN channels. *J.Gen.Physiol.* 117:519-532, 2001.
- Amitai, Y. Membrane potential oscillations underlying firing patterns in neocortical neurons. *Neuroscience.* 63:151-161, 1994.
- Arias-Montano, J.A., Floran, B., Garcia, M., Aceves, J., and Young, J.M. Histamine H_3 receptor-mediated inhibition of depolarization-induced, dopamine D_1 receptor-dependent release of [(3)H]-gamma-aminobutyric acid from rat striatal slices. *Br.J.Pharmacol.* 133:165-171, 2001.
- Armstrong, W.E. and Sladek, C.D. Evidence for excitatory actions of histamine on supraoptic neurons *in vitro*: mediation by an H_1 -type receptor. *Neuroscience* 16:307-322, 1985.
- Arrang, J.M., Garbarg, M., and Schwartz, J.C. Auto-inhibition of brain histamine release mediated by a novel class (H_3) of histamine receptor. *Nature* 302:832-837, 1983.
- Arrang, J.M., Garbarg, M., Quach, T.T., Dam, T.T., Yeramian, E., and Schwartz, J.C. Actions of betahistidine at histamine receptors in the brain. *Eur.J.Pharmacol.* 111:73-84, 1985.
- Arrang, J.M., Garbarg, M., and Schwartz, J.C. Autoinhibition of histamine synthesis mediated by presynaptic H_3 -receptors. *Neuroscience* 23:149-157, 1987.

- Arrang, J.M., Devaux, B., Chodkiewicz, J.P., and Schwartz, J.C. H₃-receptors control histamine release in human brain. *J.Neurochem.* 51:105-108, 1988.
- Arrang, J.M., Drutel, G., and Schwartz, J.C. Characterization of histamine H₃ receptors regulating acetylcholine release in rat entorhinal cortex. *Br.J.Pharmacol.* 114:1518-1522, 1995.
- Atzori, M., Lau, D., Tansey, E.P., Chow, A., Ozaita, A., Rudy, B., and McBain, C.J. H₂ histamine receptor-phosphorylation of K_{v3.2} modulates interneuron fast spiking. *Nat.Neurosci.* 3:791-798, 2000.
- Bacciottini, L., Passani, M.B., Mannaioni, P.F., and Blandina, P. Interactions between histaminergic and cholinergic systems in learning and memory. *Behav.Brain Res.* 124:183-194, 2001.
- Baghdoyan, H.A., Spotts, J.L., and Snyder, S.G. Simultaneous pontine and basal forebrain microinjections of carbachol suppress REM sleep. *J.Neurosci.* 13:229-242, 1993.
- Baudry, M., Martres, M.P., and Schwartz, J.C. H₁ and H₂ receptors in the histamine-induced accumulation of cyclic AMP in guinea pig brain slices. *Nature* 253:362-364, 1975.
- Bazhenov, M., Timofeev, I., Steriade, M., and Sejnowski, T.J. Model of thalamocortical slow-wave sleep oscillations and transitions to activated States. *J.Neurosci.* 22:8691-8704, 2002.
- Bekkers, J.M. Enhancement by histamine of NMDA-mediated synaptic transmission in the hippocampus. *Science* 261:104-106, 1993.
- Bekkers, J.M., Vidovic, M., and Ymer, S. Differential effects of histamine on the N-methyl-D-aspartate channel in hippocampal slices and cultures. *Neuroscience* 72:669-677, 1996.
- Berger, T., Senn, W., and Luscher, H.R. Hyperpolarization-activated current I_h disconnects somatic and dendritic spike initiation zones in layer V pyramidal neurons. *J.Neurophysiol.* 90:2428-2437, 2003.
- Berger, T., Larkum, M.E., and Luscher, H.R. High I_h channel density in the distal apical dendrite of layer V pyramidal cells increases bidirectional attenuation of EPSPs. *J.Neurophysiol.* 85:855-868, 2001.
- Bhargava, K.P., Kulshrestha, V.K., Santhakumari, G., and Srivastava, Y.P. Mechanism of histamine-induced antidiuretic response. *Br.J.Pharmacol.* 47:700-706, 1973.
- Bickmeyer, U., Heine, M., Manzke, T., and Richter, D.W. Differential modulation of I_h by 5-HT receptors in mouse CA1 hippocampal neurons. *Eur.J.Neurosci.* 16:209-218, 2002.
- Blandina, P., Giorgetti, M., Bartolini, L., Cecchi, M., Timmerman, H., Leurs, R., Pepeu, G., and Giovannini, M.G. Inhibition of cortical acetylcholine release and cognitive performance by histamine H₃ receptor activation in rats. *Br.J.Pharmacol.* 119:1656-1664, 1996.

- Blandina, P., Giorgetti, M., Cecchi, M., Leurs, R., Timmerman, H., and Giovannini, M.G. Histamine H₃ receptor inhibition of K⁺-evoked release of acetylcholine from rat cortex *in vivo*. *Inflamm.Res.* 45 Suppl 1:54-55, 1996.
- Bliss, T.V., Collingridge, G.L., and Morris, R.G. Introduction. Long-term potentiation and structure of the issue. *Philos.Trans.R.Soc.Lond.B.Biol.Sci.* 358:607-611, 2003.
- Bliss, T.V. and Collingridge, G.L. A synaptic model of memory: long-term potentiation in the hippocampus. *Nature* 361:31-39, 1993.
- Bobker, D.H. and Williams, J.T. Serotonin augments the cationic current I_h in central neurons. *Neuron* 2:1535-1540, 1989.
- BoSmith, R.E., Briggs, I., and Sturgess, N.C. Inhibitory actions of ZENECA ZD7288 on whole-cell hyperpolarization activated inward current (I_f) in guinea-pig dissociated sinoatrial node cells. *Br.J.Pharmacol.* 110:343-349, 1993.
- Bouthenet, M.L., Ruat, M., Sales, N., Garbarg, M., and Schwartz, J.C. A detailed mapping of histamine H₁-receptors in guinea-pig central nervous system established by autoradiography with [125I]iodobolpyramine. *Neuroscience* 26:553-600, 1988.
- Bristow, D.R., Banford, P.C., Bajusz, I., Vedat, A., and Young, J.M. Desensitization of histamine H₁ receptor-mediated inositol phosphate accumulation in guinea pig cerebral cortex slices. *Br.J.Pharmacol.* 110:269-274, 1993.
- Brown, R.E., Stevens, D.R., and Haas, H.L. The physiology of brain histamine. *Prog.Neurobiol.* 63:637-672, 2001.
- Brown, R.E., Sergeeva, O.A., Eriksson, K.S., and Haas, H.L. Convergent excitation of dorsal raphe serotonin neurons by multiple arousal systems (orexin/hypocretin, histamine and noradrenaline). *J.Neurosci.* 22:8850-8859, 2002.
- Brown, R.E., Fedorov, N.B., Haas, H.L., and Reymann, K.G. Histaminergic modulation of synaptic plasticity in area CA1 of rat hippocampal slices. *Neuropharmacology* 34:181-190, 1995.
- Brown, R.E. and Reymann, K.G. Histamine H₃ receptor-mediated depression of synaptic transmission in the dentate gyrus of the rat *in vitro*. *J.Physiol.* 496:175-184, 1996.
- Brown, R.E. and Haas, H.L. On the mechanism of histaminergic inhibition of glutamate release in the rat dentate gyrus. *J.Physiol.* 515:777-786, 1999.
- Brunel, N. Dynamics of networks of randomly connected excitatory and inhibitory spiking neurons. *J.Physiol.Paris.* 94:445-463, 2000.
- Budd, J.M. Theta oscillations by synaptic excitation in a neocortical circuit model. *Proc.Biol.Sci.* 272:101-109, 2005.

- Budde, T., White, J.A., and Kay, A.R. Hyperpolarization-activated $\text{Na}^+\text{-K}^+$ current (I_h) in neocortical neurons is blocked by external proteolysis and internal TEA. *J.Neurophysiol.* 72:2737-2742, 1994.
- Bugajski, J. and Janusz, Z. Lipolytic responses induced by intracerebroventricular administration of histamine in the rat. *Agents Actions* 11:147-150, 1981.
- Burkhalter, A. and Bernardo, K.L. Organization of corticocortical connections in human visual cortex. *Proc.Natl.Acad.Sci.U.S.A.* 86:1071-1075, 1989.
- Buzsaki, G. Two-stage model of memory trace formation: a role for "noisy" brain states. *Neuroscience* 31:551-570, 1989.
- Cangioli, I., Baldi, E., Mannaioni, P.F., Bucherelli, C., Blandina, P., and Passani, M.B. Activation of histaminergic H_3 receptors in the rat basolateral amygdala improves expression of fear memory and enhances acetylcholine release. *Eur.J.Neurosci.* 16:521-528, 2002.
- Cantrell, A.R., Smith, R.D., Goldin, A.L., Scheuer, T., and Catterall, W.A. Dopaminergic modulation of sodium current in hippocampal neurons via cAMP-dependent phosphorylation of specific sites in the sodium channel alpha subunit. *J.Neurosci.* 17:7330-7338, 1997.
- Caplan, J.B., Madsen, J.R., Raghavachari, S., and Kahana, M.J. Distinct patterns of brain oscillations underlie two basic parameters of human maze learning. *J.Neurophysiol.* 86:368-380, 2001.
- Carswell, H., Galione, A.G., and Young, J.M. Differential effect of temperature on histamine- and carbachol-stimulated inositol phospholipid breakdown in slices of guinea-pig cerebral cortex. *Br.J.Pharmacol.* 90:175-182, 1987.
- Castelfranco, A.M. and Hartline, D.K. Corrections for space-clamp errors in measured parameters of voltage-dependent conductances in a cylindrical neurite. *Biol.Cybern.* 90:280-290, 2004.
- Castro-Alamancos, M.A. Origin of synchronized oscillations induced by neocortical disinhibition *in vivo*. *J.Neurosci.* 20:9195-9206, 2000.
- Castro-Alamancos, M.A. and Rigas, P. Synchronized oscillations caused by disinhibition in rodent neocortex are generated by recurrent synaptic activity mediated by AMPA receptors. *J.Physiol.* 542:567-581, 2002.
- Cathala, L. and Paupardin-Tritsch, D. Neurotensin inhibition of the hyperpolarization-activated cation current (I_h) in the rat substantia nigra pars compacta implicates the protein kinase C pathway. *J.Physiol.* 503:87-97, 1997.
- Cathala, L. and Paupardin-Tritsch, D. Effect of catecholamines on the hyperpolarization-activated cationic I_h and the inwardly rectifying potassium I_{Kir} currents in the rat substantia nigra pars compacta. *Eur.J.Neurosci.* 11:398-406, 1999.

- Cecchi, M., Passani, M.B., Bacciottini, L., Mannaioni, P.F., and Blandina, P. Cortical acetylcholine release elicited by stimulation of histamine H₁ receptors in the nucleus basalis magnocellularis: a dual-probe microdialysis study in the freely moving rat. *Eur.J.Neurosci.* 13:68-78, 2001.
- Chang, F., Cohen, I.S., DiFrancesco, D., Rosen, M.R., and Tromba, C. Effects of protein kinase inhibitors on canine Purkinje fibre pacemaker depolarization and the pacemaker current I_f. *J.Physiol.* 440:367-84.:367-384, 1991.
- Chen, C. Hyperpolarization-activated current (I_h) in primary auditory neurons. *Hear.Res.* 110:179-190, 1997.
- Chen, S., Wang, J., and Siegelbaum, S.A. Properties of hyperpolarization-activated pacemaker current defined by coassembly of HCN1 and HCN2 subunits and basal modulation by cyclic nucleotide. *J.Gen.Physiol.* 117:491-504, 2001.
- Chen, Z., Chen, J.Q., and Kamei, C. Effect of H₁-antagonists on spatial memory deficit evaluated by 8-arm radial maze in rats. *Acta Pharmacol.Sin.* 22:609-613, 2001.
- Choe, Y. The role of temporal parameters in a thalamocortical model of analogy. *IEEE Trans.Neural Netw.* 15:1071-1082, 2004.
- Chu, M., Huang, Z.L., Qu, W.M., Eguchi, N., Yao, M.H., and Urade, Y. Extracellular histamine level in the frontal cortex is positively correlated with the amount of wakefulness in rats. *Neurosci.Res.* 49:417-420, 2004.
- Clark, E.A. and Hill, S.J. Sensitivity of histamine H₃ receptor agonist-stimulated [35S]GTP gamma[S] binding to pertussis toxin. *Eur.J.Pharmacol.* 296:223-225, 1996.
- Claro, E., Garcia, A., and Picatoste, F. Histamine-stimulated phosphoinositide hydrolysis in developing rat brain. *Mol.Pharmacol.* 32:384-390, 1987.
- Cole, K.S. *Membrane, ions, and impulses. A chapter of classical biophysics.* University of California Press. Berkeley and Los Angeles, 1968.
- Collingridge, G.L. and Bliss, T.V. Memories of NMDA receptors and LTP. *Trends.Neurosci.* 18:54-56, 1995.
- Connors, B.W. and Amitai, Y. Making waves in the neocortex. *Neuron* 18:347-349, 1997.
- Cuttle, M.F., Rusznak, Z., Wong, A.Y., Owens, S., and Forsythe, I.D. Modulation of a presynaptic hyperpolarization-activated cationic current (I_h) at an excitatory synaptic terminal in the rat auditory brainstem. *J.Physiol.* 534:733-744, 2001.
- D'Angelo, E., Nieuwenhuis, T., Maffei, A., Armano, S., Rossi, P., Taglietti, V., Fontana, A., and Naldi, G. Theta-frequency bursting and resonance in cerebellar granule cells: experimental evidence and modeling of a slow K⁺-dependent mechanism. *J.Neurosci.* 21:759-770, 2001.

- Daum, P.R., Hill, S.J., and Young, J.M. Histamine H₁-agonist potentiation of adenosine-stimulated cyclic AMP accumulation in slices of guinea-pig cerebral cortex: comparison of response and binding parameters. *Br.J.Pharmacol.* 77:347-357, 1982.
- Daum, P.R., Downes, C.P., and Young, J.M. Histamine stimulation of inositol 1-phosphate accumulation in lithium-treated slices from regions of guinea pig brain. *J.Neurochem.* 43:25-32, 1984.
- Denoyer, M., Sallanon, M., Buda, C., Kitahama, K., and Jouvet, M. Neurotoxic lesion of the mesencephalic reticular formation and/or the posterior hypothalamus does not alter waking in the cat. *Brain Res.* 539:287-303, 1991.
- Desjardins, A.E., Li, Y.X., Reinker, S., Miura, R.M., and Neuman, R.S. The influences of I_h on temporal summation in hippocampal CA1 pyramidal neurons: a modeling study. *J.Comput.Neurosci.* 15:131-142, 2003.
- Di Pasquale, E., Keegan, K.D., and Noebels, J.L. Increased excitability and inward rectification in layer V cortical pyramidal neurons in the epileptic mutant mouse Stargazer. *J.Neurophysiol.* 77:621-631, 1997.
- Dickson, C.T., Magistretti, J., Shalinsky, M.H., Fransen, E., Hasselmo, M.E., and Alonso, A. Properties and role of I_h in the pacing of subthreshold oscillations in entorhinal cortex layer II neurons. *J.Neurophysiol.* 83:2562-2579, 2000.
- DiFrancesco, D., Ferroni, A., Mazzanti, M., and Tromba, C. Properties of the hyperpolarizing-activated current (I_f) in cells isolated from the rabbit sino-atrial node. *J.Physiol.* 377:61-88, 1986.
- DiFrancesco, D. and Mangoni, M. Modulation of single hyperpolarization-activated channels (I_f) by cAMP in the rabbit sino-atrial node. *J.Physiol.* 474:473-482, 1994.
- DiFrancesco, D. Dual allosteric modulation of pacemaker (f) channels by cAMP and voltage in rabbit SA node. *J.Physiol.* 515:367-376, 1999.
- Doan, T.N. and Kunze, D.L. Contribution of the hyperpolarization-activated current to the resting membrane potential of rat nodose sensory neurons. *J.Physiol.* 514:125-138, 1999.
- Donaldson, J. and Hill, S.J. Histamine-induced hydrolysis of polyphosphoinositides in guinea-pig ileum and brain. *Eur.J.Pharmacol.* 124:255-265, 1986.
- Donaldson, J., Hill, S.J., and Brown, A.M. Kinetic studies on the mechanism by which histamine H₁ receptors potentiate cyclic AMP accumulation in guinea pig cerebral cortical slices. *Mol.Pharmacol.* 33:626-633, 1988.
- Donaldson, J., Brown, A.M., and Hill, S.J. Temporal changes in the calcium-dependence of the histamine H₁-receptor-stimulation of cyclic AMP accumulation in guinea-pig cerebral cortex. *Br.J.Pharmacol.* 98:1365-1375, 1989.

- Doreulee, N., Yanovsky, Y., Flaggmeyer, I., Stevens, D.R., Haas, H.L., and Brown, R.E. Histamine H₃ receptors depress synaptic transmission in the corticostriatal pathway. *Neuropharmacology* 40:106-113, 2001.
- Douglas, C.L., Demarco, G.J., Baghdoyan, H.A., and Lydic, R. Pontine and basal forebrain cholinergic interaction: implications for sleep and breathing. *Respir.Physiol.Neurobiol.* 143:251-262, 2004.
- Dringenberg, H.C. and Kuo, M.C. Histaminergic facilitation of electrocorticographic activation: role of basal forebrain, thalamus, and neocortex. *Eur.J.Neurosci.* 18:2285-2291, 2003.
- Dringenberg, H.C. and Vanderwolf, C.H. Involvement of direct and indirect pathways in electrocorticographic activation. *Neurosci.Biobehav.Rev.* 22:243-257, 1998.
- Drutel, G., Peitsaro, N., Karlstedt, K., Wieland, K., Smit, M.J., Timmerman, H., Panula, P., and Leurs, R. Identification of rat H₃ receptor isoforms with different brain expression and signaling properties. *Mol.Pharmacol.* 59:1-8, 2001.
- Duchen, M.R. Effects of metabolic inhibition on the membrane properties of isolated mouse primary sensory neurones. *J.Physiol.* 424:387-409, 1990.
- Edman, A., Gestrelus, S., and Grampp, W. Current activation by membrane hyperpolarization in the slowly adapting lobster stretch receptor neurone. *J.Physiol.* 384:671-90, 1987.
- Ericson, H., Blomqvist, A., and Kohler, C. Brainstem afferents to the tuberomammillary nucleus in the rat brain with special reference to monoaminergic innervation. *J.Comp.Neurol.* 281:169-192, 1989.
- Ericson, H., Kohler, C., and Blomqvist, A. GABA-like immunoreactivity in the tuberomammillary nucleus: an electron microscopic study in the rat. *J.Comp.Neurol.* 305:462-469, 1991.
- Ericson, H., Blomqvist, A., and Kohler, C. Origin of neuronal inputs to the region of the tuberomammillary nucleus of the rat brain. *J.Comp.Neurol.* 311:45-64, 1991.
- Ezeamuzie, C.I. and Philips, E. Histamine H₂ receptors mediate the inhibitory effect of histamine on human eosinophil degranulation. *Br.J.Pharmacol.* 131:482-488, 2000.
- Fernandez-Novoa, L. and Cacabelos, R. Histamine function in brain disorders. *Behav.Brain Res.* 124:213-233, 2001.
- Ferrier, G.R., Zhu, J., Redondo, I.M., and Howlett, S.E. Role of cAMP-dependent protein kinase A in activation of a voltage-sensitive release mechanism for cardiac contraction in guinea-pig myocytes. *J.Physiol.* 513:185-201, 1998.
- Fink, K., Schlicker, E., Neise, A., and Gothert, M. Involvement of presynaptic H₃ receptors in the inhibitory effect of histamine on serotonin release in the rat brain cortex. *Naunyn Schmiedebergs Arch.Pharmacol.* 342:513-519, 1990.

- Fink, K., Schlicker, E., and Gothert, M. N-methyl-D-aspartate (NMDA)-stimulated noradrenaline (NA) release in rat brain cortex is modulated by presynaptic H₃-receptors. *Naunyn Schmiedebergs Arch.Pharmacol.* 349:113-117, 1994.
- Flint, A.C. and Connors, B.W. Two types of network oscillations in neocortex mediated by distinct glutamate receptor subtypes and neuronal populations. *J.Neurophysiol.* 75:951-957, 1996.
- Foehring, R.C. and Waters, R.S. Contributions of low-threshold calcium current and anomalous rectifier (I_h) to slow depolarizations underlying burst firing in human neocortical neurons *in vitro*. *Neurosci.Lett.* 124:17-21, 1991.
- Fontanini, A. and Katz, D.B. 7 to 12 Hz activity in rat gustatory cortex reflects disengagement from a fluid self-administration task. *J.Neurophysiol.* 93:2832-2840, 2005.
- Forscher, P. and Oxford, G.S. Modulation of calcium channels by norepinephrine in internally dialyzed avian sensory neurons. *J.Gen.Physiol.* 85:743-763, 1985.
- Fransen, E., Alonso, A.A., Dickson, C.T., Magistretti, J., and Hasselmo, M.E. Ionic mechanisms in the generation of subthreshold oscillations and action potential clustering in entorhinal layer II stellate neurons. *Hippocampus.*14:368-384, 2004.
- Fraser, K.A., Poucet, B., Partlow, G., and Herrmann, T. Role of the medial and lateral septum in a variable goal spatial problem solving task. *Physiol.Behav.* 50:739-744, 1991.
- Frere, S.G. and Luthi, A. Pacemaker channels in mouse thalamocortical neurones are regulated by distinct pathways of cAMP synthesis. *J.Physiol.* 554:111-125, 2004.
- Frey, U., Huang, Y.Y., and Kandel, E.R. Effects of cAMP simulate a late stage of LTP in hippocampal CA1 neurons. *Science* 260:1661-1664, 1993.
- Frisch, C., Hasenohrl, R.U., and Huston, J.P. The histamine H₁-antagonist chlorpheniramine facilitates learning in aged rats. *Neurosci.Lett.* 229:89-92, 1997.
- Frisch, C., Hasenohrl, R.U., Krauth, J., and Huston, J.P. Anxiolytic-like behavior after lesion of the tuberomammillary nucleus E2-region. *Exp.Brain Res.* 119:260-264, 1998.
- Fuhrmann, G., Markram, H., and Tsodyks, M. Spike frequency adaptation and neocortical rhythms. *J.Neurophysiol.* 88:761-770, 2002
- Fujise, T., Yoshimatsu, H., Kurokawa, M., Oohara, A., Kang, M., Nakata, M., and Sakata, T. Satiety and masticatory function modulated by brain histamine in rats. *Proc.Soc.Exp.Biol.Med.* 217:228-234, 1998.
- Fujita, I. and Fujita, T. Intrinsic Connections in the macaque inferior temporal cortex. *J.Comp.Neurol.* 368:467-486, 1996.

- Funahashi, M., Mitoh, Y., Kohjitani, A., and Matsuo, R. Role of the hyperpolarization-activated cation current (I_h) in pacemaker activity in area postrema neurons of rat brain slices. *J.Physiol.* 552:135-148, 2003.
- Gaddum, J.H. Log normal distribution. *Nature* 156:463-466, 1945.
- Garbarg, M. and Schwartz, J.C. Synergism between histamine H_1 - and H_2 -receptors in the cAMP response in guinea pig brain slices: effects of phorbol esters and calcium. *Mol.Pharmacol.* 33:38-43, 1988.
- Garbarg, M., Tuong, M.D., Gros, C., and Schwartz, J.C. Effects of histamine H_3 -receptor ligands on various biochemical indices of histaminergic neuron activity in rat brain. *Eur.J.Pharmacol.* 164:1-11, 1989.
- Garcia, M., Floran, B., Arias-Montano, J.A., Young, J.M., and Aceves, J. Histamine H_3 receptor activation selectively inhibits dopamine D_1 receptor-dependent [3H]GABA release from depolarization-stimulated slices of rat substantia nigra pars reticulata. *Neuroscience* 80:241-249, 1997.
- Gasparini, S. and DiFrancesco, D. Action of serotonin on the hyperpolarization-activated cation current (I_h) in rat CA1 hippocampal neurons. *Eur.J.Neurosci.* 11:3093-3100, 1999.
- Gilbert, C.D. and Wiesel, T.N. Morphology and intracortical projections of functionally characterised neurones in the cat visual cortex. *Nature* 280:120-125, 1979.
- Gimbarzevsky, B., Miura, R.M., and Puil, E. Impedance profiles of peripheral and central neurons. *Can.J.Physiol.Pharmacol.* 62:460-462, 1984.
- Giorgetti, M., Bacciottini, L., Bianchi, L., Giovannini, M.G., Cecchi, M., and Blandina, P. GABAergic mechanism in histamine H_3 receptor inhibition of K^+ -evoked release of acetylcholine from rat cortex *in vivo*. *Inflamm.Res.* 46 Suppl 1:33-34, 1997.
- Giovannini, M.G., Efoudebe, M., Passani, M.B., Baldi, E., Bucherelli, C., Giachi, F., Corradetti, R., and Blandina, P. Improvement in fear memory by histamine-elicited ERK2 activation in hippocampal CA3 cells. *J.Neurosci.* 2003.Oct.8.;23.(27.):9016.-23. 23:9016-9023,
- Gomez-Ramirez, J., Ortiz, J., and Blanco, I. Presynaptic H_3 autoreceptors modulate histamine synthesis through cAMP pathway. *Mol.Pharmacol.* 61:239-245, 2002.
- Gorelova, N. and Reiner, P.B. Histamine depolarizes cholinergic septal neurons. *J.Neurophysiol.* 75:707-714, 1996.
- Gottesmann, C. Neurophysiological support of consciousness during waking and sleep. *Prog.Neurobiol.* 59:469-508, 1999.
- Gray, C.M., Konig, P., Engel, A.K., and Singer, W. Oscillatory responses in cat visual cortex exhibit inter-columnar synchronization which reflects global stimulus properties. *Nature* 338:334-337, 1989.

- Greene, R.W. and Haas, H.L. Effects of histamine on dentate granule cells *in vitro*. *Neuroscience* 34:299-303, 1990.
- Grillner, S., Hellgren, J., Menard, A., Saitoh, K., and Wikstrom, M.A. Mechanisms for selection of basic motor programs--roles for the striatum and pallidum. *Trends.Neurosci.* 28:364-370, 2005.
- Gu, Q. Neuromodulatory transmitter systems in the cortex and their role in cortical plasticity. *Neuroscience* 111:815-835, 2002.
- Guillery, R.W. and Sherman, S.M. Thalamic relay functions and their role in corticocortical communication: generalizations from the visual system. *Neuron* 33:163-175, 2002.
- Gutfreund, Y., Yarom, Y., and Segev, I. Subthreshold oscillations and resonant frequency in guinea-pig cortical neurons: physiology and modelling. *J.Physiol.* 483:621-640, 1995.
- Gutnick, M.J. and Yarom, Y. Low threshold calcium spikes, intrinsic neuronal oscillation and rhythm generation in the CNS. *J.Neurosci.Methods* 28:93-99, 1989.
- Haas, H. and Panula, P. The role of histamine and the tuberomamillary nucleus in the nervous system. *Nat.Rev.Neurosci.* 4:121-130, 2003.
- Haas, H.L. and Selbach, O. Functions of neuronal adenosine receptors. *Naunyn Schmiedebergs Arch.Pharmacol.* 2000.Nov.;362.(4.-5.):375.-81. 362:375-381,
- Haas, H.L. Histamine hyperpolarizes hippocampal neurones *in vitro*. *Neurosci.Lett.* 22:75-78, 1981.
- Haas, H.L. and Konnerth, A. Histamine and noradrenaline decrease calcium-activated potassium conductance in hippocampal pyramidal cells. *Nature* 302:432-434, 1983.
- Haas, H.L. Histamine potentiates neuronal excitation by blocking a calcium-dependent potassium conductance. *Agents Actions* 14:534-537, 1984.
- Haas, H.L. Histamine may act through cyclic AMP on hippocampal neurones. *Agents Actions* 16:234-235, 1985.
- Haas, H.L. and Greene, R.W. Effects of histamine on hippocampal pyramidal cells of the rat *in vitro*. *Exp.Brain Res.* 62:123-130, 1986.
- Haas, H.L., Sergueeva, O.A., Vorobjev, V.S., and Sharonova, I.N. Subcortical modulation of synaptic plasticity in the hippocampus. *Behav.Brain Res.* 66:41-44, 1995.
- Harris, N.C. and Constanti, A. Mechanism of block by ZD 7288 of the hyperpolarization-activated inward rectifying current in guinea pig substantia nigra neurons *in vitro*. *J.Neurophysiol.* 74:2366-2378, 1995.

- Hasenohrl, R.U., Kuhlen, A., Frisch, C., Galosi, R., Brandao, M.L., and Huston, J.P. Comparison of intra-accumbens injection of histamine with histamine H₁-receptor antagonist chlorpheniramine in effects on reinforcement and memory parameters. *Behav.Brain Res.* 124:203-211, 2001.
- Hatton, G.I. and Yang, Q.Z. Synaptically released histamine increases dye coupling among vasopressinergic neurons of the supraoptic nucleus: mediation by H₁ receptors and cyclic nucleotides. *J.Neurosci.* 16:123-129, 1996.
- Haug, T. and Storm, J.F. Protein kinase A mediates the modulation of the slow Ca²⁺-dependent K⁺ current, I(sAHP), by the neuropeptides CRF, VIP, and CGRP in hippocampal pyramidal neurons. *J.Neurophysiol.* 83:2071-2079, 2000.
- Hegstrand, L.R., Kanof, P.D., and Greengard, P. Histamine-sensitive adenylate cyclase in mammalian brain. *Nature* 260:163-165, 1976.
- Hegyí, K., Fulop, K.A., Kovacs, K.J., Falus, A., and Toth, S. High leptin level is accompanied with decreased long leptin receptor transcript in histamine deficient transgenic mice. *Immunol.Lett.* 92:193-197, 2004.
- Hellwig, B., Haussler, S., Schelter, B., Lauk, M., Guschlbauer, B., Timmer, J., and Lucking, C.H. Tremor-correlated cortical activity in essential tremor. *Lancet* 357:519-523, 2001.
- Hestrin, S. The properties and function of inward rectification in rod photoreceptors of the tiger salamander. *J.Physiol.* 390:319-333:319-333, 1987.
- Hill, S.J. Distribution, properties, and functional characteristics of three classes of histamine receptor. *Pharmacol.Rev.* 42:45-83, 1990.
- Hill, S.J., Ganellin, C.R., Timmerman, H., Schwartz, J.C., Shankley, N.P., Young, J.M., Schunack, W., Levi, R., and Haas, H.L. International Union of Pharmacology. XIII. Classification of histamine receptors. *Pharmacol.Rev.* 49:253-278, 1997.
- Hoffman, B.J., Hansson, S.R., Mezey, E., and Palkovits, M. Localization and dynamic regulation of biogenic amine transporters in the mammalian central nervous system. *Front.Neuroendocrinol.* 19:187-231, 1998.
- Hoffman, D.A. and Johnston, D. Downregulation of transient K⁺ channels in dendrites of hippocampal CA1 pyramidal neurons by activation of PKA and PKC. *J.Neurosci.* 18:3521-3528, 1998.
- Hollingsworth, E.B., Sears, E.B., and Daly, J.W. An activator of protein kinase C (phorbol-12-myristate-13-acetate) augments 2-chloroadenosine-elicited accumulation of cyclic AMP in guinea pig cerebral cortical particulate preparations. *FEBS Lett.* 184:339-342, 1985.
- Honrubia, M.A., Vilaro, M.T., Palacios, J.M., and Mengod, G. Distribution of the histamine H₂ receptor in monkey brain and its mRNA localization in monkey and human brain. *Synapse* 38:343-354, 2000.

- Horn, R. and Korn, S.J. Prevention of rundown in electrophysiological recording. *Methods Enzymol.* 207:149-55.:149-155, 1992.
- Hoshi, T. Regulation of voltage dependence of the KAT1 channel by intracellular factors. *J.Gen.Physiol.* 105:309-328, 1995.
- Hough, L.B., Khandelwal, J.K., and Green, J.P. Histamine turnover in regions of rat brain. *Brain Res.* 291:103-109, 1984.
- Hu, H., Vervaeke, K., and Storm, J.F. Two forms of electrical resonance at theta frequencies, generated by M-current, h-current and persistent Na⁺ current in rat hippocampal pyramidal cells. *J.Physiol.* 545:783-805, 2002.
- Hughes, B.A. and Takahira, M. ATP-dependent regulation of inwardly rectifying K⁺ current in bovine retinal pigment epithelial cells. *Am.J.Physiol.* 275:1372-1383, 1998.
- Huszti, Z. and Magyar, K. Regulation of histidine decarboxylase activity in rat hypothalamus *in vitro* by ATP and cyclic AMP: enzyme inactivation under phosphorylating conditions. *Agents Actions* 14:546-549, 1984.
- Hutcheon, B. and Yarom, Y. Resonance, oscillation and the intrinsic frequency preferences of neurons. *Trends.Neurosci.* 23:216-222, 2000.
- Hutcheon, B., Miura, R.M., Yarom, Y., and Putil, E. Low-threshold calcium current and resonance in thalamic neurons: a model of frequency preference. *J.Neurophysiol.* 71:583-594, 1994.
- Hutcheon, B., Miura, R.M., and Putil, E. Subthreshold membrane resonance in neocortical neurons. *J.Neurophysiol.* 76:683-697, 1996a.
- Hutcheon, B., Miura, R.M., and Putil, E. Models of subthreshold membrane resonance in neocortical neurons. *J.Neurophysiol.* 76:698-714, 1996b.
- Hutcheon, B. Subthreshold resonance in central neurons. *Ph.D. thesis*, University of British Columbia, 1996.
- Impey, S., Obrietan, K., and Storm, D.R. Making new connections: role of ERK/MAP kinase signaling in neuronal plasticity. *Neuron* 23:11-14, 1999.
- Inagaki, N., Yamatodani, A., Ando-Yamamoto, M., Tohyama, M., Watanabe, T., and Wada, H. Organization of histaminergic fibers in the rat brain. *J.Comp.Neurol.* 273:283-300, 1988.
- Inagaki, N., Toda, K., Taniuchi, I., Panula, P., Yamatodani, A., Tohyama, M., Watanabe, T., and Wada, H. An analysis of histaminergic efferents of the tuberomammillary nucleus to the medial preoptic area and inferior colliculus of the rat. *Exp.Brain Res.* 80:374-380, 1990.
- Ingram, S.L. and Williams, J.T. Opioid inhibition of I_h via adenylyl cyclase. *Neuron* 13:179-186, 1994.

- Ingram, S.L. and Williams, J.T. Modulation of the hyperpolarization-activated current (I_h) by cyclic nucleotides in guinea-pig primary afferent neurons. *J.Physiol.* 492:97-106, 1996.
- Inoue, I., Yanai, K., Kitamura, D., Taniuchi, I., Kobayashi, T., Niimura, K., and Watanabe, T. Impaired locomotor activity and exploratory behavior in mice lacking histamine H_1 receptors. *Proc.Natl.Acad.Sci.U.S.A.* 93:13316-13320, 1996.
- Itateyama, E., Chiba, S., Sakata, T., and Yoshimatsu, H. Hypothalamic neuronal histamine in genetically obese animals: its implication of leptin action in the brain. *Exp.Biol.Med.(Maywood.)* 228:1132-1137, 2003.
- Izhikevich, E.M. Resonance and selective communication via bursts in neurons having subthreshold oscillations. *Biosystems* 67:95-102, 2002.
- Izhikevich, E.M., Desai, N.S., Walcott, E.C., and Hoppensteadt, F.C. Bursts as a unit of neural information: selective communication via resonance. *Trends.Neurosci.* 26:161-167, 2003.
- Jahn, K., Haas, H.L., and Hatt, H. Patch clamp study of histamine activated potassium currents on rabbit olfactory bulb neurons. *Naunyn Schmiedebergs Arch.Pharmacol.* 352:386-393, 1995.
- Jinks, A.L. and McGregor, I.S. Modulation of anxiety-related behaviours following lesions of the prelimbic or infralimbic cortex in the rat. *Brain Res.* 772:181-190, 1997.
- John, J., Wu, M.F., Boehmer, L.N., and Siegel, J.M. Cataplexy-active neurons in the hypothalamus: implications for the role of histamine in sleep and waking behavior. *Neuron* 42:619-634, 2004.
- Jones, E.G. The thalamic matrix and thalamocortical synchrony. *Trends.Neurosci.* 24:595-601, 2001.
- Joseph, D.R., Sullivan, P.M., Wang, Y.M., Kozak, C., Fenstermacher, D.A., Behrendsen, M.E., and Zahnow, C.A. Characterization and expression of the complementary DNA encoding rat histidine decarboxylase. *Proc.Natl.Acad.Sci.U.S.A.* 87:733-737, 1990.
- Kalivas, P.W. Histamine-induced arousal in the conscious and pentobarbital-pretreated rat. *J.Pharmacol.Exp.Ther.* 222:37-42, 1982.
- Kasper, E.M., Larkman, A.U., Lubke, J., and Blakemore, C. Pyramidal neurons in layer 5 of the rat visual cortex. II. Development of electrophysiological properties. *J.Comp.Neurol.* 339:475-494, 1994.
- Kasper, E.M., Larkman, A.U., Lubke, J., and Blakemore, C. Pyramidal neurons in layer 5 of the rat visual cortex. I. Correlation among cell morphology, intrinsic electrophysiological properties, and axon targets. *J.Comp.Neurol.* 339:459-474, 1994.
- Kaupp, U.B. and Seifert, R. Molecular diversity of pacemaker ion channels. *Annu.Rev.Physiol.* 63:235-57, 2001.

- Khakh, B.S. and Henderson, G. Hyperpolarization-activated cationic currents (I_h) in neurones of the trigeminal mesencephalic nucleus of the rat. *J.Physiol.* 510:695-704, 1998.
- Khateb, A., Serafin, M., and Muhlethaler, M. Histamine excites pedunclopontine neurones in guinea pig brainstem slices. *Neurosci.Lett.* 112:257-262, 1990.
- Khateb, A., Fort, P., Pegna, A., Jones, B.E., and Muhlethaler, M. Cholinergic nucleus basalis neurons are excited by histamine *in vitro*. *Neuroscience* 69:495-506, 1995.
- King, A.J. The superior colliculus. *Curr.Biol.* 14:335-338, 2004.
- Kirischuk, S., Tuschick, S., Verkhratsky, A., and Kettenmann, H. Calcium signalling in mouse Bergmann glial cells mediated by $\alpha 1$ -adrenoreceptors and H_1 histamine receptors. *Eur.J.Neurosci.* 8:1198-1208, 1996.
- Kiyono, S., Seo, M.L., Shibagaki, M., Watanabe, T., Maeyama, K., and Wada, H. Effects of alpha-fluoromethylhistidine on sleep-waking parameters in rats. *Physiol.Behav.* 34:615-617, 1985.
- Kjaer, A., Knigge, U., Rouleau, A., Garbarg, M., and Warberg, J. Dehydration-induced release of vasopressin involves activation of hypothalamic histaminergic neurons. *Endocrinology* 135:675-681, 1994.
- Kjaer, A., Knigge, U., Jorgensen, H., and Warberg, J. Dehydration-induced renin secretion: involvement of histaminergic neurons. *Neuroendocrinology.* 67:325-329, 1998.
- Klapdor, K., Hasenohrl, R.U., and Huston, J.P. Facilitation of learning in adult and aged rats following bilateral lesions of the tuberomammillary nucleus region. *Behav.Brain Res.* 61:113-116, 1994.
- Koch, C. Cable theory in neurons with active, linearized membranes. *Biol.Cybern.* 50:15-33, 1984.
- Kohler, C., Swanson, L.W., Haglund, L., and Wu, J.Y. The cytoarchitecture, histochemistry and projections of the tuberomammillary nucleus in the rat. *Neuroscience* 16:85-110, 1985.
- Kohler, C., Ericson, H., Watanabe, T., Polak, J., Palay, S.L., Palay, V., and Chan-Palay, V. Galanin immunoreactivity in hypothalamic neurons: further evidence for multiple chemical messengers in the tuberomammillary nucleus. *J.Comp.Neurol.* 250:58-64, 1986.
- Komater, V.A., Buckley, M.J., Browman, K.E., Pan, J.B., Hancock, A.A., Decker, M.W., and Fox, G.B. Effects of histamine H_3 receptor antagonists in two models of spatial learning. *Behav.BrainRes.* 159:295-300, 2005.
- Koumi, S., Wasserstrom, J.A., and Ten Eick, R.E. Beta-adrenergic and cholinergic modulation of inward rectifier K^+ channel function and phosphorylation in guinea-pig ventricle. *J.Physiol.* 486:661-678, 1995.

- Koumi, S., Wasserstrom, J.A., and Ten Eick, R.E. beta-adrenergic and cholinergic modulation of the inwardly rectifying K^+ current in guinea-pig ventricular myocytes. *J.Physiol.* 486:647-659, 1995.
- Kubota, Y., Ito, C., Sakurai, E., Watanabe, T., and Ohtsu, H. Increased methamphetamine-induced locomotor activity and behavioral sensitization in histamine-deficient mice. *J.Neurochem.* 83:837-845, 2002.
- Laitinen, J.T. and Jokinen, M. Guanosine 5'-(gamma-[35S]thio)triphosphate autoradiography allows selective detection of histamine H_3 receptor-dependent G protein activation in rat brain tissue sections. *J.Neurochem.* 71:808-816, 1998.
- Lamas, J.A. A hyperpolarization-activated cation current (I_h) contributes to resting membrane potential in rat superior cervical sympathetic neurones. *Pflugers Arch.* 436:429-435, 1998.
- Lamberty, Y., Margineanu, D.G., Dassel, D., and Klitgaard, H. H_3 agonist imipip markedly reduces cortical histamine release, but only weakly promotes sleep in the rat. *Pharmacol.Res.* 48:193-198, 2003.
- Lampl, I. and Yarom, Y. Subthreshold oscillations of the membrane potential: a functional synchronizing and timing device. *J.Neurophysiol.* 70:2181-2186, 1993.
- Lampl, I. and Yarom, Y. Subthreshold oscillations and resonant behavior: two manifestations of the same mechanism. *Neuroscience* 78:325-341, 1997.
- Larkman, P.M. and Kelly, J.S. Modulation of I_h by 5-HT in neonatal rat motoneurons *in vitro*: mediation through a phosphorylation independent action of cAMP. *Neuropharmacology* 36:721-733, 1997.
- Lee, K.H., Broberger, C., Kim, U., and McCormick, D.A. Histamine modulates thalamocortical activity by activating a chloride conductance in ferret perigeniculate neurons. *Proc.Natl.Acad.Sci.U.S.A.* 101:6716 - 6721, 2004.
- Lee, K.H. and McCormick, D.A. Abolition of spindle oscillations by serotonin and norepinephrine in the ferret lateral geniculate and perigeniculate nuclei *in vitro*. *Neuron* 17:309-321, 1996.
- Leung, L.S. and Yu, H.W. Theta-frequency resonance in hippocampal CA1 neurons *in vitro* demonstrated by sinusoidal current injection. *J.Neurophysiol.* 79:1592-1596, 1998.
- Leurs, R., Traiffort, E., Arrang, J.M., Tardivel-Lacombe, J., Ruat, M., and Schwartz, J.C. Guinea pig histamine H_1 receptor. II. Stable expression in Chinese hamster ovary cells reveals the interaction with three major signal transduction pathways. *J.Neurochem.* 62:519-527, 1994.

- Li, S.J., Wang, Y., Strahlendorf, H.K., and Strahlendorf, J.C. Serotonin alters an inwardly rectifying current (I_h) in rat cerebellar Purkinje cells under voltage clamp. *Brain Res.* 617:87-95, 1993.
- Li, Z. and Hatton, G.I. Histamine-induced prolonged depolarization in rat supraoptic neurons: G-protein-mediated, Ca^{2+} -independent suppression of K^+ leakage conductance. *Neuroscience* 70:145-158, 1996.
- Lin, J.S., Sakai, K., and Jouvet, M. Evidence for histaminergic arousal mechanisms in the hypothalamus of cat. *Neuropharmacology* 27:111-122, 1988.
- Lin, J.S., Sakai, K., Vanni-Mercier, G., and Jouvet, M. A critical role of the posterior hypothalamus in the mechanisms of wakefulness determined by microinjection of muscimol in freely moving cats. *Brain Res.* 479:225-240, 1989.
- Lin, J.S., Sakai, K., Vanni-Mercier, G., Arrang, J.M., Garbarg, M., Schwartz, J.C., and Jouvet, M. Involvement of histaminergic neurons in arousal mechanisms demonstrated with H_3 -receptor ligands in the cat. *Brain Res.* 523:325-330, 1990.
- Lin, J.S., Sakai, K., and Jouvet, M. Hypothalamo-preoptic histaminergic projections in sleep-wake control in the cat. *Eur.J.Neurosci.* 6:618-625, 1994.
- Lin, J.S., Hou, Y., Sakai, K., and Jouvet, M. Histaminergic descending inputs to the mesopontine tegmentum and their role in the control of cortical activation and wakefulness in the cat. *J.Neurosci.* 16:1523-1537, 1996.
- Liu, Z., Bunney, E.B., Appel, S.B., and Brodie, M.S. Serotonin reduces the hyperpolarization-activated current (I_h) in ventral tegmental area dopamine neurons: involvement of $5-HT_2$ receptors and protein kinase C. *J.Neurophysiol.* 90:3201-3212, 2003.
- Lorenzon, N.M. and Foehring, R.C. Relationship between repetitive firing and afterhyperpolarizations in human neocortical neurons. *J.Neurophysiol.* 67:350-363, 1992.
- Lorincz, A., Notomi, T., Tamas, G., Shigemoto, R., and Nusser, Z. Polarized and compartment-dependent distribution of HCN1 in pyramidal cell dendrites. *Nat.Neurosci.* 5:1185-1193, 2002.
- Lovenberg, T.W., Roland, B.L., Wilson, S.J., Jiang, X., Pyati, J., Huvar, A., Jackson, M.R., and Erlander, M.G. Cloning and functional expression of the human histamine H_3 receptor. *Mol.Pharmacol.* 55:1101-1107, 1999.
- Ludwig, A., Zong, X., Jeglitsch, M., Hofmann, F., and Biel, M. A family of hyperpolarization-activated mammalian cation channels. *Nature* 393:587-591, 1998.
- Lukatch, H.S. and MacIver, M.B. Physiology, pharmacology, and topography of cholinergic neocortical oscillations *in vitro*. *J.Neurophysiol.* 77:2427-2445, 1997.

- Luthi, A., Bal, T., and McCormick, D.A. Periodicity of thalamic spindle waves is abolished by ZD7288, a blocker of I_h . *J.Neurophysiol.* 79:3284-3289, 1998.
- Maccaferri, G., Mangoni, M., Lazzari, A., and DiFrancesco, D. Properties of the hyperpolarization-activated current in rat hippocampal CA1 pyramidal cells. *J.Neurophysiol.* 69:2129-2136, 1993.
- Maccaferri, G. and McBain, C.J. The hyperpolarization-activated current (I_h) and its contribution to pacemaker activity in rat CA1 hippocampal stratum oriens-alveus interneurons. *J.Physiol.* 497:119-130, 1996.
- Magee, J.C. Dendritic hyperpolarization-activated currents modify the integrative properties of hippocampal CA1 pyramidal neurons. *J.Neurosci.* 18:7613-7624, 1998.
- Magrani, J., de, C., Varjao, B., Duarte, G., Ramos, A.C., Athanazio, R., Barbeta, M., Luz, P., and Fregoneze, J.B. Histaminergic H_1 and H_2 receptors located within the ventromedial hypothalamus regulate food and water intake in rats. *Pharmacol.Biochem.Behav.* 79:189-198, 2004.
- Manning, K.A., Wilson, J.R., and Uhlrich, D.J. Histamine-immunoreactive neurons and their innervation of visual regions in the cortex, tectum, and thalamus in the primate *Macaca mulatta*. *J.Comp.Neurol.* 373:271-282, 1996.
- Maricq, A.V. and Korenbrot, J.I. Inward rectification in the inner segment of single retinal cone photoreceptors. *J.Neurophysiol.* 64:1917-1928, 1990.
- Martinez-Mir, M.I., Pollard, H., Moreau, J., Arrang, J.M., Ruat, M., Traiffort, E., Schwartz, J.C., and Palacios, J.M. Three histamine receptors (H_1 , H_2 and H_3) visualized in the brain of human and non-human primates. *Brain Res.* 526:322-327, 1990.
- Marty, A. and Zimmerberg, J. Diffusion into the patch-clamp recording pipette of a factor necessary for muscarinic current response. *Cell Signal.* 1:259-268, 1989.
- Maruoka, F., Nakashima, Y., Takano, M., Ono, K., and Noma, A. Cation-dependent gating of the hyperpolarization-activated cation current in the rabbit sino-atrial node cells. *J.Physiol.* 477:423-435, 1994.
- Massicotte, G. Modification of glutamate receptors by phospholipase A_2 : its role in adaptive neural plasticity. *Cell Mol.Life Sci.* 57:1542-1550, 2000.
- Matzen, S., Knigge, U., and Warberg, J. Brain regulation of renin secretion involves central histaminergic neurons. *Neuroendocrinology.* 52:175-180, 1990.
- Mayer, M.L. and Westbrook, G.L. A voltage-clamp analysis of inward (anomalous) rectification in mouse spinal sensory ganglion neurones. *J.Physiol.* 340:19-45.:19-45, 1983.

- McCormick, D.A. and Prince, D.A. Post-natal development of electrophysiological properties of rat cerebral cortical pyramidal neurones. *J.Physiol.* 393:743-62.:743-762, 1987.
- McCormick, D.A. and Pape, H.C. Properties of a hyperpolarization-activated cation current and its role in rhythmic oscillation in thalamic relay neurones. *J.Physiol.* 431:291-318.:291-318, 1990a.
- McCormick, D.A. and Pape, H.C. Noradrenergic and serotonergic modulation of a hyperpolarization-activated cation current in thalamic relay neurones. *J.Physiol.* 431:319-42.:319-342, 1990b.
- McCormick, D.A. and Williamson, A. Modulation of neuronal firing mode in cat and guinea pig LGNd by histamine: possible cellular mechanisms of histaminergic control of arousal. *J.Neurosci.* 11:3188-3199, 1991.
- McCormick, D.A., Pape, H.C., and Williamson, A. Actions of norepinephrine in the cerebral cortex and thalamus: implications for function of the central noradrenergic system. *Prog.Brain Res.* 88:293-305.:293-305, 1991.
- McCormick, D.A. and Huguenard, J.R. A model of the electrophysiological properties of thalamocortical relay neurons. *J.Neurophysiol.* 68:1384-1400, 1992.
- McCormick, D.A. Neurotransmitter actions in the thalamus and cerebral cortex and their role in neuromodulation of thalamocortical activity. *Prog.Neurobiol.* 39:337-388, 1992.
- McCormick, D.A. Neurotransmitter actions in the thalamus and cerebral cortex. *J.Clin.Neurophysiol.* 9:212-223, 1992.
- McCormick, D.A. Cellular mechanisms underlying cholinergic and noradrenergic modulation of neuronal firing mode in the cat and guinea pig dorsal lateral geniculate nucleus. *J.Neurosci.* 12:278-289, 1992.
- McCormick, D.A., Wang, Z., and Huguenard, J. Neurotransmitter control of neocortical neuronal activity and excitability. *Cereb.Cortex.* 3:387-398, 1993.
- McCormick, D.A. Actions of acetylcholine in the cerebral cortex and thalamus and implications for function. *Prog.Brain Res.* 98:303-8.:303-308, 1993.
- McGinty, D. and Szymusiak, R. Hypothalamic regulation of sleep and arousal. *Front.Biosci.* 8:1074-1083, 2003.
- McGinty, D.J. Somnolence, recovery and hyposomnia following ventro-medial diencephalic lesions in the rat. *Electroencephalogr.Clin.Neurophysiol.* 26:70-79, 1969.
- Mellor, J., Nicoll, R.A., and Schmitz, D. Mediation of hippocampal mossy fiber long-term potentiation by presynaptic I_h channels. *Science* 295:143-147, 2002
- Mercer, L.P., Kelley, D.S., Haq, A., and Humphries, L.L. Dietary induced anorexia: a review of involvement of the histaminergic system. *J.Am.Coll.Nutr.* 15:223-230, 1996.

- Miyazaki, S., Imaizumi, M., and Onodera, K. Ameliorating effects of histidine on learning deficits in an elevated plus-maze test in mice and the contribution of cholinergic neuronal systems. *Methods Find. Exp. Clin. Pharmacol.* 17:57-63, 1995.
- Mochizuki, T., Yamatodani, A., Okakura, K., Takemura, M., Inagaki, N., and Wada, H. *In vivo* release of neuronal histamine in the hypothalamus of rats measured by microdialysis. *Naunyn Schmiedebergs Arch. Pharmacol.* 343:190-195, 1991.
- Monnier, M. and Hatt, A.M. Afferent and central activating effects of histamine on the brain. *Experientia* 25:1297-1298, 1969.
- Monteggia, L.M., Eisch, A.J., Tang, M.D., Kaczmarek, L.K., and Nestler, E.J. Cloning and localization of the hyperpolarization-activated cyclic nucleotide-gated channel family in rat brain. *Brain Res. Mol. Brain Res.* 81:129-139, 2000.
- Monti, J.M., Pellejero, T., and Jantos, H. Effects of H₁- and H₂-histamine receptor agonists and antagonists on sleep and wakefulness in the rat. *J. Neural Transm.* 66:1-11, 1986.
- Monti, J.M., Orellana, C., Boussard, M., Jantos, H., and Olivera, S. Sleep variables are unaltered by zolantidine in rats: are histamine H₂-receptors not involved in sleep regulation? *Brain Res. Bull.* 25:229-231, 1990.
- Monti, J.M., Jantos, H., Boussard, M., Altier, H., Orellana, C., and Olivera, S. Effects of selective activation or blockade of the histamine H₃ receptor on sleep and wakefulness. *Eur. J. Pharmacol.* 205:283-287, 1991.
- Monti, J.M. Involvement of histamine in the control of the waking state. *Life Sci.* 53:1331-1338, 1993.
- Monti, J.M., Jantos, H., Leschke, C., Elz, S., and Schunack, W. The selective histamine H₁-receptor agonist 2-(3-trifluoromethylphenyl)histamine increases waking in the rat. *Eur. Neuropsychopharmacol.* 4:459-462, 1994.
- Moosmang, S., Biel, M., Hofmann, F., and Ludwig, A. Differential distribution of four hyperpolarization-activated cation channels in mouse brain. *Biol. Chem.* 380:975-980, 1999.
- Morimoto, T., Yamamoto, Y., Mobarakeh, J.I., Yanai, K., Watanabe, T., and Yamatodani, A. Involvement of the histaminergic system in leptin-induced suppression of food intake. *Physiol. Behav.* 67:679-683, 1999.
- Morisset, S., Rouleau, A., Ligneau, X., Gbahou, F., Tardivel-Lacombe, J., Stark, H., Schunack, W., Ganellin, C.R., Schwartz, J.C., and Arrang, J.M. High constitutive activity of native H₃ receptors regulates histamine neurons in brain. *Nature* 408:860-864, 2000.
- Munakata, M. and Akaike, N. Regulation of K⁺ conductance by histamine H₁ and H₂ receptors in neurones dissociated from rat neostriatum. *J. Physiol.* 480:233-245, 1994.

- Murthy, V.N. and Fetz, E.E. Coherent 25- to 35-Hz oscillations in the sensorimotor cortex of awake behaving monkeys. *Proc.Natl.Acad.Sci.U.S.A.* 89:5670-5674, 1992.
- Nahorski, S.R., Rogers, K.J., and Smith, B.M. Histamine H₂ receptors and cyclic AMP in brain. *Life Sci.* 15:1887-1894, 1974.
- Neuman, R.S., Giles, C, Kong, F-J., and Puil, E., 1998. Histamine modulates ion channels on rat neocortical neurons. *Soc. Neurosci. Abs.* 789.3.
- Nguyen, T., Shapiro, D.A., George, S.R., Setola, V., Lee, D.K., Cheng, R., Rauser, L., Lee, S.P., Lynch, K.R., Roth, B.L., and O'Dowd, B.F. Discovery of a novel member of the histamine receptor family. *Mol.Pharmacol.* 59:427-433, 2001.
- Nicolelis, M.A., Baccala, L.A., Lin, R.C., and Chapin, J.K. Sensorimotor encoding by synchronous neural ensemble activity at multiple levels of the somatosensory system. *Science* 268:1353-1358, 1995.
- Nicoll, A., Larkman, A., and Blakemore, C. Modulation of EPSP shape and efficacy by intrinsic membrane conductances in rat neocortical pyramidal neurons *in vitro*. *J.Physiol.* 468:693-710.:693-710, 1993.
- Nishizaki, T., Nomura, T., Matsuoka, T., and Tsujishita, Y. Arachidonic acid as a messenger for the expression of long-term potentiation. *Biochem.Biophys.Res.Commun.* 254: 446-449,1999.
- Notomi, T. and Shigemoto, R. Immunohistochemical localization of I_h channel subunits, HCN1-4, in the rat brain. *J.Comp.Neurol.* 471:241-276, 2004.
- Nowak, J.Z. Histamine in the central nervous system: its role in circadian rhythmicity. *Acta Neurobiol.Exp.(Wars.)* 54 Suppl:65-82.:65-82, 1994.
- O'Connor, S.M., Berg, R.W., and Kleinfeld, D. Coherent electrical activity between vibrissa sensory areas of cerebellum and neocortex is enhanced during free whisking. *J.Neurophysiol.* 87:2137-2148, 2002.
- Oishi, R., Nishibori, M., and Saeki, K. Regional differences in the turnover of neuronal histamine in the rat brain. *Life Sci.* 34:691-699, 1984.
- Oishi, R., Itoh, Y., Nishibori, M., and Saeki, K. Effects of the histamine H₃-agonist (R)-alpha-methylhistamine and the antagonist thioperamide on histamine metabolism in the mouse and rat brain. *J.Neurochem.* 52:1388-1392, 1989.
- Oleson, D.R., DeFelice, L.J., and Donahoe, R.M. A comparison of K⁺ channel characteristics in human T cells: perforated-patch versus whole-cell recording techniques. *J.Membr.Biol.* 132:229-241, 1993.
- Olianas, M., Oliver, A.P., and Neff, N.H. Correlation between histamine-induced neuronal excitability and activation of adenylate cyclase in the guinea pig hippocampus. *Neuropharmacology* 23:1071-1074, 1984.

- Onodera, K., Yamatodani, A., Watanabe, T., and Wada, H. Neuropharmacology of the histaminergic neuron system in the brain and its relationship with behavioral disorders. *Prog.Neurobiol.* 42:685-702, 1994.
- Oohara, A., Yoshimatsu, H., Kurokawa, M., Oishi, R., Saeki, K., and Sakata, T. Neuronal glucoprivation enhances hypothalamic histamine turnover in rats. *J.Neurochem.* 63:677-682, 1994.
- Orr, E. and Quay, W.B. Hypothalamic 24-hour rhythms in histamine, histidine, decarboxylase and histamine-N-methyltransferase. *Endocrinology* 96:941-945, 1975.
- Palacios, J.M., Garbarg, M., Barbin, G., and Schwartz, J.C. Pharmacological characterization of histamine receptors mediating the stimulation of cyclic AMP accumulation in slices from guinea-pig hippocampus. *Mol.Pharmacol.* 14:971-982, 1978.
- Palacios, J.M., Wamsley, J.K., and Kuhar, M.J. The distribution of histamine H₁-receptors in the rat brain: an autoradiographic study. *Neuroscience* 6:15-37, 1981.
- Panula, P., Pirvola, U., Auvinen, S., and Airaksinen, M.S. Histamine-immunoreactive nerve fibers in the rat brain. *Neuroscience* 28:585-610, 1989.
- Pape, H.C. and McCormick, D.A. Noradrenaline and serotonin selectively modulate thalamic burst firing by enhancing a hyperpolarization-activated cation current. *Nature* 340:715-718, 1989.
- Pape, H.C. and Mager, R. Nitric oxide controls oscillatory activity in thalamocortical neurons. *Neuron* 9:441-448, 1992.
- Pape, H.C. Queer current and pacemaker: the hyperpolarization-activated cation current in neurons. *Annu.Rev.Physiol.* 58: 299-327, 1996.
- Pare, D. and Lang, E.J. Calcium electrogenesis in neocortical pyramidal neurons *in vivo*. *Eur.J.Neurosci.* 10:3164-3170, 1998.
- Passani, M.B., Bacciottini, L., Mannaioni, P.F., and Blandina, P. Central histaminergic system and cognition. *Neurosci.Biobehav.Rev.* 24:107-113, 2000.
- Passani, M.B. and Blandina, P. Cognitive implications for H₃ and 5-HT₃ receptor modulation of cortical cholinergic function: a parallel story. *Methods Find.Exp.Clin.Pharmacol.* 20:725-733, 1998.
- Payne, G.W. and Neuman, R.S. Effects of hypomagnesia on histamine H₁ receptor-mediated facilitation of NMDA responses. *Br.J.Pharmacol.* 121:199-204, 1997.
- Pedarzani, P. and Storm, J.F. PKA mediates the effects of monoamine transmitters on the K⁺ current underlying the slow spike frequency adaptation in hippocampal neurons. *Neuron* 11:1023-1035, 1993.

- Pedarzani, P. and Storm, J.F. Protein kinase A-independent modulation of ion channels in the brain by cyclic AMP. *Proc.Natl.Acad.Sci.U.S.A.* 92:11716-11720, 1995.
- Philippu, A. and Prast, H. Importance of histamine in modulatory processes, locomotion and memory. *Behav.Brain Res.* 124:151-159, 2001
- Pike, F.G., Goddard, R.S., Suckling, J.M., Ganter, P., Kasthuri, N., and Paulsen, O. Distinct frequency preferences of different types of rat hippocampal neurones in response to oscillatory input currents. *J.Physiol.* 529:205-213, 2000.
- Pillot, C., Heron, A., Cochois, V., Tardivel-Lacombe, J., Ligneau, X., Schwartz, J.C., and Arrang, J.M. A detailed mapping of the histamine H₃ receptor and its gene transcripts in rat brain. *Neuroscience* 114:173-193, 2002
- Pinault, D. and Deschenes, M. Voltage-dependent 40-Hz oscillations in rat reticular thalamic neurons *in vivo*. *Neuroscience* 51:245-258, 1992.
- Pollard, H., Moreau, J., Arrang, J.M., and Schwartz, J.C. A detailed autoradiographic mapping of histamine H₃ receptors in rat brain areas. *Neuroscience* 52:169-189, 1993.
- Prast, H., Lamberti, C., Fischer, H., Tran, M.H., and Philippu, A. Nitric oxide influences the release of histamine and glutamate in the rat hypothalamus. *Naunyn Schmiedebergs Arch.Pharmacol.* 354:731-735, 1996.
- Prast, H., Fischer, H., Tran, M.H., Grass, K., Lamberti, C., and Philippu, A. Modulation of acetylcholine release in the ventral striatum by histamine receptors. *Inflamm.Res.* 46 Suppl 1:37-38,1997.
- Prell, G.D., Morrishow, A.M., Duoyon, E., and Lee, W.S. Inhibitors of histamine methylation in brain promote formation of imidazoleacetic acid, which interacts with GABA receptors. *J.Neurochem.* 68:142-151, 1997.
- Psychoyos, S. H₁- and H₂-histamine receptors linked to adenylate cyclase in cell-free preparations of guinea pig cerebral cortex. *Life Sci.* 23:2155-2162, 1978.
- Puebla, L., Ocana, F.A., and Arilla, E. Histamine H₁-receptors modulate somatostatin receptors coupled to the inhibition of adenylyl cyclase in the rat frontoparietal cortex. *Peptides* 18:1569-1576, 1997.
- Puil, E. and Werman, R. Internal cesium ions block various K conductances in spinal motoneurons. *Can.J.Physiol.Pharmacol.* 59:1280-1284, 1981.
- Puil, E., Gimbarzevsky, B., and Miura, R.M. Quantification of membrane properties of trigeminal root ganglion neurons in guinea pigs. *J.Neurophysiol.* 55:995-1016, 1986.
- Puil, E., Gimbarzevsky, B., and Spigelman, I. Primary involvement of K⁺ conductance in membrane resonance of trigeminal root ganglion neurons. *J.Neurophysiol.* 59:77-89, 1988.

- Puil, E., Meiri, H., and Yarom, Y. Resonant behavior and frequency preferences of thalamic neurons. *J.Neurophysiol.* 71:575-582, 1994.
- Quirk, G.J., Russo, G.K., Barron, J.L., and Lebron, K. The role of ventromedial prefrontal cortex in the recovery of extinguished fear. *J.Neurosci.* 20:6225-6231, 2000
- Raes, A., Wang, Z., van den Berg, R.J., Goethals, M., Van de Vijver, G., and van Bogaert, P.P. Effect of cAMP and ATP on the hyperpolarization-activated current in mouse dorsal root ganglion neurons. *Pflugers Arch.* 434:543-550, 1997.
- Raethjen, J., Lindemann, M., Dumpelmann, M., Wenzelburger, R., Stolze, H., Pfister, G., Elger, C.E., Timmer, J., and Deuschl, G. Corticomuscular coherence in the 6-15 Hz band: is the cortex involved in the generation of physiologic tremor? *Exp.Brain Res.* 142:32-40, 2002.
- Raghavachari, S., Kahana, M.J., Rizzuto, D.S., Caplan, J.B., Kirschen, M.P., Bourgeois, B., Madsen, J.R., and Lisman, J.E. Gating of human theta oscillations by a working memory task. *J.Neurosci.* 21:3175-3183, 2001.
- Recabarren, M.P., Valdes, J.L., Farias, P., Seron-Ferre, M., and Torrealba, F. Differential effects of infralimbic cortical lesions on temperature and locomotor activity responses to feeding in rats. *Neuroscience* 134:1413-1422, 2005.
- Reiner, P.B. and Kamondi, A. Mechanisms of antihistamine-induced sedation in the human brain: H₁ receptor activation reduces a background leakage potassium current. *Neuroscience* 59:579-588, 1994.
- Reuter, H., Stevens, C.F., Tsien, R.W., and Yellen, G. Properties of single calcium channels in cardiac cell culture. *Nature* 297:501-504, 1982.
- Rhodes, S.E. and Killcross, S. Lesions of rat infralimbic cortex enhance recovery and reinstatement of an appetitive Pavlovian response. *Learn.Mem.* 11:611-616, 2004.
- Richardson, M.J., Brunel, N., and Hakim, V. From subthreshold to firing-rate resonance. *J.Neurophysiol.* 89:2538-2554, 2003.
- Richelson, E. Histamine H₁ receptor-mediated guanosine 3',5'-monophosphate formation by cultured mouse neuroblastoma cells. *Science* 201:69-71, 1978.
- Rizzuto, D.S., Madsen, J.R., Bromfield, E.B., Schulze-Bonhage, A., Seelig, D., Aschenbrenner-Scheibe, R., and Kahana, M.J. Reset of human neocortical oscillations during a working memory task. *Proc.Natl.Acad.Sci.U.S.A.* 100:7931-7936, 2003.
- Robinson, R.B. and Siegelbaum, S.A. Hyperpolarization-activated cation currents: from molecules to physiological function. *Annu.Rev.Physiol.* 65:453-480, 2003.
- Roth, A. and Hausser, M. Compartmental models of rat cerebellar Purkinje cells based on simultaneous somatic and dendritic patch-clamp recordings. *J.Physiol.* 535:445-472, 2001.

- Rouleau, A., Ligneau, X., Tardivel-Lacombe, J., Morisset, S., Gbahou, F., Schwartz, J.C., and Arrang, J.M. Histamine H₃-receptor-mediated [³⁵S]GTP gamma[S] binding: evidence for constitutive activity of the recombinant and native rat and human H₃ receptors. *Br.J.Pharmacol.* 135:383-392, 2002.
- Ruat, M., Traiffort, E., Bouthenet, M.L., Schwartz, J.C., Hirschfeld, J., Buschauer, A., and Schunack, W. Reversible and irreversible labeling and autoradiographic localization of the cerebral histamine H₂ receptor using [¹²⁵I]iodinated probes. *Proc.Natl.Acad.Sci.U.S.A.* 87:1658-1662, 1990.
- Rubio, S., Begega, A., Santin, L.J., Miranda, R., and Arias, J.L. Effects of histamine precursor and (R)-alpha-methylhistamine on the avoidance response in rats. *Behav.Brain Res.* 124:177-181, 2001.
- Sakai, N., Onodera, K., Maeyama, K., Yanai, K., and Watanabe, T. Effects of (S)-alpha - fluoromethylhistidine and metoprine on locomotor activity and brain histamine content in mice. *Life Sci.* 51:397-405, 1992.
- Sakai, N., Yamazaki, S., Onodera, K., Yanai, K., Maeyama, K., and Watanabe, T. Effects of (S)-alpha-fluoromethylhistidine and (R)-alpha-methylhistamine on locomotion of W/W^v mice. *Pharmacol.Biochem.Behav.* 46:95-99, 1993.
- Sakata, T., Yoshimatsu, H., Masaki, T., and Tsuda, K. Anti-obesity actions of mastication driven by histamine neurons in rats. *Exp.Biol.Med.(Maywood.)* 228:1106-1110, 2003.
- Sakata, T., Fukagawa, K., Ookuma, K., Fujimoto, K., Yoshimatsu, H., Yamatodani, A., and Wada, H. Modulation of neuronal histamine in control of food intake. *Physiol.Behav.* 44:539-543, 1988.
- Sakata, T., Ookuma, K., Fukagawa, K., Fujimoto, K., Yoshimatsu, H., Shiraishi, T., and Wada, H. Blockade of the histamine H₁-receptor in the rat ventromedial hypothalamus and feeding elicitation. *Brain Res.* 441:403-407, 1988.
- Sakata, T., Kurokawa, M., Oohara, A., and Yoshimatsu, H. A physiological role of brain histamine during energy deficiency. *Brain Res.Bull.* 35:135-139, 1994.
- Sakata, T., Yoshimatsu, H., and Kurokawa, M. Hypothalamic neuronal histamine: implications of its homeostatic control of energy metabolism. *Nutrition.* 13:403-411, 1997.
- Sanchez-Vives, M.V. and McCormick, D.A. Cellular and network mechanisms of rhythmic recurrent activity in neocortex. *Nat.Neurosci.* 3:1027-1034, 2000.
- Santoro, B., Chen, S., Luthi, A., Pavlidis, P., Shumyatsky, G.P., Tibbs, G.R., and Siegelbaum, S.A. Molecular and functional heterogeneity of hyperpolarization-activated pacemaker channels in the mouse CNS. *J.Neurosci.* 20:5264-5275, 2000.

- Santoro, B., Liu, D.T., Yao, H., Bartsch, D., Kandel, E.R., Siegelbaum, S.A., and Tibbs, G.R. Identification of a gene encoding a hyperpolarization-activated pacemaker channel of brain. *Cell* 93:717-729, 1998.
- Sato-Bigbee, C., Pal, S., and Chu, A.K. Different neuroligands and signal transduction pathways stimulate CREB phosphorylation at specific developmental stages along oligodendrocyte differentiation. *J.Neurochem.* 72:139-147, 1999.
- Schaefer, A.T., Helmstaedter, M., Sakmann, B., and Korngreen, A. Correction of conductance measurements in non-space-clamped structures: 1. Voltage-gated K⁺ channels. *Biophys.J.* 84:3508-3528, 2003.
- Schlicker, E., Betz, R., and Gothert, M. Histamine H₃ receptor-mediated inhibition of serotonin release in the rat brain cortex. *Naunyn Schmiedebergs Arch.Pharmacol.* 337:588-590, 1988.
- Schlicker, E., Fink, K., Hinterthaler, M., and Gothert, M. Inhibition of noradrenaline release in the rat brain cortex via presynaptic H₃ receptors. *Naunyn Schmiedebergs Arch.Pharmacol.* 340:633-638, 1989.
- Schlicker, E., Fink, K., Detzner, M., and Gothert, M. Histamine inhibits dopamine release in the mouse striatum via presynaptic H₃ receptors. *J.Neural Transm.Gen.Sect.* 93:1-10, 1993.
- Schlicker, E., Kathmann, M., Detzner, M., Exner, H.J., and Gothert, M. H₃ receptor-mediated inhibition of noradrenaline release: an investigation into the involvement of Ca²⁺ and K⁺ ions, G protein and adenylate cyclase. *Naunyn Schmiedebergs Arch.Pharmacol.* 350:34-41, 1994.
- Schmahmann, J.D. and Pandya, D.N. The cerebrocerebellar system. *Int.Rev.Neurobiol.* 41:31-60, 1997.
- Schreiber, S., Erchova, I., Heinemann, U., and Herz, A.V. Subthreshold resonance explains the frequency-dependent integration of periodic as well as random stimuli in the entorhinal cortex. *J.Neurophysiol.* 92:408-415, 2004.
- Schwabe, U., Ohga, Y., and Daly, J.W. The role of calcium in the regulation of cyclic nucleotide levels in brain slices of rat and guinea pig. *Naunyn Schmiedebergs Arch.Pharmacol.* 302:141-151, 1978.
- Schwartz, J.C., Morisset, S., Rouleau, A., Ligneau, X., Gbahou, F., Tardivel-Lacombe, J., Stark, H., Schunack, W., Ganellin, C.R., and Arrang, J.M. Therapeutic implications of constitutive activity of receptors: the example of the histamine H₃ receptor. *J.Neural Transm.Suppl.* 64:1-16, 2003
- Schwartz, J.C., Arrang, J.M., Garbarg, M., Pollard, H., and Ruat, M. Histaminergic transmission in the mammalian brain. *Physiol.Rev.* 71:1-51, 1991.

- Schwindt, P.C. and Crill, W.E. Modification of current transmitted from apical dendrite to soma by blockade of voltage- and Ca^{2+} -dependent conductances in rat neocortical pyramidal neurons. *J.Neurophysiol.* 78:187-198, 1997.
- Scroggs, R.S., Todorovic, S.M., Anderson, E.G., and Fox, A.P. Variation in I_H , I_{IR} , and I_{LEAK} between acutely isolated adult rat dorsal root ganglion neurons of different size. *J.Neurophysiol.* 71:271-279, 1994.
- Selbach, O., Brown, R.E., and Haas, H.L. Long-term increase of hippocampal excitability by histamine and cyclic AMP. *Neuropharmacology* 36:1539-1548, 1997.
- Servos, P., Barke, K.E., Hough, L.B., and Vanderwolf, C.H. Histamine does not play an essential role in electrocortical activation during waking behavior. *Brain Res.* 636:98-102, 1994.
- Seutin, V., Massotte, L., Renette, M.F., and Dresse, A. Evidence for a modulatory role of I_h on the firing of a subgroup of midbrain dopamine neurons. *Neuroreport.* 12:255-258, 2001.
- Sheng, M., McFadden, G., and Greenberg, M.E. Membrane depolarization and calcium induce c-fos transcription via phosphorylation of transcription factor CREB. *Neuron* 4:571-582, 1990.
- Sherin, J.E., Shiromani, P.J., McCarley, R.W., and Saper, C.B. Activation of ventrolateral preoptic neurons during sleep. *Science* 271:216-219, 1996.
- Sherin, J.E., Elmquist, J.K., Torrealba, F., and Saper, C.B. Innervation of histaminergic tuberomammillary neurons by GABAergic and galaninergic neurons in the ventrolateral preoptic nucleus of the rat. *J.Neurosci.* 18:4705-4721, 1998.
- Shipp, S. The functional logic of cortico-pulvinar connections. *Philos.Trans.R.Soc.Lond.B.Biol.Sci.* 358:1605-1624, 2003.
- Shipp, S. Corticopulvinar connections of areas V5, V4, and V3 in the macaque monkey: a dual model of retinal and cortical topographies. *J.Comp.Neurol.* 439:469-490, 2001.
- Shors, T.J. and Matzel, L.D. Long-term potentiation: what's learning got to do with it? *Behav.Brain Sci.* 20:597-614, 1997.
- Silva, L.R., Amitai, Y., and Connors, B.W. Intrinsic oscillations of neocortex generated by layer 5 pyramidal neurons. *Science* 251:432-435, 1991.
- Simmons, M.A. and Schneider, C.R. Regulation of M-type potassium current by intracellular nucleotide phosphates. *J.Neurosci.* 18:6254-6260, 1998.
- Smith, B.N. and Armstrong, W.E. Histamine enhances the depolarizing afterpotential of immunohistochemically identified vasopressin neurons in the rat supraoptic nucleus via H_1 -receptor activation. *Neuroscience* 53:855-864, 1993.

- Smith, B.N. and Armstrong, W.E. The ionic dependence of the histamine-induced depolarization of vasopressin neurones in the rat supraoptic nucleus. *J.Physiol.* 495:465-478, 1996.
- Snider, R.M., McKinney, M., Forray, C., and Richelson, E. Neurotransmitter receptors mediate cyclic GMP formation by involvement of arachidonic acid and lipoxygenase. *Proc.Natl.Acad.Sci.U.S.A.* 81:3905-3909, 1984.
- Soria-Jasso, L.E., Bahena-Trujillo, R., and Arias-Montano, J.A. Histamine H₁ receptors and inositol phosphate formation in rat thalamus. *Neurosci.Lett.* 225:117-120, 1997.
- Southan, A.P., Morris, N.P., Stephens, G.J., and Robertson, B. Hyperpolarization-activated currents in presynaptic terminals of mouse cerebellar basket cells. *J.Physiol.* 526:91-97, 2000.
- Spruston, N., Jaffe, D.B., Williams, S.H., and Johnston, D. Voltage- and space-clamp errors associated with the measurement of electrotonically remote synaptic events. *J.Neurophysiol.* 70:781-802, 1993.
- Stafstrom, C.E., Schwindt, P.C., Flatman, J.A., and Crill, W.E. Properties of subthreshold response and action potential recorded in layer V neurons from cat sensorimotor cortex *in vitro*. *J.Neurophysiol.* 52:244-263, 1984.
- Staines, W.A., Yamamoto, T., Daddona, P.E., and Nagy, J.I. Neuronal colocalization of adenosine deaminase, monoamine oxidase, galanin and 5-hydroxytryptophan uptake in the tuberomammillary nucleus of the rat. *Brain Res.Bull.* 17:351-365, 1986.
- Steriade, M. Impact of network activities on neuronal properties in corticothalamic systems. *J.Neurophysiol.* 86:1-39, 2001.
- Steriade, M., Gloor, P., Llinas, R.R., Lopes, d.S.F., and Mesulam, M.M. Report of IFCN Committee on Basic Mechanisms. Basic mechanisms of cerebral rhythmic activities. *Electroencephalogr.Clin.Neurophysiol.* 76:481-508, 1990.
- Steriade, M., McCormick, D.A., and Sejnowski, T.J. Thalamocortical oscillations in the sleeping and aroused brain. *Science* 262:679-685, 1993.
- Steriade, M. Awakening the brain. *Nature* 383:24-25, 1996.
- Steriade, M., Amzica, F., and Contreras, D. Synchronization of fast (30-40 Hz) spontaneous cortical rhythms during brain activation. *J.Neurosci.* 16:392-417, 1996.
- Steriade, M., Timofeev, I., Durmuller, N., and Grenier, F. Dynamic properties of corticothalamic neurons and local cortical interneurons generating fast rhythmic (30-40 Hz) spike bursts. *J.Neurophysiol.* 79:483-490, 1998.

- Storm, J.F., Winther, T., Pedarzani, P., 1996. h-current modulation by norepinephrine, serotonin, dopamine, histamine and cyclic-AMP analogues in rat hippocampal neurons. *Soc. Neurosci. Abs.* 572.9.
- Strohmann, B., Schwarz, D.W., and Puil, E. Subthreshold frequency selectivity in avian auditory thalamus. *J.Neurophysiol.* 71:1361-1372, 1994.
- Stuart, G. and Spruston, N. Determinants of voltage attenuation in neocortical pyramidal neuron dendrites. *J.Neurosci.* 18:3501-3510, 1998.
- Svoboda, K.R. and Lupica, C.R. Opioid inhibition of hippocampal interneurons via modulation of potassium and hyperpolarization-activated cation (I_h) currents. *J.Neurosci.* 18:7084-7098, 1998.
- Swett, C.P. and Hobson, J.A. The effects of posterior hypothalamic lesions on behavioral and electrographic manifestations of sleep and waking in cats. *Arch.Ital.Biol.* 106:283-293, 1968.
- Szymusiak, R., Alam, N., Steininger, T.L., and McGinty, D. Sleep-waking discharge patterns of ventrolateral preoptic/anterior hypothalamic neurons in rats. *Brain Res.* 803:178-188, 1998.
- Takagi, H., Morishima, Y., Matsuyama, T., Hayashi, H., Watanabe, T., and Wada, H. Histaminergic axons in the neostriatum and cerebral cortex of the rat: a correlated light and electron microscopic immunocytochemical study using histidine decarboxylase as a marker. *Brain Res.* 364:114-123, 1986.
- Takahashi, A. and Shimazu, T. Hypothalamic regulation of lipid metabolism in the rat: effect of hypothalamic stimulation on lipolysis. *J.Auton.Nerv.Syst.* 4:195-205, 1981.
- Takahashi, K., Tokita, S., and Kotani, H. Generation and characterization of highly constitutive active histamine H_3 receptors. *J.Pharmacol.Exp.Ther.* 307:213-218, 2003.
- Takahashi, K., Suwa, H., Ishikawa, T., and Kotani, H. Targeted disruption of H_3 receptors results in changes in brain histamine tone leading to an obese phenotype. *J.Clin.Invest.* 110:1791-1799, 2002.
- Takeshita, Y., Watanabe, T., Sakata, T., Munakata, M., Ishibashi, H., and Akaike, N. Histamine modulates high-voltage-activated calcium channels in neurons dissociated from the rat tuberomammillary nucleus. *Neuroscience* 87:797-805, 1998.
- Takigawa, T. and Alzheimer, C. G protein-activated inwardly rectifying K^+ (GIRK) currents in dendrites of rat neocortical pyramidal cells. *J.Physiol.* 517:385-390, 1999.
- Tang, X.D. and Hoshi, T. Rundown of the hyperpolarization-activated KAT1 channel involves slowing of the opening transitions regulated by phosphorylation. *Biophys.J.* 76:3089-3098, 1999.

- Tardivel-Lacombe, J., Rouleau, A., Heron, A., Morisset, S., Pillot, C., Cochois, V., Schwartz, J.C., and Arrang, J.M. Cloning and cerebral expression of the guinea pig histamine H₃ receptor: evidence for two isoforms. *Neuroreport*. 11:755-759, 2000.
- Tasaka, K., Chung, Y.H., Sawada, K., and Mio, M. Excitatory effect of histamine on the arousal system and its inhibition by H₁ blockers. *Brain Res.Bull.* 22:271-275, 1989.
- Tashiro, M., Mochizuki, H., Iwabuchi, K., Sakurada, Y., Itoh, M., Watanabe, T., and Yanai, K. Roles of histamine in regulation of arousal and cognition: functional neuroimaging of histamine H₁ receptors in human brain. *Life Sci.* 72:409-414, 2002.
- Thomas, E. and Evans, G.J. Septal inhibition of aversive emotional states. *Physiol.Behav.* 31:673-678, 1983.
- Thompson, S.M., Capogna, M., and Scanziani, M. Presynaptic inhibition in the hippocampus. *Trends.Neurosci.* 16:222-227, 1993.
- Thomson, A.M. and Bannister, A.P. Interlaminar connections in the neocortex. *Cereb.Cortex.* 13:5-14, 2003.
- Threlfell, S., Cragg, S.J., Kallo, I., Turi, G.F., Coen, C.W., and Greenfield, S.A. Histamine H₃ receptors inhibit serotonin release in substantia nigra pars reticulata. *J.Neurosci.* 24:8704-8710, 2004.
- Timofeev, I., Bazhenov, M., Sejnowski, T., and Steriade, M. Cortical hyperpolarization-activated depolarizing current takes part in the generation of focal paroxysmal activities. *Proc.Natl.Acad.Sci.U.S.A.* 99:9533-9537, 2002.
- Toftegaard, C.L., Knigge, U., Kjaer, A., and Warberg, J. The role of hypothalamic histamine in leptin-induced suppression of short-term food intake in fasted rats. *Regul.Pept.* 111:83-90, 2003.
- Tokimasa, T. and Akasu, T. Cyclic AMP regulates an inward rectifying sodium-potassium current in dissociated bull-frog sympathetic neurones. *J.Physiol.* 420:409-29.:409-429, 1990.
- Traiffort, E., Ruat, M., Arrang, J.M., Leurs, R., Piomelli, D., and Schwartz, J.C. Expression of a cloned rat histamine H₂ receptor mediating inhibition of arachidonate release and activation of cAMP accumulation. *Proc.Natl.Acad.Sci.U.S.A.* 89:2649-2653, 1992.
- Traiffort, E., Leurs, R., Arrang, J.M., Tardivel-Lacombe, J., Diaz, J., Schwartz, J.C., and Ruat, M. Guinea pig histamine H₁ receptor. I. Gene cloning, characterization, and tissue expression revealed by in situ hybridization. *J.Neurochem.* 62:507-518, 1994.
- Trautwein, W. and Hescheler, J. Regulation of cardiac L-type calcium current by phosphorylation and G proteins. *Annu.Rev.Physiol.* 52:257-74.:257-274, 1990.

- Travis, E.R., Wang, Y.M., Michael, D.J., Caron, M.G., and Wightman, R.M. Differential quantal release of histamine and 5-hydroxytryptamine from mast cells of vesicular monoamine transporter 2 knockout mice. *Proc.Natl.Acad.Sci.U.S.A.* 97:162-167, 2000.
- Tsien, R.W., Giles, W., and Greengard, P. Cyclic AMP mediates the effects of adrenaline on cardiac purkinje fibres. *Nat.New Biol.* 240:181-183, 1972.
- Tuomisto, L., Eriksson, L., and Fyhrquist, F. Vasopressin release by histamine in the conscious goat. *Eur.J.Pharmacol.* 63:15-24, 1980.
- Turbes, C.C. EEG dynamics. Brain processing of sensory and cognitive information. *Biomed.Sci.Instrum.* 28:51-58, 1992.
- Uchimura, N., Cherubini, E., and North, R.A. Cation current activated by hyperpolarization in a subset of rat nucleus accumbens neurons. *J.Neurophysiol.* 64:1847-1850, 1990.
- Ulrich, D. Dendritic resonance in rat neocortical pyramidal cells. *J.Neurophysiol.* 87:2753-2759, 2002.
- Valjakka, A., Vartiainen, J., Kosunen, H., Hippelainen, M., Pesola, P., Olkkonen, H., Airaksinen, M.M., and Tuomisto, L. Histaminergic modulation of neocortical spindling and slow-wave activity in freely behaving rats. *J.Neural Transm.* 103:1265-1280, 1996.
- van Brederode, J.F. and Spain, W.J. Differences in inhibitory synaptic input between layer II-III and layer V neurons of the cat neocortex. *J.Neurophysiol.* 74:1149-1166, 1995.
- Vanni-Mercier, G., Sakai, K., and Jouvet, M. [Specific neurons for wakefulness in the posterior hypothalamus in the cat]. *C.R.Acad.Sci.III.* 298:195-200, 1984.
- Vargas, G. and Lucero, M.T. Modulation by PKA of the hyperpolarization-activated current (I_h) in cultured rat olfactory receptor neurons. *J.Membr.Biol.* 188:115-125, 2002.
- Vargas, G. and Lucero, M.T. Dopamine modulates inwardly rectifying hyperpolarization-activated current (I_h) in cultured rat olfactory receptor neurons. *J.Neurophysiol.* 81:149-158, 1999.
- Velumian, A.A., Zhang, L., Pennefather, P., and Carlen, P.L. Reversible inhibition of I_K , I_{AHP} , I_h and I_{Ca} currents by internally applied gluconate in rat hippocampal pyramidal neurones. *Pflugers Arch.* 433:343-350, 1997.
- Viscomi, C., Altomare, C., Bucchi, A., Camatini, E., Baruscotti, M., Moroni, A., and DiFrancesco, D. C terminus-mediated control of voltage and cAMP gating of hyperpolarization-activated cyclic nucleotide-gated channels. *J.Biol.Chem.* 276:29930-29934, 2001.

- Vizuete, M.L., Dimitriadou, V., Traiffort, E., Griffon, N., Heron, A., and Schwartz, J.C. Endogenous histamine induces c-fos expression within paraventricular and supraoptic nuclei. *Neuroreport*. 6:1041-1044, 1995.
- Vizuete, M.L., Traiffort, E., Bouthenet, M.L., Ruat, M., Souil, E., Tardivel-Lacombe, J., and Schwartz, J.C. Detailed mapping of the histamine H₂ receptor and its gene transcripts in guinea-pig brain. *Neuroscience* 80:321-343, 1997.
- Volterra, A., Trotti, D., Cassutti, P., Tromba, C., Galimberti, R., Lecchi, P., and Racagni, G. A role for the arachidonic acid cascade in fast synaptic modulation: ion channels and transmitter uptake systems as target proteins. *Adv.Exp.Med.Biol.* 318:147-158, 1992.
- von Stein, A., Chiang, C., and Konig, P. Top-down processing mediated by interareal synchronization. *Proc.Natl.Acad.Sci.U.S.A.* 97:14748-14753, 2000.
- Vorobjev, V.S., Sharonova, I.N., Walsh, I.B., and Haas, H.L. Histamine potentiates N-methyl-D-aspartate responses in acutely isolated hippocampal neurons. *Neuron* 11:837-844, 1993.
- Wada, H., Inagaki, N., Yamatodani, A., and Watanabe, T. Is the histaminergic neuron system a regulatory center for whole-brain activity? *Trends.Neurosci.* 14:415-418, 1991.
- Wainger, B.J., DeGennaro, M., Santoro, B., Siegelbaum, S.A., and Tibbs, G.R. Molecular mechanism of cAMP modulation of HCN pacemaker channels. *Nature* 411:805-810, 2001.
- Wallace, D.J., Chen, C., and Marley, P.D. Histamine promotes excitability in bovine adrenal chromaffin cells by inhibiting an M-current. *J.Physiol.* 540:921-939, 2002.
- Wang, L., Gantz, I., and DelValle, J. Histamine H₂ receptor activates adenylate cyclase and PLC via separate GTP-dependent pathways. *Am.J.Physiol.* 271:613-620, 1996.
- Wang, L.D., Hoeltzel, M., Gantz, I., Hunter, R., and Del Valle, J. Characterization of the histamine H₂ receptor structural components involved in dual signaling. *J.Pharmacol.Exp.Ther.* 285:573-578, 1998.
- Wang, X.J. Ionic basis for intrinsic 40 Hz neuronal oscillations. *Neuroreport*. 5:221-224, 1993.
- Wang, Y.T., Pak, Y.S., and Salter, M.W. Rundown of NMDA-receptor mediated currents is resistant to lowering intracellular [Ca²⁺] and is prevented by ATP in rat spinal dorsal horn neurons. *Neurosci.Lett.* 157:183-186, 1993.
- Washington, B., Shaw, J.B., Li, J., Fisher, B., and Gwathmey, J. *In vivo* histamine release from brain cortex: the effects of modulating cellular and extracellular sodium and calcium channels. *Eur.J.Pharmacol.* 407:117-122, 2000.
- Watanabe, T. and Yanai, K. Studies on functional roles of the histaminergic neuron system by using pharmacological agents, knockout mice and positron emission tomography. *Tohoku.J.Exp.Med.* 195:197-217, 2001.

- Watts, A.E., Williams, J.T., and Henderson, G. Baclofen inhibition of the hyperpolarization-activated cation current, I_h , in rat substantia nigra zona compacta neurons may be secondary to potassium current activation. *J.Neurophysiol.* 76:2262-2270, 1996.
- Weiger, T., Stevens, D.R., Wunder, L., and Haas, H.L. Histamine H_1 receptors in C6 glial cells are coupled to calcium-dependent potassium channels via release of calcium from internal stores. *Naunyn Schmiedebergs Arch.Pharmacol.* 355:559-565, 1997.
- Westerink, B.H., Cremers, T.I., De Vries, J.B., Liefers, H., Tran, N., and De Boer, P. Evidence for activation of histamine H_3 autoreceptors during handling stress in the prefrontal cortex of the rat. *Synapse* 43:238-243, 2002.
- White, E.L. and Hersch, S.M. A quantitative study of thalamocortical and other synapses involving the apical dendrites of corticothalamic projection cells in mouse SmI cortex. *J.Neurocytol.* 11:137-157, 1982.
- Wieland, K., Bongers, G., Yamamoto, Y., Hashimoto, T., Yamatodani, A., Menge, W.M., Timmerman, H., Lovenberg, T.W., and Leurs, R. Constitutive activity of histamine H_3 receptors stably expressed in SK-N-MC cells: display of agonism and inverse agonism by H_3 antagonists. *J.Pharmacol.Exp.Ther.* 299:908-914, 2001.
- Williams, K. Subunit-specific potentiation of recombinant N-methyl-D-aspartate receptors by histamine. *Mol.Pharmacol.* 46:531-541, 1994.
- Williams, S.R. and Stuart, G.J. Site independence of EPSP time course is mediated by dendritic $I(h)$ in neocortical pyramidal neurons. *J.Neurophysiol.* 83:3177-3182, 2000.
- Winklhofer, M., Matthias, K., Seifert, G., Stocker, M., Sewing, S., Herget, T., Steinhauser, C., and Saaler-Reinhardt, S. Analysis of phosphorylation-dependent modulation of $K_{v1.1}$ potassium channels. *Neuropharmacology* 44:829-842, 2003.
- Wischmeyer, E. and Karschin, A. Receptor stimulation causes slow inhibition of IRK1 inwardly rectifying K^+ channels by direct protein kinase A-mediated phosphorylation. *Proc.Natl.Acad.Sci.U.S.A.* 93:5819-5823, 1996.
- Wu, J.Y. and Cohen, I.S. Tyrosine kinase inhibition reduces I_f in rabbit sinoatrial node myocytes. *Pflugers Arch.* 434:509-514, 1997.
- Wu, L.G. and Saggau, P. Presynaptic inhibition of elicited neurotransmitter release. *Trends.Neurosci.* 20:204-212, 1997.
- Wu, N., Hsiao, C.F., and Chandler, S.H. Membrane resonance and subthreshold membrane oscillations in mesencephalic V neurons: participants in burst generation. *J.Neurosci.* 21:3729-3739, 2001.
- Wulff, B.S., Hastrup, S., and Rimvall, K. Characteristics of recombinantly expressed rat and human histamine H_3 receptors. *Eur.J.Pharmacol.* 453:33-41, 2002.

- Yadin, E., Thomas, E., Grishkat, H.L., and Strickland, C.E. The role of the lateral septum in anxiolysis. *Physiol.Behav.* 53:1077-1083, 1993.
- Yamagishi, N., Callan, D.E., Goda, N., Anderson, S.J., Yoshida, Y., and Kawato, M. Attentional modulation of oscillatory activity in human visual cortex. *Neuroimage.* 20:98-113, 2003.
- Yanai, K., Son, L.Z., Endou, M., Sakurai, E., and Watanabe, T. Targeting disruption of histamine H₁ receptors in mice: behavioral and neurochemical characterization. *Life Sci.* 62:1607-1610, 1998.
- Yanai, K., Son, L.Z., Endou, M., Sakurai, E., Nakagawasai, O., Tadano, T., Kisara, K., Inoue, I., and Watanabe, T. Behavioural characterization and amounts of brain monoamines and their metabolites in mice lacking histamine H₁ receptors. *Neuroscience* 87:479-487, 1998.
- Yang, C.R., Seamans, J.K., and Gorelova, N. Electrophysiological and morphological properties of layers V-VI principal pyramidal cells in rat prefrontal cortex *in vitro*. *J.Neurosci.* 16:1904-1921, 1996.
- Yang, Q.Z. and Hatton, G.I. Electrophysiology of excitatory and inhibitory afferents to rat histaminergic tuberomammillary nucleus neurons from hypothalamic and forebrain sites. *Brain Res.* 773:162-172, 1997.
- Yates, S.L., Tedford, C.E., Gregory, R., Pawlowski, G.P., Handley, M.K., Boyd, D.L., and Hough, L.B. Effects of selected histamine H₃ receptor antagonists on telemethylhistamine levels in rat cerebral cortex. *Biochem.Pharmacol.* 57:1059-1066, 1999.
- Yu, H., Chang, F., and Cohen, I.S. Phosphatase inhibition by calyculin A increases i(f) in canine Purkinje fibers and myocytes. *Pflugers Arch.* 422:614-616, 1993.
- Yu, H., Chang, F., and Cohen, I.S. Pacemaker current I_f in adult canine cardiac ventricular myocytes. *J.Physiol.* 485:469-483, 1995.
- Zawilska, J.B., Woldan-Tambor, A., and Nowak, J.Z. Histamine H₂-like receptors in chick cerebral cortex: effects on cyclic AMP synthesis and characterization by [(3) H]tiotidine binding. *J.Neurochem.* 81:935-946, 2002.
- Zhang, L. and Krnjevic, K. Whole-cell recording of anoxic effects on hippocampal neurons in slices. *J.Neurophysiol.* 69:118-127, 1993.
- Zhou, Z. and Lipsius, S.L. Effect of isoprenaline on I_f current in latent pacemaker cells isolated from cat right atrium: ruptured vs. perforated patch whole-cell recording methods. *Pflugers Arch.* 423:442-447, 1993.
- Zong, X., Eckert, C., Yuan, H., Wahl-Schott, C., Abicht, H., Fang, L., Li, R., Mistrik, P., Gerstner, A., Much, B., Baumann, L., Michalakis, S., Zeng, R., Chen, Z., and Biel, M. A novel mechanism of modulation of hyperpolarization-activated cyclic nucleotide-gated channels by SRC kinase. *J.Biol.Chem.*, Epub ahead of print, 2005.

